National Library of Canada
Acquisitions and Bibliographic Services Branch
395 Wellington Street
Ottawa, Ontario
K1A 0N4

Bibliothèque nationale du Canada
Direction des acquisitions et des services bibliographiques
395, rue Wellington
Ottawa (Ontario)
K1A 0N4

Your file Votre référence

Our file Notre référence

NOTICE

The quality of this microform is heavily dependent upon the quality of the original thesis submitted for microfilming. Every effort has been made to ensure the highest quality of reproduction possible.

If pages are missing, contact the university which granted the degree.

Some pages may have indistinct print especially if the original pages were typed with a poor typewriter ribbon or if the university sent us an inferior photocopy.

Reproduction in full or in part of this microform is governed by the Canadian Copyright Act, R.S.C. 1970, c. C-30, and subsequent amendments.

AVIS

La qualité de cette microforme dépend grandement de la qualité de la thèse soumise au microfilmage. Nous avons tout fait pour assurer une qualité supérieure de reproduction.

S'il manque des pages, veuillez communiquer avec l'université qui a conféré le grade.

La qualité d'impression de certaines pages peut laisser à désirer, surtout si les pages originales ont été dactylographiées à l'aide d'un ruban usé ou si l'université nous a fait parvenir une photocopie de qualité inférieure.

La reproduction, même partielle, de cette microforme est soumise à la Loi canadienne sur le droit d'auteur, SRC 1970, c. C-30, et ses amendements subséquents.

Canada

Almost-Symmetrical Time-Varying ARMA Model and Its Applications for Separation of Signals with Overlapping Fourier Spectra

Wen Tong

A Thesis
in
The Department
of
Electrical and Computer Engineering

Presented in Partial Fulfillment of the Requirements
for the Degree of Doctor of Philosophy at
Concordia University
Montreal, Quebec, Canada

April 1993

ISBN 0-315-97648-9

Canada

ABSTRACT

Almost-Symmetrical Time-Varying ARMA Model and Its Applications for Separation of Signals with Overlapping Fourier Spectra

Wen Tong, Ph.D
Concordia University, 1993

An almost-symmetrical time-varying (ASTV) ARMA model is proposed and investigated in this thesis. It is shown that such a model can be implemented by a cascade connection of time-varying null and anti-null operators. The existence and implementation of a time-varying null operator (in MA form) is associated with the Wronskian (W-system) of the linearly independent components of the signal under analysis. The signal space spanned by the W-system constitutes a null singularity of the time-varying null operator. It is shown that such a time-varying null operator can not be decomposed by using root-factorization and is not commutable with any other time-varying or time-invariant operators. Any signal that does not belong to the space of the W-system will be distorted by such a null operator, thus precluding signal separation. It is shown that in order to fulfill the signal separation task a special property called transparency has to be established. Such a transparency may be achieved by introducing an anti-null operator (AR) perfectly symmetrical to the null operator (MA), resulting in an ARMA model. Any signal that belongs to the space spanned by the W-system is rejected, while signals not belonging to the signal space will pass this ARMA model with no distortion. Two kinds of local instabilities which are inherent to the proposed system are investigated and several BIBO global stability tests are established.

The proposed model is used for the separation of broad-band signals with overlapping Fourier spectra. Two basic approaches are investigated: (1) nonlinear phase-unwarping procedure followed by time-invariant almost-symmetrical ARMA filtering, and (2) time-varying signal-controlled almost-symmetrical ARMA filtering. Phase-unwarping procedure is implemented by a specially designed non-equally spaced sampling strategy. It is shown that such a strategy is able to transform any constant-envelope signal of arbitrary phase into a new constant-envelope signal of given phase, but in a new time-domain (in particular, an FM signal is transformed into a sinewave of fixed frequency). Several

algorithms for the recovery of a signal corrupted by a strong, constant-envelope interference are investigated.

The ASTV-ARMA model is then successfully applied to solve two specific problems: (1) the blind deconvolution of a linear channel driven by a non-stationary source, and (2) separation of broad-band signals with overlapping spectra, by proposing a cross-coupled signal controlled ASTV-ARMA model. It is shown that the uniqueness of the proposed blind deconvolution procedure is guaranteed. The stability of the equilibria of the cross-coupled ASTV-ARMA model is investigated; it is shown that this model always converges to a solution resulting in a complete separation of the superimposed FM signals.

Acknowledgments

I would like to express my profound gratitude and appreciation to Prof. Eugene I. Plotkin and Prof. M. N. S. Swamy, my thesis supervisors, for their expert guidance, persistent encouragement and support through the entire course of this research. With their deep intellectual insight, high standards in research, kind understanding and patience, they have not only contributed immensely their ideas, time, and devotion to the direction of this work, but also made great efforts to develop my ability to think independently, originally and logically, to be rigorous and disciplined in research, and not unimportantly, to write passable English. I am happy to have not only one but two such wonderful supervisors.

I am indebted to my friends and colleagues at the *Center for Signal Processing and Communications* for providing me a warm, friendly enthusiastic atmosphere. Sincere thanks also to Drs. D. Wulich, Y.Yoganandam and V. Shatalov, and Mr. R. Agarwal and other fellow graduate students (in H-847 and GM-905) for their valuable discussions and helps.

Special thanks go to my parents in China, who have extended their generous support and confidence all these years.

Last but not least, I wish to extend my deepest thanks to my wife, Qiaozhen for her encouragement and patience throughout the whole span of this undertaking when she studied in ETH in Zurich, Harvard University and Universite de Montreal. She truly shared each step of progress of this thesis and always supported me with her love and understanding.

This thesis was made possible through a joint doctoral program between Concordia University and Southeast University; I would like to pay my respect to Dr. M.N.S. Swamy who initiated this kind of joint doctoral program for the first time between China and the Western World. The research was supported partly by the Canadian International Development Agency (CIDA), under the joint doctoral program between Concordia University and Southeast University, and partly supported by the NSERC through grants awarded to Dr. Plotkin and Dr. Swamy.

Dedicated

to

My Late Grandpa

and

to

China

Time-Variant Involves Time-Invariant

Time-Invariant Involves Time-Variant

Dao-De-Jing Chapter 2.4

***Lao Tze* (Philosopher B.C. 560-457)**

TABLE OF CONTENTS

Chapter 9 CONCLUSIONS

Appendices

1. A floppy disk is included.

LIST OF FIGURES

LIST OF TABLES

LIST OF SYMBOLS AND ABBREVATIONS

$a_i(k)$	time-varying coefficients of null operator
$A(k)$	companion matrix for time-varying null operator
α	symmetrical factor
$\gamma_i^A(k)$	partial coefficient for amplitude
$\partial A(k)$	variation rate of time-varying system $A(k)$
$E\{\ \}$	ensemble average operation
$F(\Omega, \omega)$	displacement kernel function on the unit disc
$\varphi_i(k)$	element function of W-system
$h(n, k)$	impulse response of a time-varying system when the impulse is applied a time m
$\aleph_1$	time-varying null operator representing signal space S_1
$\Re$	real variables
$\rho_A(k)$	Maximum module the of eigen values of the matrix $A(k)$
$\rho_{i,j}$	signal separation ratio
$\psi(k)$	instantaneous phase of signal
t_k	non-equally spaced sampling instant
$\Theta(q^{-1})$	equalizer
$\Im(q^{-1})$	the channel impulse response
$V(Y(j))$	Lyapunov function associated with $Y(j)$
$W(k)$	time-varying coefficients of null operator estimated by Gauss-Newton Algorithm
W_o^N	N-dimensional Wronskian constructed with respect to operator o
Ω_i^N	signal subspace S_1 with dimension N
Z^+	positive integers set

ARMA	Autoregressive Moving Average
BIBO	Bounded Input Bounded Output
AS	Almost Symmetrical
ASTV	Almost Symmetrical Time-Varying
CC-AA	Cross-Coupled Almost Symmetrical ASTV-ARMA
C-M	Choi-Mcmillan
ESS	Equally Spaced Sampling
FM	Frequency Modulation
FMS	Frequency Modulated Sinusoids
G-N	Gauss-Newton
LIF	Linear Independent Functions
LIFK	Local Instability of the First Kind
LISK	Local Instability of the Second Kind
LTI	Linear Time Invariant
LTV	Linear Time-Varying
MA	Moving Average
NESS	Non-Equally Spaced Sampling
QAM	Quadric Amplitude Modulation
TV	Time-varying

Chapter

1

Introduction

Our objective in this research is to develop a linear time-varying model for the separation of superimposed signals whose Fourier spectra overlap. In this work, we introduce the concept and the design methodology of an Almost-Symmetrical Time-Varying ARMA (ASTV-ARMA) model. Several basic properties related to this special time-varying model are investigated. Some applications of this model related to the separation of signals with overlapping Fourier spectra are presented.

1.1. Problems and Approach

1.1.1. Signal Modelling

Most of the existing signal models are *time-invariant* rational linear ones, such as auto-regressive(AR), moving-average(MA) and auto-regressive moving-average (ARMA) models. These models are also called *parametric models*. For decades, the time-invariant parametric model has been a subject of intensive study in the filed of signal processing. The properties and applications of these time-invariant models are well known. In a certain sense, time-invariant signal modelling is equivalent to the problem of signal filtering based on a knowledge of the Fourier spectrum of the signal under analysis.

It is an established fact that a time-invariant model is optimal for a signal possessing a *rational Fourier spectrum*; that is a given signal with a rational Fourier spectrum, one can find an exact *finite order* time-invariant model. However, if the Fourier spectrum of the signal is not rational, only an *infinite order* time-invariant parametric model can be associated with such a signal. On the other hand, it is possible to find *a finite order time-varying parametric model* to model a signal with a non-rational Fourier spectrum.

It is also a known fact an ideal separation of signals by time-invariant filtering may be achieved only if the Fourier spectra of the superimposed signals are located in non-overlapping frequency ranges. However, in the case where the Fourier spectra are overlapping within the same frequency bandwidth, then the separation of such signals becomes impossible by using a conventional linear time-invariant filter. In what follows, we will show that the proposed time-varying ARMA model may be effectively used for solving the problem of signal separation, even if the Fourier spectra of the signals are located within the same frequency bandwidth, i.e. the spectra are completely overlapping.

The main aim of this thesis is to develop a systematic approach to the design of *time-varying linear parametric model* associated with a given class of signals. Our efforts are also devoted to the problem of signal separation, especially in the case of superimposed signals with overlapping Fourier spectra.

1.1.2. Parametric Modeling and W-System

We establish our concept of signal parametric modelling by exploring the relationship between a homogeneous parametric model and its fundamental solutions. If a signal can be represented by a linear combination of a complete set of independent functions, such a set of linear independent functions constitute a system of fundamental solutions (W-system) for a particular linear homogenous equation. Thus the signal may be considered as a solution of this linear homogeneous equation. We define such a homogenous equation as the MA parametric model associated with this signal. If the coefficients of this homogenous equation are fixed values, the parametric model is a time-invariant one; if at least one of the coefficients of this model is time-varying, then the model is a time-varying one.

If a signal can be represented by a certain W-system, then the output of the parametric model associated with such a signal is zero. Therefore such a parametric

model may be treated as a *null operator* with respect to the given signal. The signal space spanned by the W-system constitutes a *null singularity* of the model associated with such a W-system. Conversely, given a null operator one can always find a W-system which represents the null singularity. The relationship between a null operator and its null singularity is a very important key to the parametric modelling of a signal. According to our definition of the null operator/singularity, it is not difficult to see that any *MA model (linear FIR filter) is a null operator* associated with a certain signal and that the signal modelling problem may be considered as one of designing the null operator for the given signal.

On the other hand, given an arbitrary signal, its harmonic expansion usually requires many terms (generally, infinite number of terms). However, such a signal may be expanded by certain non-harmonic or even non-orthogonal basis. The non-harmonic system usually represents a linear time-varying model. Since our choice of system of functions is not necessarily restricted to harmonic systems, this leaves room for more efficient modelling by exploiting time-varying models. By efficient modelling, we mean that the order of the time-varying null operator associated with a given signal is lower than the choice of the W-system associated with the time-invariant model.

Usually the W-system for a linear time-varying null operator is not an harmonic system, which means the Fourier spectra of two different W-systems of functions may be located in the same frequency range. We will show that the key to the separation of the superimposed signals is that these signals may be represented by different W-systems even though these W-systems may have overlapping Fourier spectra.

Generally, for purposes of signal processing, time-invariant filters are designed based on the knowledge of the Fourier spectra of the signals under analysis (or their auto-correlation functions in case of stationary random signals). *Since the process of construction of a time-varying parametric model is essentially independent of the knowledge of the Fourier spectrum of the signal,* such a model may be used for separation of a certain class of signals with overlapping Fourier spectra.

1.2. Almost-Symmetrical Time-Varying ARMA Model

In many cases a time-varying model is treated as a time-invariant one by assuming the parameters of the signal under analysis are almost of constant values, during a certain observation time interval. Therefore, a time-invariant model is used to analyze such signals. This assumption is not always justified, and in some cases, the parameters of the signal vary very fast. In such a case we cannot approximate a time-varying model by using a time-invariant one.

Our effort in this work is to find a true time-varying model for the signal, rather than imposing certain assumptions in order to treat the signal model as a time-invariant one. In particular, our interest is concentrated on the fast time-varying model. We consider a linear time-varying model as a general linear model, and the time-invariant model is a special case of the time-varying model. If the linear model is a time-varying one, then *the Wronskian* of the W-system associated with the such a signal model is not of a fixed value, but *changes with time*. If the Wronskian is a of fixed value, then the signal model associated with this Wronskian becomes a time-invariant one. It is shown that the root-factorization, which is commonly used in the time-invariant case, is invalid for decomposing a liner time-varying model, and that the time-varying model is not commutable with other time-varying or time-invariant models. This result leads to a more explicit criterion which allows us to classify time-varying and time-invariant models.

It is known that any linear time-varying system will produce spurious spectrum components. Such additional spectrum components are usually undesired artifacts in the output, and this is a major drawback of using a linear time-varying operator in the signal processing context. On the other hand, signals *which do not belong to the null singularity* are distorted by the time-varying null operator. In this situation, separation can not be achieved. In order to restore the signal which does not belong to the null singularity, we introduce a time-varying anti-null operator which is perfectly symmetrical to the time-varying null operator. The combined operator (symmetrical ARMA model) becomes a *transparent* one for any signal, but it possesses a certain null singularity for the particular W-system.

It is also shown that such a perfect symmetrical operator is not physically realizable. A physically realizable one-sided almost symmetrical time-varying operator, which

allows us to achieve almost ideal transparency, is introduced.

After presenting the definition and the design approach to the time-varying modelling of a signal, we outline the basic idea of using ASTV-ARMA model for signal separation. Any signal S_1 which is represented by a linear combination of a W-system will be annihilated by the null operator (MA). By combining the symmetrical anti-null operator, a transparent operator Q_1^a is obtained. Thus any other signal S_2 which does not belong to the signal subspace spanned by the W-system will pass the transparent operator without any change. Therefore, two superimposed signals can be separated by using the transparent operator Q_1^a as shown in Fig.1.1-a.

Moreover, the signal subspace can be further partitioned by defining different transparent operators as illustrated in Fig.1.1-b. The transparent operator Q_1^a is associated with the signal subspace Ω_1; therefore, any signal that belongs to the subspace Ω_1 will be annihilated at the output of operator Q_1^a while the signal that belongs to the other signal subspace will pass this operator transparently. In this way the W-system defines an operator Q_i^a and conversely the operator defines a signal subspace Ω_i. Thus the signal space is partitioned by the transparent operators $\{Q_i^a\}$.

1.3. A Brief Review of Literature

Our research in this thesis belongs to the field of Structural Signal Processing, and a recent comprehensive review of this field can be found in [1.2]. It has its origin from a Russian school (see Ref. in [1.2]) and found remarkable developments in this field during the eighties[1.2]-[1.4],[1.7]-[1.17]. Structural signal processing presents a very generalized theory of parametric signal modeling. Some very important aspects of structural signal processing are given below.

1. *Design of Function Elimination Filters, (Null Filters, Parametric Invariant Filters) which operate on an entire class of signals regardless of the values of their parameters.[1.2],[1.7]-[1.15]*

2. *Design of a parametric null operator based on arbitrarily chosen building blocks.[1.13]*

3. *Separation of signals, occupying the same frequency band.[1.27],[1.29]*

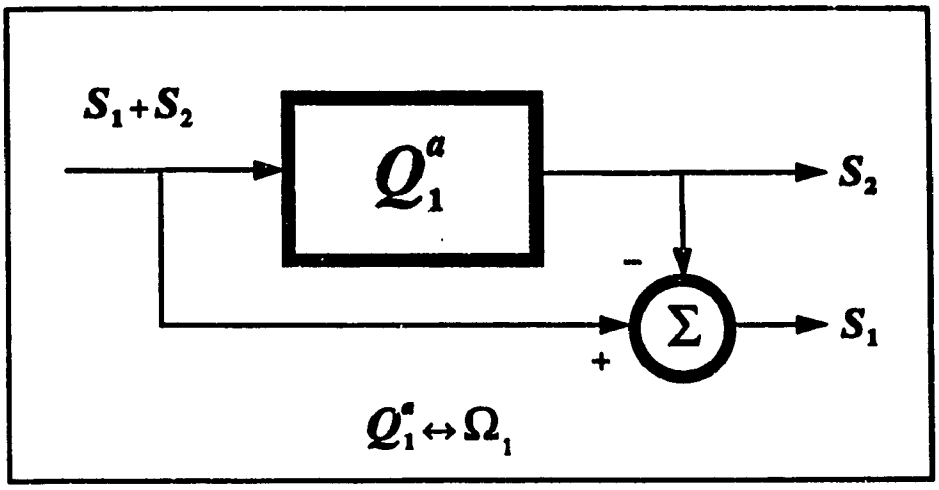

a) Signal Separation

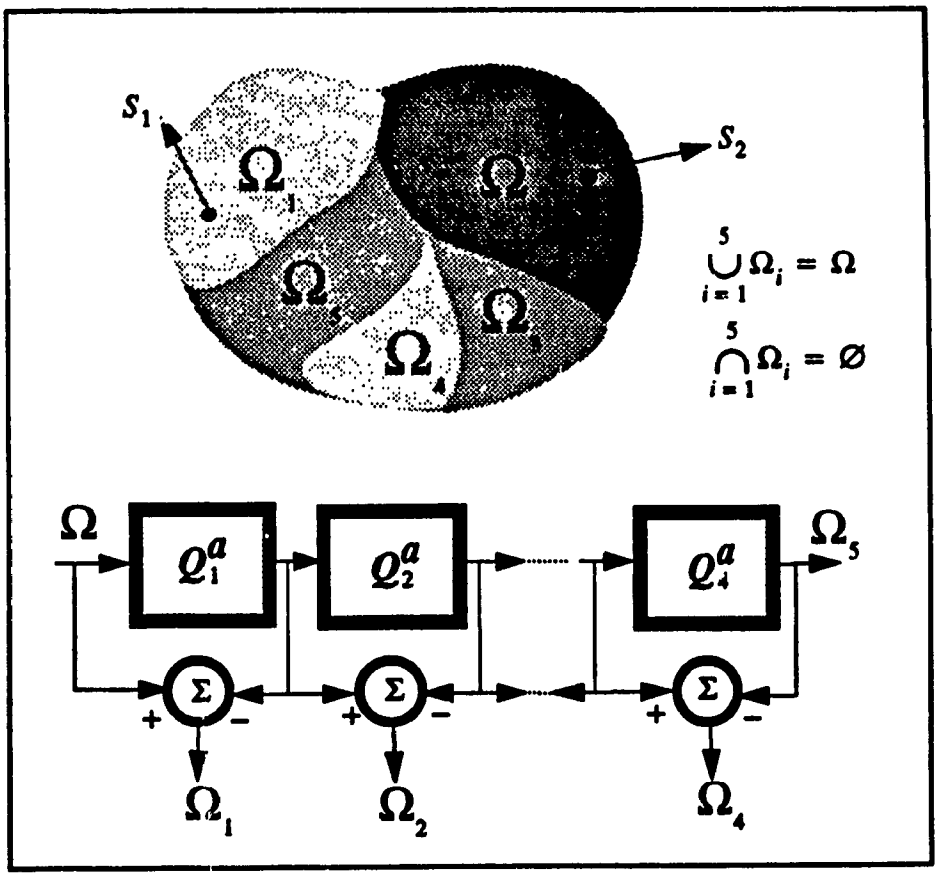

b) Partition of Signal Space and Transparent Operators

Fig.1.1 Signal Separation and Transparent Operator

As to the Function Elimination Filters, which fall into the category of non-linear signal processing, considerable results are available in [1.2], [1.3]. The results obtained in this thesis belong to the area of structural signal processing with particular emphasis on the theory and application of linear time-varying structural modelling. First attempt to time-varying structural modelling for the design of a time-varying null filter may be found in [1.7], [1.17] and [1.25]. Later, this time-varying null filter was reintroduced as a *signal-controlled time-varying filter*, and successfully applied to the problem of rejection of frequency varying interference [1.16]-[1.18],[1.21],[1.25]-[1.28]. The stability of this signal controlled time-varying null-filter was studied in [1.30]. The transparency property of such a signal-controlled null-filter is discussed in [1.26].

It should be mentioned that a discrete time symmetrical ARMA model *as applied to a time-invariant system* had been also introduced by Pisarenko in 1973 [1.32]; he obtained this special ARMA model from the singular value decomposition of the covariance matrix used in the estimation of the fixed frequencies of harmonic signals. This model in the time-invariant case is equivalent to the so called *constrained notch filter*. Rao[1.23] and Nehorai [1.24] applied the constrained notch filter with an adaptive algorithm to estimate the parameters of sinusoids, and to retrieve the sinusoids from white additive noise. Rao used the *complete parametric model*, while Nehorai used a *minimum parametric model*; both of them used one-sided symmetrical ARMA model, which implies that the zeros of the notch filter are located on the unit disc, while the poles are constrained to be on the radii of the zeros and located inside the unit disc, at a distant α form the origin tending to the unit disc boundary; i.e. $\alpha \rightarrow 1^-$. Note that for $\alpha = 1$, these models become perfectly symmetrical in the sense of the above discussion. Nehorai further proposed the use of the time-varying symmetrical factor $\alpha(k)$ [1.24] to improve the convergence time. Rao [1.23] presented an analysis of the tracking behavior of the adaptive algorithm for this almost-symmetrical ARMA model. However all their results are based on the assumption that the symmetrical ARMA model is a time-invariant one.

1.4. Outline of the Thesis

The thesis consists of two parts: in the first part the theory of the ASTV-ARMA model and its properties are discussed, and in the second part the ASTV-ARMA model

is applied to separate signals with overlapping Fourier spectra. The thesis is organized as follows.

In Chapter 2, we present the concept and rules for the design of a linear time-varying null operator; several basic properties of such a time-varying null operator are then discussed. We show that if a signal can be represented by an N-dimensional Wronskian system, then one can find a time-varying null operator to represent such a signal, provided that the Wronskian is positive.

In Chapter 3, we show that the synthesis of a higher-order time-varying null operator can be achieved by using lower-order Wronskians combined with certain pivot rules. Two algorithms are discussed, the Choi-McMillan and the Sylvester algorithms. We show that the time-varying operator can not be decomposed by using root-factorization, and that it is also non-commutable with other time-varying and/or time-invariant null operators. These restrictions place a very serious limitation on the applicability of such operators to signal processing purposes.

In Chapter 4, we show that if the time-varying null operator is combined with a perfect symmetrical anti-null operator, a transparent operator can be built. In this case and only in this case do the transparency and symmetry properties allow the time-varying null operator to be commutable with the time-varying anti-null operator. By exploring the properties of the impulse response of the anti-null time-varying operator, we show clearly the role the anti-null operator plays in the construction of a transparent system. On the other hand, it is shown that a perfect transparent operator is not physically realizable. It is also shown that the one-sided almost symmetrical time-varying transparent system is physically realizable. A trade-off between the requirement of ideal transparency and the duration of the observation time, as applied to almost symmetrical time-varying operator, is also investigated.

In Chapter 5, a general study of a linear time-varying anti-null operator is carried out. We present two kinds of local instabilities which exclusively belong to linear time-varying autonomous systems. It is shown that for a linear time-varying system the module of the eigenvalues of a time-varying system can be temporally outside the unit disc, and the system may be still globally BIBO stable; however it is also shown that even if the module of the eigenvalues of the system is strictly inside the unit disc, the system may become globally unstable. General tests for the necessary and sufficient condition for the stability of a linear time-varying system are presented. Also it is

proved that a second-order almost anti-null operator based on the W-system is BIBO globally stable. The main steps for the design of an almost symmetrical ARMA model are illustrated in Fig.1.2

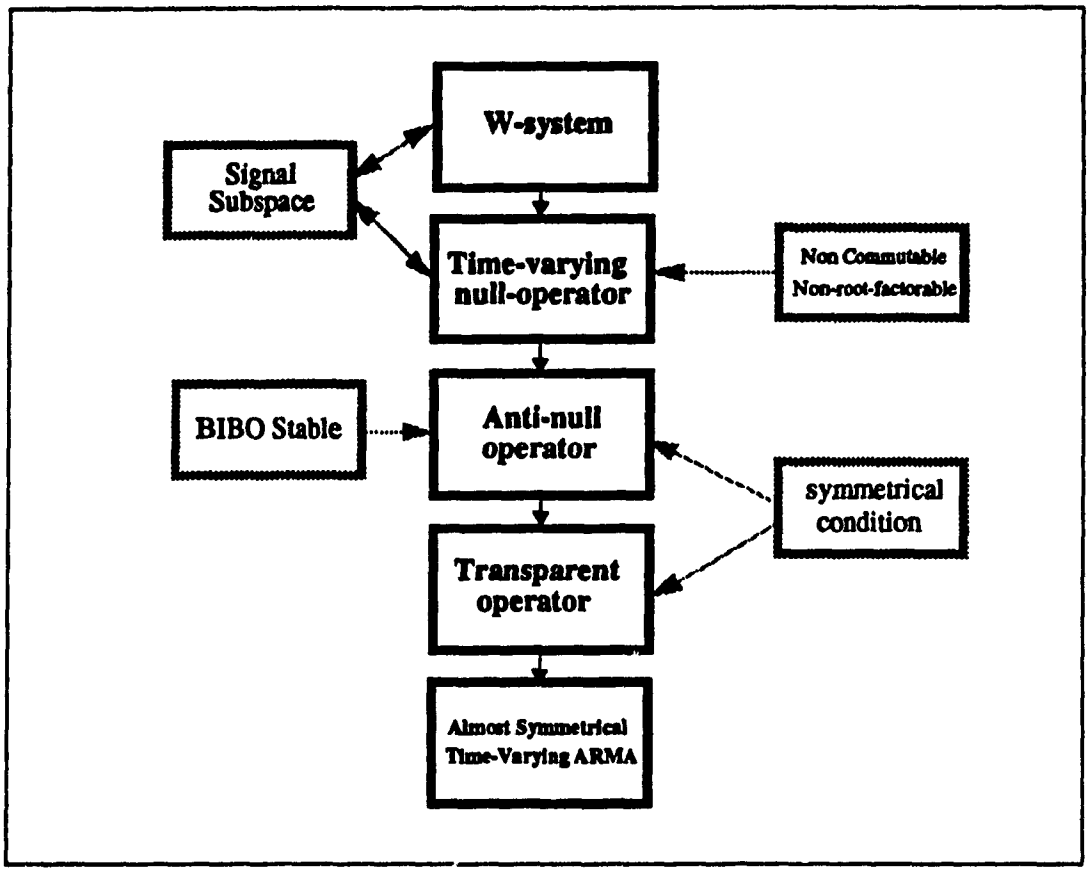

Fig.1.2 Design of ASTV-ARMA Model

Chapters 6 to 8 mainly focus on the applications of the ASTV-ARMA model to the problem of separation of signals with overlapping Fourier spectra (see Fig.1.3).

In Chapter 6, we first study the application of signal separation based on a non-equally spaced sampling technique. By introducing the Dirichlet series expansion, we show that the Fourier spectrum can be transformed into a new desired one by an appropriate choice of the non-equally spaced sampling strategy. It is also shown that the non-equally spaced sampling plays a fundamental role in transforming a time-varying system into another time-varying system or in special cases into a time-

invariant one. Based on this property, we show that it is possible to separate a constant-envelope signal from an arbitrary signal through the non-equally spaced sampling technique. We also investigate the use of phase controlled ASTV-ARMA to separate an FM signal from other signals. A phase perturbation analysis is carried out, and a closed loop scheme is suggested to improve the separation performance. In addition we also carry out a theoretical analysis of the tracking capability of the commonly used adaptive algorithm, the Gauss-Newton algorithm, and show that such an algorithm possesses an inherent threshold effect when applied to track signals with fast time-varying parameters.

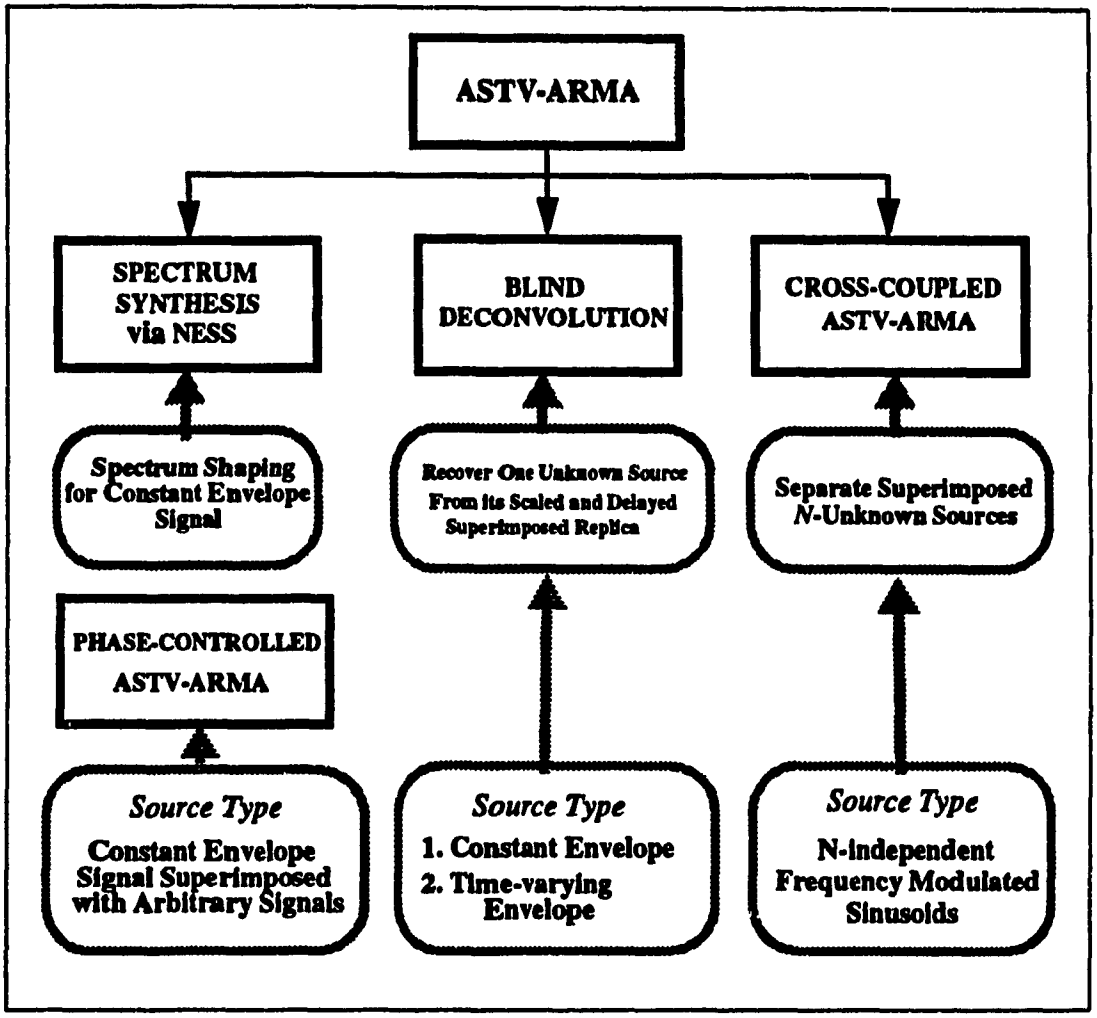

Fig.1.3 Using ASTV-ARMA Model to Separate Signals with Overlapping Fourier Spectra

In Chapter 7, we study the blind deconvolution problem, where one has to estimate

both the unknown source and the channel (whose transfer function is unknown) from the data observed at the channel output, no other auxiliary access to the source being available. Two blind deconvolution schemes, namely the one-sensor scheme and the two-sensor scheme are considered. The proposed blind deconvolution schemes are shown to converge to the desired deconvolution solution. Several examples are presented to show the advantages of using the proposed blind deconvolution algorithm.

In Chapter 8, we present a Cross-Coupled ASTV-ARMA(CC-AA) model and show that such a special structure can be used to separate superimposed frequency modulated sinusoids. The stability of the equilibria of the CC-AA model and its trajectory variation properties are also investigated. Based on these results, we show that CC-AA always converges to the solution resulting in a complete separation of the superimposed FM signals.

Finally, Chapter 9 briefly summarizes the main results in this thesis and points out some future research directions.

1.5. Main Contributions of the Thesis

The main contribution of this thesis is centered around the theory of time-varying almost-symmetrical ARMA models and their applications to the problem of separation of signals with overlapping Fourier spectra.

Basic Properties of Time-Varying Null Operators: The design of a time-varying null-operator and properties of the associated W-system are investigated.

Transparent Operator and Symmetry Condition: It is shown that a transparent operator can be constructed by combining a time-varying null operator and a time-varying anti-null operator. The trade-off between the observation time and transparency of the ASTV-ARMA model is studied.

BIBO Global Stability of Time-Varying Autonomous System: Local instabilities of first and second kind are investigated. Necessary and sufficient tests for global BIBO stability of a linear time-varying system are presented.

Spectrum Synthesis via Non-Equally Spaced Sampling: It is shown that by using non-equally spaced sampling technique, it is possible to transform a linear time-varying system into another time-varying or even time-invariant system; in particular, any constant-envelope frequency varying signal can be transformed into a sinewave with a fixed frequency.

Blind Deconvolution of a Non-Stationary Source: Blind deconvolution of a time-varying parameter source based on a second-order ASTV-ARMA model is proposed; such a model guarantees the unique convergence to the true deconvolution.

Cross-Coupled ASTV-ARMA Model: This system is proposed to separate superimposed sinusoids whose Fourier spectra are completely overlapping. The uniqueness of separation is established.

Many of the results obtained in this thesis have been published in [1.17] [1.21] [1.26][1.27] [1.28] [1.29] [1.30] [1.31].

References

[1.1] A.V. Opennheim and R.W. Schafer,"*Digital Signal Processing*", Prentice-Hall, Eglewood Cliffs, N.J. 1975.

[1.2] E.I. Plotkin and M.N.S. Swamy," Structural Signal Processing-Current Trends", *ASME, Diagnostics, Vehicle Dynamics and Special Topics*, Book No. H0508E, pp. 37-45, Sept. 1989.

[1.3] E.I. Plotkin and M.N.S. Swamy," Nonlinear Signal Processing Based on Parameter Invariant Moving Average", *Proceedings of Canadian Conference of Electrical and Computer Engineering*, Vol. 2, pp. TM3.11.1-4, Sept. 1992

[1.4] E.I. Plotkin, A.M. Zayezdny, L.M. Roytman and M.N.S. Swamy," Simulation of Modulated Signal", *Journal of Franklin Institute*, Vol. 318 No.1, pp. 15-28, July,1984

[1.5] A.M. Zayezdny and I. Druckmann,"A New Method of Signal Description and Its Application to Signal Processing", *Signal Processing*, Vol. 22, pp. 153-178, Feb. 1991

[1.6] S.C. Scoular, I.B. Rogozkin and M.S. Chenykov, " Review of Soviet Research on Linear Time-Variant Discrete System", *Signal Processing*, Vol. 30, pp. 85-101, Jan. 1993

[1.7] E.I. Plotkin and M.N.S. Swamy," Multistage Implementation of Parameter Invariant Null Filter and Its Application to Discrimination of Closely Spaced Sinusoids", *Proceedings of ISCAS88*, pp. 767-770, June, 1988

[1.8] E.I. Plotkin and M.N.S. Swamy," Shift-Invariant Nonlinear Null Filters for Cancellation of AR-Signals with Unknown Parameters", *Proceedings ISCAS87*, pp. 855-858, May, 1987

[1.9] E.I. Plotkin, L.M. Roytman and M.N.S. Swamy," A New Approach to Suppression of Finite Length Pulse Interference Using Modified Linear Predictor", *IEEE Trans. on ASSP*, No.3, pp. 622-629, 1983

[1.10] E.I. Plotkin,"Function Elimination Filters to Reject a N-order Exponential Signal", *Proceedings of the European Conference on Circuits Theory and Design*, pp. 422-427, 1978

[1.11] E.I. Plotkin,"Use of Function Elimination Filters to Reject Quasideterminiatic Interference in ASK-System", *Int. Journal of Circuits Theory and Applications*, Vol. 6, pp. 75-81, 1978

[1.12] L. Kazovsky, E.I. Plotkin and A.M. Zayezdny," Nonlinear Suppression of AR-Impulsive Noise in Binary Communications", *Signal Processing*, Vol. 7, pp. 31-44, 1984

[1.13] E.I. Plotkin,"Notch Filter Based on Identical Building Blocks with Arbitrary Transfer Function", *Int. Journal on Circuits Theory and Applications*, Vol. 1.8, pp. 31-37, 1980

[1.14] E.I. Plotkin,"Using Linear Prediction to Design a Function Elimination Filter to Reject Sinusoidal Interference", *IEEE Trans. ASSP*, Vol. 27, No. 3, pp. 501-506, 1979

[1.15] E.I. Plotkin and D. Wulich,"A Comparative Study of Two Adaptive Algorithms for Suppression of a Narrowband Interference", *Signal Processing*, Vol.4, No.1, Jan. 1982

[1.16] D. Wulich, E.I. Plotkin and M.N.S. Swamy,"Synthesis of Discrete Time-Variant Null Filters for Frequency Varying Signals using Time-Warping Technique", *IEEE Trans. on Circuits and Systems*, Vol.37, pp. 977-990, Aug. 1990

[1.17] D. Wulich, E.I. Plotkin and M.N.S. Swamy and W. Tong,"PLL Synchronized Time-Varying Constrained Notch Filter for Retrieving a Weak Multiple Sine Signal Jammed by FM Interference", *IEEE Trans. on Signal Processing*, Vol. 40, No. 11, pp. 2866-2870, Nov. 1992

[1.18] D. Wulich, E.I. Plotkin and M.N.S. Swamy,"Constrained Notch Filtering of Non-Uniformly Spaced Samples for Enhancement of an Arbitrary Signal Corrupted by a Strong FM Interference", *IEEE Trans. on Signal Processing*, Vol. 39, No. 10, pp. 2359-2363, Oct. 1991

[1.19] E.I. Plotkin, L.M. Roytman and M.N.S. Swamy,"Non-Uniform Sampling of Bandlimited Modulated Signals", *Signal Processing*, Vol. 4, pp. 295-303, 1982

[1.20] E.I. Plotkin and M.N.S. Swamy," Signal Reconstruction from the Non-Equally Spaced

Samples with Application to Jitter Error Reduction and Bandwidth Compression", *Proceedings ISSPA87*, pp. 337-341, Aug. 1987

[1.21] W. Tong, E.I. Plotkin, D. Wulich and M.N.S. Swamy,"Self-Synchronized Signal Controlled Constrained Notch Filter for Rejection of Non-Stationary Interference", *Proceedings ICASSP91*, Vol. 3 pp. 1937-1940, May 1990

[1.22] E.I. Plotkin, M.N.S. Swamy and Y. Yoganandam,"A Novel Iterative Method for the Reconstruction of Signals From Nonuniform Spaced Samples", submitted to *Signal Processing*

[1.23] B.D. Rao and R. Peng,"Tracking Characteristic of the Constrained IIR Adaptive Notch Filter", *IEEE Trans. on ASSP*, Vol. 36, pp. 1466-1479, Sept.1988

[1.24] A. Nehorai," A Minimum Parameter Adaptive Notch Filter with Constrained Poles and Zeros", *IEEE Trans on ASSP*, Vol. 33, pp. 983-996, Aug.1985

[1.25] D. Wulich, E.I. Plotkin and M.N.S. Swamy and W. Tong,"PLL Synchronized Time-Varying Constrained Notch Filter for Retrieving a Weak Multiple Sine Signal Jammed by FM Interference", *IEEE Trans. on Signal Processing*, Vol. 40, No. 11, pp. 2866-2870, Nov. 1992

[1.26] D. Wulich, E.I. Plotkin, M.N.S. Swamy and W. Tong," Externally Controlled Time-Varying Notch Filter", *Proceedings ISCAS91*, pp. 2061-2064, June 1991.

[1.27] W. Tong, E.I. Plotkin, M.N.S. Swamy and D. Wulich,"Closed-Loop Self-Synchronized Signal Controlled Constrained Notch Filter with Application for Rejection of Arbitrary Frequency Variation Speed Sinusoidal Interference", *Proceedings ISCAS91*, pp. 1440-1443, June 1991.

[1.28] Wen Tong, E.I. Plotkin, D. Wulich and M.N.S. Swamy,"Self-Synchronized Signal Controlled Constrained Notch Filter for Rejection of Non-Stationary Interference", Proceedings ICASSP91, pp. 1937-1940, May 1991

[1.29] W. Tong, E.I. Plotkin and M.N.S. Swamy,"Cross-Coupled Constrained Null Filter and Separation of Superimposed Frequency Modulated Sinusoids", *Proceedings ISCAS92*, pp. 1479-1482, May 1992.

[1.30] Wen Tong, D. Wulich, Eugene I. Plotkin and M.N.S. Swamy," Stability of Tow Second Order Time-Varying Constrained Notch Filters with Externally Controlled Coefficients", *Proceedings of Canadian Conference of Electrical and Computer Engineering*, pp. 795-798, Sept. 1990

[1.31] Wen Tong, E.I. Plotkin and M.N.S. Swamy,"Blind Deconvolution of Linear System Driven by Non-Stationary Source Based on Almost-Symmetrical Time-Varying ARMA Model" *Proceedings ISCAS93*, pp. 1479-1482, 1993

[1.32] V.F. Pisarenko,"The Retrieval of Harmonics from a Covariance Fuction", *Geophysical J. Royal Astronomical Soc.* Vol. 33, pp. 347-366, 1973

Chapter 2

Time-Varying Null Operators

2.1. Introduction

In this chapter, we introduce the concept of a time-varying null operator, and its associated signal space. Several basic properties of such a time-varying null-operator are presented. The existence of a time-varying null operator is associated with the positiveness of the Wronskian which defines the geometrical properties of the signal subspace, and hence the properties of the signals under analysis.

It is shown that in many cases, time-varying models based on the proposed time-varying null operators is much more efficient than the conventional time-invariant ones.

2.2. Preliminaries

In 1815, the Polish Mathematician *Hoene Wronski* published his celebrated memoir *"Philosophie de la Technie Algorithmique"*, where he gave the following fundamental result (as presented in [2.1])

Let $\{\varphi_i(t)\}_{i=1}^{N}$ $t \in \Re$, *be a system of any N functions which are continuous together with their first (N-1) derivatives. The necessary and sufficient*

condition for such a system of functions $\{ \varphi_1(t), \varphi_2(t), \ldots \varphi_N(t) \}$ *to be the linear independent solutions of a homogeneous equation is that the following determinant*

$$W^N_{\frac{d}{dt}}(\varphi_1(t), \varphi_2(t), \ldots, \varphi_N(t)) = \begin{vmatrix} \varphi_1(t) & \varphi_2(t) & \ldots & \varphi_N(t) \\ \varphi'_1(t) & \varphi'_2(t) & \ldots & \varphi'_N(t) \\ \ldots & \ldots & \ldots & \ldots \\ \varphi_1^{[N-1]}(t) & \varphi_2^{[N-1]}(t) & \ldots & \varphi_N^{[N-1]}(t) \end{vmatrix} \neq 0 \qquad (2.2.1)$$

be non-vanishing at any instant $t \in \Re$

Such a determinant $W^N_{\frac{d}{dt}}(\varphi_1(t), \varphi_2(t), \ldots, \varphi_N(t))$ is called the *Nth-order Wronskian* with respect to the base operation $\frac{d}{dt}$.

In 1880, *F. Casorati* [2.2] presented a discrete version of the Wronskian for a system of discrete functions $\{\varphi_i(k)\}_{i=1}^N$, $k \in Z^+$

$$W^N_D(\varphi_1(k), \varphi_2(k), \ldots, \varphi_N(k)) = \begin{vmatrix} \varphi_1(k) & \varphi_2(k) & \ldots & \varphi_N(k) \\ D\varphi_1(k) & D\varphi_2(k) & \ldots & D\varphi_N(k) \\ \ldots & \ldots & \ldots & \ldots \\ D^{N-1}\varphi_1(k) & D^{N-1}\varphi_2(k) & \ldots & D^{N-1}\varphi_N(k) \end{vmatrix} \neq 0 \quad \forall k \in Z^+ \qquad (2.2.2)$$

where D *denotes a shift operator,* $D^m \varphi_i(k) = \varphi_i(k-m)$.

Later, *Bortolotti* [2.2] extended this idea to a very general functional setting. He stated:

If $\{\varphi_i(t)\}_{i=1}^N$ *be a system of analytic functions having a common domain of convergence, and* O *be a one-to-one mapping functional operation, the necessary and sufficient condition for such a system of functions being associated with a homogeneous equation with coefficients with respect to* O *is*

$$W^N_O(\varphi_1(t), \varphi_2(t), \ldots, \varphi_N(t)) = \begin{vmatrix} \varphi_1(t) & \varphi_2(t) & \ldots & \varphi_N(t) \\ O\varphi_1(t) & O\varphi_2(t) & \ldots & O\varphi_N(t) \\ \ldots & \ldots & \ldots & \ldots \\ O^{N-1}\varphi_1(t) & O^{N-1}\varphi_2(t) & \ldots & O^{N-1}\varphi_N(t) \end{vmatrix} \neq 0 \qquad (2.2.3)$$

These three results, provide a concrete base for the theory of linear equations and a

mathematical tool for linear signal processing.

It is well known that for a system of N linearly independent functions $\{ \varphi_1(t), \varphi_2(t), \ldots \varphi_N(t) \}$ there exists ***a unique monic homogeneous equation*** of order N given by

$$Q_o(x) \equiv \frac{W_o^{N+1}(\varphi_1(t), \varphi_2(t), \ldots, \varphi_N(t), x(t))}{W_o^N(\varphi_1(t), \varphi_2(t), \ldots, \varphi_N(t))} = 0 \tag{2.2.4}$$

where, W_o^{N+1} is an augmented Wronskian. Such a homogeneous equation also defines a linear operator $Q_o(x)$. Choosing different base operators will result in different operators $Q_o(x)$: for example, Wronski used the differential operator, while Casarati chose a shift operator. Such an operator can be explicitly expressed as a linear homogeneous equation in the form

$$\left[1 + a_1(t) O + a_2(t) O^2 + \ldots + a_N(t) O^N\right] x(t) = 0 \tag{2.2.5}$$

where

$$a_l(t) = (-1)^{l+1} \frac{M_o^N(\varphi_1(t), \varphi_2(t), \ldots, \varphi_l(t), \varphi_{l+1}(t), \ldots, \varphi_N(t))}{W_o^N(\varphi_1(t), \varphi_2(t), \ldots, \varphi_N(t))}$$

and $M_o^N(\ldots)$ is the minor of W_o^{N+1} with respect to the Laplace expansion of $x(t)$.

Bortolotti's result is of special interest, since it provides a mathematical support to the so called ***structural signal processing***, where the operator O can be treated as an arbitrarily chosen building block. This thesis is an attempt to extend this concept to time-varying structural signal processing. Throughout this thesis, we restrict ourselves to the *linear time-varying discrete equation* [1], and the operator O is the delay operator D. In this case, the linear time-varying operator is expressed as the homogenous equation

$$\boxed{[1 + a_1(k) q^{-1} + a_2(k) q^{-2} + \ldots + a_N(k) q^{-N}] x(k) = 0} \tag{2.2.6}$$

1. By time-varying we also mean shift-variant.

Although in discrete-time situation, the determinant $W_D^N(\varphi_1(k), \varphi_2(k), ..., \varphi_N(k))$ is called Casaratian, in view of Wronski's earlier discovery, in this thesis we term this discrete determinant as Wronskian.

Note that the *Wronskian* $W^N(k)$ is a positive function[1], i.e. $\text{sgn}\{W^N(k)\} = Const \quad \forall k \in Z^+$. The system of functions $\{\varphi_i(k)\}_{i=1}^N$ which constitute the Wronskian is called a ***Wronskian system of functions***, and the elements of the ***W-matrix*** are formed by the elements of the Wronskian, and is denoted as $[W^N(k)]$.

Following two lemmas can be found in [2.1], and we restate them here, without proof, for the time-varying situation.

Lemma 2.2.1 *If the Wronskian is a positive function, then there exists a unique linear homogeneous equation whose fundamental solution is a W-system of functions.*

Lemma 2.2.2 *Given a linear homogeneous equation, one can find a system of fundamental solutions such that the Wronskian of this system of functions constitute a positive function.*

An *Nth*-order ***time-varying null operator*** is defined by the homogeneous equation (2.2.6). A linear span of W-system of functions $\{\varphi_i(k)\}_{i=1}^N$ constitutes an N-dimensional ***signal space***. Such a signal space is a ***null singularity*** of the time-varying null operator.

From Lemmas 2.2.1, and2.2.2, we can see that the time-varying null operator and the associated signal space are uniquely determined.

2.3. Basic Properties of W-System of Functions and Null Operator

In what follows, we present several basic properties of W-system of functions, and

1. A function is called positive, iff its sign remains unchanged over the entire observation time.

its associated null operator.

Proposition 2.3.1 *The order N of a W-system of periodic functions* $\{\varphi_i(k)\}_{i=1}^{N}$ *must be even.*

Proof: Let $\varphi_i(k) = \varphi_i(k-N+1) \quad i = 1, 2, \ldots, N$

Then for odd N the determinant $W^N(k)$ changes sign

$$\begin{vmatrix} \varphi_1(k) & \varphi_2(k) & \cdots & \varphi_N(k) \\ \varphi_1(k-1) & \varphi_2(k-1) & \cdots & \varphi_N(k-1) \\ \cdots & \cdots & \cdots & \cdots \\ \varphi_1(k-N+1) & \varphi_2(k-N+1) & \cdots & \varphi_N(k-N+1) \end{vmatrix} = - \begin{vmatrix} \varphi_1(k-N+1) & \varphi_2(k-N+1) & \cdots & \varphi_N(k-N+1) \\ \varphi_1(k-1) & \varphi_2(k-1) & \cdots & \varphi_N(k-1) \\ \cdots & \cdots & \cdots & \cdots \\ \varphi_1(k) & \varphi_2(k) & \cdots & \varphi_N(k) \end{vmatrix}$$

Q.E.D.

In particular, the order of the Wronskian for sinusoidal signals must be even.

Proposition 2.3.2 *[Szeago]* [2.4]*The order N of an orthogonal polynomial W-system of functions must be even.*

Proposition 2.3.3 *If the last coefficient of an Nth-order null operator is given as* $a_N(k) = (-1)^N$, *then such a null operator is time-invariant and the Wronskian associated with this null operator is time-invariant.*

Proof: By (2.2.5), if $a_N(k) = (-1)^N$, then $W^N(k) = W^N(k-1) = W^N$, the Wronskian is a constant, and shift-invariant. The following minors are shift invariant too

$$\left| \varphi_i(k) \ \ldots \ \varphi_i(k-l) \ \varphi_i(k+l) \ \ldots \ \varphi_i(k) \right|_{i=1}^{N} = \tilde{W}_l^N$$

and thus the coefficients are shift invariant

$$a_l(k) = (-1)^l \frac{\tilde{W}_l^N}{W^N} = a_l \qquad \forall k \in Z^+$$

Q.E.D.

Certainly, if a Wronskian is time-varying, its associated null operator is time-

varying too.

Proposition 2.3.4 *If the Wronskian of a system of functions* $\{\varphi_i(k)\}_{i=1}^{N}$ *is of a fixed value, the coefficients of the Nth-order null operator are mirror symmetric or anti-symmetric:*

$$a_l(k) = (-1)^N a_{N-l}(k) \qquad l = 1, 2, \ldots [N/2]$$

where [ ] *denotes the nearest integer.*

Proof: Since a Wronskian is a fixed value, i.e. time-invariant, the null operator remain the same if we *inverse the time direction* $k' = -k$

$$W^N(k) = W^N(-k) \qquad \forall k \in Z^+ \tag{2.2.7}$$

The coefficients of the null operator can be written as

$$a_l(k) = (-1)^l \frac{\tilde{W}_l^N(k)}{W^N(k)} \tag{2.2.8}$$

where

$$\tilde{W}_l^N(k) = \begin{vmatrix} \varphi_1(k) & \varphi_2(k) & \cdots & \varphi_N(k) \\ \cdots & \cdots & \cdots & \cdots \\ \varphi_1(k-l+1) & \varphi_2(k-l+1) & \cdots & \varphi_N(k-l+1) \\ \varphi_1(k-l-1) & \varphi_2(k-l-1) & \cdots & \varphi_N(k-l-1) \\ \cdots & \cdots & \cdots & \cdots \\ \varphi_1(k-N) & \varphi_2(k-N) & \cdots & \varphi_N(k-N) \end{vmatrix} \tag{2.2.9}$$

In the reversed time, we have

$$\tilde{W}_{ll}^N(-k) = \begin{vmatrix} \varphi_1(-k) & \varphi_2(-k) & \cdots & \varphi_N(-k) \\ \cdots & \cdots & \cdots & \cdots \\ \varphi_1(-k+l-1) & \varphi_2(k+l-1) & \cdots & \varphi_N(k+l-1) \\ \varphi_1(-k+l+1) & \varphi_2(k+l+1) & \cdots & \varphi_N(k+l+1) \\ \cdots & \cdots & \cdots & \cdots \\ \varphi_1(-k+N) & \varphi_2(-k+N) & \cdots & \varphi_N(-k+N) \end{vmatrix} = \tilde{W}_{N-l}^N(k) \tag{2.2.10}$$

Therefore,

$$a_{N-l}(k) = (-1)^{N-l}\frac{\tilde{W}^N_{N-l}(k)}{W^N(k)} = (-1)^{N-l}\frac{\tilde{W}^N_l(-k)}{W^N(-k)} = (-1)^N a_l(k)$$

Q.E.D.

Proposition 2.3.5 *The eigenvalue functions of the W-matrix should be positive, and the W-system of functions is congruent to unitary transformation (which means that the Wronskian is invariant to a transformation of the coordinate system)*

Proof: Denoting a W-matrix as $W^N(k)$, let U U^* be $N \times N$ matrices, such that $UU^* = U^*U = I$. Let $\lambda_1(k), \lambda_2(k), \ldots, \lambda_N(k)$ be the eigen values of the W-matrix $[W^N(k)]$. Suppose by applying a unitary transformation, we have a new W-matrix

$$[W^N(k)]^* = U[W^N(k)]U^* = \begin{bmatrix} \lambda_1(k) & & 0 \\ & \ldots & \\ 0 & & \lambda_N(k) \end{bmatrix}$$

Thus $det[W^N(k)]^* = \lambda_1(k)\lambda_2(k)\ldots\lambda_N(k)$. It is well known that

$$det[W^N(k)] = \lambda_1(k)\lambda_2(k)\ldots\lambda_N(k)$$

Therefore $det[W^N(k)]^* = det[W^N(k)]$, and $\lambda_l(k) \neq 0 \quad l = 1, 2\ldots N$ which means no eigenvalue function $\lambda_l(k)$ changes the sign.

Q.E.D.

Proposition 2.3.6 *If $\chi(s)$ is an arbitrary continuous monotonic function on $[\tau_1,\tau_2]$, $\chi(\tau_1) = a$ and $\chi(\tau_2) = b$, then the time transformation $t = \chi(s)$ transforms the W-system of functions $\{\varphi_i(k)\}_{i=1}^N$ on $[a,b]$ into a new W-system of functions $\{\varphi_i(\chi(s))\}_{i=1}^N$ on $[\tau_1,\tau_2]$.*

Proof: This property can be proved by directly invoking the continuity argument of functions[2.5]. It is not difficult to see that the Wronskian of the new system of functions remains positive.

Q.E.D.

Proposition 2.3.7 *There exists a time warping function* $\chi(s)$, *which is a continuous monotonic function on* $[\tau_1,\tau_2]$, *that transforms a time-varying Wronskian on* $[a,b]$ *into a new time-invariant Wronskian,*

$$W_D^N(\varphi_1(\chi(s)), \varphi_2(\chi(s)), \ldots, \varphi_N(\chi(s))) = Constant$$

Proof: Consider the integral of the positive function $W^N(t)$ as

$$\int_{s_k}^{s_{k+1}} W^N(t)\,dt = Const$$

such that there exists a one-to-one correspondence between $\{1, 2, \ldots\}$ and $\{s_1, s_2, \ldots\}$; thus a time-transformation $t = \chi(s)$ can be established, which will transform the Wronskain $W^N(t)$ into a constant. *Q.E.D.*

This indicates that using the transformation $t = \chi(s)$, one can convert a certain time-varying null operator into another *new time-varying null operator*; more interestingly, through such a transformation, a time-varying null operator can be converted into a *time-invariant* one. We will further explore this property in Chapter 6, to show using a non-equally spaced sampling strategy to convert a time-varying null operator into a time-invariant one.

2.4. Wronskian and the Order of Signals

Definition 2.5.1 If a signal $x(k)$ can be uniquely expressed as a linear combination of a W-system of functions $\{\varphi_i(k)\}_{i=1}^N$, then such a signal is called an *Nth-order signal.*

Example 1 *All bounded positive finite interval functions* $x(k) > 0 \quad \forall k \in [0,N]$ *are 1st-order signals.*

Proof: The 1st-order Wronskian $W^1(k) = x(k-1) > 0$

Q.E.D.

Example 2 *Sinusoidal function* $\sin(\psi(k) + \phi_0)$, $k \in Z^+$ *is a 2nd-order signal.*

Proof: The 2nd-order Wronskain $W^2(k) = \sin(\psi(k) - \psi(k-1)) > 0$. Here the instantaneous frequency of the sinusoid should be positive and satisfy the Nyquest criterion, i.e. $0 < \psi(k) - \psi(k-1) < \pi$

Q.E.D.

Example 3 Consider an FM signal $s(k) = \sin\psi(k)$, its instantaneous frequency is a single tone modulated one, i.e.

$$\psi(k) = \omega_o k + \frac{\Delta\omega}{\omega_m}\sin(\omega_m k)$$

By using the first-kind Bessel function $J_n(\ )$

$$s(k) = e^{j\omega_o k}\sum_{l=-\infty}^{\infty} J_n\left(\frac{\Delta\omega}{\omega_m}\right) e^{jlk\omega_o}$$

Such an FM signal can be represented by a time-invariant null operator of an infinite order

$$\aleph = \prod_{l=1}^{\infty}\left[1 - 2\cos(l\omega_m)\,q^{-1} + q^{-2}\right]$$

On the other hand, as shown in Chapter 6, an FM signal can be represented by using only *a second order time-varying null operator*

$$\aleph_k = 1 - \frac{\sin[\psi(k) - \psi(k-2)]}{\sin[\psi(k-1) - \psi(k-2)]}q^{-1} + \frac{\sin[\psi(k) - \psi(k-1)]}{\sin[\psi(k-1) - \psi(k-2)]}q^{-2}$$

Thus the order of a signal may be drastically reduced by using time-varying systems.

2.5. W-System of Functions and Associated Span of Signal Subspace

Let us consider a W-system of functions that spans a signal space, then we have the following properties of a Wronskian.

Lemma 2.4.1 *The Nth-order Wronskian is the square root measure of the volume of the N-dimensional parallelogram signal space spanned by the W-system of functions.*

Proof: $\Phi_l(k) = \left[\varphi_l(k)\ \varphi_l(k-1)\ \ldots\ \varphi_l(k-N+1)\right]^T$, $l = 1, 2, \ldots, N$, and thus the W-

matrix can be written as

$$[W^N(k)] = \left[\vec{\Phi}_1(k)\ \vec{\Phi}_2(k)\ \ldots\ \vec{\Phi}_N(k)\right]$$

Consider the Gramian matrix given by

$$G(k) = [W^N(k)]\,[W^N(k)]^T = \begin{bmatrix} \langle\vec{\Phi}_1(k)|\vec{\Phi}_1(k)\rangle & \langle\vec{\Phi}_1(k)|\vec{\Phi}_2(k)\rangle & \ldots & \langle\vec{\Phi}_1(k)|\vec{\Phi}_N(k)\rangle \\ \langle\vec{\Phi}_2(k)|\vec{\Phi}_1(k)\rangle & \langle\vec{\Phi}_2(k)|\vec{\Phi}_2(k)\rangle & \ldots & \langle\vec{\Phi}_2(k)|\vec{\Phi}_N(k)\rangle \\ \ldots & \ldots & \ldots & \ldots \\ \langle\vec{\Phi}_N(k)|\vec{\Phi}_1(k)\rangle & \langle\vec{\Phi}_N(k)|\vec{\Phi}_1(k)\rangle & \ldots & \langle\vec{\Phi}_N(k)|\vec{\Phi}_N(k)\rangle \end{bmatrix}$$

where $\langle\ |\ \rangle$ denotes an inner product

$$det(G(k)) = [det(W^N(k))]^2$$

It is well known that the Gramian $det(G(k))$ is the volume of a parallelogram spanned by the vectors $\vec{\Phi}_1(k), \vec{\Phi}_2(k) \ldots \vec{\Phi}_N(k)$, see Fig.2.1, thus the Wronskian $W^N(k)$ is the square-root of the volume of the parallelogram of the signal subspace.

Q.E.D.

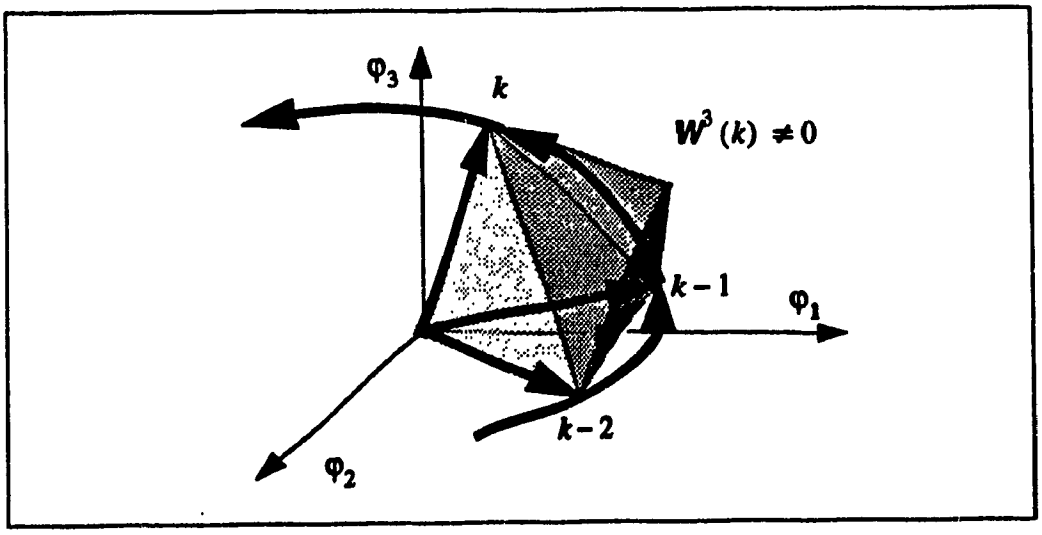

Fig.2.1 The Volume of a Parallelogram of a Signal Subspace

In the case where the Wronskian is time-varying, Lemma 2.4.1 implies that the volume of the signal subspace is constantly expanding or contracting. However, if there

exist a time-varying null operator representing such a signal subspace, the value of the volume of the subspace should never vanish, i.e. the subspace does not collapse to an *(N-1)* or less dimensional space. Especially, in the case of a 2nd-order W-system of functions, the Wronskian or the volume of the signal subspace is equivalent to the so called *frequency weighted energy.*

Lemma 2.4.2 *Wronskian is the square-root measure of the generalized local covariance of the signal subspace.*

$$Cov(\vec{\Phi}_l, \vec{\Phi}_m) = \frac{1}{N-1} d^2(\vec{\Phi}_l(k), \vec{\Phi}_m(k))$$

where $d^2(\vec{\Phi}_l(k), \vec{\Phi}_m(k)) = \langle \vec{\Phi}_l(k) - \vec{\Phi}_m(k) | \vec{\Phi}_l(k) - \vec{\Phi}_m(k) \rangle$

Proof: Consider the Gramian of two vectors; we have

$$[\vec{\Phi}_l(k), \vec{\Phi}_m(k)][\vec{\Phi}_l(k), \vec{\Phi}_m(k)]^T = \begin{bmatrix} \langle \vec{\Phi}_l(k) | \vec{\Phi}_l(k) \rangle & \langle \vec{\Phi}_m(k) | \vec{\Phi}_l(k) \rangle \\ \langle \vec{\Phi}_l(k) | \vec{\Phi}_m(k) \rangle & \langle \vec{\Phi}_m(k) | \vec{\Phi}_m(k) \rangle \end{bmatrix}$$

$$= \| \vec{\Phi}_l(k) \|_2 + \| \vec{\Phi}_m(k) \|_2 - 2\langle \vec{\Phi}_l(k) | \vec{\Phi}_m(k) \rangle$$

Since $d^2(\vec{\Phi}_l(k), \vec{\Phi}_m(k)) = = \| \vec{\Phi}_l(k) \|_2 + \| \vec{\Phi}_m(k) \|_2 - 2\langle \vec{\Phi}_l(k) | \vec{\Phi}_m(k) \rangle$, it is clear that the second order Wronskian is the square root of a local generalized covariance of two functions $[\vec{\Phi}_l(k), \vec{\Phi}_m(k)]$. This can be easily extended to the case of an Nth-order Wronskian.

Q.E.D.

2.6. Some Geometrical Meanings Related to W-System of Functions

In this section, we interpret the properties of a W-system of functions by its geometrical meaning, especially by exploring the inherent relationship between the signal subspace decomposition and its geometrical properties. We use some classical results in function theory and give interpretation from the point of view of signal

processing.

Denote a Wronskian curve Λ, in the N-dimensional Euclidean space as

$$\Lambda(k) = \{\varphi_1(k), \varphi_2(k), ..., \varphi_N(k)\} \in \Re^{N \times N}$$

Then the following properties hold and the proofs may be found in Ref. [2.3].

Proposition 2.6.1 *[Gantmacher + Krein][2.3] For a W-System of functions, the curve Λ associated with such a system of functions in the N-dimensional space is a convex one.*

Proposition 2.6.2 *[Riesz] [2.3]The smallest closed convex hull $\wp$ of a convex curve Λ constitutes a set of points $C = [c_1\ c_2\ ...c_N]$ which admitting the generalized moment representation*

$$c_k = \int_0^N \varphi_1(t)\, d\sigma(t) \qquad k = 1, 2...N$$

where $\sigma(t)$ is a distribution function in the Stieltjes integral sense

$$\int_0^N d\sigma(t) = 1$$

This property is very interesting one, since the time-varying volume of the signal subspace is associated with the time-varying null operator, while the smallest volume is the convex hall given by proposition 2.6.2. Considering the Proposition 2.3.7 and 2.3.8 together, the above result implies that there exists a certain distribution function $\sigma(t)$ to transform the time-varying volume of a signal subspace into a time-invariant one.

Proposition 2.6.3 *[Minkovski] [2.3]Any point C, which is exterior to a convex body $\wp$ can be separated from $\wp$ by a hyperplane.*

Proposition 2.6.4 *[2.3]The curve Λ does not intersect itself and no hyperplane intersects such a curve more that N times.*

Theorem 2.6.1 *There exists a unique time-varying null operator with respect to a particular convex body in N- dimensional space, this null operator annihilates such*

a convex body.

Proof: By Propositions 2.6.1, and 2.6.2, it is seen that for a convex body in an N-dimensional space, there must exist a shortest convex curve on such a convex body, such that the coordinates of this curve constitute a W-system of functions. Then by Lemma 2.2.2, a unique time-varying null operator can be constructed based on this W-system of functions; therefore, such a signal subspace or convex body constitutes a null singularity to the time-varying null operator.

Q.E.D.

Corollary 2.6.1 *Two signal subspaces which represent two different time-varying null operators must be represented by convex bodies which are separable by a hyperplane*

Proof: By Proposition 2.6.3 and Proposition 2.6.4, we see that any signal which does not fall into the span of a signal subspace, may by geometrically separated by a hyperplane. That is such a signal is not the null singularity of the time-varying null operator. Therefore, it is true that the two signal subspaces in the N-dimensional space are separable by a hyperplane.

Q.E.D.

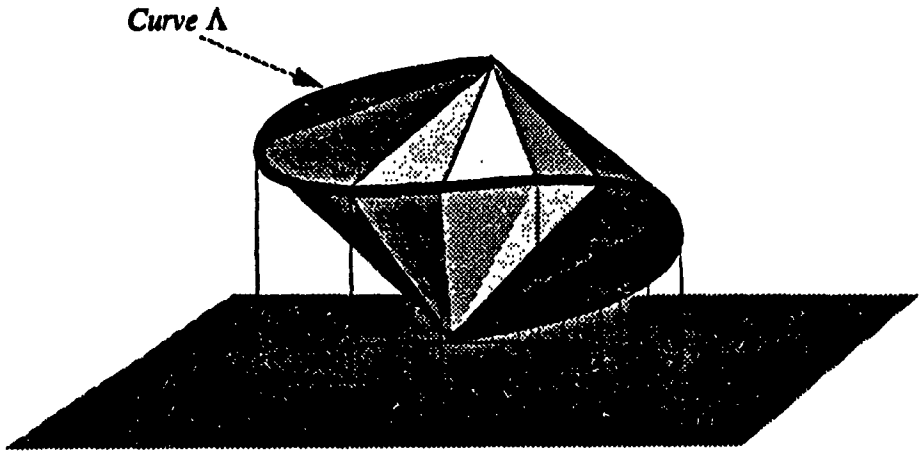

Fig.2.2 A Signal Subspace is a Convex Body in N-D Space

Corollary 2.6.1 gives a geometrical explanation as to why and what kind of signals can be separated by using time-varying null operators. Fig. 2.2 highlights this explanation.

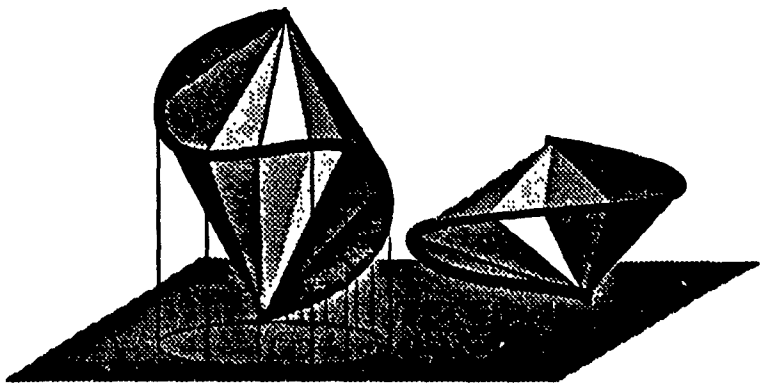

Fig.2.3 Two Separable Signal Subspaces

References

[2.1] W. Hurewicz, "*Lectures on Ordinary Differential Equtions*", John Wiley & Sons, Inc., New York, 1958

[2.2] T. Muir, "*Theory of Determinants*", Volume 1-4, Dover Publications, Inc. New York, 1906

[2.3] M.G. Krein, "The Ideas of Chebysev and Markov in the Limiting Values of Integrals and their Developments", *Translations of American Mathematical Society*, Vol.64 pp.1-122, 1968

[2.4] G. Szego, "*Collected Papers*" Volume 3, (1945-1972) R.Askey.Ed, Birkhauser, 1982

[2.5] C.Caratheodory," *Theory of Functions*", Chelesa Publisher Company, 1958

Chapter

3

Higher-Order Time-Varying Null Operator

3.1. Introduction

In this chapter, we study Higher-Order Time-Varying (HOTV) Null Operators. It is shown that a HOTV null operator can be designed based on lower-order null operators. This is accomplished by decomposing the higher dimensional Wronskian into a set of lower order Wronskians; each lower order Wronskian is associated with a certain subspace of the W-system of functions of the corresponding HOTV null operator. Two algorithms for decomposing a higher dimensional Wronskian are discussed, one is the Choi-McMillan pivot-condensing algorithm, while the other is the Sylvester pivot-growing algorithm.

The decomposition of a HOTV null operator has two major differences compared to its time-invariant counterpart: (1) the non-applicability of root-factorization for decomposing a HOTV null operator *(non-factorable)*; (2) the non-commutability with any other time-varying or time-invariant null operator (*non-commutable*).

In light of non-factorable and non-commutable properties of a HOTV null operator, difference between slow-time-varying and fast-time-varying system can be clarified.

3.1.1. Preliminaries on the Decomposition of Signal Space

In what follows, we discuss the decomposition of the signal space defined by a W-system. As discussed in Chapter 2, an *Nth*-order W-system of functions defines an *N*-dimensional signal space Ω_N, which is associated with an *Nth*-order time-varying null operator $\aleph^{(N)}$. Let us consider an *Nth*-order W-system $W^N\{\varphi_1(k) \ldots \varphi_N(k)\}$. It is well known that choosing any $M(<N)$ functions from such a W-system, one may organize a subsystem of linear independent functions (LIF) to span a subspace Ω_1^M. The remaining LIFs of this W-system of functions may constitute another subspace Ω_2^{N-M} with dimension *(N-M)*

$$\Omega_1^M \cup \Omega_2^{N-M} = \Omega_N \,, \quad \Omega_1^M \cap \Omega_2^{N-M} = \varnothing$$

where Ω_N represents a complete set, i.e. $\Omega_1^M \oplus \Omega_2^{N-M} = \Omega_N$ where $\oplus$ represents the direct sum. Then the signal space is partitioned into two subspaces. Notice that the choice of the LIFs to construct a subspace is *arbitrary*. However, under the principle of structural signal processing, we impose a certain structure on the subspace: the subsystem of LIFs constitute a *signal subspace*, i.e. the Wronskain of such a signal subspace ought to exist, and thus there exists a time-varying null operator associated with a chosen signal subspace.

Hence, by *signal space decomposition,* we mean that for an *Nth*-order W-system of functions *(i.e. N*-dimensional signal space), there exists a particular set of *M* LIFs, which constitute a W-System of functions with a dimension $M < N$.

Example 3.1 Given two sinusoidal signals $s_1(k) = \sin\psi_1(k)$ and $s_2(k) = \sin\psi_2(k)$ with different frequencies $\psi_1(k) - \psi_1(k-1) \neq \psi_2(k) - \psi_2(k-1)$. Denoting $\bar{s}_1(k) = \cos\psi_1(k)$ and $\bar{s}_2(k) = \cos\psi_2(k)$, it can be shown that

$$W^4(s_1(k), \bar{s}_1(k), s_2(k), \bar{s}_2(k)) > 0$$

Thus, $\{s_1(k), \bar{s}_1(k), s_2(k), \bar{s}_2(k)\}$ constitutes a W-system of functions. However, one may check that only $\{s_1(k), \bar{s}_1(k)\}$ and $\{s_2(k), \bar{s}_2(k)\}$ represent the subset of LIF. with the Wronskians

$$\sin(\psi_1(k) - \psi_1(k-1)) > 0, \quad \sin(\psi_2(k) - \psi_2(k-1)) > 0$$

Since the phases $\psi_1(k)$ and $\psi_2(k)$ are independent, the determinant

$W^2(s_1(k), s_2(k)) = \sin(\psi_1(k) - \psi_2(k-1))$ is not guaranteed to be positive, therefore such a determinant can not be a Wronskian. $\{s_1(k), s_2(k)\}$ can constitute a signal subspace, because $\sin\psi_1(k)$, $\cos\psi_2(k)$ can not be the solutions of the same second order linear homogeneous equation.

3.2. Design of A Higher-Order Null Operator

Suppose that the fundamental solution of an *Nth*-order homogenous equation with time-varying coefficients is given as

$$\{ \varphi_1(k), \varphi_2(k), \ldots \varphi_N(k) \} \tag{3.2.1}$$

As already shown in Chapter 2, the time-varying null operator can be constructed by using an augmented $(N+1) \times (N+1)$ Wronskian:

$$W_{aug}^{N+1} = \begin{vmatrix} \varphi_1(k) & \varphi_2(k) & \ldots & \varphi_N(k) & x(k) \\ \varphi_1(k-1) & \varphi_2(k-1) & \ldots & \varphi_N(k-1) & x(k-1) \\ \ldots & \ldots & \ldots & \ldots & \ldots \\ \varphi_1(k-N) & \varphi_2(k-N) & \ldots & \varphi_2(k-N) & x(k-N) \end{vmatrix} = 0 \tag{3.2.2}$$

Equation (3.2.2) means that a signal vector $X(k) = \left[x(k) \ \ldots \ x(k-N)\right]^T$ falls into an N-dimensional subspace spanned by the independent basis $\{ \varphi_1(k), \ldots, \varphi_N(k) \}$ where $\forall l \in \{1, 2, \ldots, N\}$. Such a signal vector $X(k)$ will be cancelled by an *Nth*-order time-varying null operator which is associated with the signal subspace. Moreover, the *Nth*-order time-varying null operator can be expressed as a linear homogeneous equation

$$x(k) + a_1(k)x(k-1) + \ldots + a_N(k)x(k-N) = 0 \tag{3.2.3}$$

For convenience of presentation, we denote,

$$P\begin{pmatrix} i_1 & i_2 & \ldots & i_p \\ k_1 & k_2 & \ldots & k_p \end{pmatrix} = \begin{vmatrix} \varphi_{i_1}(k-1) & \varphi_{i_2}(k-1) & \ldots & \varphi_{i_p}(k-1) \\ \varphi_{i_1}(k-2) & \varphi_{i_2}(k-2) & \ldots & \varphi_{i_p}(k-2) \\ \ldots & \ldots & \ldots & \ldots \\ \varphi_{i_1}(k-p) & \varphi_{i_2}(k-p) & \ldots & \varphi_{i_p}(k-p) \end{vmatrix}$$

By using direct minor expansion of the augmented Wronskian W_a^{N+1}, along with the last column of (3.2.2), the coefficients of the time-varying null operator are explicitly given as

$$a_i(k) = (-1)^{i+k} \frac{P^N\begin{pmatrix} i_1\ i_2 \cdots i_{i-1}\ i_{i+1} \cdots i_N \\ k_0\ k_1 \cdots k_{i-1}\ k_{i+1} \cdots k_N \end{pmatrix}}{W^N\begin{pmatrix} i_1\ i_2 \cdots i_N \\ k_1\ k_2 \cdots k_N \end{pmatrix}} \qquad i = 1, 2, \ldots, N \tag{3.2.4}$$

In what follows, we present two algorithms which allows us to express an *Nth*-order determinant using lower order determinants. Such a decomposition leads us to an efficient approach for the design of higher dimensional Wronskians by using ones with low dimensions. It will be seen that the decomposition of a higher-order determinant into lower-order determinants will not only reduce the computational burden, but also provides a key for the decomposition of higher order time-varying null operators into lower-order ones.

3.2.1. Choi-McMillan Pivot-Condensing Algorithm [3.1]

The idea of pivot-condensing algorithm is to find an iterative procedure to reduce the dimension of the determinants. This can be accomplished by organizing certain sub-determinants as elements of a new determinant such that after every iteration the dimension of determinant is reduced by one. To be more precise, let us consider following Wronskain of order N

$$W^N = \begin{vmatrix} \varphi_{11} & \varphi_{12} & \cdots & \varphi_{1,N} \\ \varphi_{21} & \varphi_{22} & \cdots & \varphi_{2,N} \\ \cdots & \cdots & \cdots & \cdots \\ \varphi_{N,1} & \varphi_{N,2} & \cdots & \varphi_{N,N} \end{vmatrix} \tag{3.2.5}$$

After first iteration, we have a new determinant W^{N-1} with dimension of $(N-1)$

$$W^{N-1} = \begin{vmatrix} \varphi_{11}^{(1)} & \varphi_{12}^{(1)} & \cdots & \varphi_{1,n-1}^{(1)} \\ \varphi_{21}^{(1)} & \varphi_{22}^{(1)} & \cdots & \varphi_{2,n-1}^{(1)} \\ \cdots & \cdots & \cdots & \cdots \\ \varphi_{n-1,1}^{(1)} & \varphi_{n-1,2}^{(1)} & \cdots & \varphi_{n-1,n-1}^{(1)} \end{vmatrix} \tag{3.2.6}$$

where the elements of Wronskian W^{N-1} is given as

$$\varphi_{i,j}^{(1)} = (\varphi_{i,j}\varphi_{i+1,j+1} - \varphi_{i,j+1}\varphi_{i+1,j})$$

After second iteration, the new Wronskian becomes

$$W^{N-2} = \begin{vmatrix} \varphi_{11}^{(2)} & \varphi_{12}^{(2)} & \cdots & \varphi_{1,n-2}^{(2)} \\ \varphi_{21}^{(2)} & \varphi_{22}^{(2)} & \cdots & \varphi_{2,n-2}^{(2)} \\ \cdots & \cdots & \cdots & \cdots \\ \varphi_{n-2,1}^{(2)} & \varphi_{n-2,2}^{(2)} & \cdots & \varphi_{n-2,n-2}^{(2)} \end{vmatrix}$$

where,

$$\varphi_{i,j}^{(2)} = \frac{1}{\varphi_{i+1,j+1}} (\varphi_{i,j}^{(1)} \varphi_{i+1,j+1}^{(1)} - \varphi_{i,j+1}^{(1)} \varphi_{i+1,j}^{(1)})$$

Notice that at each iteration the value of the determinant is unchanged although the dimension of the Wronskian is reduced consecutively.

$$W^N = W^{N-1} = \ldots = W^1 \tag{3.2.7}$$

Fig.3.1 illustrates the Choi-McMillan(C-M) pivot-condensing for a 4×4 Wronskian.

The C-M algorithm is listed in Table 3.1. The computational flow diagram is shown in Fig.3.2, which illustrates the pivot-condensing algorithm for a 4×4 Wronskain. The C-M algorithm is of particular interest from a computational efficiency point of view, and is suitable for hardware implementation.

The C-M algorithm can be used to construct a higher-order Wronskian by using lower order Wronskians in a multi-layer structure, i.e. *Wronskian of Wronskians* as shown in Fig.3.2. The multilayer structure of Fig.3.2 is of special interest in the construction of non-linear annihilators [3.5].

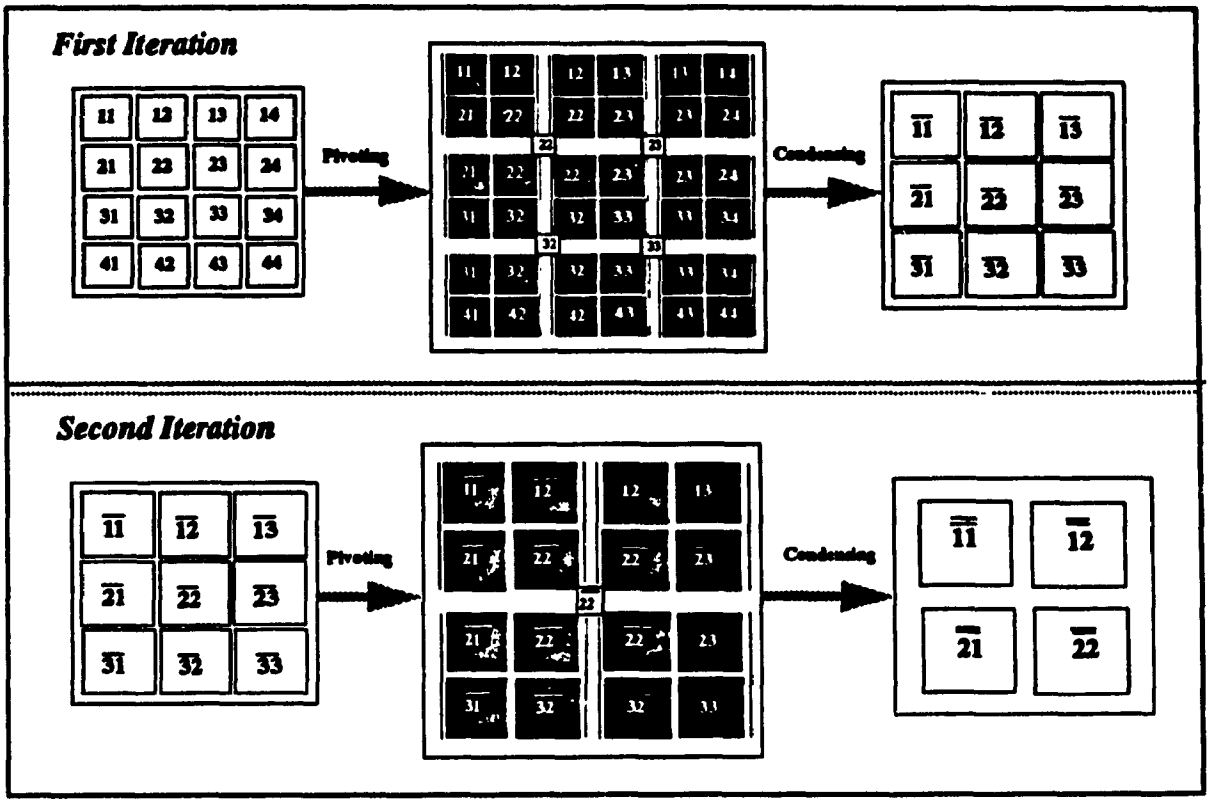

Fig.3.1 An Example of C-M Algorithm

Table 3.1: Choi-McMillan Pivot-Condensing Algorithm

Set $\varphi_{i,j}^{(1)} = \varphi_{i,j}$ and $\varphi_{i,j}^{(0)} = \varphi_{i,j}$

For $k=1$ to $N-1$

For $i=1$ to $N-k$

For $j=1$ to $N-k$

$$\varphi_{i,j}^{(k+1)} = \frac{1}{\varphi_{i+1,j+1}^{(k-1)}} \left(\varphi_{i,j}^{(k)} \varphi_{i+1,j+1}^{(k)} - \varphi_{i,j+1}^{(k)} \varphi_{i+1,j}^{(k)}\right)$$

end

end

end

$$W^N = W^1 = \varphi_{1,1}^{(N)}$$

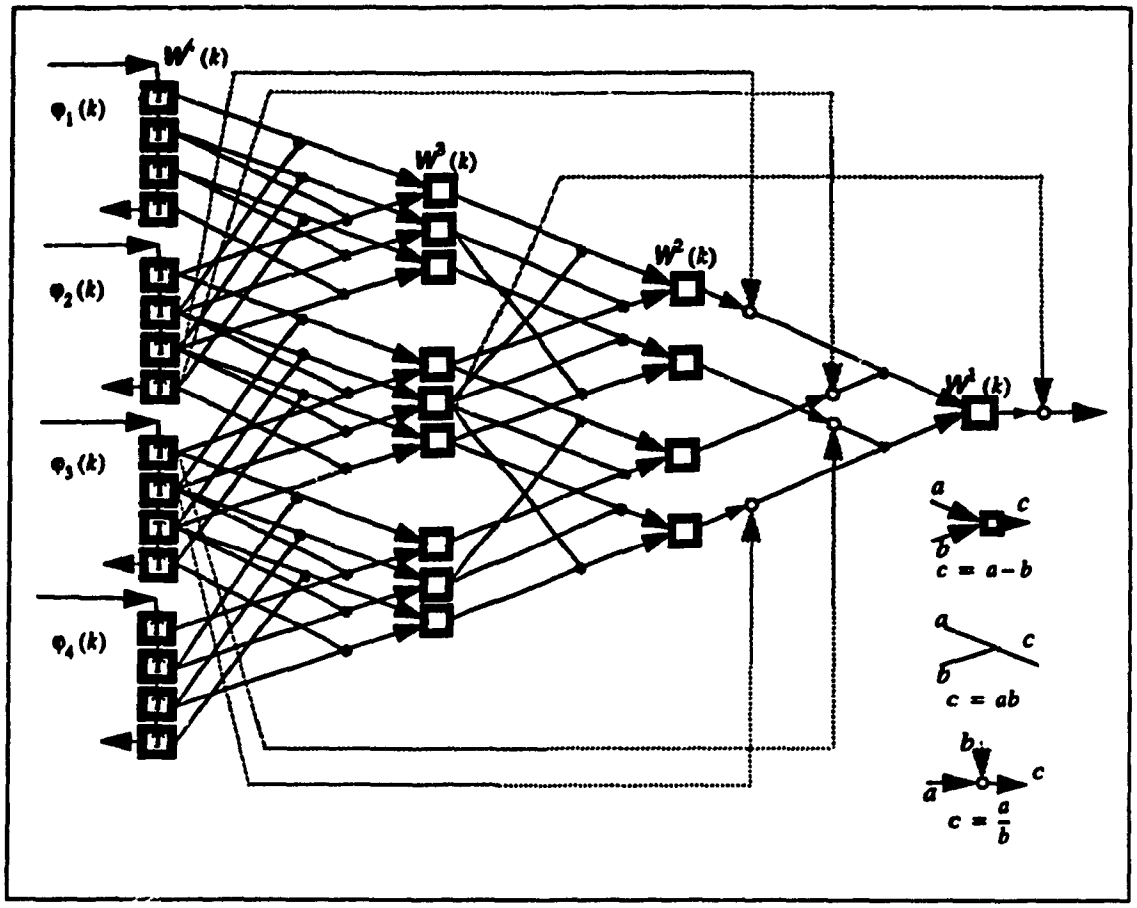

Fig.3.2 Computational Flow Diagram for C-M Pivot-Condensing Algorithm

3.2.2. Sylvester Algorithm

Sylvester algorithm [3.2] states that

$$W^N = \sum_{1 \le \begin{pmatrix} i_1 < i_2 < \dots < i_P \\ k_1 < k_2 < \dots < k_Q \end{pmatrix} \le N} (-1)^{\sum_{r=1}^{P} i_r + \sum_{r=1}^{Q} k_r} P^P \begin{pmatrix} i_1 & i_2 & \dots & i_P \\ k_1 & k_2 & \dots & k_P \end{pmatrix} P^Q \begin{pmatrix} i'_1 & i'_2 & \dots & i'_Q \\ k'_1 & k'_2 & \dots & k'_Q \end{pmatrix} \quad (3.2.8)$$

where $i_1 < i_2 < \dots < i_P$ and $i'_1 < i'_2 < \dots < i'_P$ constitute a *complete system of indices* of $1, 2, \dots, N$, also $k_1 < k_2 < \dots < k_Q$ and $k'_1 < k'_2 < \dots < k'_Q$, become a complete system

of indices and the promotion of indices i_j and k_l takes all possible values between I and N, and $P+Q=N$.

Sylvester algorithm (3.2.8) shows that the computation of a $N\times N$ determinant W^N may be done by calculating a sum of products of *two* smaller dimensional determinants $P^P P^Q$, the number of such combinations of products is $\binom{N}{P}$. Moreover, Sylverster algorithm can be further performed on the determinants P^P and P^Q, thus breaking them into smaller ones. Fig.3.3 illustrates an example of Sylvester algorithm to compute a 4×4 determinant using various combinations of two 2×2 determinants.

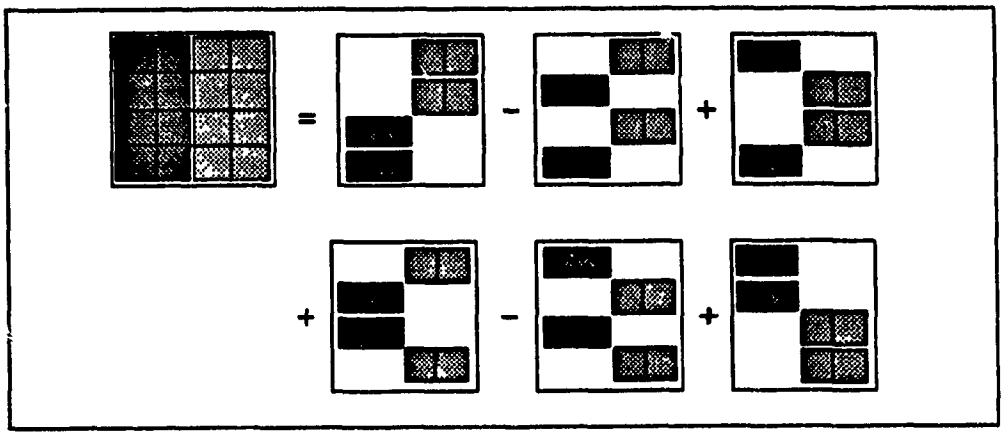

Fig.3.3 Example of Sylvester Algorithm

Consider a $N\times N$ Wronskian, with $N=2^S$. The decomposition of the Wronskian is carried out by reducing the Wronskians to $N/2^l$ dimension at step l.

$$W^N = \sum_{1\le \begin{pmatrix} i_1^{(1)}<i_2^{(1)}<\ldots<i_{N/2^l}^{(1)} \\ k_1^{(1)}<k_2^{(1)}<\ldots<k_{N/2^l}^{(1)} \end{pmatrix} \le N} (-1)^{\sum_{n=1}^{l}\left(\sum_{\nu=1}^{P} i_\nu^{(n)}+\sum_{n=1}^{Q} k_\nu^{(n)}\right)} \prod_{n=1}^{l} P^{\frac{N}{2^l}} \begin{pmatrix} i_1^{(n)} & i_2^{(n)} & \ldots & i_{N/2^l}^{(n)} \\ k_1^{(n)} & k_2^{(n)} & \ldots & k_{N/2^l}^{(n)} \end{pmatrix} \tag{3.2.9}$$

where $i_1^{(1)}<i_2^{(1)}<\ldots<i_{N/2^P}^{(1)} i_1^{(2)}<i_2^{(2)}<\ldots<i_{N/2^P}^{(2)}\ldots$ and $i_1^{(l)}<i_2^{(l)}<\ldots<i_{N/2^P}^{(l)}\ldots$ constitute a *complete system of indices (1,2,...,N)*. This is true also for indices $k_1^{(n)}<k_2^{(n)}<\ldots<k_{N/2^l}^{(n)}$.

The algorithm performing the Sylvester pivoting decomposition is illustrated in Table 3.2. which starts from the elements of the Wronskian matrix.

Table 3.2: Sylvester Pivoting Decomposition Algorithm

For $i_j^{(1)} = 1 \ldots N$ and $i_j^{(1)} \neq i_{m1}^{(1)}$

For $k_j^{(1)} = 1 \ldots N$ and $k_j^{(1)} \neq k_{m1}^{(1)}$

For $i_j^{(2)} = 1 \ldots N$ and $i_j^{(2)} \neq i_{m1}^{(2)} \neq i_{m2}^{(1)}$

For $k_j^{(2)} = 1 \ldots N$ and $k_j^{(2)} \neq k_{m1}^{(2)} \neq k_{m2}^{(1)}$

$\vdots$

For $i_j^{(S)} = 1 \ldots N$ and $i_j^{(S)} \neq i_{m1}^{(S)} \neq i_{m2}^{(S-1)} \ldots \neq i_{mS}^{(1)}$

For $k_j^{(S)} = 1 \ldots N$ and $k_j^{(S)} \neq k_{m1}^{(S)} \neq k_{m2}^{(S-1)} \ldots \neq k_{mS}^{(1)}$

$$W^N = W^N + (-1)^{\sum_{n=1}^{S} (i_j^{(n)} + k_j^{(n)})} \varphi_{i_j^{(1)}, k_j^{(1)}} \varphi_{i_j^{(2)}, k_j^{(2)}} \cdots \varphi_{i_j^{(S)}, k_j^{(S)}}$$

end
end
end
end
end
end

$\forall j, m1, \ldots, mS \in \{1, 2, \ldots N\}$

Unlike the C-M algorithm, Sylvester algorithm uses smaller Wronskians combined with certain pivots to construct a higher dimensional Wronskian. It is in fact a pivot-growing algorithm.

Sylvester algorithm is very useful to show the relationship between a higher-order Wronskian and the lower-order Wronskians. Using this algorithm, we can show that a higher-order time-varying null operator can be decomposed into lower-order ones.

Example: Let us consider two FM signals with phases $\psi_1(k)$ and $\psi_2(k)$. The Wronskian for the first signal $\sin\psi_1(k)$ (FM-1) is $\sin(\psi_1(k) - \psi_1(k-1))$ and the Wronskian for the second signal $\sin\psi_2(k)$ (FM-2) is $\sin(\psi_2(k) - \psi_2(k-1))$. The

4th-order Wronskain associated with these two FM signals is

$$W^4 = \begin{vmatrix} \sin\psi_1^{(0)} & \cos\psi_1^{(0)} & \sin\psi_2^{(0)} & \cos\psi_2^{(0)} \\ \sin\psi_1^{(1)} & \cos\psi_1^{(1)} & \sin\psi_2^{(1)} & \cos\psi_2^{(1)} \\ \sin\psi_1^{(2)} & \cos\psi_1^{(2)} & \sin\psi_2^{(2)} & \cos\psi_2^{(2)} \\ \sin\psi_1^{(3)} & \cos\psi_1^{(3)} & \sin\psi_2^{(3)} & \cos\psi_2^{(3)} \end{vmatrix} = \begin{cases} \sin\dot{\psi}_1^{(0)} \sin\dot{\psi}_2^{(2)} - \sin\ddot{\psi}_1^{(0)} \sin\dot{\psi}_2^{(1)} \\ + \sin\ddot{\psi}_1^{(0)} \sin\dot{\psi}_2^{(1)} + \sin\dot{\psi}_1^{(1)} \sin\ddot{\psi}_2^{(0)} \\ -\sin\ddot{\psi}_1^{(1)} \sin\dot{\psi}_2^{(0)} + \sin\dot{\psi}_1^{(2)} \sin\dot{\psi}_2^{(0)} \end{cases} \tag{3.2.10}$$

where,

$$\begin{aligned} \dot{\psi}_l^{(m)} &= \psi_l(k-m) - \psi_l(k-m-1) \\ \ddot{\psi}_l^{(m)} &= \psi_l(k-m) - \psi_l(k-m-2) \\ \dddot{\psi}_l^{(m)} &= \psi_l(k-m) - \psi_l(k-m-3) \end{aligned} \tag{3.2.11}$$

By repeatedly applying the Sylvester rule(3.2.9), we can show that the Wronskain for N FM signals can be expressed as

$$W^N = \sum_{1<n_1<m_i<Ni=1} \prod^{N/2} (-1)^{\sum_{i=1}^{N/2}(m_i+n_i)} \sin\left[\psi_i^{(m_i)} - \psi_i^{(n_j)}\right] \tag{3.2.12}$$

Notice that if the instantaneous frequencies of FM-1 and FM-2 are fixed values,i.e. these two FM signals become just sinusoids with fixed frequencies, then the right-hand-side (RHS) of (3.2.10) is shift invariant

$$\sin\psi_m^{(i)}(k) = \sin\psi_m^{(j)}(k)$$

Then the 4th-order Wronskian in (3.2.10) can be expressed as a product of two second order Wronskians of FM-1 and FM-2

$$W^4 = 8\sin\dot{\psi}_1^{(0)} \sin\dot{\psi}_2^{(0)} \tag{3.2.13}$$

This example shows that, in general, a 4×4 Wronskian (3.2.10) for 2 -FM signals can not be constructed by directly using two 2×2 Wronskians $\sin\dot{\psi}_1^{(0)}$ (for FM-1) and $\sin\dot{\psi}_2^{(0)}$ (for FM-2). Such construction is made possible only by using extra pivot-

terms as given in (3.2.10). The complexity of the two algorithms discussed above is illustrated in Table 3.3.

Table 3.3: Comparison of C-M and Sylvester Algorithms

Algorithm	Multiplication	Division	Pivots
Choi-McMillan	$1.5N^3$	$0.5N^3$	2×2
Sylvester	$(\sqrt{2})\,2^N N^{5/2}$	No	$P+Q=N$

3.3. Root-Factorization of Time-Varying Null Operator

Let us consider a HOTV null operator given by

$$\aleph^{(N)} = 1 + \sum_{l=1}^{N} a_l(k)\, q^{-l} \tag{3.3.1}$$

which is associated with an N-dimensional signal space

$$\Omega^N = \Omega_1^{N_1} \oplus \Omega_2^{N_2} \oplus \ldots \oplus \Omega_s^{N_M} \text{ and } \sum_{s=1}^{M} N_s = N$$

A signal subspace Ω^{N_s} can be represented by a time-varying null operator $\aleph^{(s)}$ of order s:

$$\aleph^{(s)} = 1 + \sum_{n_s=1}^{N_s} \bar{a}_{n_s}(k)\, q^{-n_s}$$

By the decomposition of a HOTV null operator, we mean the representation of the HOTV null operator by using individual lower-order null operators,

$$\aleph^{(N)} = \chi^M(\aleph^{(1)}, \aleph^{(2)}, \ldots, \aleph^{(M)}) \tag{3.3.2}$$

In particular, if the decomposition operation can be written as

$$\chi^M = \prod_{s=1}^{M} \aleph^{(s)}$$

such a decomposition is equivalent to the standard *root-factorization*, that is, a cascade

connection of the individual lower-order time-varying null operators $\aleph^{(s)}$.

Note that for a time-invariant null operator such a decomposition is always possible simply by root-factorizing of the higher-order null operator into lower-order polynomial forms.

Theorem 3.3.1 *A HOTV-null operator can not be decomposed by using root-factorization.*

Proof: Without loss of generality, suppose $M = 2$ and $P+Q = N$. The coefficients of the HOTV-null operator (3.3.1) are expressed in (3.2.4), and for the decomposed *Pth* order time-varying null operator, the coefficients become

$$a_{P,i}^{*}(k) = (-1)^{i_i+k_i}\frac{W^{P}\begin{pmatrix} i_1\ i_2 \cdots i_{i-1}\ i_{i+1} \cdots i_P \\ k_0\ k_1 \cdots k_{i-1}\ k_{i+1} \cdots k_P \end{pmatrix}}{W^{P}\begin{pmatrix} i_1\ i_2 \cdots i_P \\ k_1\ k_2 \cdots k_P \end{pmatrix}} \qquad i = 1, 2, \ldots, P \tag{3.3.3}$$

Similarly, we can find the expression for a *Qth*- order time-varying null operator; let the coefficients be denoted as $a_{Q,i}^{*}(k)$ and $i = 1, 2, \ldots, Q$. If the root-factorization is used for the decomposition then

$$a_i(k) = \sum_{n,m=1}^{m+n=i} a_{P,m}^{*}(k)\, a_{Q,n}^{*}(k-P) \tag{3.3.4}$$

On the other hand, the denominator of the left-hand-side (LHS) of (3.3.4) is expressed as (3.2.8), while the denominator of the RHS of (3.3.4) is

$$W^{P}\begin{pmatrix} i_1\ i_2 \cdots i_P \\ k_1\ k_2 \cdots k_P \end{pmatrix} W^{Q}\begin{pmatrix} i_1 & i_2 & \cdots & i_Q \\ k_1-P & k_2-P & \cdots & k_Q-P \end{pmatrix} \tag{3.3.5}$$

Since (3.3.5) is only one term of (3.2.8), the rest of $\binom{N}{P}-1$ terms are not the same as (3.2.8). Therefore, the denominators of LHS and RHS of (3.3.4) are not the same and thus (3.3.4) is not valid.

Q.E.D.

Corollary 3.3.1 *The condition for the existence of root-factorization decomposition of an Nth-order null operator is that the lower-order Wronskians be shift invariant ones.*

Proof: The denominator of LHS of (3.3.4) is written as

$$W^N = \sum_{1 \le \begin{pmatrix} i_1 < i_2 < \dots < i_P \\ k_1 < k_2 < \dots < k_Q \end{pmatrix} \le N} (-1)^{\sum_{r=1}^{P} i_r + \sum_{r=1}^{Q} k_r} P^P \begin{pmatrix} i_1 \; i_2 \; \cdots \; i_P \\ k_1 \; k_2 \; \cdots \; k_P \end{pmatrix} P^Q \begin{pmatrix} i'_1 \; i'_2 \; \cdots \; i'_Q \\ k'_1 \; k'_2 \; \cdots \; k'_Q \end{pmatrix}$$

If Wronskians $W^P(k)$ and $W^P(k)$ are shift invariant, i.e.

$$W^P(k) = W^P(k-l) \quad \text{and} \quad W^Q(k) = W^Q(k-l) \quad \forall l \in \{1, 2 \dots N\}$$

then it can be shown that all possible pivots of P^P and P^Q are shift invariant too. Thus, the Wronskian W^N can be expressed as a product of two lower-order Wronskians up to a constant scale, i.e.

$$W^N = c\, W^P W^Q$$

where c is a constant value, and thus the equation (3.3.4) is valid.

Q.E.D.

Theorem 3.3.1 and Corollary 3.3.1 in fact are valid for any linear time-varying system. Root-factorization can not be applied for the decomposition of a higher-order time-varying system unless the system is time-invariant. It will be shown in Chapter 4 (by introducing the so-called anti-null time-varying operator) that an *Nth*-order time-varying null operator can be *pseudo factorized*. The signal space is partitioned into subspaces by connecting in cascade the lower-order ASTV-ARMA models.

If the root-factorization approximately leads to the decomposition of a HOTV-null operator, such a HOTV-null operator can be treated as a slow-time-varying null operator. By Corollary 3.3.1, if the parameters of a time-varying system does not change significantly during the time interval N, that is, if the Wronskian is locally almost shift-invariant, then such a system may be considered as a *slow time-varying* system.

Example 3.2 Consider two single-tone modulated FM signals. A 4th-order time-varying null operator is constructed by using (3.2.4). The time-varying roots obtained by root-factorization are shown in Fig.3.4. For each FM signal we can construct a second order time-varying null operator and the loci of time-varying the roots shown in Fig.3.4. It is seen that the loci of the roots for the true 2nd-order time-varying null operator and the 2nd-order time-varying null operator obtained by using root-factorization are not the same.

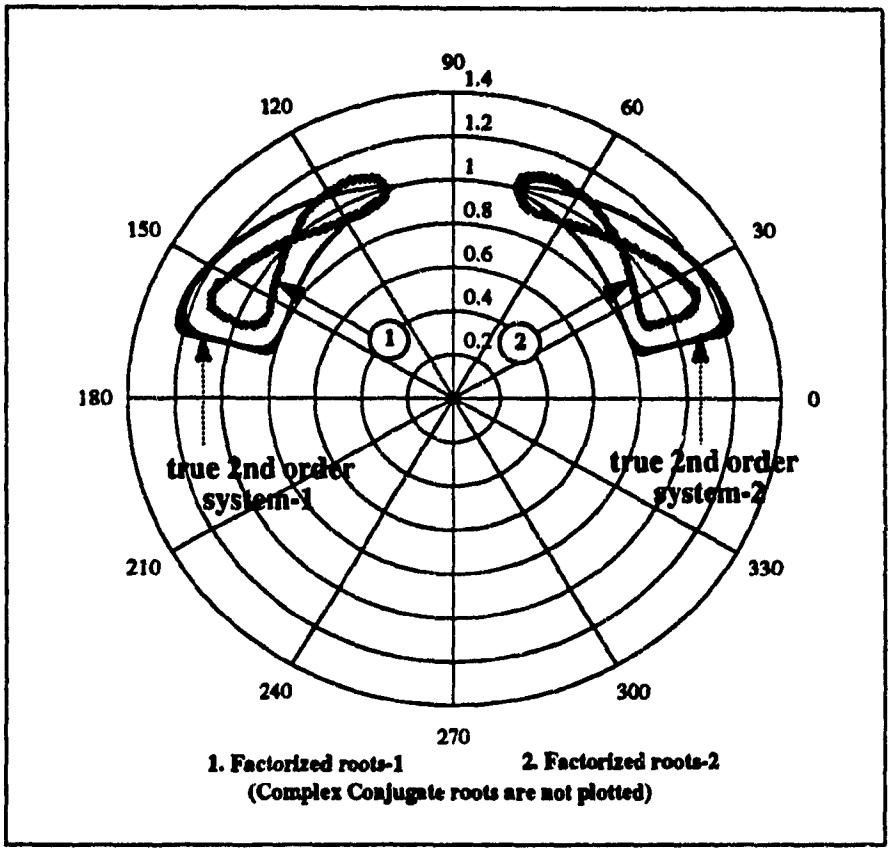

Fig.3.4 Invalidity of the Root-Factorization for the Decomposition of a Time-Varying Null Operator

3.4. Commutability of Time-Varying Null Operator

In this section, we investigate the commutability of two time-varying null operators. Based on the concept of commutability of two linear systems, the classification of *fast time-varying* and *slow time-varying* systems is introduced.

Consider two linear time-varying null operators, $\aleph_1$ and $\aleph_2$, whose impulse responses are

$$\begin{aligned} \aleph_1 \qquad & h_1(m,k) = h_1(m,0) + \sum_{j=0}^{k-1} \partial h_1(m,j) \\ \aleph_2 \qquad & h_2(n,k) = h_2(n,0) + \sum_{j=0}^{k-1} \partial h_2(n,j) \end{aligned} \tag{3.4.1}$$

where $m = 1, 2, \ldots, N$, $m = 1, 2, \ldots M$ are coefficient indices for $h_1(m,k)$ and $h_2(m,k)$ respectively, and $h_1(m,0)$ are the initial values of the time-varying coefficients, which correspond to the time-invariant parts of the impulse response. The

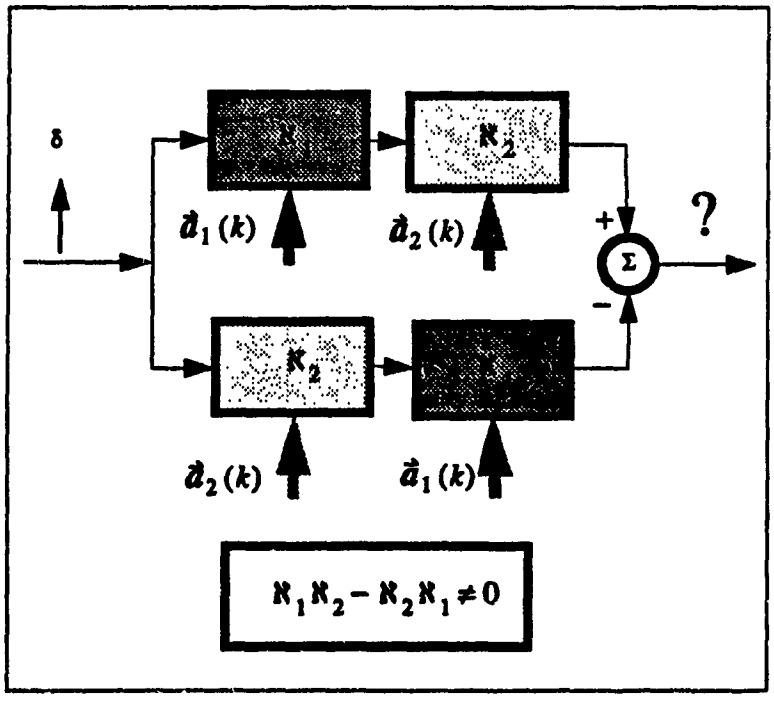

Fig.3.5 Non-Commutability of Two Time-Varying Null Operators

variation of the time-varying parts of the impulse response is denoted as $\partial h_1(m,j)$. The cascade connection of $\aleph_1$ and $\aleph_2$ is given by $\aleph_1\aleph_2$, similarly $\aleph_2\aleph_1$ denotes $\aleph_2$ followed by $\aleph_1$.

Definition 3.4.1 Two systems are *commutable*, if the impulse response of $\aleph_1\aleph_2$ is the same as that of $\aleph_2\aleph_1$ within a multiplying constant.

The impulse response of system $\aleph_1\aleph_2$ may be written as

$$H_{12}(k) = \sum_{m=0}^{N+M} h_1(m,k)\, h_2(k-m,k) \tag{3.4.2}$$

Substituting (3.4.1) into (3.4.2), we have

$$\begin{aligned} H_{12}(k) &= \sum_{m=0}^{N+M}\left(h_1(m,0)+\sum_{i=0}^{k-1}\partial h_1(m,i)\right)\left(h_2(k-m,0)+\sum_{j=0}^{k-1}\partial h_2(k-m,j)\right) \\ &= \sum_{m=0}^{N+M} h_1(m,0)\, h_2(k-m,0) + \sum_{m=0}^{N+Mk-1}\sum_{j=0} h_1(m,0)\,\partial h_2(k-m,j) \\ &+ \sum_{m=0}^{N+Mk-1}\sum_{i=0}\partial h_1(m,i)\, h_2(k-m,0) + \sum_{m=0}^{N+Mk-1}\sum_{i=0}^{k-1}\sum_{j=0}\partial h_1(m,i)\,\partial h_2(k-m,j) \end{aligned} \tag{3.4.3}$$

Similarly, the impulse response of system $\aleph_2\aleph_1$ is

$$\begin{aligned} H_{21}(k) &= \sum_{m=0}^{N+M} h_2(m,0)\, h_1(k-m,0) + \sum_{m=0}^{N+Mk-1}\sum_{j=0} h_2(m,0)\,\partial h_1(k-m,j) \\ &+ \sum_{m=0}^{N+Mk-1}\sum_{i=0}\partial h_2(m,i)\, h_1(k-m,0) + \sum_{m=0}^{N+Mk-1}\sum_{i=0}^{k-1}\sum_{j=0}\partial h_2(m,i)\,\partial h_1(k-m,j) \end{aligned} \tag{3.4.4}$$

Theorem 3.4.1 *Linear time-varying null-operators are not commutable.*

$$\aleph_1\aleph_2 - \aleph_2\aleph_1 \neq 0 \tag{3.4.5}$$

Proof: From (3.4.3) and (3.4.4), since the time-invariant parts of the impulse

response $H_{12}(k)$ and $H_{21}(k)$ are the same, we have

$$\begin{aligned}\varsigma(k) &= H_{12}(k) - H_{21}(k) \\ &= \sum_{m=0}^{N+Mk-1}\sum_{j=0} [h_1(m,0)\,\partial h_2(k-m,j) - \partial h_2(m,j)\,h_1(k-m,0)] \\ &+ \sum_{m=0}^{N+Mk-1}\sum_{j=0} [\partial h_1(m,j)\,h_2(k-m,0) - h_2(m,0)\,\partial h_1(k-m,j)] \\ &+ \sum_{m=0}^{N+Mk-1}\sum_{i=0}^{k-1}\sum_{j=0} [\partial h_1(m,i)\,\partial h_2(k-m,j) - \partial h_2(m,i)\,\partial h_1(k-m,j)]\end{aligned} \tag{3.4.6}$$

since $\partial h_1(m,j) \neq \partial h_2(m,j) \neq 0 \quad \forall m,j \in Z^+$, therefore, $\varsigma(k) \neq 0 \ \forall k \in Z^+$

Q.E.D.

Corollary 3.4.1 *A sufficient condition for two linear systems to be commutable is that both systems $\aleph_1$ and $\aleph_2$ are time-invariant*

Proof: From(3.4.6),

$$\begin{cases} \partial h_1(i,j) = 0 \\ \partial h_2(i,j) = 0 \end{cases} \qquad \forall i,j \in Z^+$$

This implies $\varsigma(k) = 0$

Q.E.D.

Corollary 3.4.2 *A time-varying null operator is not commutable with a time-invariant null operator.*

Proof: Suppose that $\aleph_2$ is time-invariant, i.e. $\partial h_2(i,j) = 0$ thus

$$\varsigma(k) = \sum_{m=0}^{N+Mk-1}\sum_{j=0} [\partial h_1(m,j)\,h_2(k-m,0) - h_2(m,0)\,\partial h_1(k-m,j)]$$

If $\varsigma(k) = 0$, then $\partial h_1(k-m,j) = 0$

Q.E.D.

A time-varying system is slow-time-varying if it is commutable with a time-invariant system, i.e.

$$\sum_{k=k_0}^{M+N} \zeta^2(k) = \varepsilon \approx 0$$

Corollary 3.4.3 *(Weak Time-Varying) Two time-varying null operators* $\aleph_1$ *and* $\aleph_2$ *are slow time-varying if* $\exists \varepsilon > 0$

$$\| \partial h_1(i,j) \|_2 \| \partial h_2(i,j) \|_2 \ll \frac{\varepsilon}{(M+N) \| h_1(i,j) \|_2 \| h_2(i,j) \|_2} \tag{3.4.7}$$

Proof: Taking the Euclidean norm on (3.4.6), and by applying the Cauchy-Schwartz inequality, one can show that (3.4.7) holds.

Q.E.D.

Corollary 3.4.3 provides an interesting condition for the so called weak time-varying system. Such a system can be treated as an almost time-invariant one.

It should be noted that in a very special case, which we will discuss in Chapter 4, under a certain symmetry constraint, a time-varying (even a fast time-varying) ARMA model becomes a commutable one.

Non-commutability is a fundamental feature of a time-varying system. It in fact provides an explanation as to why the decomposition of a linear time-varying null operator can not be performed by using root-factorization.

3.5. Trajectory Equation of Higher-Order Time-Varying Null Operator

An *Nth*-order time-varying null operator, whose coefficients are functions of time, can be expressed by a trajectory in an *N*-dimensional parametric space. In this section, we give an expression for the trajectory of an *Nth*-order time-varying null operator. This expression will be used in Chapter 5 to derive stability conditions for a time-varying

anti-null operator, and in Chapter 8 to solve the problem of blind-signal separation.

Lemma 3.6.1 *The trajectory of a linear time-varying null operator is expressed by the following orbit equation*

$$\gamma_N(k) + a_1(k)\gamma_{N-1}(k) + a_2(k)\gamma_{N-2}(k) + \ldots + a_N(k) = 0 \qquad (3.5.1)$$

where

$$\gamma_{N-l}(k) = (-1)^l \begin{vmatrix} a_1(k) & 1 & & 0 \\ a_2(k) & a_1(k) & 1 & \\ \ldots & \ldots & \ldots & \ldots \\ a_{l-1}(k) & a_{l-2}(k) & \ldots & 1 \\ a_l(k) & a_{l-1}(k) & \ldots & a_1(k) \end{vmatrix}_{l \times l}$$

Proof: see Appendix 3.1.

Q.E.D.

The stability of a linear time-varying null operator depends on the variation properties of such a trajectory (see Chapter 5).

3.6. Wronskian-Like Determinant for Gaussian Random Signals

Let us consider a case where the signal is represented by a random stationary Gaussian process. As was shown, the construction of a null operator depends on the positiveness of a certain determinant associated with the set of linearly independent solutions. If such a determinant is positive with probability close to unity, we call this determinant a *Wronskian-like determinant*. Then it is possible to construct a high order null operator for a random signal. In what follows, we study the case where the signal space is spanned by Gaussian random signals. It can be shown that under certain conditions, the random determinant associated with such a signal space approaches the

Wronskian-like determinant.

Consider N realizations of a stationary random Gaussian source, with zero mean and variance σ, given by the matrix

$$A = [a_{ij}] \qquad i,j = 1,2,\ldots,N$$

where each element a_{ij} is an independent Gaussian distributed random variable. It is known that the joint distribution function of the elements a_{ij} is [3.3]

$$\frac{1}{\sigma^{N^2}(2\pi)^{N^2/2}} exp\left[-\frac{\sum_{i=1}^{N}\sum_{j=1}^{N} a_{i,j}}{2\sigma^2}\right] \prod_{i=1}^{N}\prod_{j=1}^{N} da_{i,j} \tag{3.6.1}$$

In order to investigate the positiveness of matrix A, one may work with the definite matrix given by

$$B = A^T A = [b_{i,j}] \qquad i,j = 1,2,\ldots,N$$

If at least one eigen value of matrix B becomes zero, then the determinant of matrix A vanishes. The joint distribution of elements $b_{i,j}$ is [3.4]

$$\frac{[det(B)]^{-1/2}}{(2^{1/2}\sigma)^{N^2}\pi^{N(N-1)/4}\prod_{i=1}^{N}\Gamma(\frac{N+1-i}{2})} exp\left[-\frac{\sum_{i=1}^{N} b_{i,j}}{2\sigma^2}\right] \prod_{i=1}^{N}\prod_{j=1}^{N} db_{i,j} \tag{3.6.2}$$

The joint distribution of n random eigenvalues $\lambda_1, \lambda_2, \ldots \lambda_n$ of the matrix B can be written as

$$K_N exp\left[-\frac{\sum_{i=1}^{N}\lambda_i}{2\sigma^2}\right] \prod_{i<j}(\lambda_i - \lambda_j) \prod_{i=1}^{N} \lambda_i^{-1/2} d\lambda_i \tag{3.6.3}$$

where,

$$K_N = \frac{\pi^{N/2}}{(2\sigma^2)^{N^2/2} \prod_{i=1}^{N} \left[\Gamma(\frac{i}{2})\right]^2}$$

Lemma 3.7.1 *The probability of the smallest eigen value λ_n of matrix B may be expressed as*

$$Prob\,(\lambda_o < 2\sigma^2 rN) < (\frac{2r}{e^{r-1}})^N \frac{1}{4(r-1)(r\pi N)^{1/2}} \qquad (3.6.4)$$

where $r > 1$

Proof: See Appendix 3.2.

Q.E.D.

Example 3.3 Consider a zero mean Gaussian random process with variance σ^2. Using Lemma 3.7.1, we find the probability of the Wronskian-like determinant crossing zero (changing sign) are 17% ($\sigma^2 = 0.5$) and 4% ($\sigma^2 = 0.1$). The dimension of Wronskian is N=4. The Wronskian-like determinant is plotted in Fig. 3.6

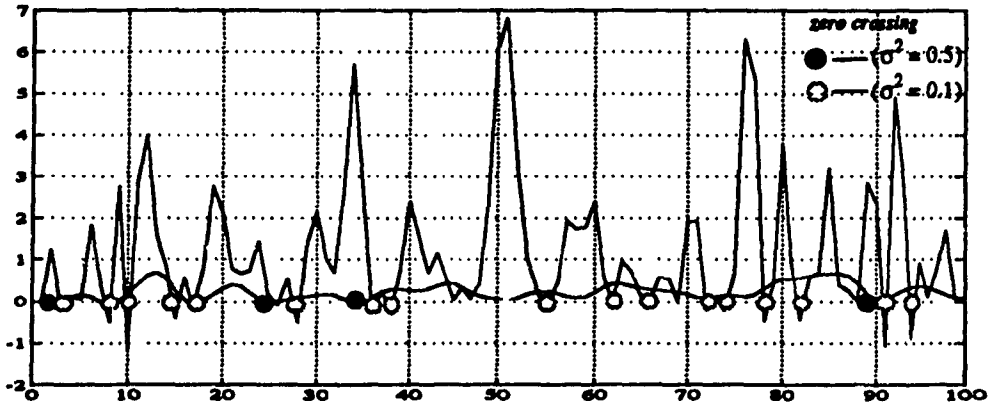

Fig.3.6 Zero Crossing of Gaussian Wronskian-Like Determinant

Example 3.4 In this example, we use a second order time-varying null operator to cancel a speech signal. Two randomly time-varying coefficients are calculated using a Wronskian-like determinant, where such a determinant was constructed by using this speech signal and its Hilbert transform, these being taken as two independent functions. As is shown in Fig.3.7, an almost perfect cancellation has been achieved.

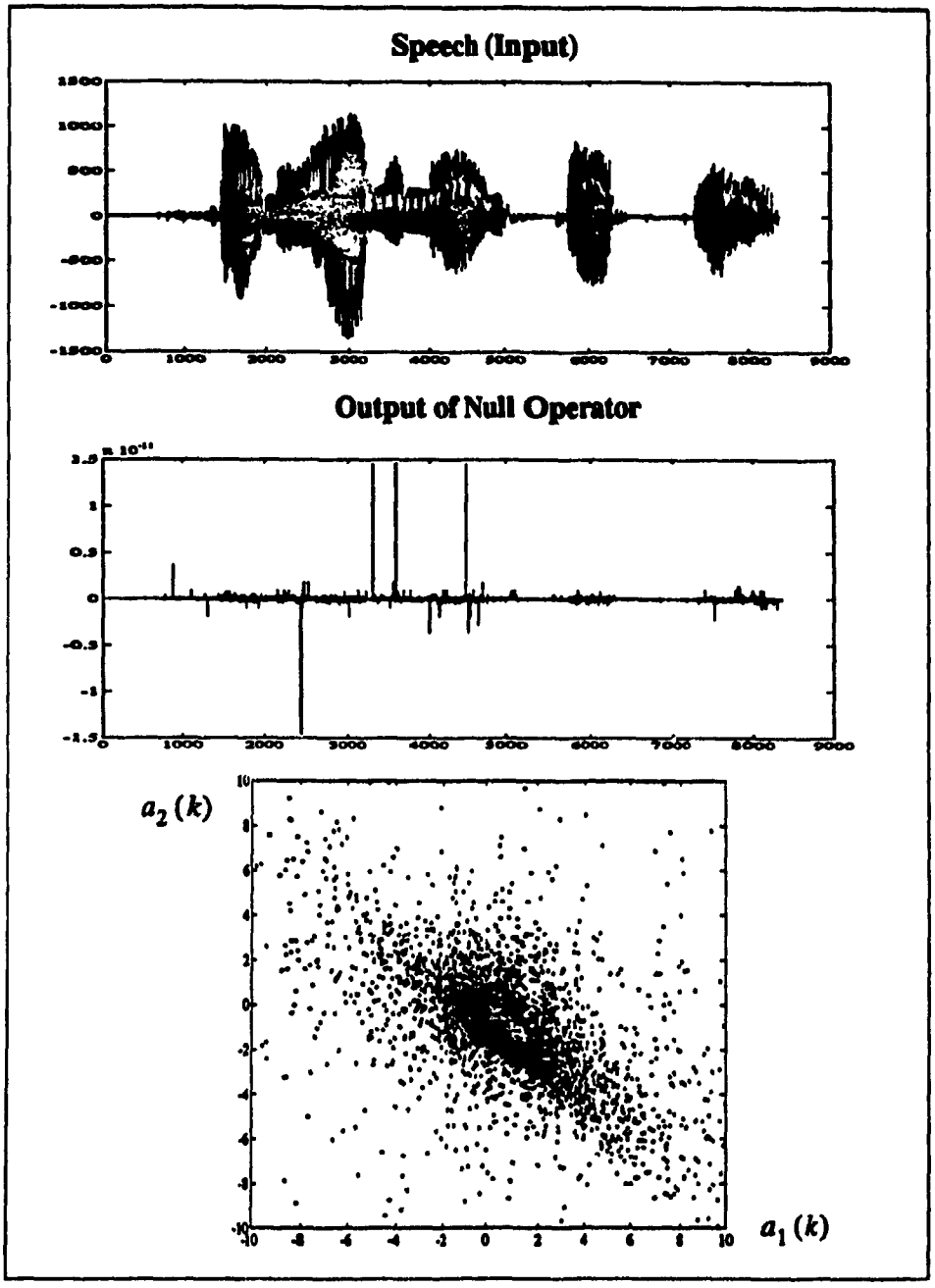

Fig.3.7 Speech Cancellation Using Second-Order Time-Varying Null Operator

References

[3.1] R. H. MacMillan, "Contractants: A New Method for the Numerical Evaluation of Determinants", *Journal of the Royal Aeronautical Society*, Vol. 59, pp. 772-773, Nov. 1955

[3.2] F R. Gantmacher, " *Theory of Matrices*", Vol.1-2, Chelsea Publishing Company, New York, 1959

[3.3] H. Cramer, "*Mathematical Methods of Statistics*", Princeton University Press, 1946

[3.4] S. Wilks,"*Mathematical Statistics*", Wiley, New York, 1962

[3.5] E.I. Plotkin and M.N.S. Swamy," Nonlinear Signal Processing Based on Parameter Invariant Moving Average", *Proceedings of Canadian Conference of Electrical and Computer Engineering*, pp. TM3.11.1-4, Sept. 1992

Chapter 4

Anti-Null Operator and Almost-Symmetrical Time-Varying ARMA Model

4.1. Introduction

In this Chapter, we construct a time-varying anti-null operator. We show that for signal processing purposes, it is important to combine the time-varying null and anti-null operators into one block as a *transparent operator*. The main purpose of such an anti-null operator is to compensate for the distortions which are created by the use of the time-varying null operator.

It is shown that the proposed transparent operator which contains time-varying null and anti-null operators possesses a new property: it exhibits transparency to any other signal that is not eliminated by the null operator.

In this chapter a detailed analysis of the impulse response of the time-varying anti-null operator is presented,. Using two kinds of representation of the impulse response of an anti-null operator, the properties of the transparent operator are investigated. It is also shown that a higher-order time-varying null operator can be pseudo factorized into lower-order ones, and the signal subspaces can be separated by using corresponding transparent operators.

It is shown that a physically implementable anti-null operator can not be perfectly symmetric to a null-operator. An one-sided almost-symmetrical transparent operator is introduced and the trade-off between the transparency and the observation time of such an operator is analyzed.

The results presented show the importance and applicability of the proposed

transparent operator to signal separation and interference suppression.

The aim of this chapter is to design a special time-varying transparent operator which can be used to carry out signal separation, such an operator must fullfil two objectives; (1) to have null singularity, (2) to be transparent.

Given an N-dimensional W-system of functions, it spans an N-dimensional signal subspace Ω_1. Consider two signals, $S_1 \in \Omega_1$ and $S_2 \in \bar{\Omega}_1$; $\Omega_1 \cap \bar{\Omega}_1 = \varnothing$ $\Omega_1 \cup \bar{\Omega}_1 = I$. We seek a transparent operator Q_1,such that

$$\begin{array}{ll} \text{I} & Q_1[S_1] = 0 \\ \text{II} & Q_1[S_1 + S_2] = S_2 \end{array} \tag{4.1.1}$$

Now let us recall the basic properties of the time-varying null operator $\aleph_1$ [1] discussed in Chapter 2 and Chapter 3

$$\begin{array}{ll} \text{I} & \aleph_1[S_1] = 0 \\ \text{II} & \aleph_1[S_2] = \tilde{S}_2 \neq S_2 \\ \text{III} & \aleph_1[S_1 + S_2] = \tilde{S}_2 \end{array} \tag{4.1.2}$$

It is seen that the time-varying null operator fulfills our first objective. However, *the time-varying null operator also distorts any signal which does not belong to the signal space* Ω_1.

In order to meet the second objective, one has to construct an inverse operator such that by combining it with the time-varying null operator $\aleph_1$ the second objective is achieved. We call such an operator as anti-null operator $\aleph_1^{\dagger}$; in fact, it compensates the distortion in signal space $\bar{\Omega}_1$. Before discussing the properties of such an inverse operator, we present the following definitions.

Definition 4.2.1 The *transparency* of a linear operator Q_1, means that any

1. Time-varying null operator having null singularity with respect to signal subspace Ω_1.

signal passes such an operator without any distortion, except the signals which satisfy its null singularity, i.e. $Q_1[S] = S$, if $\forall S \in \bar{\Omega}_1$, and $\Omega_1 \cup \bar{\Omega}_1 = I$, $\Omega_1 \cap \bar{\Omega}_1 = \varnothing$.

Definition 4.2.2. The anti-null operator $\aleph_1\dagger$ is an inverse operator such that $\aleph_1\aleph_1\dagger = Q_1$, and Q_1 preserves the null-singularity of $\aleph_1$.

4.2. Transparency and Symmetry of Operator Q_1

4.2.1. Symmetry Condition

Theorem 4.2.1 *(Main Result) The necessary and sufficient condition for a time-varying operator Q_1 to be transparent to any signal other than its null singularity is that the time-varying anti-null operator be perfectly symmetrical to the time-varying null operator.*

Proof: Suppose we are given an *Nth*-order time-varying null operator, $\aleph_1[\ ] = 1 + \sum_{n=1}^{N} a_n(k)\, O^n$, and an input signal $x(k)$ which does not belong to the null singularity of $\aleph_1$. Let us consider an Mth-order non-homogenous anti-null operator $\aleph_1\dagger[\ ] = 1 + \sum_{m=1}^{M} b_m(k)\, O^m$. Thus the output $y(k)$ of the combined null and anti-null operators is written as

$$\left(1 + \sum_{n=1}^{N} a_n(k)\, O^n\right) x(k) = \left(1 + \sum_{m=1}^{M} b_m(k)\, O^m\right) y(k) \tag{4.2.1}$$

The input-output relationship (4.2.1) can be expressed as

$$y(k) = \left(\frac{1 + \sum_{n=1}^{N} a_n(k)\, O^n}{1 + \sum_{m=1}^{M} b_m(k)\, O^m}\right) x(k) \tag{4.2.2}$$

Hence (4.2.2) can be regarded as a new operator for input $x(k)$, which is written as

$$\overline{Q_1} = \frac{1 + \sum_{n=1}^{N} a_n(k)\, O^n}{1 + \sum_{m=1}^{M} b_m(k)\, O^m} = 1 - p_1(k)\, O + p_2(k)\, O^2 + \ldots \tag{4.2.3}$$

$$= 1 + \sum_{l=1}^{\infty} (-1)^l p_l(k)\, \sigma^l$$

The combined operator $\bar{Q}_1$ is in fact an infinite order homogenous linear operator. From Appendix 4.1, we know that the coefficients of such an operator $\bar{Q}_1$ are given as

$$p_l(k) = \begin{vmatrix} b_1(k) - a_1(k) & 1 & & \mathbf{O} \\ b_2(k) - a_2(k) & b_1(k) & 1 & \\ b_3(k) - a_3(k) & b_2(k) & b_1(k) & 1 \\ b_3(k) - a_3(k) & b_3(k) & b_2(k) & b_1(k) \quad \cdots \\ \cdots & \cdots & \cdots & \cdots \quad \cdots \end{vmatrix}_{l \times l} \tag{4.2.4}$$

Proof of necessity: In order to achieve transparency, i.e. $y(k) = x(k)$, the coefficients $p_l(k) = 0 \quad \forall l \in Z^+$. By (4.2.4) we have

$$p_1(k) = b_1(k) - a_1(k) = 0 \quad \Rightarrow b_1(k) = a_1(k) \tag{4.2.5}$$

By induction, suppose $b_1(k) = a_1(k), b_2(k) = a_2(k), \ldots b_n(k) = a_n(k)$ and $p_1(k) = p_2(k) = \ldots = p_n(k) = 0$ we have from (4.2.5)

$$p_{n+1}(k) = [b_{n+1}(k) - a_{n+1}(k)] \begin{vmatrix} 1 & & & \mathbf{O} \\ b_1(k) & 1 & & \\ b_2(k) & b_1(k) & 1 & \\ \cdots & \cdots & \cdots & \cdots \\ b_n(k) & b_{n-1}(k) & b_{n-2}(k) & \ldots 1 \end{vmatrix}$$

$$= b_{n+1}(k) - a_{n+1}(k) = 0 \tag{4.2.6}$$

Hence, if $p_l(k) = 0 \quad \forall l \in Z^+$, one must have

$$b_n(k) = a_n(k) \qquad n = 1, 2, \ldots, max\{M,N\} \tag{4.2.7}$$

Proof of sufficiency: If the time-varying null operator and the time-varying anti-null operator are symmetrical, i.e.

$$b_n(k) = a_n(k) \quad n = 1, 2, \ldots, max\{M,N\}$$

then by (4.2.4) we have

$$p_l(k) = 0 \quad \forall l \in Z^+ \tag{4.2.8}$$

Q.E.D.

This is a very elegant result, since to find an anti-null operator for constructing a transparent operator, no additional efforts need be made; such an anti-null operator is simply a non-homogeneous operator which is perfectly symmetric to the homogeneous null operator. Further, the symmetrical condition is valid for an arbitrarily chosen operation building block O.

In the case of a discrete time-varying null operator, where our interests are focused, the transparent operator may be expressed by the following simple ARMA canonical form

$$\left[1+\sum_{i=1}^{N} a_i(k)\,q^{-i}\right]y(k) = \left[1+\sum_{i=1}^{N} a_i(k)\,q^{-i}\right]x(k) \quad , \qquad (4.2.9)$$

Such a canonical form defines a perfect symmetrical linear time-varying transparent operator Q_1. We shall further explore this operator in connection with the separation of superimposed signals with overlapping Fourier spectra. In order to discuss the symmetry property, we now define the so-called one-sided almost-symmetrical operator, where the symmetry is broken as far as the non-homogenous part of the perfect symmetrical operator Q_1 is concerned.

Definition 4.2.1 A one-sided almost-symmetric operator Q^{α}_{1} is defined as

$$\left[1+\sum_{i=1}^{N} \alpha^i a_i(k)\,q^{-i}\right]y(k) = \left[1+\sum_{i=1}^{N} a_i(k)\,q^{-i}\right]x(k) \qquad (4.2.10)$$

where, $\alpha \rightarrow 1^{-}$, is called the symmetric factor, and the anti-null operator of Q^{α}_{1} is defined as $\aleph_1^{\alpha\dagger}$.

The most negative aspect in using a time-varying operator for signal processing application is that a time-varying operator generates spurious spectral components, which are not found in the input signal. Such spurious spectral components generated by the time-varying operator are undesired components at the output and these components could be even stronger than the useful signal. This is one of the major reasons why time-varying filters are not widely used in the signal processing context. However, Theorem 4.2.1 indicates that there exists a special symmetrical time-varying

operator such that the spurious spectral components will not appear at the output of such a time-varying operator if the transparency property is guaranteed. Moreover, if a signal does not belong to the null singularity of such a transparent operator, then the Fourier spectra of the output and input of such an operator become identical.

4.3. Transparency and Commutability of Operators $\aleph_1$ and $\aleph_1\dagger$

Theorem 4.3.1 *A symmetrical time-varying operator Q_1 is transparent, iff its time-varying null operator and time-varying anti-null operator are commutable*

Proof: Let us first consider the case when Q_1 is given by the cascade connection $\aleph_1\dagger\,\aleph_1$.

The Fourier spectrum of the output of the null-operator $\aleph_1$ is given as

$$O_{Null}(j\omega) = X(j\omega) + \sum_{l=1}^{N} A_l(j\omega) \otimes [X(j\omega)\, e^{jl\omega}] \tag{4.3.1}$$

$$= X(j\omega) + \sum_{l=1}^{N} [A_l(j\omega)\, e^{-jl\omega}] \otimes X(j\omega)$$

ant the output Fourier spectrum of the combined operator is

$$Y_1(j\omega) = X(j\omega) + \sum_{n=1}^{N} [A_n(j\omega)\, e^{-jn\omega}] \otimes X(j\omega) \tag{4.3.2}$$

$$- \sum_{n=1}^{N} [A_n(j\omega)\, e^{-jn\omega}] \otimes Y_1(j\omega)$$

We now consider the case when the operator is given by the cascade connection $\aleph_1\,\aleph_1\dagger$.

The output of the anti-null operator is given as

$$Z(j\omega) = X(j\omega) - \sum_{n=1}^{N} [A_n(j\omega)\, e^{-jn\omega}] \otimes Z(j\omega) \tag{4.3.3}$$

and the output Fourier spectrum of the combined operator $\aleph_1\,\aleph_1\dagger$ yields

$$Y_2(j\omega) = Z(j\omega) + \sum_{n=1}^{N} [A_n(j\omega)\, e^{-jn\omega}] \otimes Z(j\omega) \tag{4.3.4}$$

$$= X(j\omega) - \sum_{n=1}^{N} [A_n(j\omega)\, e^{-jn\omega}] \otimes Z(j\omega)$$

$$+ \sum_{n=1}^{N} [A_n(j\omega)\, e^{-jn\omega}] \otimes \left[X(j\omega) - \sum_{n=1}^{N} [A_n(j\omega)\, e^{-jn\omega}] \otimes Z(j\omega) \right]$$

Then Fourier spectrum of the output difference can be expressed as

$$Y_1(j\omega) - Y_2(j\omega) =$$

$$- \sum_{n=1}^{N} [A_n(j\omega)\, e^{-jn\omega}] \otimes \left[Y_1(j\omega) - Z(j\omega) - \sum_{n=1}^{N} [A_n(j\omega)\, e^{-jl\omega}] \otimes Z(j\omega) \right] \tag{4.3.5}$$

Proof of Sufficiency: if $\aleph_1 \aleph_1\dagger$ and $\aleph_1\dagger \aleph_1$ are commutable, then

$$Y_1(j\omega) - Z(j\omega) - \sum_{l=1}^{N} [A_l(j\omega)\, e^{-jl\omega}] \otimes Z(j\omega) = 0 \tag{4.3.6}$$

which results in

$$Y_1(j\omega) = Y_2(j\omega) = X(j\omega) \tag{4.3.7}$$

thus implying the transparency of the operators $\aleph_1 \aleph_1\dagger$ and $\aleph_1\dagger \aleph_1$.

Proof of Necessity: If the operator $\aleph_1 \aleph_1\dagger$ is transparent, i.e. $Y_1(j\omega) = X(j\omega)$, we have (4.3.6), and (4.3.5) that

$$Y_1(j\omega) - Y_2(j\omega) = 0$$

Hence, the operators $\aleph_1 \aleph_1\dagger$ and $\aleph_1\dagger \aleph_1$ are commutable.

Q.E.D.

It is easily seen that if the time-varying null operator is symmetric to the time-varying anti-null operator, then the time-varying null and anti-null operators are commutable, and the corresponding operator Q_1 is transparent. It is also easy to see that the one-sided almost-symmetrical time-varying null and anti-null operators are commutable and transparent, iff $\alpha \rightarrow 1^-$.

It should be noted that a necessary condition for an operator to be transparent is that its impulse response must be a δ-function, but this is not a sufficient condition. This is due to the fact that there exists the trivial case of a zero-order operator, or the direct connector, which is a transparent operator, but does not contain any null singularity.

4.4. Impulse Response of Time-Varying Anti-Null Operator $\aleph_1\dagger$

Consider a time-varying null operator, $\aleph_1[\ ] = 1 + \sum_{i=1}^{N} a_i(k)\, q^{-i}$. Let us embed such a time-varying null operator into a matrix representation

$$N_1 = \begin{bmatrix} \cdots & \cdots & \cdots & \cdots & & \\ \cdots & a_N(k_0) & \cdots & a_1(k_0) & 1 & \mathbf{0} \\ & \cdots & \cdots & \cdots & \cdots & \cdots \\ & & a_N(k_0-L+1) & \cdots & a_1(k_0-L+1) & 1 \\ & \mathbf{0} & & a_N(k_0-L) & \cdots & a_1(k_0-L) \quad 1 \ \cdots \\ & & & & \cdots & \cdots \quad \cdots \ \cdots \end{bmatrix}_{\infty\times\infty} \tag{4.4.1}$$

Given a signal vector $\hat{S}_2$, which does not belong to the null space of matrix N_1, i.e., $\hat{S}_2 \notin \Omega_{\aleph}$, to find the matrix representation of an anti-null operator is equivalent to finding an inverse matrix $N_1\dagger$, such that the transparency property, $N_1\dagger N_1 \hat{S}_2 = \hat{S}_2$ is satisfied.

Since matrix N_1 is a lower triangular banded matrix with unit diagonal entries, denoting its inverse as $N_1\dagger = [n_{ij}^*]$, it is well known that the inverse matrix can be written as [4.1]

$$\boxed{\begin{aligned} n_{ii}^* &= 1 && i = -\infty, \ldots, +\infty \\ n_{ij}^* &= -\sum_{l=i-N}^{i} a_l(k_0-i+1)\, n_{l,j}^* && \begin{matrix} j = -\infty, \ldots, +\infty \\ i = j+1, \ldots +\infty \end{matrix} \\ n_{ij}^* &= 0 && j > i \end{aligned}} \tag{4.4.2}$$

Now, let us consider an *Nth*-order time-varying null operator $\aleph_1$ with time-varying coefficients $a_l(k) \quad \forall l = 1, 2, \ldots N$. The impulse response of the time-varying anti-null operator $\aleph_1\dagger$ is *time-dependent*. In what follows, we give two kinds of presentation

for the impulse response of anti-null operator $\aleph_1\dagger$.

4.4.1. A Coefficient Based Presentation

The impulse response of $\aleph_1\dagger$ can be represented by its coefficients. Suppose that at time k_o an impulse $\delta(k-k_o)$ is applied to such an anti-null operator, then the input vector may be written as

$$\hat{S} = \left[\ldots 0 \underset{k_o}{1} 0 \ldots\right]^T.$$

The impulse response of the anti-null operator is given by the elements of the k_0th column of matrix $N_1\dagger$, and can be expressed as

$$h_{k_o}(k) = -\sum_{l=1}^{N} a_l(k)\, h_{k_o}(k-l)\, U(k-k_o)$$

where, $U(k-k_o)$ is a unit step function. This corresponds to the impulse response of an *Nth*-order AR system. Thus the output of the anti-null operator can be expressed as

$$y(k) = \sum_{k_o=0}^{\infty} x(k_o)\, h_{k_o}(k) = -\sum_{k_o=0}^{\infty} x(k_o) \sum_{l=1}^{N} a_l(k)\, h_{k_o}(k-l)\, U(k-k_o) \quad (4.4.3)$$

4.4.2. A W-System Based Presentation

An anti-null operator $\aleph_1\dagger$ is symmetrical to a null operator $\aleph_1$, and the coefficients of this null operator are constructed based on its W-system $\{\varphi_i(k)\}_{i=1}^{N}$. Therefore, the anti-null operator is in fact a function generator such that the impulse response of $\aleph_1\dagger$ is a causal function represented by a linear combination of functions $\{\varphi_i(k)\}_{i=1}^{N}$, and given by

$$h_{k_o}(k) = \sum_{l=1}^{N} w_l^{(k_o)}\, \varphi_l(k)\, U(k-k_o) \quad (4.4.4)$$

where, $\{w_l^{(k_o)}\}_{l=1}^{N}$ is a set of N weights, which satisfy the boundary condition at time k_o

$$\begin{aligned} &\sum_{l=1}^{N} w_l^{(k_o)}\, \varphi_l(k_o) = 1 \\ &\sum_{l=1}^{N} w_l^{(k_o)}\, \varphi_l(k_o+m) = n_{mk_o}{}^{*} \\ &m = 1, 2, \ldots, N \end{aligned} \quad (4.4.5)$$

where $n_{mk_o}^{*}$ is given by (4.4.2). From the N-linear equations (4.4.5), values of the weights $w_l^{(k_o)}$ can be obtained. Thus $h_{k_o}(k)$ satisfies the null condition of its corresponding time-varying null operator.

4.5. Some Additional Properties of the Anti-Null Operator

4.5.1. Using Anti-Null Operator to Reconstruct the Signal S_2

As mentioned earlier, any linear time-varying null operator $\aleph_1$ will introduce a certain amount of distortion to the signal $S_2 \in \overline{\Omega}_1$. Hence in order to keep the signal S_2 to be transparent at the output of the operator, a symmetric time-varying anti-null operator must be cascade connected to the null operator; in this case, the time-varying anti-null operator is used as a time-dependent interpolator in the reconstruction of the output signal.

Anti-null operator is a ***pure causal time-dependent interpolator*** and the interpolation function is a linear combination of the W-system of functions $\{\varphi_i(k)\}_{i=1}^{N}$. The interpolator can be written as

$$K_k(k) = \sum_{l=1}^{N} w_l^{(k_o)} \varphi_l(k)\, U(k-k_o) \quad \text{and} \quad K_{k_o}(k) \subset V_{k_o}$$

where $V_{k_o} = [k_o, \infty)$ and $V_1 \supset V_2 \supset \ldots \supset V_{k_o} \supset \ldots$

The input sequence of the anti-null operator is $x(k)$, thus the output of the anti-null operator is

$$y(k) = \sum_{k_o=0}^{\infty} x(k_o) K_{k_o}(k) = \sum_{k_o=0}^{\infty} \sum_{l=1}^{N} x(k_o) w_l^{(k_o)} \varphi_l(k)\, U(k-k_o) \qquad (4.5.1)$$

First, we show that the anti-null operator will play an important role in the reconstruction of $\bar{S}_2$, which is distorted by $\aleph_1$

$$\aleph_1[S_2] = \sum_{i=0}^{N} a_i(k)\, s_2(k-i) = \bar{s}_2(k) \qquad (4.5.2)$$

Applying the anti-null operator $\aleph_1^{\dagger}$

$$\aleph_1^{\dagger} \aleph_1[S_2] = \sum_{k_o=0}^{\infty} \sum_{l=1}^{N} \bar{s}_2(k_o)\, \hat{w}_l^{(k_o)} \varphi_l(k)\, U(k-k_o) \qquad (4.5.3)$$

Substituting (4.5.2) into (4.5.3)

$$\aleph_1^{\dagger}\aleph_1[S_2] = \sum_{k_o=0}^{\infty}\left(\sum_{i=0}^{N} a_i(k_o)\, s_2(k_o-i)\right)\sum_{l=1}^{N}\hat{w}_l^{(k_o)}\varphi_l(k)\,U(k-k_o) \tag{4.5.4}$$

Hence,

$$\aleph_1^{\dagger}\aleph_1[S_2] = \sum_{k_o=0}^{\infty}\sum_{i=1}^{N}\hat{w}_l^{(k_o)}\sum_{l=1}^{N} a_l(k_o)\,\varphi_l(k_o-l) \tag{4.5.5}$$

$$+\sum_{k_o=0}^{\infty} s_2(k_o)\,\delta(k-k_o) = S_2$$

Thus the signal $\tilde{s}_2(k)$ is reconstructed to S_2 by using anti-null operator.

4.5.2. Using Anti-null Operator $\aleph_1^{\dagger}$ to Pre-Distort the Signal Space

If a symmetrical anti-null operator is cascaded by a time-varying null operator, the input signal is pre-distorted by this anti-null operator. Such a pre-distortion of the signal space $\overline{\Omega}_1$ will be compensated by the time-varying null operator. The pre-distortion of the signal space is in fact an operation to pre-expand the signal space by the W-system. Let us consider a signal $S_2 = s_2(k)$ as an input of the anti-null operator $\aleph_1^{\dagger}$. Using the interpolation relationship given by (4.5.1), the output of the anti-null operator may be expressed as

$$\aleph_1^{\dagger}[S_2] = \sum_{k_o=0}^{\infty}\sum_{l=1}^{N} s_2(k_o)\, w_l^{(k_o)}\varphi_l(k)\,U(k-k_o) \tag{4.5.3}$$

where the interpolation weights $\{w_l^{(k_o)}\}_{l=1}^{N}$ can be obtained by using (4.4.5). If the output of the anti-null operator is now fed into the corresponding null operator, the output of the combined operator $\aleph_1\aleph_1^{\dagger}$ becomes

$$\aleph_1\aleph_1^{\dagger}[S_2] = \sum_{l=0}^{N} a_l(k)\sum_{k_o=0}^{\infty}\sum_{i=1}^{N} s_2(k_o)\, w_l^{(k_o)}\varphi_i(k-l)\,U(k-k_o-l) \tag{4.5.4}$$

$$\aleph_1\aleph_1^{\dagger}[S_2] = \sum_{k_o=0}^{\infty} s_2(k_o)\sum_{i=0}^{N}\sum_{l=0}^{N} a_l(k)\, w_l^{(k_o)}\varphi_i(k-l)\,U(k-k_o-l) \tag{4.5.5}$$

Since any linear combination of the W-system of functions will satisfy the null singularity of the null operator, by considering the boundary condition (4.4.5) we see that

$$\aleph_1 \aleph_1^{\dagger}[S_2] = \sum_{k_o=0}^{\infty} \sum_{l=1}^{N} s_2(k_o)\,\delta(k-k_o) = S_2(k) \tag{4.5.6}$$

Now, let us consider the same operation on S_1

$$\aleph_1^{\dagger}[S_1] = \sum_{k_o=0}^{\infty} \sum_{l=1}^{N} s_1(k_0)\,\bar{w}_l^{(k_o)}\,\varphi_l(k)\,U(k-k_o) \tag{4.5.7}$$

As in (4.5.3), the weights $\{\bar{w}_l^{(k_o)}\}_{l=1}^{N}$ may be evaluated by using (4.4.5). Applying the null operator to (4.5.7), we have

$$\aleph_1 \aleph_1^{\dagger}[S_1] = \sum_{l=0}^{N} a_l(k) \sum_{k_o=0}^{\infty} \sum_{i=1}^{N} s_1(k_0)\,\bar{w}_l^{(k_o)}\,\varphi_i(k-l)\,U(k-k_o-l) \tag{4.5.8}$$

The above relationship may be expressed as

$$\aleph_1 \aleph_1^{\dagger}[S_1] = \sum_{k_o=0}^{\infty} \sum_{i=0}^{N} \sum_{l=0}^{N} a_l(k)\,s_1(k_0)\,\bar{w}_l^{(k_o)}\,\varphi_i(k-l)\,U(k-k_o-l) \tag{4.5.9}$$

$$\aleph_1 \aleph_1^{\dagger}[S_1] = \sum_{k_o=0}^{\infty} \sum_{l=1}^{N} a_l(k_o)\,s_1(k_o-l) = 0 \qquad k \le N \tag{4.5.10}$$

$$\aleph_1 \aleph_1^{\dagger}[S_1] = \sum_{k_o=0}^{\infty} \sum_{i=1}^{N} s_1(k_0)\,\bar{w}_l^{(k_o)} \sum_{l=1}^{N} a_l(k)\,\varphi_i(k-l) = 0 \qquad k \ge N$$

It is seen that the anti-null operator plays an important role in the design of the transparent operator Q_1, and it is also seen that the anti-null operator can be used as an interpolator to reconstruct the signal space which is distorted by the time-varying null operator except for its null singularity, or it can be used to pre-expand the signal space by using the W-system of functions. Through the above analysis, it is shown in a constructive fashion that the anti-null operator plays a crucial role in the transparency property of the combined time-varying operator; besides, it also provides an explanation of the mechanism of transparency.

Lemma 4.5.1 *The time-varying null operator and its symmetrical anti-null operator possess following two basic properties.*

$$\boxed{\aleph_1[S_1+S_2]=\tilde{S}_2 \quad \aleph_1^{\dagger}[\tilde{S}_2]=S_2} \qquad \boxed{\aleph_1^{\dagger}[S_1+S_2]=\underline{S}_1+\underline{S}_2 \quad \aleph_1[\underline{S}_1+\underline{S}_2]=S_2} \tag{4.5.11}$$

Proof: (1) By null condition

$$\aleph_1[S_1]=\sum_{l=0}^{N} a_l(k)\,s_1(k-l)=0 \tag{4.5.12}$$

Therefore, $\aleph_1[S_1+S_2]=\tilde{S}_2$, and from (4.5.6), we get $\aleph_1^{\dagger}[\tilde{S}_2]=S_2$.

(2) Using (4.5.3) and (4.5.7), we have $\aleph_1^{\dagger}[S_1+S_2]=\underline{S}_1+\underline{S}_2$. Using (4.5.5) and (4.5.10), we obtain $\aleph_1[\underline{S}_1+\underline{S}_2]=S_2$

Q.E.D.

4.6. Higher-Order Time-Varying Transparent Operator

Lemma 4.6.1 *The time-varying null operator and the time-varying anti-null operators are pairwise commutable*

$$\boxed{\prod_{i=1}^{M}\aleph_i^{\dagger}\aleph_i=\prod_{j=1}^{M}\aleph_j\aleph_j^{\dagger}} \tag{4.6.1}$$

Proof: Based on Theorem 4.3.1, we known that $\aleph_i$ and $\aleph_i^{\dagger}$ are commutable, i.e. $Q_i=\aleph_i^{\dagger}\aleph_i=\aleph_i\aleph_i^{\dagger}$. By Lemma 4.5.1, we know that the operator Q_i is transparent to signal $S\in\Omega_i$, and the transparency is independent of the permutation of the index i.

Q.E.D.

Theorem 4.6.1 *A higher order operator Q_1 can be decomposed into lower order ones.*

$$Q_1^{[N]} = \prod_{i=1}^{M} Q^{[i]} \tag{4.6.2}$$

Proof: Suppose an *Nth*-order time-varying transparent operator $Q_1^{[N]}$ represents the signal space Ω_1 and $\Omega_1 \oplus \overline{\Omega}_1 = \Omega$. The signal space Ω_1 can be decomposed into subspaces as (according to the definition in Chapter 3)

$$\Omega_1 = \Omega_{l_1}^{(1)} \oplus \Omega_{l_2}^{(1)} \oplus \ldots \oplus \Omega_{l_M}^{(1)} \quad \text{and} \quad \sum_{i=1}^{M} l_i = N$$

Each subspace $\Omega_{l_i}^{(1)}$ is represented by a transparent operator $Q^{[i]}$ with order l. Since we have $Q^{[i]} = \aleph_i \aleph_i^{\dagger}$, by Lemma 4.6.1 we obtain (4.6.2).

Q.E.D.

As it is shown in Chapter 3, a higher-order time-varying null operator can not be decomposed into a lower-order ones by using root-factorization, see (3.3.2) in section 3.3. However, if we combine each lower-order time-varying null operator with its corresponding anti-null operator as one lower-order transparent operator, such a decomposition can be represented in a factorization form.

Corollary 4.6.1 *A higher order time-varying null operator can be pseudo factorized into lower-order ones by combining the lower-order null operators with the corresponding anti-null operators*

$$\chi = \prod_{i=1}^{M} \aleph_i \aleph_i^{\dagger} \tag{4.6.3}$$

Proof: According to Theorem 4.6.1, we known that if a higher dimensional signal space can be decomposed into lower dimensional subspaces $\Omega_{l_i}^{(1)}$, then the cascade connection of the lower order transparent operators $Q^{[i]} = \aleph_i \aleph_i^{\dagger}$ representing the corresponding subspaces will result in a higher-order transparent operator; such an operator exactly represents the direct sum of these signal subspaces. Therefore a higher-

order time-varying null operator may be pseudo factorized in the form given by (4.6.3).

Q.E.D.

Recall that in Chapter 3, we showed that a higher-order time-varying null operator can neither be decomposed by root-factorization nor can it be represented as a product of the lower order ones. Corollary 4.5.1 shows that if it is combined with the corresponding anti-null time-varying operator, a cascade connection (pesudo product) of lower-order time-varying null operator can represent the higher-order time-varying null operator.

Lemma 4.6.2 *The signal space can be partitioned and separated by using the decomposed operator* Q_i

$$\prod_{\substack{i=1 \\ i \notin \Xi}}^{M} Q_i\left[\sum_{i=1}^{M} S_i\right] = \sum_{i \in \Xi} S_i \tag{4.6.4}$$

Proof: Since a signal space is defined by a transparent operator, by Theorem 4.6.1, a higher-order transparent operator can be decomposed into lower-order transparent operators in cascade connection; therefore, singal space is partitioned by the decomposed lower-order transparent operators. Furthermore, the parititioned signal spaces have no intersections.

Q.E.D.

Theorem 4.6.3 *(Separability of Signals) If two signal subspaces can be represented by two different time-varying null operators, then these two signal subspaces can be separated by using the operators* Q_1 *and* Q_2.

Proof: If for a certain signal subspace Ω_1 there exists a time-varying null operator, then the corresponding transparent operator can be constructed. If the same is true for the signal subspace Ω_2 and $\Omega_1 \cap \Omega_2 = \varnothing$, then the signals belonging to the signal subspaces Ω_1 and Ω_2 can be respectively separated by the transparent operators Q_1 and Q_2.

Q.E.D.

4.7. Almost-Symmetrical Operator Q_1^{α}

4.7.1. Discussion of N-Uncertain Initial States of Operator $\aleph_1$

Our discussion in the previous section about the transparency of the perfect symmetrical operator Q_1 is based on the assumption that the system is in the steady state. Obviously this is an ideal case; since any physical system has to be causal, once the input is applied to the system at a certain time instant, the system contains a priori unknown initial states.

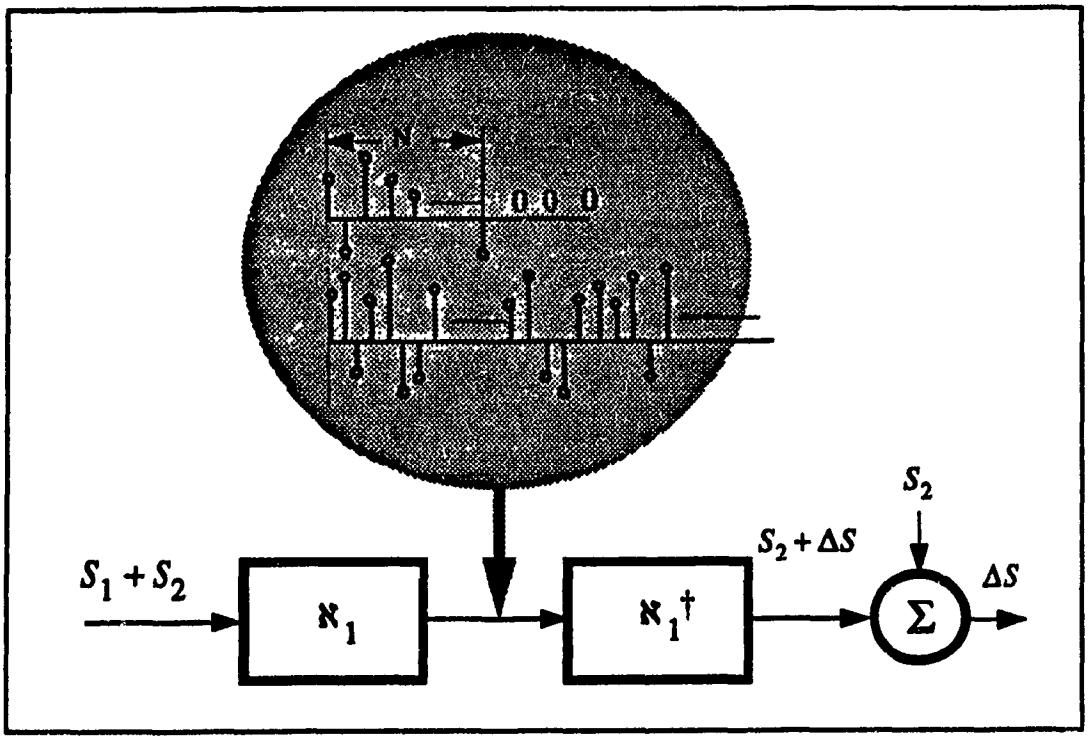

Fig.4.1 N- a priori Unknown Initial States in Operator Q_1^{+}

Let us elaborate this point in more detail. Suppose an input signal is applied to an *Nth*-order null operator $\aleph_1$. Because there are *N* initial states in the null operator, then the null condition will not be satisfied, at the first *N* samples. Thus, the null operator will produce *N* uncertain outputs, and these *N* uncertain outputs will be fed into the anti-null operator, $\aleph_1^{\dagger}$. This, in turn, produces an undesired residual output ΔS, (see Fig.4.1), while in the ideal case, the output for S_1 should be zero.

4.7.2. Residual ΔS Generated From N-Uncertainty Initial States

Consider a time-varying null operator, $1 + \sum_{i=1}^{N} a_i(k)\, q^{-i}$. Let us embed such a time-varying null operator into a matrix representation

$$N_1^{[k]} = \begin{bmatrix} 1 & & & & & & \\ a_1(k-1) & 1 & & & & & \\ \cdots & \cdots & \cdots & & & \mathbf{0} & \\ a_N(k-N+1) & a_{N-1}(k-N+1) & \cdots & 1 & & & \\ & \cdots & \cdots & \cdots & \cdots & & \\ \mathbf{0} & a_N(k-L+2) & a_{1-1}(k-L+2) & \cdots & a_1(k-L+2) & 1 & 0 \\ & & a_N(k-L+1) & a_{N-1}(k-L+1) & \cdots & a_1(k-L+1) & 1 \end{bmatrix}_{L\times L} \tag{4.7.1}$$

Also, let the input signal vector, $\mathring{S}_1 = \left[s_1(k), s_1(k-1), \ldots s_1(k-L+1)\right]$ and the signal vector $\mathring{S}_2 = \left[s_2(k), s_2(k-1), \ldots s_2(k-L+1)\right]$, where $L \geq N+1$. Since the initial condition of the time-varying null operator is arbitrary, the first N samples of the output of the null operator is non-zero, i.e.

$$N_1^{[k]} \mathring{S}_1 = \left[\underbrace{x_0 \ldots x_N}_{\mathrm{N}} 0 \ldots 0\right]^T \tag{4.7.2}$$

where the N non-zero values is generated due to the N unknown initial conditions of the time-varying null operator. We will show that these non-zero elements will cause a residual output of the anti-null operator, and such a residual output is only produced from signal $\mathring{S}_1$, which are supposed to be perfectly cancelled by the time-varying null operator $N_1^{[k]}$. Furthermore the non-zero elements can be expressed as

$$x_j = \sum_{m=0}^{j} a_m(k-j+1)\, x(k+m) \qquad j = 0, 1, \ldots, N \tag{4.7.3}$$

Now let us find the out of the anti-null matrix $(N_1^{[k]})^{-1} = \left[n_{ij}^{*}\right]$. It is well known that the *exact inverse* of the lower-triangular-banded matrix $N_1^{[k]}$, is another lower-

triangular-banded matrix[4.1], which can be found by using the following formula

$$\begin{aligned} n_{ii}^{*} &= 1 && i = 1,2,\ldots L \\ n_{ij}^{*} &= -\sum_{l=j}^{i} a_l(k-i+1)\,n_{lj}^{*} && i = 1,2,\ldots,N \\ n_{ij}^{*} &= -\sum_{l=i-N} a_l(k-i+1)\,n_{lj}^{*} && j = 1,2,\ldots,L-1 \\ & && i = N+1,\ldots L \\ n_{ij}^{*} &= 0 && j>i \end{aligned} \tag{4.7.4}$$

The output of inverse of matrix is

$$[N_1^{[k]}]^{-1} N_1^{[k]} \hat{S}_1 = \Delta\hat{S}_1 \neq 0 \tag{4.7.5}$$

$$[N_1^{[k]}]^{-1} N_1^{[k]} \hat{S}_2 = \hat{S}_2 \tag{4.7.6}$$

At the output of the anti-null operator, it can be seen that at the output of the anti-null operator, $\hat{S}_2$ ideally transparently passes the anti-null operator, while $\hat{S}_1$ is not ideally cancelled by the null operator, therefore it has a residual output at the anti-null operator, such a residual output $\Delta S = \Delta\hat{S}_1$ can be expressed as

$$\Delta\hat{S}_1 = \left[\Delta s_1(k)\ \Delta s_1(k-1)\ \ldots\ \Delta s_1(k-L+1)\right]^T$$

where,

$$\begin{aligned} \Delta s_1(k-i+1) &= \sum_{j=1}^{i}\sum_{m=0}^{j} n_{ij}^{*}\, a_m(k-j+1)\,x(k-m) && i = 1,2,\ldots,N-1 \\ \Delta s_1(k-i+1) &= \sum_{j=1}^{N-1}\sum_{m=0}^{N-1} n_{ij}^{*}\, a_m(k-j+1)\,x(k-m) && i = N,N+1,\ldots,L \end{aligned} \tag{4.7.7}$$

4.8. Trade-off Between Transparency and Observation Time

As we have already seen, because of the N uncertain initial conditions, the causal transparent operator Q_1^{+} can not provide ideal transparency. In what follows, we investigate the trade-off between transparency and observation time, and show that

transparency can not be achieved within a short observation time, but it can be almost ideally attained by introducing a certain strategy to control the symmetrical nature of operator Q_1^+ .

Let us consider the null matrix (4.7.1). If we introduce a one-sided symmetrical factor in the anti-null operator and denote such null matrix as $N_1^{\alpha[k]}$.

$$N_1^{\alpha[k]} = \begin{bmatrix} 1 & & & & & \\ \alpha a_1(k-1) & 1 & & & \mathbf{0} & \\ \cdots & \cdots & & & & \\ \alpha^2 a_N(k-N+1) & \alpha a_{N-1}(k-N+1) & 1 & & & \\ & \cdots & \cdots & \cdots & & \\ & \alpha^N a_N(k-L+2) & \cdots & \alpha a_1(k-L+2) & 1 & 0 \\ \mathbf{0} & & \alpha^N a_N(k-L+1) & \cdots & \alpha a_1(k-L+1) & 1 \end{bmatrix}_{L\times L} \tag{4.8.1}$$

We know from (4.7.2) that the anti-null matrix $[N_1^{\alpha[k]}]^{-1} = [n^{*\alpha}_{ij}]$ can be expressed as

$$\begin{aligned} & n^{*\alpha}_{ii} = 1 && i = 1, 2, \ldots L \\ & n^{*\alpha}_{ij} = -\sum_{l=j}^{i} \alpha^l a_l(k-i+1)\, n^{*\alpha}_{lj} && i = 1, 2, \ldots, N-1 \\ & n^{*\alpha}_{ij} = -\sum_{l=i-N}^{i} \alpha^l a_l(k-i+1)\, n^{*\alpha}_{lj} && \begin{matrix} j = 1, 2, \ldots, L-1 \\ i = N+1, \ldots L \end{matrix} \\ & n^{*\alpha}_{ij} = 0 && j > i \end{aligned} \tag{4.8.2}$$

In the case where the one-sided almost-symmetrical operator Q_1^+ is used, i.e using $N_1^{[k]}$ as null matrix and $[N_1^{\alpha[k]}]^{\cdot}$ as anti-null matrix, then the residual output for S_1 is given as

$$\Delta s_1(k-L+1) = -\sum_{j=1}^{N-1} \sum_{l=L-N}^{L} \sum_{m=0}^{N-1} \alpha^l a_l(k-L+1)\, n^{*\alpha}_{lj} a_m(k-j+1)\, x(k-m) \tag{4.8.3}$$

After some manipulation, we find

$$\Delta s_1(k-L+1) = o(\alpha^L) \tag{4.8.4}$$

Since $\alpha < 1$, $\Delta s_1(k-L+1) \to 0$ as $L \to \infty$

Since the operator Q_1^+ is not perfectly symmetrical, perfect transparency can not be achieved for S_2 and the residual output error of S_2 is

$$\delta \hat{S}_2 = \hat{S}_2 - [N_1^{\alpha[k]}]^{-1}(N_1^{[k]})\hat{S}_2 = [N_1^{\alpha[k]}]^{-1}(N_1^{\alpha[k]} - N_1^{[k]})\hat{S}_2 \qquad (4.8.5)$$

Denoting

$$N_1^{\alpha[k]} - N_1^{[k]} = \begin{bmatrix} 0 & & & & & & & \\ \delta a_1(k) & 0 & & & & & & \\ \delta^2 a_2(k-1) & \delta a_1(k-1) & & & & & & \\ \cdots & \cdots & \cdots & & & & & \\ 0 & \delta^N a_N(k-1) & \cdots & \delta a_1(k-N) & & & & \\ & \cdots & \cdots & \cdots & \cdots & \cdots & & \\ & 0 & \delta^N a_N(k-L+1) & \cdots & \delta a_1(k-L+1) & 0 & \cdots & \\ & 0 & 0 & \delta^N a_N(k-L) & \cdots & \delta a_1(k-L) & 0 & \end{bmatrix}$$

where $\alpha^p - 1 = \delta^p$. If $\alpha \to 1^-$ then $\delta \to 0^-$, and we have

$$\Delta s_2(k-L+1) = -\sum_{j=1}^{L-1}\sum_{m=1}^{N-1}\sum_{l=L-N}^{L} \alpha^l a_l(k-L+i)\, n^*_{ij}\, \delta^m a_m(k-j+1)\, x(k-m) \qquad (4.8.6)$$

It is easy to find that

$$\Delta s_2(k-L+1) = o(\alpha\delta) \qquad (4.8.7)$$

so the total residual out-put of the one-sided almost-symmetrical operator Q_1^+ is given by

$$\Delta s(k-L+1) = \Delta s_1(k-L+1) + \Delta s_2(k-L+1) = o(\alpha^{L-N}) + o(\alpha\delta) \qquad (4.8.8)$$

In what follows, we present computer simulation results to illustrate the transparency properties of a second-order almost-symmetrical time-varying operator Q_1^{α}. Fig 4.2a-c show the case where the null condition is not satisfied at the first N samples.

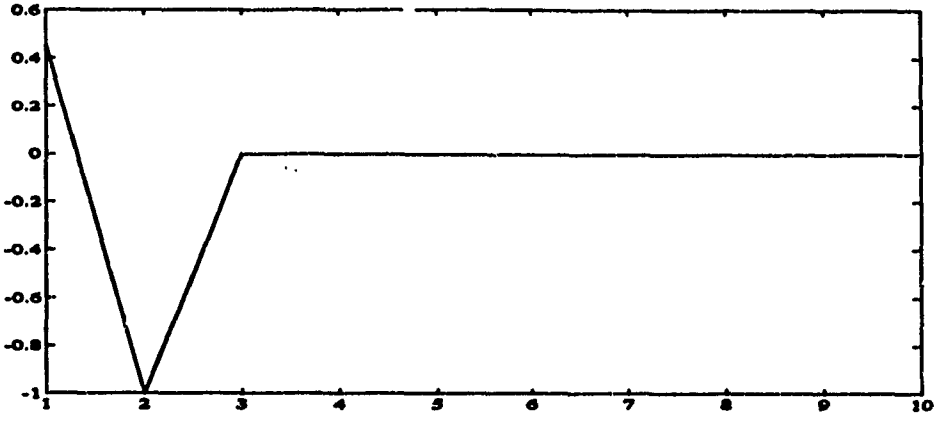

Fig.4.2.a Output of Second Order Time-Varying Null Operator $\aleph_1$ (Input is S_1) Notice that the First Two Samples do not Satisfy the Null Condition

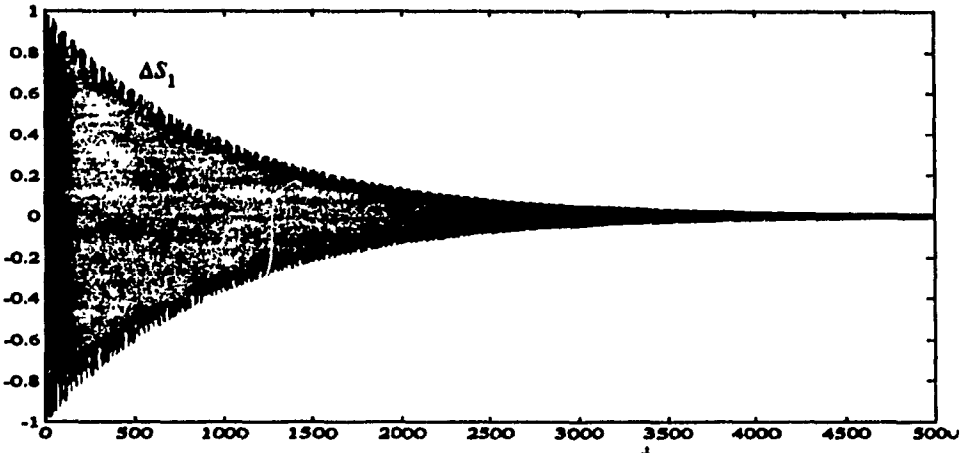

Fig.4.2.b The Output Residual ΔS_1 of Anti-Null Operator $\aleph_1^{\alpha\dagger}$ with Input Given as in Fig.4.2.a

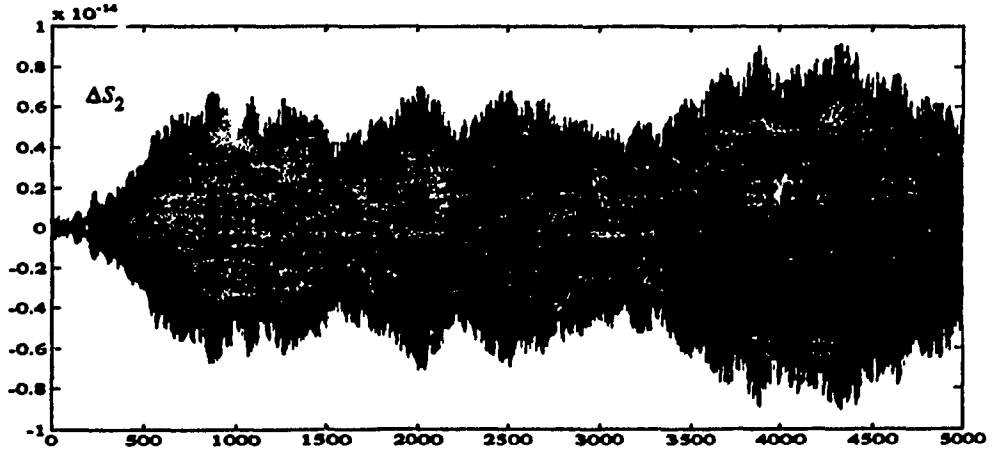

Fig.4.2.c The Output of Residual ΔS_2 of Transparent Operator Q^{α}_1

4.8.1. General Condition on Symmetrical Factor

Discussion 1 If the symmetrical factor is a fixed value $\alpha < 1$, then the residual from S_1, $\Delta s_1(L) \to 0$ as observation time $L \to \infty$. More precisely, for $L = 2/(1-\alpha)$, we have $\Delta s_1(L) = 0.1\Delta s_1(0)$. However, if $\alpha \neq 1$, i.e. $\delta \neq 0$, the residual from S_2, $\Delta s_2(L) \neq 0$, thus perfect transparency can not achieved. On the other hand, the residual $\Delta s_2(L)$ can be uniformly approached to an arbitrarily small value, if the symmetrical factor approaches unity, i.e. $\alpha \to 1^-$. This means the observation time L must be sufficiently long enough so that the residual $\Delta S_1(L)$ uniformly approaches an arbitrarily small value too. In conclusion, transparency can be achieved with arbitrary accuracy, if (1) the symmetrical factor $\alpha \to 1^-$, and (2) the observation time $L \to \infty$.

Discussion 2 Within a finite observation interval, transparency can not be achieved perfectly. Based on the analysis above, we know that we have to trade-off transparency with observation time, and therefore, one must find a trade-off between the symmetrical factor α and the observation time L. Naturally, the question arises, as to how to chose the symmetrical factor α, for given a finite observation time, such that the transparency of the one-sided almost-symmetrical operator Q_1^+ may be achieved optimally under

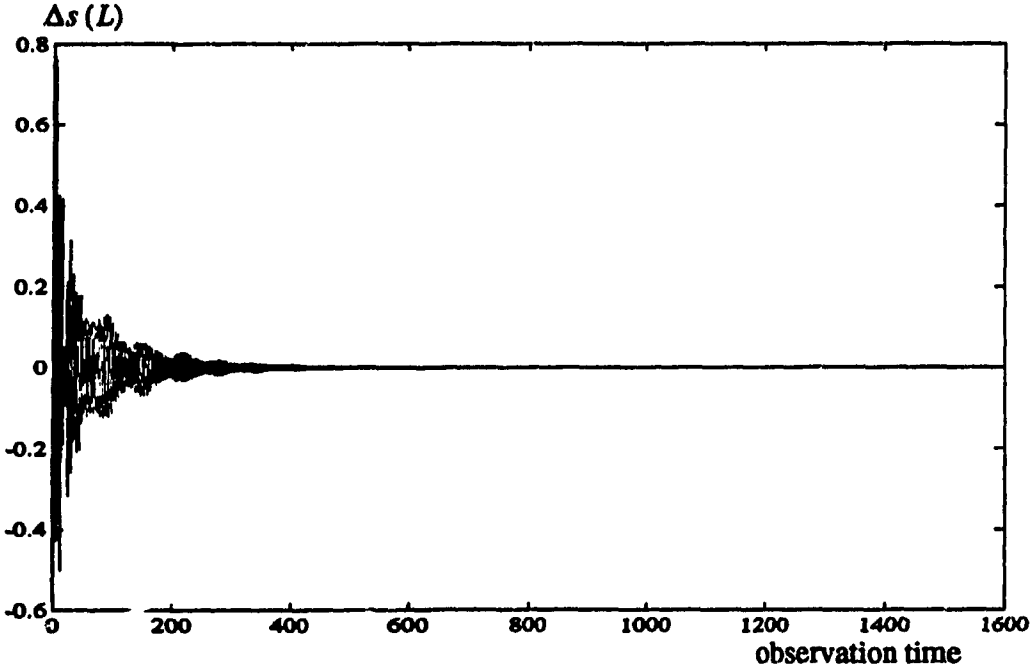

Fig.4.3 The Residual Out of One-Sided Almost-Symmetrical Time-Varying Transparent Operator with Exponential Time-varying Symmetrical Factor

certain criteria. This is a very interesting issue to be investigated. One possible solution

is to chose a time-varying symmetrical factor α. The symmetrical factor is varied according to a pre-determined rule; for example, the symmetrical factor exponentially approaching unity (as suggested in [4.4]). Fig.4.3 shows an example where the residual output approaches zero as the symmetrical factor exponentially approaches unity.

Discussion 3 How to overcome the symmetry property of the transparent operator Q_1 and to implement it as a physically realizable operator Q_1^+ is still an open issue. The introduction of the one-sided almost-symmetrical operator Q_1^α is one possible simple way.

4.8.2. Almost-Symmetrical Time-Varying ARMA Model

We adopt the conventional terminology in the signal processing context, and call the one-sided almost-symmetrical transparent operator as ***Almost-Symmetrical Time-Varying ARMA Model*** in the subsequent Chapters. This special ARMA model is described in (4.2.10).

4.9. Examples of Using Anti-Null Operator

In what follows, we present three examples to show the importance of the design of anti-null operators.

Example 4.1 Consider a second-order fast time-varying one-side almost symmetrical operator, whose coefficients are fast time-varying and constructed based on a single-tone modulated wide-band FM signal. The input signal is a sinusoid with a fixed frequency, whose Fourier spectrum is shown Fig.4.4.-1. Fig.4.4.-2 illustrates the output of the time-varying null operator; the true sinusoid is distorted by the spurious spectral lines introduced by the time-varying null operator. Notice that the circled spectral lines are undesired ones which are even stronger than the true spectral lines. As the symmetric factor approaches unity, the spurious spectral lines are compensated for, and they disappear at the output.

Example 4.2 Consider a piece-wise-constant image corrupted by a 100% uniform noise. (The Fourier spectrum of the image and noise are overlapping). We use three methods to cancel the noise: (1) Standard median filter with a window size 2 by

2, (2) A null operator for DC image with a window size 2 by 2 given by

$$y(i,j) = (1 - q_1^{-1} - q_2^{-1} + q_1^{-1}q_2^{-1})\,x(i,j)$$

and (3) An almost-symmetrical transparent operator with a window size 2 by 2 given by

$$(1 - \alpha q_1^{-1} - \alpha q_2^{-1} + \alpha^2 q_1^{-1} q_2^{-1})\,y(i,j) = (1 - q_1^{-1} - q_2^{-1} + q_1^{-1}q_2^{-1})\,x(i,j)$$

In Fig.4.5-a the input signal to noise ratio is -6dB, while in Fig.4.5-b the input signal to noise ratio is -12dB.

Example 4.3. A image is superimposed by a 2-D FM signal

$$e(i,j) = \sin[\omega_1 i + \beta_1 \sin(\omega_{m1} i) + \omega_2 j + \beta_2 \sin(\omega_{m2} j)]$$

The Fourier spectrum of the image and the Fourier spectrum of the 2-D FM signal overlap. We use two operators to separate the image from the 2-D FM signal: (1) a 2nd-Order time-varying 2-D null operator (see Appendix 4.3); (2)a 2nd-order almost-symmetrical time-varying operator. The results show that it is very important to combine null and anti-null operators to achieve signal separation, and are illustrated in Fig. 4.6.

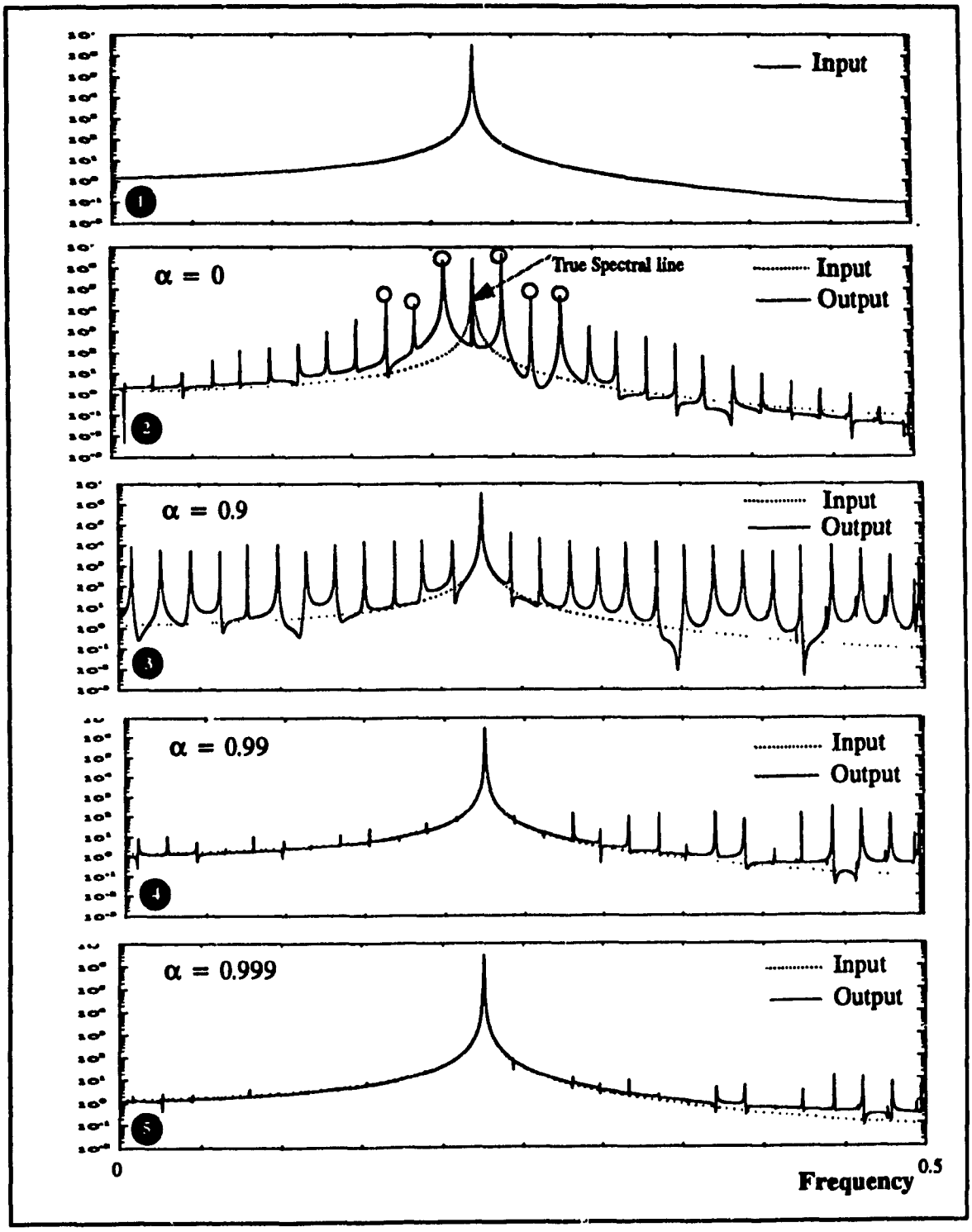

Fig.4.4 Fourier Spectrum of Input and Output of One-Sided Almost-Symmetrical Operator Q_1^{α}

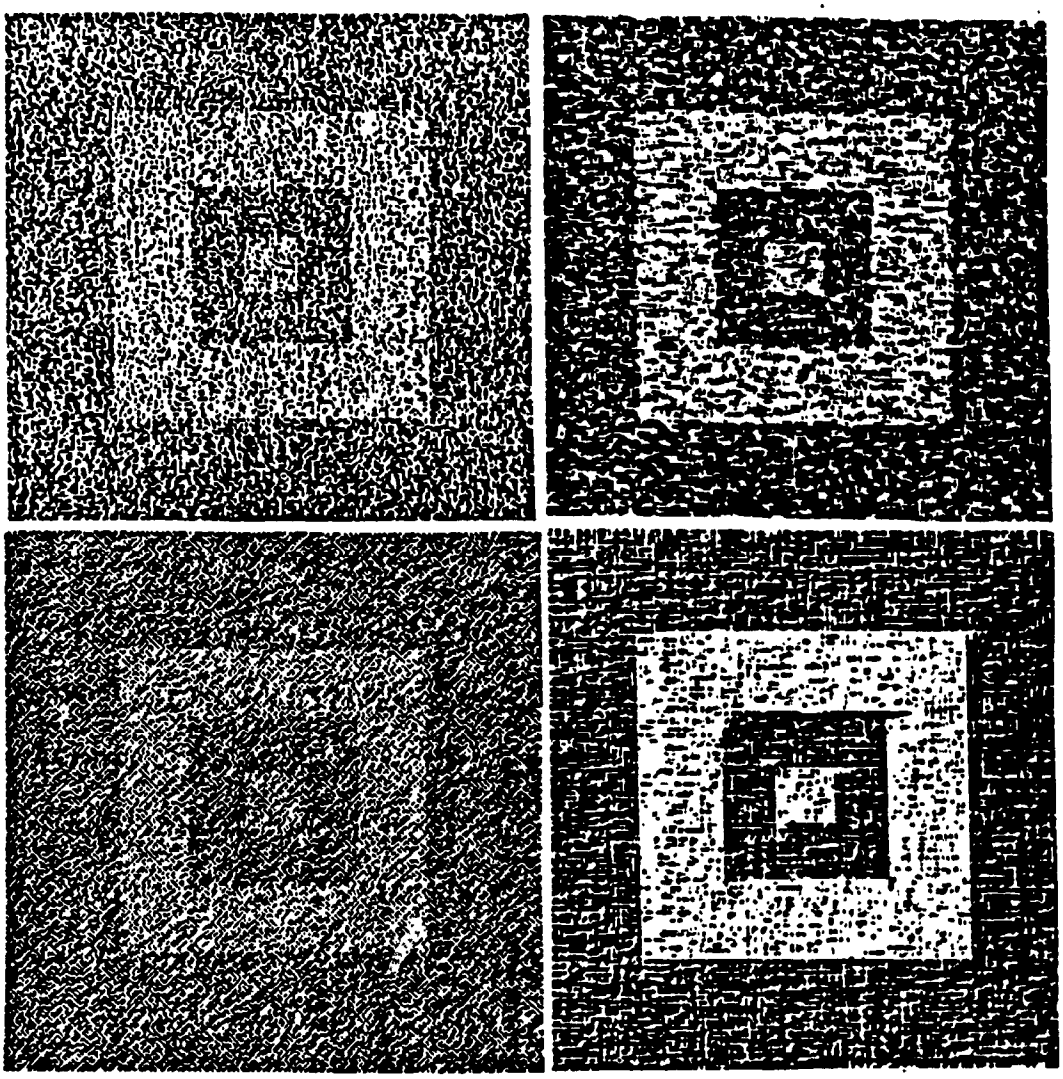

A	B
C	D

A. Input Noisy Image *B.2 by 2 Standard Median Filtering*
C. 1st-Order -2D Null Operator Output
D. 1st-Order -2D Transparent Operator Output

Fig.4.5.a Noise Cancellation Using 1st-Order 2-D Transparent Operator

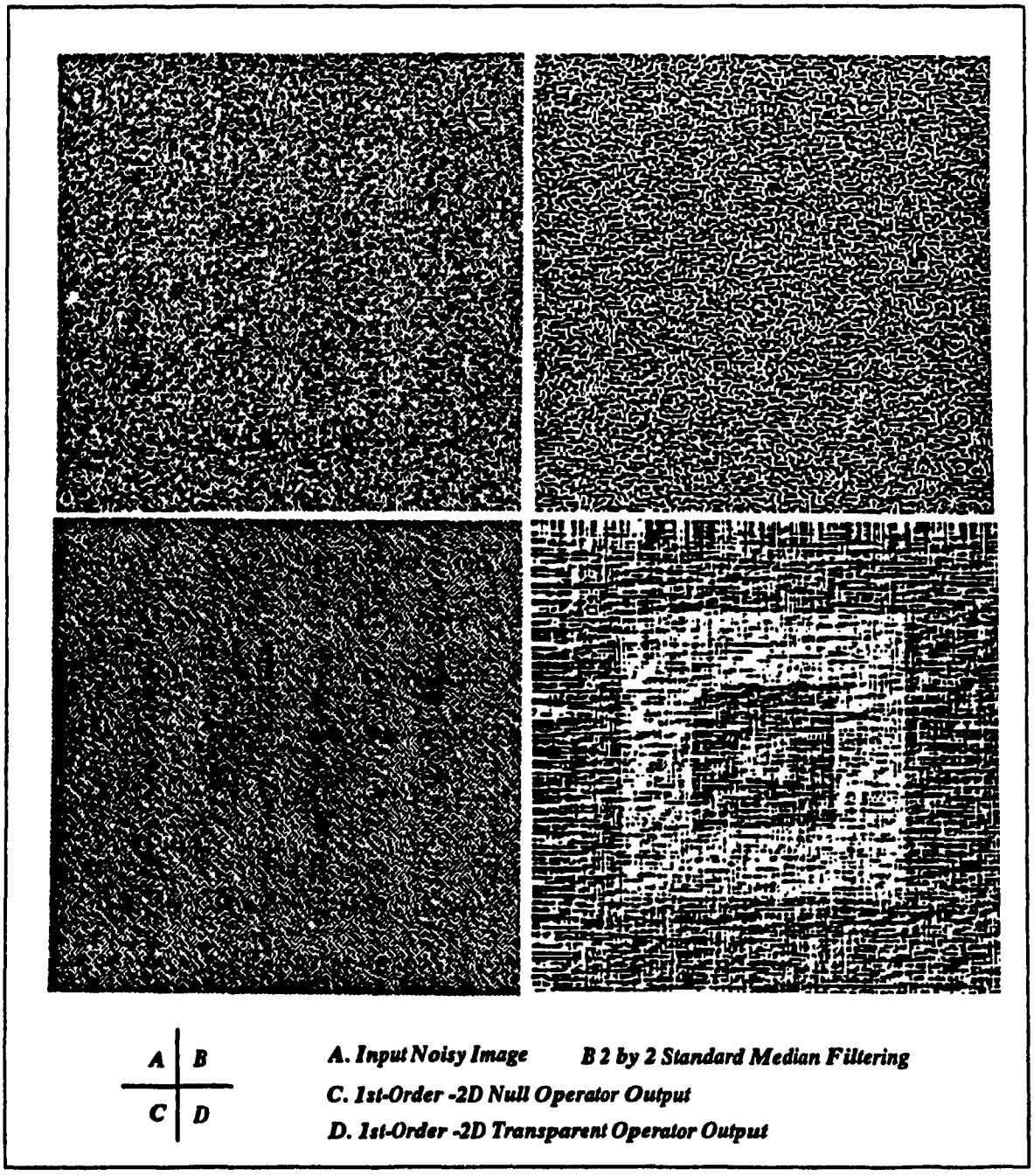

Fig.4.5.b Noise Cancellation Using 1st-Order 2-D Transparent Operator (Strong Noise Case)

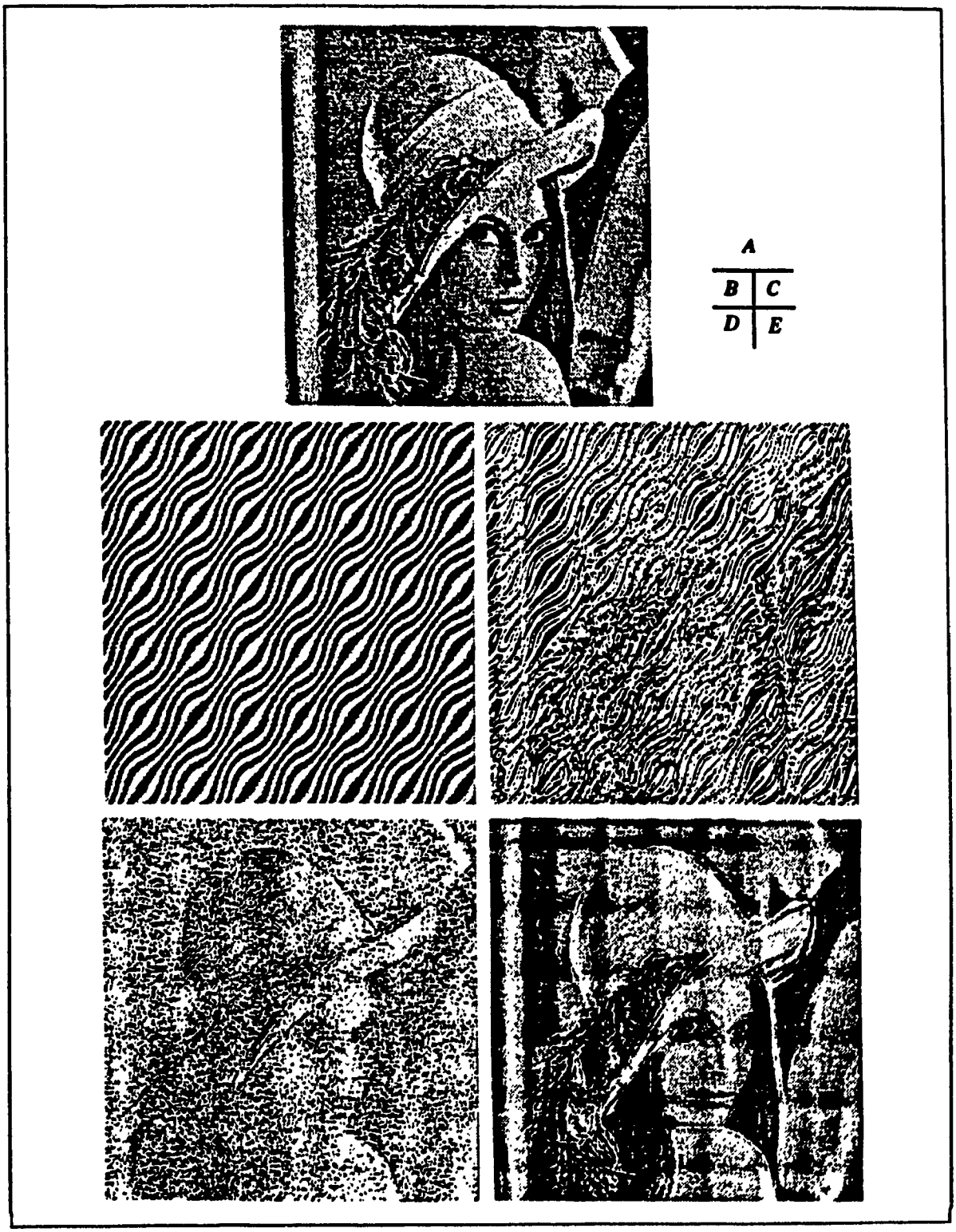

Fig.4.6 Separation of 2-D Signals with Overlapping Fourier Spectra Using Time-Varying Transparent Operator (A)-The Original Image (B)-2-D FM Signal. (C)-Superimposed Image with 2-D FM Signal (D)-Output of 2-D Time-Varying Null Operator (E)-Output of 2-D Time-Varying Transparent Operator

References

[4.1] G. H. Golub and C.F. Van Loan, "*Matrix Computations*", John Hopkins University Press, 1983

[4.2] D. Wulich, E. I. Plotkin, M. N. S. Swamy and W. Tong, "Externally Controlled Time-Varying Notch Filter", *Proceedings ISCAS91*, pp.2061-2064, 1991, Singapoure.

[4.3] B. D. Rao and R. Peng, "Tracking Characteristic of the Constrained IIR Adaptive Notch Filter", *IEEE Trans. on ASSP*, Vol. 36, pp.1466-1479, Sept. 1988

[4.4] A. Nehorai, "A Minimum Parameter Adaptive Notch Filter with Constrianed Poles and Zeros", *IEEE Trans on ASSP* Vol. 33, pp. 983-996, Aug. 1985

Chapter 5

Stability of Linear Time-Varying Autonomous System

5.1. Introduction

In previous Chapters, we investigated the theoretical aspects of the design of a *ASTV-ARMA Model* which combines a linear time-varying null operator and an anti-null operator. In this chapter, the stability issues related to such a model will be discussed. Although there are many comprehensive results on stability of linear time-invariant (LTI) systems [5.1] [5.2], unfortunately few results are known about the stability of discrete linear time-varying (LTV) systems [5.1] [5.3]. In this chapter, we present some new results on the BIBO stability of LTV systems.

In LTI system, the stability condition may be described by the *location* of the poles of transfer function of the system. The LTI system is absolutely stable iff these poles are located inside the unit disc. However, a direct extension of these results to the LTV system is not applicable, since the transfer function becomes a function of time. For a LTV system the most adequate description is based on the eigenvalues of a corresponding companion matrix. It should be pointed out that only in the case of an LTI system, these eigenvalues are equivalent to the poles of the transfer function.

We will show that for a BIBO stable LTV system, the module of the eigenvalues of the system are not necessarily inside the unit disc. On the other hand, we also show that even in the case where the module of the eigenvalues of an LTV system are inside the unit disc, it is not sufficient to make the LTV system BIBO stable.

We present two newly discovered *local instabilities* of a LTV system. An investigation of such local instability properties leads to the establishment of new criteria for the stability of a LTV system. These results should provide an insight and clear some of the issues that researchers have faced while using time-varying filters in their work.

A detailed study is carried out for the first and second-order LTV systems. It is interesting to note that the admissible area of the first and second order LTV systems for modelling a second-order analytical signal is much wider than Jury's classical result [5.2]. Especially, the stability of the discrete Mathieu equation is studied.

5.2. Preliminaries

Note that for any given LTV-ARMA model, the MA part is always stable. The stability problem arises only from the AR part [1]. Let us consider the following Nth-order LTV autonomous system with real time-varying coefficients

$$y_k = -a_1(k)\,y_{k-1} - a_2(k)\,y_{k-2} - \ldots - a_N(k)\,y_{k-N} \tag{5.2.1}$$

or in a state space representation form

$$Y(k+1) = A(k)\,Y(k) \tag{5.2.2}$$

where $Y(k) = \left[y_{k-1}\; y_{k-2} \cdots y_{k-N}\right]^T$ and the state transition matrix which is also called the *companion matrix* is given by

$$A(k) = \begin{bmatrix} -a_1(k) & -a_2(k) & \ldots & -a_N(k) \\ 1 & 0 & \ldots & 0 \\ 0 & 1 & \ldots & 0 \\ \ldots & \ldots & \ldots & \ldots \\ 0 & \ldots & 0 & 1 \end{bmatrix} \tag{5.2.3}$$

In the time-invariant case, $A(k)$ is a fixed value matrix A and the BIBO stability of such a system was given a century ago by Lyapunov in 1892 [5.4], and for its discrete

1. We only discuss the 1-D LTV model.

time version by Kalman and Bertram in 1960 [5.5] which states: *given an arbitrary symmetric positive definite matrix* $Q \in \Re^{N\times N}$ *there exists a symmetric positive definite matrix* $\Pi \in \Re^{N\times N}$ *such that* Π *is the unique solution of the linear matrix equation*

$$A^T \Pi A - \Pi = -Q \tag{5.2.4}$$

iff the module of the eigen values of the companion matrix A are less than unity. The positiveness of matrix Π is associated with the Lyapunov energy function being monotonicly decreasing.

In the following sections, we will extend this result to a LTV system, and will establish several criteria for the BIBO stability of an *Nth*-order LTV system. Before proceeding to derive the main results, we need to chose and justify our definition of a special norm for the matrix $A(k)$.

Definition 5.2.1 *The spectral radius* $\rho(A)$ *of a matrix A is*

$$\rho(A) = max\{|\lambda|:\ \lambda \ is\ an\ eigen\ value\ of\ A\ \}$$

Lemma 5.2.1 *Let A be a* $N\times N$ *matrix and* $\varepsilon > 0$ *be given. There exists a matrix norm* $\| \ \|^\dagger$ *such that* $\rho(A) < \|A\|^\dagger < \rho(A) + \varepsilon$

Proof: By Shur triangularization theorem [5.6], there exists a unitary matrix U and an upper triangular matrix Δ such that $A = U^H \Delta U$, where H denotes the Hermitian transpose.

Let us introduce the diagonal matrix $D(t) = diag(t, t^2, \ldots, t^N)$ and compute

(5.2.5)

$$D(t)\Delta D(t)^{-1} = \begin{bmatrix} \lambda_1 & t^{-1}d_{12} & t^{-2}d_{13} & \ldots & t^{-n+1}d_{1N} \\ 0 & \lambda_2 & t^{-1}d_{23} & \ldots & t^{-n+2}d_{2N} \\ 0 & 0 & \lambda_3 & \ldots & t^{-n+3}d_{3N} \\ & \ldots & \ldots & \ldots & \\ 0 & 0 & 0 & \ldots & t^{-1}d_{N-1,N} \\ 0 & 0 & 0 & 0 & \lambda_N \end{bmatrix}$$

Thus, for $t > 0$ large enough, the sum of all the absolute values of the off-diagonal entries of (5.2.6) gives

$$\sum_{i=1}^{N} t^{-j+1} d_{ij} < \varepsilon \qquad \forall j \in 1, 2, \ldots N$$

In particular, if t is large enough, by definition of the maximum column sum matrix norm $\| \ \|_1$

$$\left\| D(t) \Delta D(t)^{-1} \right\|_1 \leq \max_{1 \leq j \leq N} \sum_{i=1}^{N} t^{-j+1} d_{ij} + \lambda_j \leq \rho(A) + \varepsilon \tag{5.2.6}$$

Thus given a matrix B, we define

$$\|B\|^{\dagger} \equiv \left\| D(t)\, U^H B U D(t)^{-1} \right\|_1 = \left\| \left(UD(t)^{-1}\right)^{-1} B \left(UD(t)^{-1}\right) \right\|_1$$

Therefore $\| \ \|^{\dagger}$ is a matrix induced norm with $\|A\|^{\dagger} \leq \rho(A) + \varepsilon$. Since for any matrix induced norm it should have the lower bound

$$\|A\|^{\dagger} \geq \rho(A)$$

then it is easy to show that as $t \rightarrow \infty$

$$\rho(A) = inf\{\|A\|^{\dagger}\}$$

Q.E.D.

The purpose of this lemma is to chose the module of the eigenvalues or the spectral radius of the matrix A as a particular norm[1] in order to derive BIBO stability results. It will be seen that these results can be explicitly expressed in terms of the module of the eigen values, thus leading to a purely algebraic procedure for checking the BIBO stability of LTV systems.

---

1. In this chapter we denote the matrix induced norm as $\|A(k)\| \equiv \rho_A(k)$

5.3. BIBO Stability of Nth-Order Discrete Linear Time-Varying System

In what follows, we first present derivation of the main results, then state several theorems on the BIBO stability for a LTV system. We start from the regularization of the module of the eigen values in the situation where this module can temporarily be outside the unit disc. Moreover, if the LTV system is BIBO globally stable, then it is possible to convert such a LTV system into a new-time-domain based on the eigen value regularization. In such a situation LTV system is locally unstable in the sense that the output of the LTV system generates a burst. We shall show that with such kind of a local instability, the system may be globally BIBO stable.

5.3.1. Constructing a System in New-Time-Domain without Local Instability of the First Kind

Definition 5.3.1 *For a LTV system* $A(k)$, *if* $\exists k \in Z^{+}$ *such that* $\rho_A(k) > 1$, *then this is called local instability of the first kind (LIFK).*

Let us consider a LTV system which possesses LIFK. In what follows, we will show that under certain conditions, the companion matrices can be converted into a new time-domain, where the new system has no LIFK.

Suppose, $\rho_A(k) > 1 \quad \exists C^{(l)} = [m^{(l)}, m^{(l)} + L^{(l)}]$ where and $C^{(l)}$ is a finite integer interval, such that $k \in C^{(l)}$, we have

$$\frac{1}{L^{(l)}} \sum_{i=m^{(l)}}^{m^{(l)}+L^{(l)}} \rho_A(i) \le 1 \tag{5.3.1}$$

If the sub-sets $C^{(l)}$ are *at most countable infinity*, and pairwise disjoint

$$\bigcap_{l=1}^{\infty} C^{(l)} = \varnothing$$

one can organize a new sub-set such that

$$Z_s = \bigcup_{l=1}^{\infty} C^{(l)}$$

Thus the positive integer set Z^+ is partitioned into two sub-sets $Z^+ = Z_s \cup \bar{Z}_s$, with $Z_s \cap \bar{Z}_s = \varnothing$; moreover $\bar{Z}_s$ is the union of sub-sets $D^{(l)}$ isolated by sub-sets $C^{(l-1)}$ and $C^{(l)}$, therefore, $\bar{Z}_s = \bigcup_{l=1}^{\infty} D^{(l)}$ and $\bigcap_{l=1}^{\infty} D^{(l)} = \varnothing$, thus

$$\bigcup^{\infty} (C^{(l)} \bigcup_{l=1}^{\infty} D^{(l)}) = Z^+ \tag{5.3.2}$$

On the other hand, for each finite integer interval $C^{(l)}$ where the module of the eigen values of the state transition matrix $A(k)$ may exceed unity, we denote a new state

$$A(k^{(l)}) = A(m^{(l)}) A(m^{(l)} + 1) \ldots A(m^{(l)} + L^{(l)}) \tag{5.3.3}$$

By Cauchy-Schwartz inequality

$$\| A(k^{(l)}) \| \le \| A(m^{(l)}) \| \| A(m^{(l)} + 1) \| \ldots \| A(m^{(l)} + L^{(l)}) \| \tag{5.3.4}$$

and we have

$$\| A(k^{(l)}) \|^{\frac{1}{L^{(l)}}} \le \left(\prod_{k=m^{(l)}}^{m^{(l)}+L^{(l)}} \| A(k) \| \right)^{\frac{1}{L^{(l)}}} \le \frac{1}{L^{(l)}} \sum_{k=m^{(l)}}^{m^{(l)}+L^{(l)}} \| A(k) \| = \bar{\rho}_A(k^{(l)}) \le 1 \tag{5.3.5}$$

This implies that the module of the eigen values of the new state transition matrix in the new-time-domain is less than unity. $\| A(k^{(l)}) \| \le 1$

If we denote the new sub-sets as $E^{(l)} = \{k^{(l)}\}$, that is, for each interval $C^{(l)}$, the $L^{(l)} - m^{(l)}$ states are replaced by one single new state $A(k^{(l)})$, then we may combine the ordered sequence of the sub-sets $D^{(l)}$ and the newly constructed sub-sets $E^{(l)}$, such that

$$\bigcup^{\infty} (E^{(l)} \bigcup_{l=1}^{\infty} D^{(l)}) = Z^+ \tag{5.3.6}$$

Let us explicitly *denote the new time as* $j \in Z^+$. Thus a new sequence of state

transition matrices in the new-time-domain can be written as

$$Y(j+1) = A(j)Y(j) \tag{5.3.7}$$

In the new-time-domain, $\rho_A(j) \leq 1$, therefore no local instability of the first kind appears. Before we proceed to carry out an analysis of (5.3.7) in the new-time-domain, let us note that the set of new time $j \in Z^+$ constructed under the eigen value regularization condition (5.3.5) and the ordered sequence condition (5.3.6) is a set of full measure, see [5.7].

5.3.2. Local Instability of Second Kind in New-Time-Domain

In the new-time-domain, for a LTV system having no LIFK, there may exist a local instability of LTV, even though such a LTV system is globally BIBO stable. This phenomena exclusively belongs to the LTV system and such a local instability is observed from the Lyapunov function associated with the LTV system in the new-time-domain.

Let us construct a Lyapunov function in the new-time-domain

$$V(Y(j)) = Y^T(j)\Pi(j)Y(j) \tag{5.3.8}$$

where $\Pi(j)$ is a positive definite matrix. The difference of the Lyapunov function is written as

$$V_{j+1}(Y(j+1)) - V_j(Y(j)) = Y^T(j)\,[A^T(j)\Pi(j+1)A(j) - \Pi(j)]\,Y(j)$$

If a LTV system in the new-time-domain is BIBO stable, then the Lyapunov function should be bounded and asymptotically decreasing. Since the system is time-varying then it is not necessary that the Lyapunov function monotonously decrease, it may locally increase, thus the LTV in the new-time-domain may contain local instability.

Definition 5.3.2 *In the new-time-domain, if* $\exists j \in Z^+$, *such that* $\|\Pi(j+1) - \Pi(j)\| > 1$, *then this is called local instability of the second kind (LISK).*

Our objective is to find the positive definite matrix $\Pi(j)$, and the condition such that the Lyapunov function $V_j(Y(j))$ is asymptotically decreasing. Let us consider the matrix $\Pi(j+1)$ as a solution of the following matrix equation

$$A^T(j)\Pi(j+1)A(j) - \Pi(j+1) = -I \tag{5.3.9}$$

Performing a chain substitution

$$\begin{aligned}\Pi(j+1) &= I + A^T(j)\Pi(j+1)A(j) \\ &= I + A^T(j)A(j) + (A^T(j))^2\Pi(j+1)(A(j))^2 \\ &= I + \sum_{l=1}^{\infty}(A^T(j))^l(A(j))^l\end{aligned} \tag{5.3.10}$$

It is easy to see $\Pi(j+1)$ is a symmetric positive definite matrix; taking the norm on (5.3.10) we have

$$\begin{aligned}\|\Pi(j+1)\| &\le \|I\| + \sum_{l=1}^{\infty}\left\|(A^T(j)A(j))^l\right\| \\ &\le \|I\| + \sum_{l=1}^{\infty}\left\|A^T(j)A(j)\right\|^l \le \|I\| + \sum_{l=1}^{\infty}\|A(j)\|^{2l}\end{aligned} \tag{5.3.11}$$

Using the condition $\rho_A(j) \le 1$ and the matrix norm in Lemma 5.2.1, we obtain

$$1 \le \|\Pi(j)\| \le \frac{1}{1-\rho_A^2(j-1)} = \Gamma_\rho(j)$$

This implies that the Lyapunov function in the new-time-domain is bounded by

$$\|Y(j)\|^2 \le V(Y(j)) \le \Gamma_\rho(j)\|Y(j)\|^2 \tag{5.3.12}$$

Next, it is necessary to find the condition that the Lyapunov function $V(Y(j))$ is decreasing.

Denote $\|\partial A(j)\| = \|A(j) - A(j-1)\|$ as *variation rate* of a LTV system $A(j)$.

From Appendix 5.1, we know

$$\|\Pi(j+1) - \Pi(j)\| \le 2\|\partial A(j)\|\Gamma_p^2(j)\rho_A(j) \tag{5.3.13}$$

Now if the Lyapunov function is strictly decreasing, then this requires that

$$\begin{aligned} V(Y(j+1)) - V(Y(j)) &= Y^T(j)(-I + \Pi(j+1) - \Pi(j))Y(j) \\ &\le -\|Y(j)\| + \|\Pi(j+1) - \Pi(j)\|\|Y(j)\| \\ &\le 0 \end{aligned}$$

Hence, we have

$$\|\Pi(j+1) - \Pi(j)\| \le 1 \qquad \forall j \in Z^+ \tag{5.3.14}$$

Under this condition, given arbitrary $Y(0) \le \infty$, the Lyapunov function will uniformly tend to vanish: $V(Y(j)) \to 0$ as $j \to \infty$. Therefore, the LTV system in the new time domain is BIBO stable.

Since the coefficients of the LTV system are constantly time-varying, hence the module of the eigenvalues is time-varying too. This leads to a possibility to relax the condition in (5.3.14), that is $\exists j \in Z^+$ such that $\|\Pi(j+1) - \Pi(j)\| > 1$ and therefore $V(Y(j+1)) - V(Y(j)) > 0$ which means the LTV system in the new time domain can be locally unstable, even if the system is globally stable.

It is interesting to study the condition for the global BIBO stability of a LTV system in the presence of the LISK. Let us denote an increment of the Lyapunov function as:

$$\delta_j = V(Y(j)) - V(Y(j-1)) \tag{5.3.15}$$

If at an instant j, or a certain time interval in the new-time-domain, the Lyapunov function is not decreasing (for example, $\delta_j > 0$, if $\exists \Xi^{(j)} = [n^{(j)}, n^{(j)} + L^{(j)}]$ where $j \in \Xi^{(j)}$), but

$$\sum_{\Xi^{(j)}} \delta_j \le 0 \tag{5.3.16}$$

then over the long observation interval the Lyapunov function remains a decreasing one,

$$V(Y(n^{(j)}+L^{(j)}))-V(Y(n^{(j)}+L^{(j)}-1))+\ldots+V(Y(j))$$

$$-V(Y(j-1))+V(Y(n^{(j)}+1))-V(Y(n^{(j)}))\le 0 \qquad (5.3.17)$$

Now we are in the position to state the results of BIBO stability of LTV system.

5.3.3. Necessary and Sufficient Condition for BIBO Stability of LTV System

Theorem 5.3.1 *(Necessary Condition) If the system is globally BIBO stable, the module of the Centroid of the eigen values of the LTV system must be inside the unit disc,.*

$$\lim_{L\to\infty}\frac{1}{L}\sum_{k=1}^{L}\rho_A(k)<1 \qquad (5.3.18)$$

Proof: For a LTV system in the presence of LIFK, the output energy in the subset Z_s becomes

$$\frac{1}{N}\sum_{i=1}^{\infty}\|A(k^{(i)})Y(k^{(i)})\|\le\frac{1}{N}\sum_{i=1}^{\infty}\|A(k^{(i)})\|\|Y(k^{(i)})\|_2\le\frac{max\{\|Y(k^{(i)})\|\}}{N}\sum_{i=1}^{\infty}\bar{\rho}_A^2(i)$$

Since $\bar{\rho}_A(i)<1$,

$$\lim_{N\to\infty}\frac{1}{N}\sum_{i=1}^{\infty}\bar{\rho}_A^2(i)<\infty \qquad (5.3.19)$$

Assuming the LTV system is BIBO stable in the new-time-domain, $max\{Y(k^{(i)})\}<\infty$. Therefore, the system output energy in the subset Z_s is bounded. Therefore, (5.3.19) represents the necessary condition for BIBO stablility in the presence of LIFK. It follows that a LTV system must satisfy (5.3.18).

Q.E.D.

Corollary 5.3.1 *The necessary condition for a LTV system to be BIBO stable is*

$$\lim_{L\to\infty}\frac{1}{L}\sum_{k=1}^{L}|a_N(k)|<1 \tag{5.3.20}$$

Proof: Since for the Nth-order LTV system, the N eigen values are the N roots of (5.2.1) and

$$a_N(k) = \lambda_N(k)\lambda_{N-1}(k)\ldots\lambda_1(k)$$

hence

$$|a_N(k)|^{1/N} = |\lambda_N(k)\lambda_{N-1}(k)\ldots\lambda_1(k)|^{1/N} \le \rho_A(k)$$

using (5.3.18)

$$\lim_{L\to\infty}\frac{1}{L}\sum_{k=1}^{L}|a_N(k)|^{1/N}<1$$

Q.E.D.

It is easy to see that Theorem 5.3.1 gives a more relaxed condition for a LTV system to be stable compared to a LTI system, (for a LTI system, even if a single pole of the system is located outside the unit disc, the system becomes unstable). However, due to the nature that the eigen value of a LTV system are continuously time-varying, the instantaneous module of the system eigen values could be located inside or outside the unit disc, as long as the centroid of the these time-varying eigen values is placed inside the unit disc.

Note that for a BIBO stable LTI system, the absolute value of the last coefficient in (5.2.1) must be less than unity. For a LTV system to be BIBO stable, it is necessary to test the condition (5.3.20).

In what follows, we provide a strong condition for a LTV system to be BIBO stable, provided the system does not contain the LISK.

Theorem 5.3.2 *(Sufficient Condition) If a LTV system does not contain LISK and satisfies the following condition,*

$$\| \partial A(j) \| \le \frac{(1-\rho_A^2(j))^2}{2\rho_A(j)} \tag{5.3.21}$$

then such a LTV system is BIBO stable.

Proof: If the LTV system does not have LISK, which requires $\| \Pi(j+1) - \Pi(j) \| \le 1$, we have from (5.3.13)

$$2\| \partial A(j) \| \Gamma_p^2(j) \rho_A(j) \le 1$$

Thus we arrive at (5.3.21).

Q.E.D.

Corollary 5.3.2. *(Eigen Value Test) If a LTV system does not posses LISDK and satisfies the following test,*

$$\left| \sum_{i=1}^{N} \lambda_i(j) - \lambda_i(j-1) \right| \le \frac{(1-\lambda_N^2(j))^2}{2|\lambda_N(j)|} \tag{5.3.22}$$

where, $|\lambda_N(j)|, |\lambda_{N-1}(j)|, \ldots, |\lambda_1(j)|$ *are the module of eigen values of system* $A(j)$ *in decreasing order, then the system is BIBO stable.*

Proof: From (5.3.21), we need to find the eigen values of the system variation matrix, i.e.

$$|I - \lambda(j) \partial A(j)| = \begin{vmatrix} \lambda(j) - (a_1(j) - a_1(j-1)) & -(a_2(j) - a_2(j-1)) & \ldots & -(a_N(j) - a_N(j-1)) \\ \lambda(j) & 0 & \ldots & 0 \\ \ldots & \ldots & \ldots & \ldots \\ 0 & 0 & \ldots & \lambda(j) \end{vmatrix}$$

$$= \lambda^{N-1}(\lambda - (a_1(j) - a_1(j-1))) = 0 \tag{5.3.23}$$

which implies

$$\|\partial A(j)\| = |a_1(j) - a_1(j-1)| \tag{5.3.24}$$

and because

$$a_1(j) = \sum_{i=1}^{N} \lambda_i(j)$$

(5.3.21) can be written as (5.3.22).

Q.E.D.

Corollary 5.3.3. *(Coefficient Test) Sufficient condition of (5.3.21) can be expressed as a weak test of the coefficients of a LTV-system (5.2.1)*

$$2|a_1(j) - a_1(j-1)| \le \frac{\left(1 - \sqrt[N]{a_N^2(j)}\right)^2}{\sqrt[N]{|a_N(j)|}} \tag{5.3.25}$$

Proof: Let us denote the right hand side of (5.3.21) as $R(\rho_A(j))$, then take the derivative w.r.t. $\rho_A(j)$

$$\frac{\partial}{\partial \rho_A(j)} R(\rho_A(j)) = -\frac{(1+3\rho_A^2(j))(1-\rho_A^2(j))}{2\rho_A^2(j)} \le 0$$

Because

$$|a_N(j)| \le \rho_A^N(j) \tag{5.3.26}$$

thus, substituting (5.3.24) and (5.3.26) into (5.3.21) we have (5.3.25). *Q.E.D.*

Remark 5.3.3 Theorem 5.3.2. gives the condition for BIBO stability of a LTV system without LISK. Corollary 5.3.2. gives a test to check the sufficiency condition given in Theorem 5.3.2. However it is computationaly very intensive to verify (5.3.22), while Corollary 5.3.3 presents a relatively simple test which only needs the use of two coefficients of the system. But, as one can see in the proof, (5.3.25) is a weaker condition than (5.3.22).

In what follows, we present the BIBO stability condition of a LTV system in the presence of LISK.

Theorem 5.3.3 *(Sufficient Condition) In the presence of LISK, a sufficient condition for LTV system to be BIBO stable is*

$$\lim_{L\to\infty}\frac{1}{L}\sum_{j=n}^{n+L}\left(1-2\frac{\|\partial A(j)\|\rho_A(j)}{(1-\rho_A^2(j))^2}\right)\geq 0 \tag{5.3.27}$$

Proof: In the presence of LISK, the Lyapunov function may not be monotonically decreasing, but globally decreasing. The difference of the Lyapunov functions can be expressed as

$$V(Y(j+1))-V(Y(j))\leq -\|Y(j)\|+\|\Pi(j+1)-\Pi(j)\|\|Y(j)\|$$

Thus (5.3.16) can be written as

$$\sum_{\Xi^{\Omega}}\delta_j=-\sum_{\Xi^{\Omega}}\|Y(j)\|+\sum_{\Xi^{\Omega}}\|\Pi(j+1)-\Pi(j)\|\|Y(j)\|\leq 0$$

Using (5.3.13), we have (5.3.27)

Q.E.D.

Corollary 5.3.4 *A weak condition to test the BIBO stability (5.3.27) is given as follows*

$$\lim_{L\to\infty}\sum_{j=n}^{n+L}\|\partial A(j)\|^2\frac{\rho_A^2(j)}{(1-\rho_A^2(j))^4}\leq\frac{1}{4} \tag{5.3.28}$$

Proof: For the Lyapunov function in the new-time-domain to be decreasing during a long observation time requires

$$-\sum_{\Xi^{\Omega}}\|Y(j)\|+\sum_{\Xi^{\Omega}}\|\Pi(j+1)-\Pi(j)\|\|Y(j)\|\leq 0$$

By Hodel inequality, we have

$$-\sum_{\Xi^{\Omega}}\|Y(j)\|+\left(\sum_{\Xi^{\Omega}}\|\Pi(j+1)-\Pi(j)\|^2\right)^{1/2}\left(\sum_{\Xi^{\Omega}}\|Y(j)\|^2\right)^{1/2}\leq 0 \tag{5.3.29}$$

Using the inequality

$$\frac{\sum_{\Xi(J)} \| Y(j) \|^2}{\left(\sum_{\Xi(J)} \| Y(j) \| \right)^2} \leq 1$$

leads to

$$\sum_{\Xi(J)} 4 \| \partial A(j) \|^2 \Gamma_p^4(j) \rho_A^2(j) \leq 1$$

Q.E.D.

Theorem 5.3.3. is in fact an extension of Theorem 5.3.2. for the case when the LTV system contains LISK.

From Theorem 5.3.2, and Theorem 5.3.3, it is not difficult to see that the sufficient conditions for a LTV system to be BIBO globally stable indicate that the variation rate of the system in the new-time-domain should satisfy a certain constraint. Since the variation of the coefficients of the LTV system implies an "energy pumping", which means that the controlling coefficients are pumping energy into the system. A fast variation of the system corresponds to a situation of pumping more energy. So for a BIBO stable system, the variation can not be too fast in a global sense, (locally it may be fast which corresponds to the Lyapunov function locally increasing).

5.3.4. Other Forms of the BIBO Stability Test

As we have already seen, the BIBO stability test for a LTV system is expressed through Theorems 5.3.1,5.3.2 , and 5.3.3 . The necessary condition (5.3.20) is easy to check, while the sufficient condition is much more computationally involved, because one has to check these conditions at each time instant. One of the possible directions to establish a relatively simple algebraic test is to transform *these conditions into a test of the sign of a multivariable function, with each variable prescribed within a certain range of variation*[5.9]. In what follows, we present such a technique for 1st-order and 2nd-order LTV systems.

Consider the simplest 1st-order LTV system without LIFK:

$$y_j = -a_1(j) y_{j-1} \tag{5.3.30}$$

where $|a_1(j)| < 1$. We have the following lemma.

Lemma 5.3.2 *The 1st-order LTV system (5.3.30) is stable if the following non-negative test of two variables is satisfied*

$$1-3a_1^4(j)+8a_1^3(j)a_1(j-1)-4a_1^2(j)a_1^2(j-1)-2a_1^2(j) \geq 0 \qquad (5.3.31)$$

Proof: By (5.3.24) we know, $\|\partial A(j)\| = |a_1(j) - a_1(j-1)|$ and $\rho_A(j) = |a_1(j)|$. Thus (5.3.21) can be written as

$$|a_1(j) - a_1(j-1)| \leq \frac{(1-a_1^2(j))^2}{2|a_1(j)|}$$

By squaring both sides of above equation, we have (5.3.31)

Q.E.D.

The non-negative sign of LHS of (5.3.31) imposes a certain condition on the variation of $a_1(j)$. Conversly, if we know the admissible area or the variation law of the coefficients, then we can substitute such a relationship into (5.3.31) to check for the stability of the corresponding system.

Consider a 2nd-order LTV system without LIFK:

$$y_j = -a_1(j)y_{j-1} - a_2(j)y_{j-2} \qquad (5.3.32)$$

where $|a_2(j)| < 1$.

Lemma 5.3.3 *The 2nd-order LTV system (5.3.32) is stable if the following non-negative test of two variables is satisfied*

$$\begin{aligned} &1 + a_2^4(j) - 4a_2^3(j) + 6a_2^2(j) - 4a_2(j) - 4a_2(j)a_1^2(j) \\ &+ 8a_2(j)a_1(j)a_1(j-1) - 4a_2(j)a_1(j-1) \geq 0 \end{aligned} \qquad (5.3.33)$$

Proof: From (5.3.24), we have $\|\partial A(j)\| = |a_1(j) - a_1(j-1)|$ and because $a_1(j)$ and $a_2(j)$ are real values, $\rho_A(j) = \sqrt{|a_2(j)|}$. Thus, using (5.3.21), we

have

$$|a_1(j) - a_1(j-1)| \le \frac{(1-|a_2(j)|)^2}{2\sqrt{|a_2(j)|}} \tag{5.3.34}$$

Expanding (5.3.34) we have (5.3.33).

Q.E.D.

In chapter 3, we presented a general trajectory equation of an *Nth*-order anti-null operator, if the variation of the coefficients are a priori known. It is possible to write the trajectory equation and then substitute the relationship of such an equation into the test, to check for the BIBO stability.

5.4. Examples of LTV System in the Presence of LIFK and LISK

5.4.1. LIFK of 2nd-Order System

Example 5.1 A 2nd-Order LTV system for modeling a constant envelope signal with arbitrary frequency modulation law.

Suppose the instantaneous frequency is an arbitrary random positive function of time, $\dot{\psi}(k)$. If the FM signal is written as $s_k = \sin\psi(k)$, then we can find a second order null operator such that

$$s_k + a_1(k)\, s_{k-1} + a_2(k)\, s_{k-2} = 0$$

Its corresponding anti-null operator can be written as

$$y_k = -\alpha a_1(k)\, y_{k-1} - \alpha^2 a_2(k)\, y_{k-2} \tag{5.4.1}$$

We already know that the Wronskian associated with (5.4.1) is $\Delta_0(k) = \sin\dot{\psi}(k)$. It is interesting that the orbit of the trajectories of the LTV

system (5.4.1) may be expressed as (*orbit equation*):

$$a_1^2(k) + a_2^2(k) + 2a_1(k)\,a_2(k)\cos\psi(k-1) = 0 \tag{5.4.2}$$

where

$$a_2(k) = \frac{\Delta_0(k)}{\Delta_{-1}(k)} \tag{5.4.3}$$

$$a_1(k) = -a_2(k)\sqrt{1-\Delta_{-1}^2(k)} - a_2(k-1) \tag{5.4.4}$$

First, using (5.4.3) it is easy to determine the admissible area of the system given by (5.4.1), which is shown in Fig.5.1. We also present the admissible area of the LTV systems associated with AM/FM signal $s_k = A(k)\sin\psi(k)$ and exponentialy damped FM signal (EX/FM) $s_k = exp(-\gamma k)\sin\psi(k)$. It is interesting to compare the admissible area of these three systems to the classical Jury triangle area used for the stability test of a second-order LTI system (associated with an exponentially damped sinusoid of fixed frequency).

It is seen that the *maple leaf* like area representing AM/FM signal spans a larger area. The AM/FM and EX/FM area depend on a signal envelope. For the constant envelope FM signal, its area consists of two semi-infinite strips. Given a FM signal with arbitrary frequency modulation law, its trajectory described by the orbit equation (5.4.2) must be confined inside these two semi-infinite strips.

Now we investigate the stability of (5.4.1) by applying our BIBO stability theory developed in the last section. We first look at the LIFK and check the necessary condition(5.3.23) for such a LTV system to be BIBO stable.

For a second-order LTV system (5.4.1), we known

$$\rho_A(k) = \alpha\sqrt{a_2(k)} \tag{5.4.5}$$

Substitution of (5.4.3) in (5.4.5) gives

$$\rho_A(k) = \alpha\sqrt{\frac{\Delta_0(k)}{\Delta_{-1}(k)}} \tag{5.4.6}$$

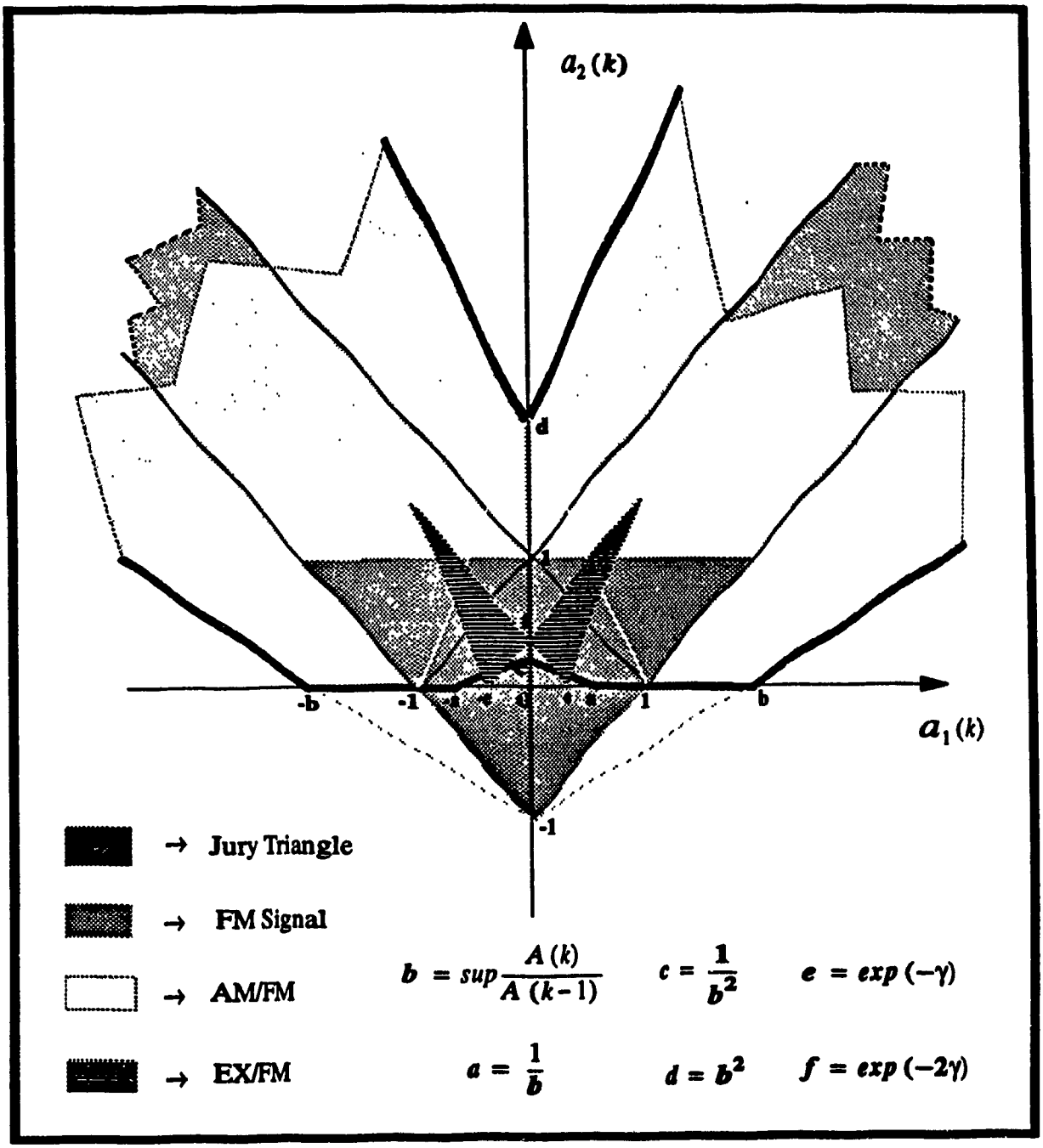

Fig.5.1 Admissible Areas of LTV Systems Representing FM, AM/FM and EX/FM Signals

Since the Wronskian is time-varying, we have for a certain period of time $\rho_A(k) > 1$; this implies that the LTV system (5.4.1) contains LIFK. In what follows, we shall prove that the necessary condition for (5.4.1) to be BIBO stable is satisfied in

the presence of LIFK. For a second-order LTV system, (5.4.5) may be written as

$$\sqrt{\Delta_0(k+1)} = \alpha \frac{\rho_A(k+1)}{\alpha} \sqrt{\Delta_0(k)}$$

which can be expressed as

$$\sqrt{\Delta_0(k+L)} = \left\{ exp\left[\frac{1}{L} \sum_{l=1}^{L} ln\left(\frac{\rho_A(k+1)}{\alpha} \right) \right] \right\}^{L} \sqrt{\Delta_0(k)} \tag{5.4.7}$$

or

$$\left(\frac{\Delta_0(k+L)}{\Delta_0(k)} \right)^{\frac{1}{2L}} = exp\left[\left(\frac{1}{L} \sum_{l=1}^{L} ln\left(\frac{\rho_A(k+1)}{\alpha} \right) \right) \right] \tag{5.4.8}$$

Taking the limit of (5.4.8) for $L \to \infty$ we get

$$\lim_{L \to \infty} \left(\frac{\Delta_0(k+L)}{\Delta_0(k)} \right)^{\frac{1}{2L}} = exp\left[E\left(ln\left(\frac{\rho_A(k)}{\alpha} \right) \right) \right]$$

where E denotes the mathematical expectation operation. Since the Wronskian is a bounded value, and the FM signal is a constant-envelope signal, we can see that

$$\lim_{L \to \infty} \left(\frac{\Delta_0(k+L)}{\Delta_0(k)} \right)^{\frac{1}{2L}} \to 1$$

and

$$exp\left[E\left(ln\left(\frac{\rho_A(k)}{\alpha} \right) \right) \right] \to 1$$

Hence we have, by using Jenson's formula,

$$E\left(ln\left(\frac{\rho_A(k)}{\alpha} \right) \right) \to 0$$

Thus,

$$ln\left(E\left(\frac{\rho_A(k)}{\alpha} \right) \right) \to 0$$

and hence,

$$E(\rho_A(k)) \rightarrow \alpha$$

Thus the necessary condition for (5.4.1) to be BIBO stable is $\alpha < 1$.

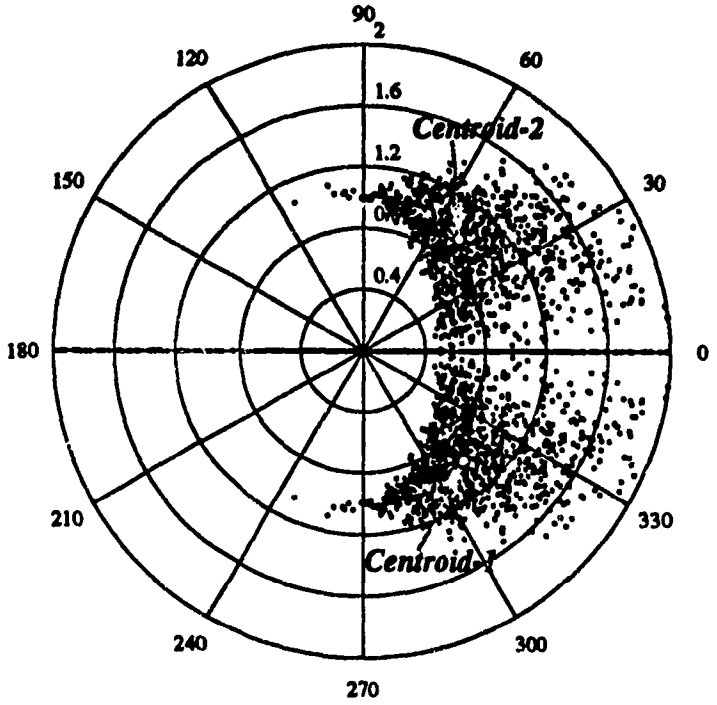

Fig.5.2 Instantaneous Eigen Value Scattering of a 2nd-Order LTV System

Fig.5.2 shows *instantaneous* eigen values of a second order LTV system constructed based on an FM signal modulated by random Gaussian noise.

It car be seen that although the instantaneous eigen values may be scattered in a wide range around the boundary of the unit disc, however for the BIBO stable system the centroid for the eigen values is still inside the unit disc.

In Fig. 5.1, the Jury triangle is the admissible area where the module of the system eigen values is less than unity. Notice that the admissible areas for FM, AM/FM and EX/FM signals are not necessarily constrained to be inside the Jury triangle, which means LTV systems representing these signals might have their instantaneous module of eigen values larger than unity (therefore the system contains LIFK).

The LTV system (5.4.1) constructed will satisfy the necessary condition for the BIBO global stability, if the debiasing factor $\alpha < 1$, although such a system may contain LIFK within a significantly long observation interval.

Next, we are going to check the LISK in the new time domain by testing the sufficiency condition (5.3.21). We denote the RHS of (5.3.33) as $P(j)$. Using the relationship (5.4.3) and (5.4.4), it can be shown that (5.3.33) can be written as

$$P(j) = \sum_{i=0}^{3} c_i(j)\, a_2^i(j) \tag{5.4.9}$$

where,

$$c_0(j) = \Delta_{-2}^3$$

$$c_1(j) = -4\Delta_{-2}^3 - \Delta_{-2}^3(1-\Delta_{-1}^2)$$

$$c_2(j) = 6\Delta_{-2}^3 + 2\Delta_{-2}^3\sqrt{1-\Delta_{-1}^2}\,(\sqrt{1-\Delta_{-2}^2} - \sqrt{1-\Delta_0^2}) - 2\sqrt{\Delta_0\Delta_{-2}}\Delta_{-2}^2(1-\Delta_{-1}^2)$$
$$+ 2\Delta_{-1}\Delta_{-2}^2\sqrt{\Delta_0\Delta_{-2}}\sqrt{1-\Delta_{-1}^2}\sqrt{1-\Delta_{-2}^2} - \Delta_{-1}\Delta_{-2}^2(1-\Delta_{-1}^2)$$

$$c_3(j) = -4\Delta_{-2}^3 - \Delta_{-2}^3(\sqrt{1-\Delta_{-1}^2} - \sqrt{1-\Delta_0^2}) + 4(\Delta_{-1}\Delta_{-2})\sqrt{\Delta_0\Delta_{-2}}\sqrt{1-\Delta_{-1}^2}\sqrt{1-\Delta_{-2}^2}$$
$$- 2\Delta_0\Delta_{-2}^2(\sqrt{1-\Delta_{-1}^2} - \sqrt{1-\Delta_0^2})(\sqrt{1-\Delta_{-1}^2} - \sqrt{1-\Delta_{-2}^2}) - \Delta_{-1}^2\Delta_{-2}(1-\Delta_{-2}^2)$$
$$+ 2\Delta_{-1}\Delta_{-2}^2(\sqrt{1-\Delta_{-1}^2}\sqrt{1-\Delta_{-2}^2}) + 4\Delta_{-2}^2\sqrt{\Delta_0\Delta_{-2}}\sqrt{1-\Delta_{-1}^2}(\sqrt{1-\Delta_{-1}^2} - \sqrt{1-\Delta_0^2})$$

$$c_4(j) = -\Delta_{-2}^3(1-\Delta_{-2}^2)^2 + \Delta_{-2}^3 - \Delta_{-2}^2\sqrt{\Delta_0\Delta_{-2}}(\sqrt{1-\Delta_{-1}^2} - \sqrt{1-\Delta_0^2})^2$$
$$- 4\Delta_{-1}\Delta_{-2}\sqrt{\Delta_0\Delta_{-2}}\sqrt{1-\Delta_{-2}^2}(\sqrt{1-\Delta_{-1}^2} - \sqrt{1-\Delta_0^2}) - \Delta_{-1}\Delta_{-2}^2(\sqrt{1-\Delta_{-1}^2} - \sqrt{1-\Delta_0^2})^2$$
$$-2\Delta_1^2\sqrt{\Delta_0\Delta_{-2}}(1-\Delta_{-2}^2) - 2\Delta_{-1}^2\Delta_{-2}\sqrt{1-\Delta_{-2}^2}(\sqrt{1-\Delta_{-1}^2} - \sqrt{1-\Delta_0^2})$$

where the Wronskian $\Delta_l = \Delta_0(j+l)$ and $0 \le \Delta_j \le 1$, the variable $0 \le a_2(j) \le 1$. In what follows we have to check that $P(j) \ge 0$, which may be accomplished by checking

the following conditions:

$$P(j)|_{a_2(j)=0} = c_0(j) \geq 0 \tag{5.4.10}$$

$$\frac{\partial}{\partial a_2(j)} P(j)\Big|_{a_2(j)=0} = c_1(j) < 0 \tag{5.4.11}$$

$$\frac{\partial^2}{\partial a^2{}_2(j)} P(j)\Big|_{a_2(j)=0} = 2c_2(j) > 0 \tag{5.4.12}$$

$$\frac{\partial^3}{\partial a^3{}_2(j)} P(j)\Big|_{a_2(j)=0} = 3c_3(j) < 0 \tag{5.4.13}$$

$$\frac{\partial^4}{\partial a^4{}_2(j)} P(j)\Big|_{a_2(j)=0} = 24c_4(j) > 0 \tag{5.4.14}$$

It is easy to see that (5.4.9) and (5.4.10) are satisfied. We can show that (5.4.11), (5.4.12) and (5.4.13) are also satisfied.

We may claim now that the LTV system (5.4.1) is strictly BIBO stable in the new--time-domain. Therefore, such a system is always BIBO globally stable.

Fig. 5.3 presents $P(k)$ for the same example as shown in Fig.5.2. Notice that this plot shows the system in real time-domain, the zero value locations shown in the plot represents the occurrence of LIFK.

Fig.5.4 shows the function $P(j)$ in the new-time-domain, (5.4.9) is positive.

Remark 5.4.3 In this example, the system has only LIFK, the Lyapunov function in new-time-domain is monotonically decreasing.

Remark 5.4.4 LIFK is in fact a common phenomena in many applications. For example, Macchi and Jeidane-Saidane [5.10] observed LIFK while carrying out a study of adaptive ADPCM coding of audio signals. They have shown that the system may be even a chaotic one because of the presence of LIFK. Sethares et al. [5.11] also found LIFK in the adaptive echo canceller, they termed LIFK as the pole going outside the unit disc. Although they use eloquent arguments to explain the LIFK, no rigorous analysis has been advanced. The theory presented in this Chapter serves as a step

towards such an endeavour.

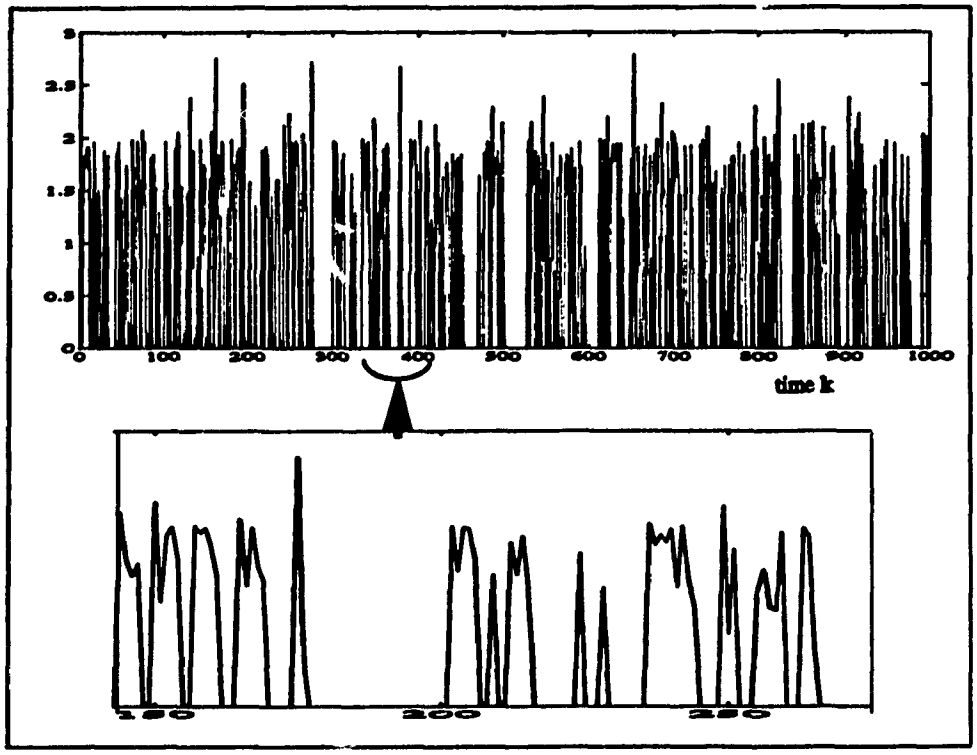

Fig.5.3 $P(k)$ *Function in Real Time Tomain*

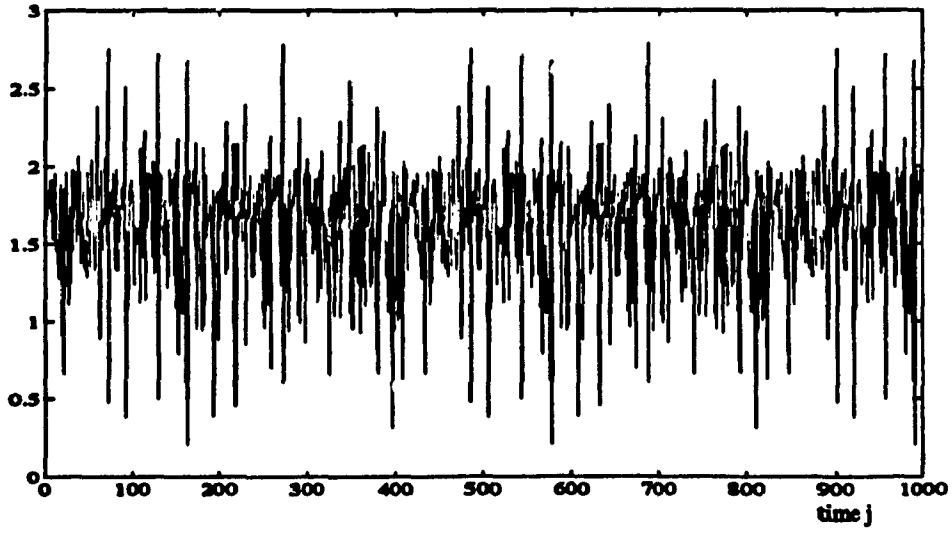

Fig.5.4 $P(k)$ *Function in New Time Tomain*

Before we proceed to consider the next example, we present the following two conjectures about the BIBO stability of a LTV system

Conjecture 5.1 The BIBO stability of a higher-order LTV AR system can not be determined by a knowledge of the BIBO stability of its roots-factorized lower order LTV systems and vice versa.

Conjecture 5.2 If the coefficients of a LTV AR system are constructed based on the Wronskian system of functions, such a LTV system is BIBO globally stable.

Next, we are going to present an example of a LTV system, which possesses a fixed module of the eigen values and located inside the unit disc. However, it will be shown that such a LTV system is in fact unstable.

5.4.2. Example of a Global BIBO Unstable LTV System [5.14]

Consider the following 2nd-Order LTV system

$$A(k) = \begin{bmatrix} -1+1.5\cos^2 k & 1-1.5\sin k\cos k \\ -1-1.5\sin k\cos k & -1+1.5\sin^2 k \end{bmatrix} \tag{5.4.15}$$

The characteristic equation of (5.4.14) becomes

$$\lambda^2 + 0.5\lambda - 1.5 = 0$$

Therefore the two eigen values of (5.4.14) are given as

$$\lambda_{1,2} = -\frac{1}{4} \pm \frac{\sqrt{-5}}{4}$$

and

$$\rho_A = \frac{1}{\sqrt{2}}$$

Hence the system (5.4.14) does not have LIFK. Let us check the sufficiency conditions.

Since,

$$\|\partial A(k)\| = \sin 1$$

we have

$$\frac{2\rho_A\|\partial A(k)\|}{(1-\rho_A^2)^2} = 4\sqrt{2}\sin 1 = 4.76\ldots > 1$$

Thus test (5.3.26) fails. Checking

$$\lim_{L\to\infty}\frac{1}{L}\sum_{j=n}^{n+L}\left(1-2\frac{\|\partial A(j)\|\rho_A}{(1-\rho_A^2)^2}\right) = \lim_{L\to\infty}\frac{1}{L}\sum_{j=n}^{n+L}(1-4\sqrt{2}\sin 1) = -\infty$$

and thus test (5.3.30) fails too. So we claim system (5.4.14) is BIBO unstable.

In fact it is easy to find even the state transition matrix for such a system

$$Y(k) = \Phi(k,0)\,Y(0)$$

with

$$\Phi(k,0) = \begin{bmatrix} e^{0.5k}\cos k & -e^{-k}\sin k \\ -e^{0.5k}\sin k & e^{-k}\cos k \end{bmatrix}$$

Obviously the system is unstable.

Remark 5.4.5 This is a good example to demonstrate that for a LTV system, although the module of the eigen values are located inside the unit disc, the system becomes globally unstable due to LISK.

5.4.3. BIBO Stability of a Discrete Mathieu Equation System

The discrete Mathieu equation is given as[5.12]

$$y_k = -\alpha a_1(k)y_{k-1} - \alpha^2 a_2(k)y_{k-2} \tag{5.4.16}$$

where the coefficients are specially chosen to be

$$a_2(k) = 1 \tag{5.4.17}$$

$$a_1(k) = -2\cos\dot{\psi}(k) \tag{5.4.18}$$

where

$$\psi(k) = f_o k + \frac{\Delta f}{f_m}\sin f_m k$$

and

$$\dot{\psi}(k) = \psi(k) - \psi(k-1) = f_o + \frac{\Delta f}{f_m}\cos(\frac{1}{2})\sin(f_m k - \frac{1}{2})$$

The module of the eigen value of the system (5.4.15) is

$$\rho_A = \alpha \qquad \alpha < 1$$

Therefore the system has no LIFK.

$$\|\partial A(k)\| = 2|\cos\dot{\psi}(k) - \cos\dot{\psi}(k-1)|$$

$$= 2\left|\sin\left[\frac{\Delta f}{f_m}\cos(\frac{1}{2})\sin f_m \cos(f_m k - \frac{1}{2})\right]\sin\left[2f_o + \frac{\Delta f}{f_m}\cos(\frac{1}{2})\cos f_m \sin(f_m k - \frac{f_m+1}{2})\right]\right| \tag{5.4.19}$$

Denote

$$P(k) = \frac{2\rho_A\|\partial A(k)\|}{(1-\rho_A^2)^2} = \frac{2\alpha\|\partial A(k)\|}{(1-\alpha^2)^2}$$

We chose following parameter values

$$\alpha = 0.9 \quad f_o = 2\pi\cdot 0.1 \quad \Delta f \in [0.1\cdot f_o f_o] \quad f_m \in [0.1\times f_o f_o]$$

The BIBO stability area is shown in Fig.5.5. The dark area represents the test given

by (5.3.26) which is valid. The grey area plus the dark area show that the test (5.3.30) is also valid, i.e.

$$\lim_{L\to\infty}\frac{1}{L}\sum_{j=n}^{n+L}\left(1-2\alpha\frac{\|\partial A(j)\|}{(1-\alpha^2)^2}\right)\geq 1$$

The white area shows the BIBO global unstable area.

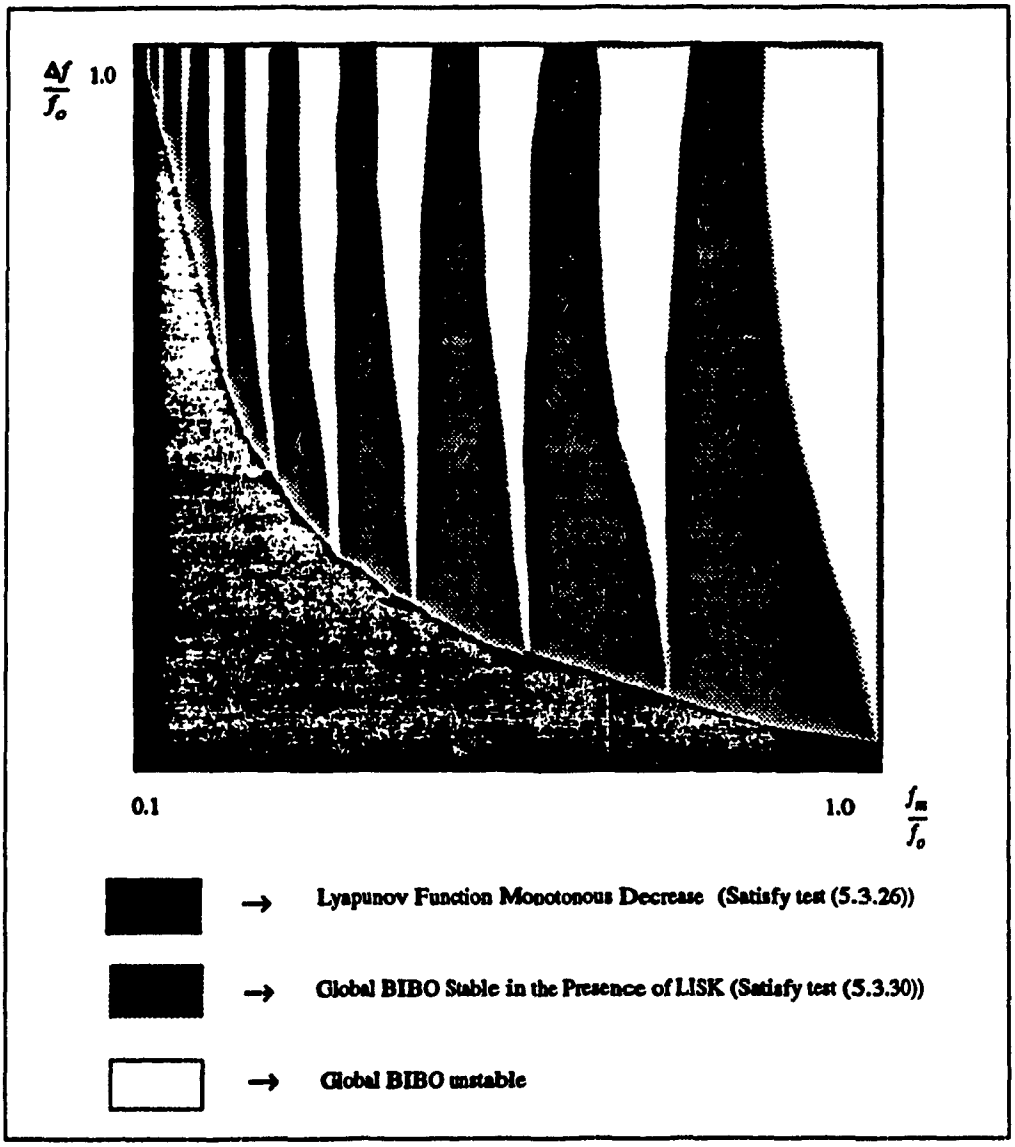

Fig.5.5 Theoretical Test of BIBO Stability Results of Discrete Mathieu Equation

Remark 5.4.6 Discrete Mathieu equation has a rich phenomenon of stability. It is very interesting to see that the discrete Mathieu equation may have LISK,or not have LISK, or it may be globally unstable.

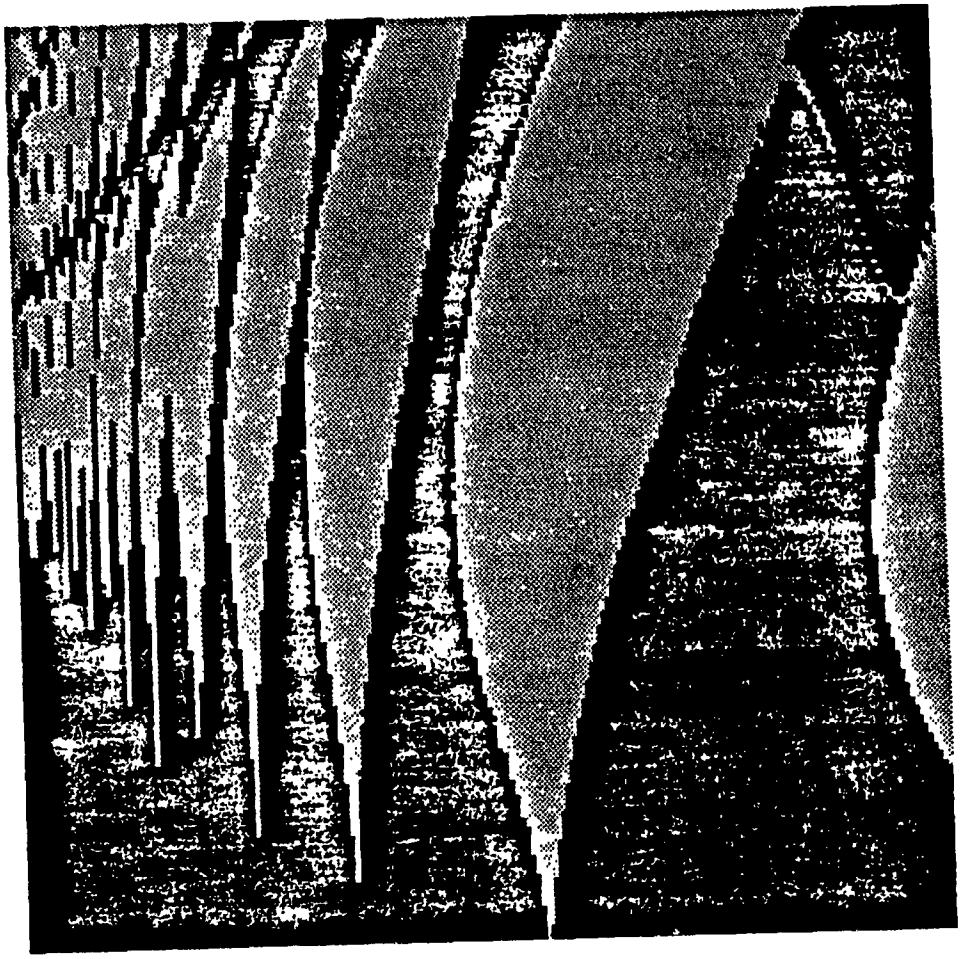

Fig.5.6 Computer Simulation Results for BIBO Stability of Discrete Mathieu Equation

Fig.5.7 Representing BIBO Stability of Mathiue Equation in a Standard Mathieu Diagram

References

[5.1] F. M. Gallier and C. A. Desoer, "*Linear System Theory*", Springer-Verlag, New York, 1991

[5.2] E. I. Jury, "*Inners and Stability of Dynamic Systems*" Wiley, New York 1975

[5.3] H. D. Angelo, "*Linear Time-Varying Systems: Analysis and Synthesis*", Allyn and Bacon, Boston, 1970

[5.4] M. A. Lyapunov, "Obshchaya zadacha ob ustoichivosti dvisheniya", *Math. Soc. Karkov*, 1892

[5.5] R. E. Kalman and J.E. Bertam, "Control System Analysis and Design via the Second Method of Lyapunov: Part II Discrete Systems", *J. of Basic Eng. Trans. ASME.*, Vol. 82 No. 2, pp. 394-400, June 1960

[5.6] G. H. Golub and C.F. Van Loan, "*Matrix Computations*", John Hopkins University Press, 1983

[5.7] Shilov and Gurevich, "*Integral, Measure, and Derivative: A Unified Approach*", Prentice-Hall Inc. 1966

[5.8] Wen Tong, D. Wulich, Eugene I. Plotkin and M. N. S. Swamy, "Stability of Two Second Order Time-Varying Constrained Notch Filters with Externally Controlled Coefficients", *Proceedings of Canadian Conference of Electrical and Computer Engineering*, pp. 795-798, Sept. 1990

[5.9] E. Walach and E. Zeheb, "Sign Test of Multivariable Real Polynomials", *IEEE Trans. on Circuits and System*, Vol. 27, No. 7, July 1980

[5.10] O. Macchi and M. Jeidane-Saidane, "Adaptive IIR Filtering and Chaotic Dynamics: Application to Audiofrequency Coding", *IEEE Trans. on Circuits and Systems*, Vol. 36, No. 4, April 1989

[5.11] W. A. Sethares, C. R. Johnson Jr. and C. E. Rohrs, "Bursting in Adaptive Hybrids", *IEEE Trans. on Communications*, Vol. 37, No. 8, pp. 791-799, August 1989

[5.12] J. A. Richards, "Modeling Parametric Processes: A Tutorial Review", *Proceeding of IEEE*, Vol. 65, No. 11, Nov. 1977

[5.13] S.C. Scoular, I.B. Rogozkin and M.S. Chernykov, "Review of Soviet Research on Linear Time-Variant Discrete System", *Signal Processing*, Vol. 30, pp. 85-101, 1993

[5.14] H.K. Khalil, "*Non-linear Systems*" MacMillan Publishing Company, New York, 1992

Chapter

6

Separation of a Constant-Envelope Signal with Time-Varying Frequency From an Arbitrary Signal with Overlapping Fourier Spectra

6.1. Fourier Spectrum Synthesis via Non-Equally Spaced Sampling

6.1.1. Introduction

In this section, we propose an algorithm which can transform a class of non-stationary signals into a new time-domain such that the non-stationary signal becomes a stationary one. The new technique is based on the design of the Non-Equally Spaced Sampling (NESS) strategy. We will present a theoretical analysis of the NESS from the point of view of spectrum synthesis (shaping) in a new time-domain. A NESS strategy is used to transform the spectrum of given shape into a desired one. An on-line NESS strategy is proposed to implement such a spectrum shaping. We introduce a NESS displacement kernel function, and show its role in spectrum shaping. Several new properties of NESS are discussed. We also provide a necessary condition for the stability of the algorithm namely the convergence of the proposed NESS. It is proven that it is possible to transform any constant-envelope signal (stationary or nonstationary) into a sinusoidal counterpart in the transformed time-domain with *a priori* assigned frequency variations. In particular, it is also possible to transform a constant-envelope signal into a sinusoid with *a fixed* and *a priori* known frequency. A simple level-crossing algorithm, which fulfills the task of on-line spectrum synthesis is presented.

6.1.2. Definitions

Let us consider a real signal $x(t)$ $t \in \Re^+$. Let the signal be sampled at time instants $t = nT$ $n \in Z^+$; Let the equally spaced samples (ESS) be denoted as $x_n = x(nT)$. The Non-Equally Spaced Sampling (NESS) instants are denoted as $\{t_k\}$, where $k \in Z^+$. The samples associated with such a NESS are given by $x_k = x(t_k)$. For convenience of discussion, we explicitly define two different time-domains.

Definition 6.1.1

$\aleph$ = {n | the index of ESS instant}

κ = {k | the index of NESS instant}

$\aleph$ represents the real-time domain, while κ represents the new transformed-time-domain associated with each specific realization of NESS, and there exists a non-decreasing positive function which constitutes a one-to-one mapping between the real-time-domain $\aleph$ and transformed-time-domain κ.

In what follows, we define three different transformations of a signal $x(t)$

Definition 6.1.2

Transform-1

$$X^{\aleph}(z) = Z\{x_n\} = \sum_{n=0}^{\infty} x_n z^{-n} \tag{6.1.1}$$

Transform-2

$$X^{D}(q) = D\{x(t_k)\} = \sum_{k=0}^{\infty} x(t_k)\, e^{-qt_k} \tag{6.1.2}$$

where $q = \sigma + j\omega$

Transform-3

$$X^{\kappa}(z) = Z\{x_k\} = \sum_{k=0}^{\infty} x_k z^{-k} \tag{6.1.3}$$

The first transform is the standard Z-transform of the ESS sequence of signal $x(t)$ in the real-time-domain, i.e. the $\aleph$-time-domain. The second one is the so-called *Dirichlet transform*, which takes into account the information of NESS instants $\{t_k\}$. Dirichlet studied such an expansion to prove his celebrated theorem on primes in arithmetical progression and such a transform is a very useful tool in the theory of

analytic numbers[6.2]. The third transform is the Z-transform of the NESS sequence in the transformed-time-domain, where the NESS samples *are treated as a regular ESS sequence*. It is readily seen that the D-transform is nothing but the Laplace transform of the continuous signal $x(t)$, with a Dirac function located at the NESS instant t_k. The unique feature of the D-transform is that it preserves the information of NESS (given by instant$\{t_k\}$). In what follows, the D-transform is used to establish the relationship between the Z-transform in $\aleph$-time-domain and the Z-transform in the κ-time-domain; this relationship will lead to an explicit expression of the Fourier spectrum in the $\aleph$-time-domain and its counterpart in κ-time-domain.

6.1.3. Convergence of D-Transform and NESS Displacement Function

Before investigating the relationship between the three transforms defined in different time-domains, we present the conditions for convergence of the D-transform. Although *for the same signal* different NESS will result in different D-transforms, the following conditions must be satisfied independent of the NESS strategy.

The NESS instants $\{t_k\}$ are a strictly increasing sequence of real numbers such that $t_k \to \infty$, as $k \to \infty$, iff [6.2]

$$\textbf{Condition I:} \qquad \lim_{k\to\infty} sup \frac{ln(k)}{t_k} = 0 \tag{6.1.4}$$

$$\textbf{Condition II:} \qquad \lim_{k\to\infty} sup \frac{ln|x(t_k)|}{t_k} = \sigma_o \tag{6.1.5}$$

The D-transform(6.1.3) is holomorphic in a half-plane with $Re\{q\} = \sigma > \sigma_o$.

Therefore, the inverse D-Transform can be written as

$$\frac{r!}{2\pi j}\int_{\sigma-j\infty}^{\sigma+j\infty} \frac{X(q)}{q^{r+1}} e^{qt} dq = \sum_{k=0}^{n} \zeta_k (t-t_k)^r \tag{6.1.6}$$

where $t \in [t_k, t_{k-1}]$ and $\sigma > \sigma_o$. If the D-Transform is known, then the NESS instants $\{t_k\}$ can be obtained by setting $r = 1$ and the NESS sequence $x(t_k) = \zeta_k$ can be found by setting $r = 0$. It should be noted here that the *convolution property* of the Z-transform no longer valid for the D-transform, since it deals with non-equally spaced

sequence.

Now suppose that the NESS can be regarded as a displacement (jittered version) from ESS instants, then we may denote such a displacement by δ_k, so that the NESS instant becomes $t_k = kT + \delta_k$. Introducing a NESS *displacement function* by

$$f_k(-q) = e^{-q\delta_k} \tag{6.1.7}$$

and using Z-transform, and keeping q as a fixed value, we get

$$F(-q, z) = \sum_{k=0}^{\infty} e^{-q\delta_k} z^{-k} \tag{6.1.8}$$

The function $F(-q, z)$ is called a *displacement kernel function*, the inverse Z-transform of $F(-q, z)$ relates to the NESS displacement function

$$e^{-q\delta_k} = \frac{1}{2\pi j} \oint_c z^{k-1} F(-q, z)\, dz \tag{6.1.9}$$

If the displacement kernel function $F(-q, z)$ is known, then the NESS instants can be determined by using (6.1.9). With such a displacement kernel function, we obtain a new expression for the D-transform of the NESS signal $x(t_k)$ in terms of the Z-transform of the NESS sequence $X^K(z)$ in the κ-time-domain

$$X^D(q) = \frac{1}{2\pi j} \oint_c F(-q, \xi) X^K(\xi^{-1} e^{qT}) \frac{d\xi}{\xi} \tag{6.1.10}$$

It should be noted here that such a displacement kernel function establishes a useful connection between the D-transform and the Z-transform through (6.1.10). Based on this relationship, we will present several important new properties of the NESS.

6.1.4. New Properties of Non-Equally Spaced Sampling

The Fourier spectrum of a ESS sequence in κ-time-domain is obtained by substituting $z = e^{j\omega}$ into its Z-transform $X^K(z)$. The spectrum of the D-transform of the NESS sequence can be obtained by substituting $q = j\omega$ into $X^D(q)$. Since the NESS instant is preserved in the D-transform, by comparing the definition of

transform-1 and transform-2, we see that the spectrum of the D-transform $X^D(j\omega)$ is identical to the spectrum of $X^{\aleph}(e^{j\omega})$. By exploiting this important relationship, we have the following properties.

Lemma 6.1.1 *(Convlutional) The Fourier spectrum of signal $x(t)$ in the $\aleph$-time-domain and its counterpart in the κ-time-domain are related by*

$$X^{\aleph}(\omega) = \frac{1}{2\pi}\int_{-\pi}^{\pi} X^{\kappa}(\omega+\Omega)\,F(\Omega,\omega)\,d(\Omega T) \tag{6.1.11}$$

Proof: This result is proved by substituting $q = e^{j\omega}$ and $\xi = e^{j\Omega}$ into (6.1.10) and by taking the contour C to be the unit disc.

Q.E.D.

This Fourier spectrum convolution Lemma 6.1.1 associated with the NESS displacement kernel function plays a key role in the analysis and synthesis of the Fourier spectrum in the κ-time-domain by using the NESS technique. The link between the Fourier spectrum in the $\aleph$-time-domain and the κ-time-domain is established by the integral equation in complex domain given by(6.1.11). Our interest is focused on an explicit expression of such an NESS displacement kernel function. It is easy to show

$$F(\Omega,\omega) = \sum_{k=0}^{\infty} e^{j\omega\delta_{k_e}-j\Omega kT} \tag{6.1.12}$$

For any pair of Fourier spectrum $X^{\aleph}(\omega)$ and $X^{\kappa}(\omega)$ in $\aleph$-time and κ-time domains respectively, which satisfy the integral equation (5.0.11), there exists a NESS strategy that can fulfill the spectrum synthesis task by transforming $X^{\aleph}(\omega)$ into $X^{\kappa}(\omega)$.

The expression of the NESS displacement kernel function (6.1.12) indicates that the kernel function $F(\Omega,\omega)$ should be an *entire function* if the expansion of the Fourier kernel of the NESS displacement function converges [6.8]. So this leads to a necessary condition for NESS to perform such a spectrum synthesis.

According to the convergence property of the entire function of exponential type

[6.8], the *necessary condition* for the stability of NESS is given by

$$\lim_{k \to \infty} \frac{\delta_k}{k} = 0 \tag{6.1.13}$$

Conditions (6.1.13), and (6.1.4) respectively provide an *asymptotic upper bound* and *an asymptotic lower bound* for the NESS displacement δ_k.

Lemma 6.1.2 *(Parseval Property) A NESS is an energy conservation process, i.e., the energy of a signal remains the same after applying NESS.*

Proof: Substitute of (6.1.12) into (6.1.11) we get

$$X^{\aleph}(\omega) = \frac{1}{2\pi} \int_{-\pi}^{\pi} X^{K}(\omega + \Omega) \sum_{l=0}^{\infty} e^{j\omega\delta_l} e^{-jl\Omega T} d(\Omega T) \tag{6.1.14}$$

Using the definition of the Fourier transform $X^{K}(\omega)$ given by

$$X^{K}(\omega + \Omega) = \sum_{k=0}^{\infty} x_k e^{-j(\omega + \Omega)kT} \tag{6.1.15}$$

yields

$$X^{\aleph}(\omega) = \frac{1}{2\pi} \int_{-\pi}^{\pi} \sum_{k=0}^{\infty} x_k e^{-j(\omega + \Omega)kT} \sum_{l=0}^{\infty} e^{j\omega\delta_l} e^{-jl\Omega T} d(\Omega T) \tag{6.1.16}$$

or

$$X^{\aleph}(\omega) = \frac{1}{2\pi} \int_{-\pi}^{\pi} \sum_{k=0}^{\infty} \sum_{l=0}^{\infty} x_k e^{-j\omega kT} e^{-j\Omega kT} e^{j\omega\delta_l} e^{-jl\Omega T} d(\Omega T) \tag{6.1.17}$$

Using the orthonormal properties

$$\int_{-\pi}^{\pi} \sum_{m=0}^{\infty} \sum_{k=0, k \neq m}^{\infty} e^{-j\Omega kT} e^{-jm\Omega T} d(\Omega T) = 0 \tag{6.1.18}$$

Also

$$\int_{-\pi}^{\pi} \sum_{l=0}^{\infty} \sum_{k=0}^{\infty} e^{j\omega kT} e^{j\omega\delta_l} d\omega T = 0 \tag{6.1.19}$$

due to the fact that a NESS displacement $\delta_l \neq lT$, $\forall l \in Z^{+}$. Thus we have

$$\int_{-\pi}^{\pi} |X^{\aleph}(\omega)|^2 d\omega = \sum_{k=0}^{\infty} x_k x_k^* = \int_{-\pi}^{\pi} |X^{\kappa}(\omega)|^2 d\omega \tag{6.1.20}$$

Q.E.D

Similar to the standard Parseval property between time and frequency domains, Lemma 6.1.2 establishes a new Parseval relationship between real time-domain and the transformed one.

Based on Lemma 6.1.2, it follows that any NESS, (which satisfies the integral Equation (6.1.11)), will *not change the total energy* of the signal in the κ-time-domain. However, the energy distribution e.g. the Fourier power spectrum, may be completely different from its counterpart in the real time domain. So the basic idea of using NESS technique to spectral synthesis rests upon this interesting mechanism of transformation of distribution of energy in the spectral domain. Therefore, the objective of spectral synthesis for a given signal is reduced to finding an appropriate NESS strategy.

Lemma 6.1.3 (*Duality*) *The Fourier spectra* $X^{\aleph}(\omega)$ *and* $X^{\kappa}(\Omega)$ *have dual counterparts in the* κ*-time-domain and the* ℵ*-time-domain, respectively.*

Proof: With the convolution Lemma 6.1.1

$$X^{\aleph}(\omega+\Omega) = \frac{1}{2\pi}\int_{-\pi}^{\pi} X^{\kappa}(\omega+\Omega+\hat{\Omega})\, F(\omega+\Omega, \hat{\Omega})\, d\hat{\Omega}T \tag{6.1.21}$$

and using (6.1.21), we evaluate

$$\frac{1}{2\pi}\int_{-\pi}^{\pi} X^{\aleph}(\omega+\Omega)\, F(\omega, \Omega)\, d(\Omega T)$$

$$= \frac{1}{4\pi^2}\int_{-\pi-\pi}^{\pi\ \pi} X^{\kappa}(\omega+\Omega+\hat{\Omega})\, F(\omega+\Omega, \hat{\Omega})\, F(\omega, \Omega)\, d(\Omega T)\, d(\hat{\Omega}T) \tag{6.1.22}$$

Let $\varpi = \omega+\Omega+\hat{\Omega}$, then (6.1.22) yields

$$\frac{1}{4\pi^2}\int_{-\pi-\pi}^{\pi\ \pi} X^{\kappa}(\varpi)\, F(\varpi-\hat{\Omega}, \hat{\Omega})\, F(\varpi-\Omega-\hat{\Omega}, \Omega)\, d(\Omega T)\, d(\hat{\Omega}T)$$

$$= \frac{1}{4\pi^2}\int_{-\pi-\pi}^{\pi\ \pi} X^{\kappa}(\varpi) \sum_{l=0}^{\infty} e^{j\varpi\delta_l} e^{-j\Omega\delta_l} e^{-jl\hat{\Omega}T} \sum_{k=0}^{\infty} e^{j\varpi\delta_k} e^{-j\Omega\delta_k} e^{-j\hat{\Omega}\delta_k} e^{-jk\Omega T}\, d(\Omega T)\, d(\hat{\Omega}T)$$

$$= X^{\kappa}(\varpi) \tag{6.1.23}$$

The last equality invokes the orthonormal property.

Q.E.D.

Lemma 6.1.3 simply states an interchange property of the Fourier spectrum in the $\aleph$-time-domain and the κ-time-domain. If a wideband signal in the $\aleph$-time-domain is transformed into a narrowband signal in the κ-time-domain by NESS, then a narrowband signal in the $\aleph$-time-domain will be transformed into a wideband signal in the κ-time-domain by the same NESS, and vice versa. This property is very useful in a situation where the Fourier spectrum of two (or several) signals are overlapped in the real-time-domain. It leads to a possibility of finding a NESS strategy which makes their Fourier spectra separated in a new-time-domain.

6.1.5. Spectrum Synthesis as Applied to a Constant Envelope Signal via NESS

To find NESS instants by directly solving (6.1.11) is an almost impossible task, because it is very difficult to solve the integral equation in the complex domain. In what follows, we consider one particular situation which allows us to find the solution of this problem without solving (6.1.11).

Theorem 6.1.1 *(Existence) Each analytic constant-envelope signal in the $\aleph$-time-domain can be converted into a sinusoid with an a priori known frequency in the κ-time-domain via a NESS.*

Proof: Suppose in the κ-time-domain the signal is a sinusoid with a fixed frequency ω_o, therefore, its Fourier spectrum in κ-time-domain is

$$X^{\kappa}(\omega+\Omega) = \pi[\delta(\omega+\Omega+\omega_o)+\delta(\omega+\Omega-\omega_o)] \tag{6.1.24}$$

Substituting (6.1.24) into (6.1.12)

$$X^{\aleph}(\omega) = \sum_{k=0}^{\infty} e^{j\omega_o\delta_k} e^{-j(\omega-\omega_o)kT} \tag{6.1.25}$$

or

$$X^{\aleph}(\omega) = \sum_{k=0}^{\infty} e^{j\omega_o\delta_k} e^{j\omega_o kT} e^{-j\omega kT}$$

By definition of the discrete Fourier transform (DFT),

$$x_n = x(nT) = e^{j(\omega_o nT + \omega_o \delta_n)} \tag{6.1.26}$$

$$|x_n| = 1 \tag{6.1.27}$$

Thus $X^{\kappa}(\omega)$ represents a single spectral line at frequency ω_0 in κ-time-domain.

Q.E.D.

By Theorem 6.1.1, a constant envelope signal $x_n = e^{j\Psi(n)}$, where $\Psi(n)$ is an arbitrary phase function, can be converted to a single sinusoid with a frequency ω_o. It is seen that ω_o depends on the sampling frequency, and NESS displacement depends on the frequency variation of the signal in the $\aleph$-time-domain. In what follows, we present a level- crossing algorithm to create NESS instants; it is an *on-line* algorithm, which has a very clear physical interpretation, see [6.10].

Corollary 6.1.1 *Any constant-envelope signal can be converted into a sinusoid via the level-crossing detection of the non-linear equation*

$$t_k = \Psi^{-1}\left[\frac{2\pi k}{N}\right] \tag{6.1.28}$$

Proof: Substituting with $t_k = kT + \delta_k$ into (6.1.26) gives

$$x_k = e^{j\left[\frac{2\pi k}{N}\right]} \tag{6.1.29}$$

Q.E.D.

In (6.1.29), N is the number of the samples during the interval in which the phase of signal $\Psi(t)$ advances by 2π radians, thus the frequency of the sinusoid in κ-time-domain $\omega_o = 2\pi/N$. Note that Corollary 6.1.1 is true based on the fact that in parctice an over sampling strategy is used, i.e. N is larger enough. The main advantage of this algorithm is that we do not need to find the Fourier displacement kernel by solving the integral equation (6.1.11) in order to find the NESS instant $\{t_k\}$.

In light of Theorem 6.1.1 and Corollary 6.1.1, a more general result may be formulated.

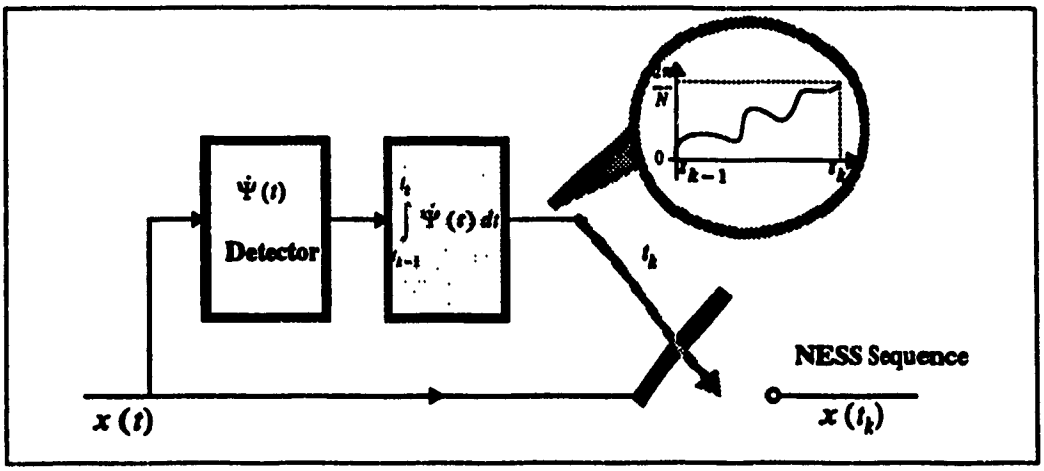

Fig.6.1 A Level-Crossing Algorithm Used for Generating NESS Sequence

Theorem 6.1.2 *(Main Result) Each constant-envelope signal in the ℵ-time-domain with arbitrary instantaneous frequency may be converted into an FM signal in the κ-time-domain with a priori known frequency variation law.*

Proof: Given an FM signal in the κ-time-domain with a known frequency variation law, the phase of such an FM signal as

$$\psi^{\kappa}(k) = \omega_o kT + \delta\psi_k$$

Assuming that the NESS displacement sequence is $\{\delta_k\}$ then we may find the Fourier spectrum of such an FM signal in the ℵ-time-domain to be:

$$X^{\aleph}(\omega) = \frac{1}{2\pi}\int_{-\pi}^{\pi}\sum_{k=0}^{\infty}\sum_{l=0}^{\infty} e^{j\psi^{\kappa}(k)} e^{-j\omega kT} e^{-j\Omega kT} e^{-jl\Omega T} d(\Omega T)\, d(\hat{\Omega}T)$$

$$= \sum_{k=0}^{\infty} e^{j(\omega_0 kT + \delta\psi_k + \omega_0\delta_k)} e^{-j\omega Tk} = \sum_{k=0}^{\infty} e^{j\phi(k)} e^{-j\omega Tk} \qquad (6.1.30)$$

Hence $\phi(k) = \psi^{\kappa}(k) + \delta\psi_k + \omega_0\delta_l$ which implies that one can always find the NESS displacement sequence $\{\delta_k\}$ to transform a given phase $\phi(k)$ in the ℵ-time-domain into a new phase $\psi^{\kappa}(k)$ in the κ-time-domain.

Q.E.D.

In practice, the transformation of a constant envelope signal into an FM one by NESS is carried out in a manner similar to the one presented in Fig.6.1; here the threshold is not a fixed one, it is time-varying according to the pre-designed frequency variation law.

Lemma 6.1 gives a general approach to spectrum synthesis based on NESS technique. A practical solution of spectrum synthesis for a class of signals with a constant-envelope is provided by Theorem 6.1.1, Corollary 6.1.1, and Theorem 6.1.2. However, the existence and practical implementation of a NESS for a given arbitrary analytical signal to be converted to a signal with an arbitrary assigned spectrum in the κ-time-domain is still an *open issue*.

Note that the spectrum synthesis or the spectrum transform is of particular interest for problems of signal separation. As already shown, a constant-envelope signal can be converted into a sinusoid with an *a priori* known frequency, thus we can use a simple second order time-invariant AS-ARMA model to separate signals in the κ-time-domain. Such an idea has been already successfully used in anti-jamming of strong FM signals [6.18] [6.11] [6.16].

It should be noted that (6.1.24) also suggests a new method for detecting the instantaneous frequency by using information about NESS displacement. The proposed NESS algorithm is a level crossing algorithm, which is different from the classical Rice's zero-crossing method. Rice's method is based only on the zero-crossing information of the waveform of the FM signal, while our method uses the level-crossing of the phase information.

6.1.6. Examples of NESS Spectrum Synthesis and Signal Separation

Consider a constant-envelope FM signal $r(t) = e^{j\Psi(t)}$, where the instantaneous frequency is modulated by a *sine* function, The phase of $r(t)$ is expressed as

$$\Psi_r(t) = \omega_c t + \frac{\Delta\omega}{\omega_m}\sin(\omega_m t) \tag{6.1.31}$$

It is well known that the Bessel expansion of such an FM signal is given by

$$r_n = e^{j\omega_c n}\sum_{l=-\infty}^{\infty} J_n\left(\frac{\Delta\omega}{\omega_m}\right) e^{jnl\omega_m} \tag{6.1.32}$$

where $J_n(\cdot)$ is the First kind Bessel function of order n.

A). Transforming an FM Signal into a Sinusoid in *K*-Time-Domain

Find the NESS instants as

$$t_k = \Psi_r^{-1}\left[\frac{2\pi k}{N}\right] \tag{6.1.33}$$

then $r(t)$ is transformed into a harmonic in the κ-time-domain

$$r_k = e^{j\left[\frac{2\pi}{N}k+\phi\right]} \tag{6.1.34}$$

On the other hand, let us consider a sinusoid with a fixed frequency ω_s in the $\aleph$-time-domain

$$s_n = e^{j\left[\omega_s n+\phi_0\right]} \tag{6.1.35}$$

After the NESS, it is transformed into the FM signal given by

$$s^*_k = e^{j\frac{\omega_s}{\omega_r}\left[\frac{2\pi}{N}\right]k}\sum_{n=-1}^{\infty} J_n(\Delta\omega)\, e^{jn\frac{\omega_m}{\omega_r}\left[\frac{2\pi}{N}\right]k} \tag{6.1.36}$$

Example 6.1.1 We present an example of separation of two weak sinusoids corrupted by a strong FM signal. Fig 6.2 shows the input mixture, here we assume that the phase of an FM signal is known.

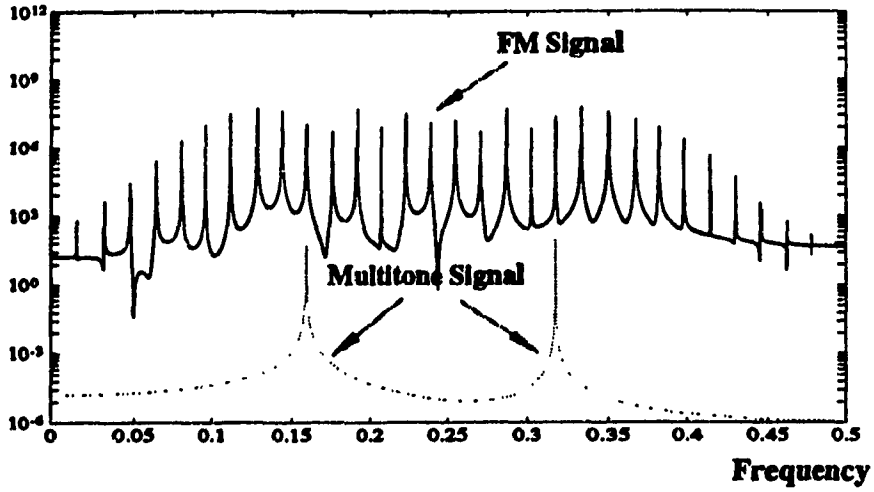

Fig.6.2 Fourier power spectrum of input mixture in κ-time-domain
(One strong wideband FM signal and two weak sinusoids)

After applying the NESS procedure to the input mixture, the wideband FM signal is concentrated as a single spectrum line, while the two sinusoids are transformed into a wideband FM signal in the κ-time-domain, see Fig.6.3

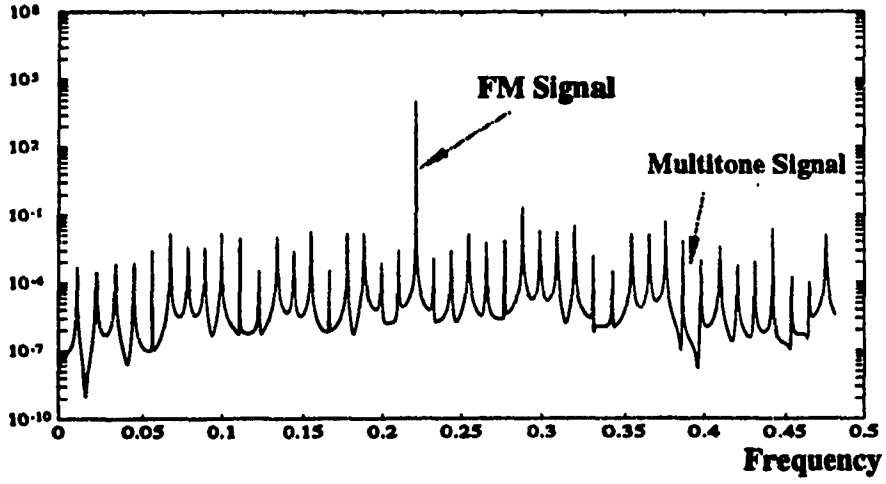

Fig.6.3 Fourier Power Spectrum of Input Mixture in K-Time-Domain

B). Transforming of a Time-Varying AS-ARMA Mode into a Time-Invariant One

One of the interesting issue is that the NESS can transform a time-varying AS-ARMA model in the $\aleph$-time-domain into a time-invariant one in the κ-time-domain. To show this, let us consider an FM signal in the $\aleph$-time-domain. The *Wronskian* associated with such a signal is time-dependent

$$\begin{aligned}\Delta_{\Psi_r}(k) &= \sin\left(\Psi_r(k) - \Psi_r(k-1)\right) \\ &= \sin\left(\omega_c + \frac{2\Delta\omega}{\omega_m}\cos\left[\omega_m\left(k-\frac{1}{2}\right)\right]\sin\left[\frac{\omega_m}{2}\right]\right)\end{aligned} \tag{6.1.37}$$

Hence the two coefficients of the 2nd-order AS-ARMA model are written as

$$a_2^{\aleph}(k) = \frac{\sin\left(\omega_c + \frac{2\Delta\omega}{\omega_m}\cos\left[\omega_m\left(k-\frac{1}{2}\right)\right]\sin\left[\frac{\omega_m}{2}\right]\right)}{\sin\left(\omega_c + \frac{2\Delta\omega}{\omega_m}\cos\left[\omega_m\left(k-\frac{3}{2}\right)\right]\sin\left[\frac{\omega_m}{2}\right]\right)} \tag{6.1.38}$$

After applying NESS, the *Wronskain* becomes a constant in the κ-time-domain:

$$\Delta_{\Psi_r}(k) = \sin\left[\Psi_r(t_k) - \Psi_r(t_{k-1})\right] = \sin\left[\frac{2\pi}{N}\right] \tag{6.1.39}$$

Then the coefficients of AS-ARMA model becomes

$$a_2^{\kappa}(k) = \frac{\Delta_{\Psi_r}(k)}{\Delta_{\Psi_r}(k-1)} = 1 \quad a_1^{\kappa}(k) = -2\cos\left[\frac{2\pi}{N}\right] \tag{6.1.40}$$

Therefore, by using the NESS given in (6.1.34), the ***time-varying*** AS-ARMA model is transformed into a ***time-invariant*** one.

We can use a second order AS-ARMA model to cancel the FM signal in the κ-time-domain. The transfer function of such a time-invariant AS-ARMA model is in fact a notch filter, and is given by

$$H(z) = \frac{1 - 2\cos\left[\frac{2\pi}{N}\right]z^{-1} + z^{-2}}{1 - 2\alpha\cos\left[\frac{2\pi}{N}\right]z^{-1} + \alpha^2 z^{-2}} \tag{6.1.41}$$

where $\alpha \to 1^{-}$ is the symmetrical factor as defined in previous Chapters.

After elimination of the FM signal in the κ-time-domain, the two sinusoids remains unchanged due the transparency property AS-ARMA model. The spectrum of the separated two sinusoids in κ-time-domain is shown in Fig.6.4

The above processing is performed to separate one FM signal from other arbitrary signals, under the assumption that the instantaneous phase of FM signal is known. Such a processing strategy can be carried out in a cascade manner to *separate multiple FM signals*, although their Fourier spectrum may be *completely overlap*, this separation of superimopsed FM signals can be achived if the instantaneous phase of each FM signal is *a priori* known.

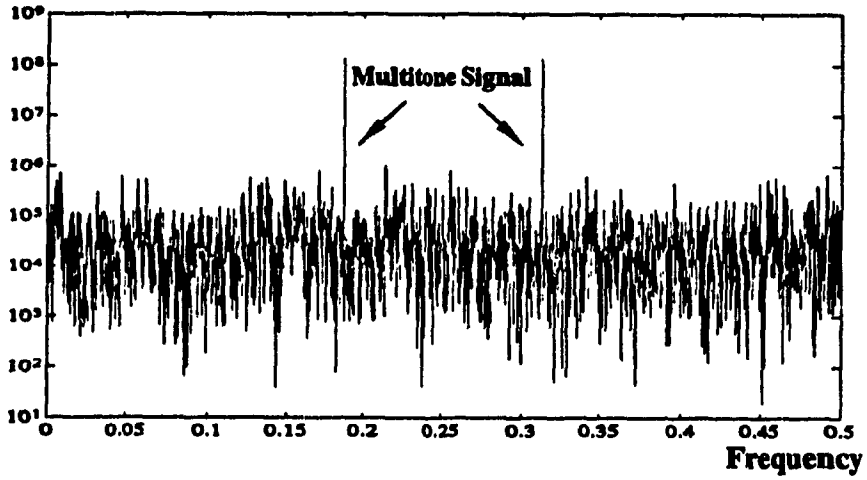

Fig.6.4 The Fourier power spectrum of two Reconstructed weak sinusoids in κ-time-domain

Example 6.1.2 Consider two linear chirp FM singles FM-1 and FM-2, FM-1 possesses a positive chirping rate, and FM-2 has a negative one. Suppose the phase of FM-2 is a priori known. Based on such a phase, NESS is carried out to convert FM-2 into a spectral line in the κ-time-domain with a known frequency. Using the time-invariant AS-ARMA model to cancel FM-2 in κ-time-domain, then FM-1 is reconstructed from the NESS samples, and thus FM-2 and FM-1 are separated, see Fig.6.5.

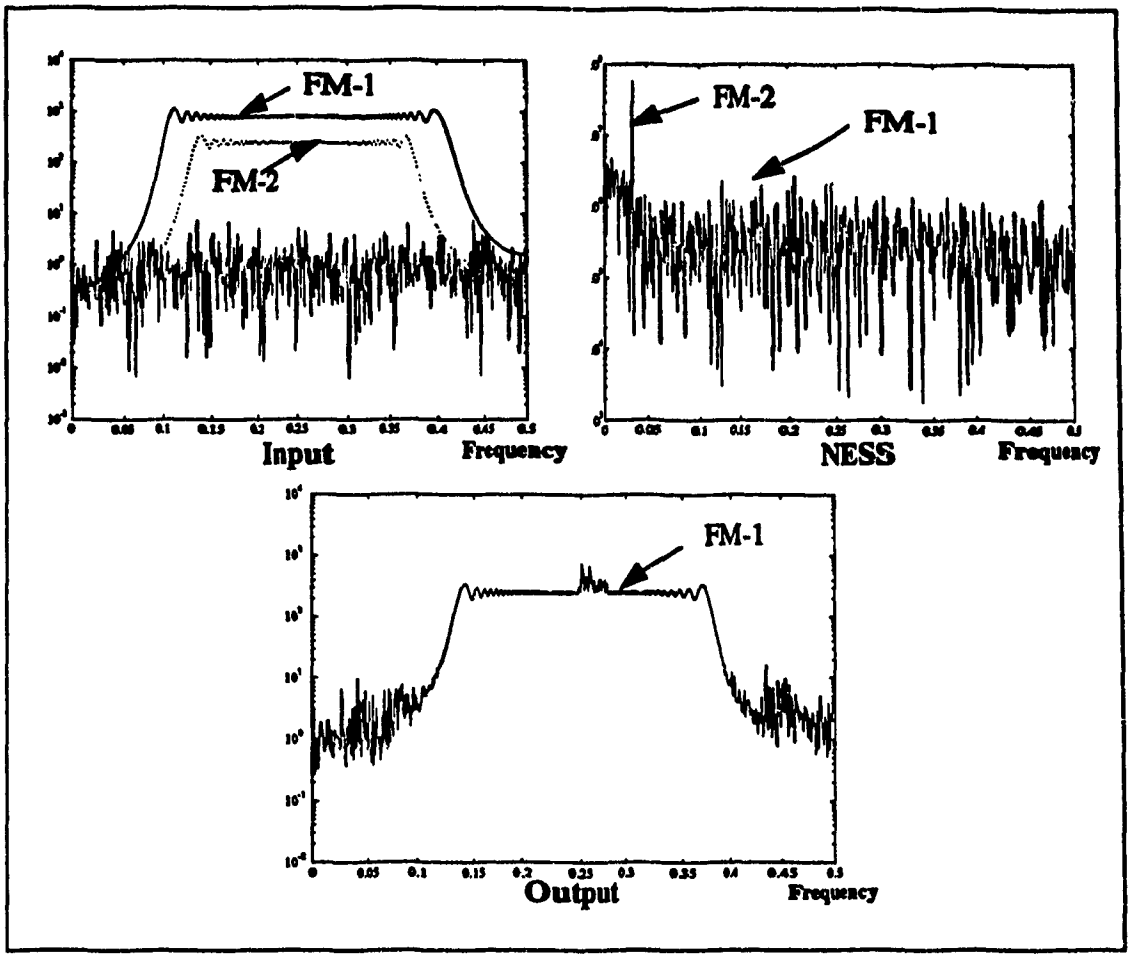

Fig.6.5 Separation of Two Chirp Signals with Overlapping Spectra

6.2. A Closed-Loop Phase Controlled ASTV-ARMA Model

6.2.1. Introduction

In the previous section, we presented an approach for the separation of constant-envelope FM signals, by using the NESS technique. However, such a separation algorithm requires *a priori* knowledge of the instantaneous phase. We may refer to such a processing as the phase-controlled processing or phase-controlled NESS. The situation remains the same, as applying to a time-varying AS-ARMA model, where time-varying coefficients solely depend on the instantaneous phase. In practice, however, a blind separation is required, i.e. the exact instantaneous phase is not available *a priori*, but has to be estimated from an input mixture. Due to the presence of other signals, and background noise, such an estimation will always contain errors, and this will cause a degradation in the performance of the separation. In this section, we present an analysis of the separation performance in the case of a strong constant-envelope FM signal with unknown parameters mixed with other signals. A new closed-loop scheme has been proposed [6.11], which improves the performance even though the phase estimation contains errors.

Before we proceed with the analysis, let us clarify the equivalence between the separation procedure based on NESS discussed in last section, and by using a direct form of a time-varying AS-ARMA model.

As for the NESS procedure, if the phase of the FM signal is known then the level-crossing algorithm will generate exact NESS time instants $\{t_k\}$, which are the ideally synchronized NESS instants, and thus the NESS can transform a constant-envelope signal into a sinusoid with a fixed frequency in the new-time-domain. Nevertheless, if the phase estimation contains an error, then the NESS instants generated by the level-crossing algorithm, are no longer ideally synchronized; it will not concentrate the whole energy of the FM signal into a single spectrum line in the new-time-domain. As for the use of the direct form of time-varying AS-ARMA model with time-varying coefficients, if such coefficients are calculated by using the true phase of the FM signal, then a perfect separation can be achieved; however, if the coefficients are calculated by using an estimated phase then the coefficients deviate from their true values, and an

ideal separation becomes impossible.

In order to improve the performance of separation, and to make the applications more attractive in practice, we propose a novel closed-loop scheme, wherein the influence of the phase estimation error will be automatically reduced. This process is referred to as the *self-synchronization* process; the condition which leads to this self-synchronization is also given.

6.2.2. Statement of the Problem

Consider an input mixture, consisting of a constant-envelope signal $r(k)$, an arbitrary signal $s(k)$, and a background noise $n(k)$,

$$x(k) = r(k) + s(k) + n(k) \qquad k \in Z^{+} \tag{6.2.1}$$

where, $r(k) = A_r exp\{j[\Psi_r(k) + \varphi_r]\}$, the instantaneous frequency $\dot{\Psi}(k)$ is a random positive function (under the Nyquist sampling criterion, its supreme value is less than π), envelope A_r and initial phase φ_r are fixed but unknown values. The other signal can be written as $s(k) = A_s(k) exp\{j\Psi_s(k)\}$, and $n(k)$ is a weak background zero-mean white Gaussian noise with a variance σ_n^2. We further make the assumption $A_r > |A_s(t)| \gg \sigma_n^2$, for $\forall t \in (0, T)$

In the input mixture, the constant-envelope signal is a dominant one; under this condition a phase estimation can be performed by using any standard technique, e.g. the phase-locked loop, or the Hilbert transform. The Fourier spectra of the components of the input mixture are completely overlapping. Our goal is to retrieve the weak signal $s(k)$.

We perform the separation of the input mixture $x(t)$, by applying a second order time-varying AS-ARMA model. Denote the two time-varying coefficients which are calculated by using the true phase of $r(k)$ as $a_1[k, \Psi_r(k)]$ and $a_2[k, \Psi_r(k)]$. In this situation, the coefficients are controlled by the true phase of $r(k)$. Therefore, perfect separation of $r(k)$ from the other signal is achieved once the FM signal $r(k)$ exactly satisfies the MA part of the AS-ARMA model constructed by using the true

phase $\Psi_r(k)$ to control the coefficients $a_1[k, \Psi_r(k)]$ and $a_2[k, \Psi_r(k)]$, i.e.

$$r(k) + a_1[k, \Psi_r(k)]\, r(k-1) + a_2[k, \Psi_r(k)]\, r(k-2) = 0 \qquad (6.2.2)$$

Method of evaluation of these two time-varying coefficients are given in Chapter 2. Unfortunately, the true phase $\Psi_r(k)$ is not available in the task of blind separation. In what follows, we present an analysis of separation performance where the time-varying coefficients of the ASTV-ARMA model are controlled by the phase of the input mixture $\Psi_x(k)$, which is taken as an estimate of $\Psi_r(k)$.

6.2.3. Phase Perturbation Analysis

It is well known that the instantaneous phase of the input mixture $x(k)$ may be represented as:

$$\Psi_x(k) = \Psi_r(k) + \delta\psi(k) \qquad (6.2.3)$$

where the *perturbation term* $\delta\psi(k)$ is caused by the presence of the signal $s(k)$. If the influence of the background noise is neglected, then we have[1]

$$\delta\psi(k) = arctan\frac{A_s(k)\sin\Phi(k)}{A_r + A_s(k)\cos\Phi(k)}, \qquad (6.2.4)$$

where $\Phi(k) = \Psi_s(k) - \Psi_r(k)$. Denote $\beta_k = \frac{A_s(k)}{A_r}$. Under the assumption that the FM signal is a strong one, we have $\beta_k < 1 \ \forall k \in Z^+$. Note that the average value of the ratio $\bar{\beta}_k$ should be less than $-8dB$, so that the phase estimation is performed above the detection threshold to avoid the phase warping in (6.2.3). If the signal $r(k)$ is much stronger than the signal $s(k)$, i.e. $\beta_k \ll 1$ we may express the perturbation term in the form

$$\delta\psi(k) = \frac{A_s(k)}{A_r}\sin\Phi(k) = \beta_k \sin\Phi(k) \qquad (6.2.5)$$

Lemma 6.2.1 *The phase perturbation part of the input mixture signal can be*

1. This expression is valid under the assumption that the phase detector operates above the detection threshold

expanded in terms of the Bessel functions as

$$e^{j\delta\psi(k)} = \prod_{l=1}^{\infty}\prod_{m=-1}^{+1}\sum_{n=-\infty}^{\infty} J_n\left(\frac{\beta^{l+m}}{2^{|m|}(l+m)}\right)e^{jn(m+l)\Phi(k)} \tag{6.2.6}$$

Proof: First we expand (6.2.4) into a trigonometrical function series as

$$\delta\psi(k) = \sum_{p=0}^{\infty}\frac{(-1)^p}{2p+1}\left[\beta_k\sin\Phi(k)\sum_{l=0}^{\infty}(-1)^l(\beta_k\cos\Phi(k))^l\right]^{2p+1} \tag{6.2.7}$$

After some tedious manipulation of (6.2.7), we arrive at the following compact expression

$$\delta\psi(k) = \sum_{n=0}^{\infty}\sum_{m=-1}^{+1}(-1)^n\left(\frac{1}{2}\right)^{|m|}\frac{\beta^{n+m}}{n+m}\sin(n+m)\Phi(k) \tag{6.2.8}$$

To prove that (6.2.8) represents an expansion of (6.2.4), we take the partial derivative of $\psi(k)$ with respect to $\Phi(k)$; from (6.2.4) we have

$$\begin{aligned}\frac{\partial}{\partial\Phi(k)}\delta\psi(k) &= \frac{1}{1+\left(\dfrac{A_s(k)\sin\Phi(k)}{A_r(k)+A_s(k)\cos\Phi(k)}\right)^2}\\ &= \frac{(1+\beta_k\cos\Phi(k))^2}{1+\beta_k\cos\Phi(k)+\beta_k^2}\\ &= \frac{1+\beta_k\cos\Phi(k)}{2}\left(\frac{1}{1+\beta_k e^{-j\Phi(k)}}+\frac{1}{1+\beta_k e^{j\Phi(k)}}\right)\\ &= \sum_{n=0}^{\infty}(-1)^n(1+\beta_k\cos\Phi(k))\beta^n\cos n\Phi(k)\end{aligned} \tag{6.2.9}$$

However, by applying (6.2.7)

$$\frac{\partial}{\partial\Phi(k)}\delta\psi(k) = \sum_{n=0}^{\infty}(-1)^n(1+\beta_k\cos\Phi(k))\beta^n\cos n\Phi(k) \tag{6.2.10}$$

Comparing (6.2.9) and (6.2.10), we see that they are the same, therefore, expression (6.2.7) is true. Using first kind Bessel functions to expand the perturbation term

$exp\{j\delta\psi(k)\}$, we obtain (6.2.6)

Q.E.D.

Since the phase estimation error can be regarded as a perturbation applied to the true phase $\Psi_r(k)$, this perturbation in the controlling phase results in a performance degradation, i.e. introduces a residual signal of $r(k)$. Let us denote this residual signal as $\tilde{r}(k)$. We define the ratio of the energy of the residual signal $\tilde{r}(k)$ to the energy of the signal $s(k)$ as the separation performance index (SPI)

$$\rho_k = \frac{\|\tilde{r}(k)\|_2^2}{\|s(k)\|_2^2} \tag{6.2.11}$$

In the case of complete separation, $\rho_k \to 0$.

Next, we are going to evaluate the separation performance when the controlling phase contains a perturbation. Before doing so, we need to invoke some properties of the first kind Bessel function $J_n(\ )$

I. $$J_{-n}(\beta) = (-1)^n J_n(\beta) \tag{6.2.12}$$

II. $$J_n(\beta+\gamma) = \sum_{k=-\infty}^{\infty} J_k(\beta) J_{n+k}(\gamma) \tag{6.2.13}$$

III. $$|J_n(\beta)| \le \frac{c(\frac{\beta}{2})^n}{n!} \qquad c \text{ is a constant} \tag{6.2.14}$$

IV. $$J_n(\beta) \approx (\frac{n}{|n|}) \frac{1}{2^{|n|}|n|!} m^{|n|} \quad \beta \ll 1 \quad n \neq 0 \quad n \in Z \tag{6.2.15}$$

Theorem 6.2.1 *The separation performance index, as given by (6.2.11), is lower bounded by 0dB.*

Proof: The input mixture is written as

$$x(k) = A_r e^{j\Psi_r(k)} + A_s(k) e^{j\Psi_s(k)}$$

$$= A_r e^{j\Psi_s(k)} e^{-j\delta\psi(k)} + A_s(k) e^{j\Psi_s(k)}$$

By applying Lemma 6.2.1,

$$x(k) = A_r e^{j\Psi_x(k)} \prod_{l=1}^{\infty} \prod_{m=-1}^{+1} \sum_{n=-\infty}^{\infty} J_n\left(\frac{\beta^{l+m}}{2^{|m|}(l+m)}\right) e^{jn(m+l)\Phi(k)} + A_s(k) e^{j\Psi_s(k)} \tag{6.2.16}$$

Using the upperbound of the Bessel function (6.2.14), we can neglect the high order terms of index $l \gg 1$. Using the anti-symmetrical property (6.2.12) and the additive property (6.2.13) together with (6.2.15), yields

$$x(k) = A_r e^{j\Psi_x(k)} \sum_{n=0}^{\infty} \frac{\beta_k^n}{2^n n!} e^{jn\Phi(k)} + A_s(k) e^{j\Psi_s(k)} \tag{6.2.17}$$

Since the ASTV-ARMA model is controlled by the phase $\Psi_x(k)$, so $A_r e^{j\Psi_x(k)}$ is cancelled at the output; therefore, the residual signal $\tilde{r}(k)$ can be expressed as

$$\tilde{r}(k) = A_r \beta_k \sum_{m=0}^{\infty} \frac{\beta_k^m}{2^m m!} e^{j(m+1)\Phi(k)} \tag{6.2.18}$$

Now, the value of the separation performance index is evaluated as

$$\rho = \frac{\|\tilde{r}(k)\|_2^2}{\|s(k)\|_2^2} \le \sum_{m=0}^{\infty} \frac{\beta_k^m}{2^m m!} = e^{\frac{1}{2}\beta_k} \tag{6.2.19}$$

It is easy to see that for a strong constant-envelope signal $r(k)$, i.e. $\beta_k \to 0$, the separation performance index $\rho_k \to 0dB$

Q.E.D.

According to Theorem 6.2.1, if the ASTV-ARMA model is controlled by the phase estimated from the input mixture, the power of the residual signal at the output equals the power of the signal which passes the ASTV-ARMA model transparently.

It is found that if the average ratio of the power between the signals $s(k)$ and $r(k)$ is less than $-8dB$, i.e. above the detecting threshold of phase $\Psi_k(k)$, the value of the separation performance index falls in the range $0dB$ to $0.3dB$

Theorem 6.2.1 is important for the purely phase controlled ASTV-ARMA model. It exhibits the limitation of blind separation of a constant-envelope signal from an arbitrary signal.

Let us consider the following cases for phase- controlled ASTV-ARMA models:

CASE-I: Input: $r(k)$ Coefficients: $a_1[k, \Psi_x(k)]$ $a_2[k, \Psi_x(k)]$

CASE-II: Input: $x(k)$ Coefficients: $a_1[k, \Psi_r(k)]$ $a_2[k, \Psi_r(k)]$

It is clear that in CASE-I, the time-varying coefficients are controlled by the phase of input mixture $x(k)$, while in CASE-II, these coefficients are controlled by the phase of the FM component only.

Theorem 6.2.2 (*Sensitivity*) *The energy of the residual outputs in CASE-I and CASE-II are the same.*

Proof: By the analysis presented in (6.2.16)-(6.2.19), the output of CASE-I is $\tilde{r}(k)$ and the output of CASE-II is $s(k)$, due to the transparency of ASTV-ARMA model. According to Theorem 6.2.1. they have the same energy.

Q.E.D.

Theorem 6.2.2 allows us to establish the sensitivity of the coefficients of the phase-controlled ASTV-ARMA model; any perturbation at the input will cause the same amount of perturbation in controlling the phase of the coefficients. Finally, the energy at the output is equal to the energy of the equivalent input perturbation.

In what follows, we will show the possibility for further improvement of the separation performance by using a closed-loop phase controlled ASTV-ARMA model.

6.2.4. A Closed-Loop Phase Controlled ASTV-ARMA Model

In order to further improve the separation performance, we employ a closed-loop scheme to reduce the perturbation in the controlling phase. A block diagram of the closed- loop phase-controlled ASTV-ARMA model is illustrated in Fig. 6.6.

Since the signal $s(k)$ passes the ASTV-ARMA model transparently, the output of the ASTV-ARMA model contains two parts, the signal $s(k)$ and the residual signal $\tilde{r}(k)$. If the output of the ASTV-ARMA model is directly fedback, and substrated from

the input mixture, then the input of the phase detector contains the signal $r(k)$ and the residual signal $\tilde{r}(k)$. Hence we have to evaluate a new phase-perturbation term caused by the feedback part of the residual signal $\tilde{r}(k)$.

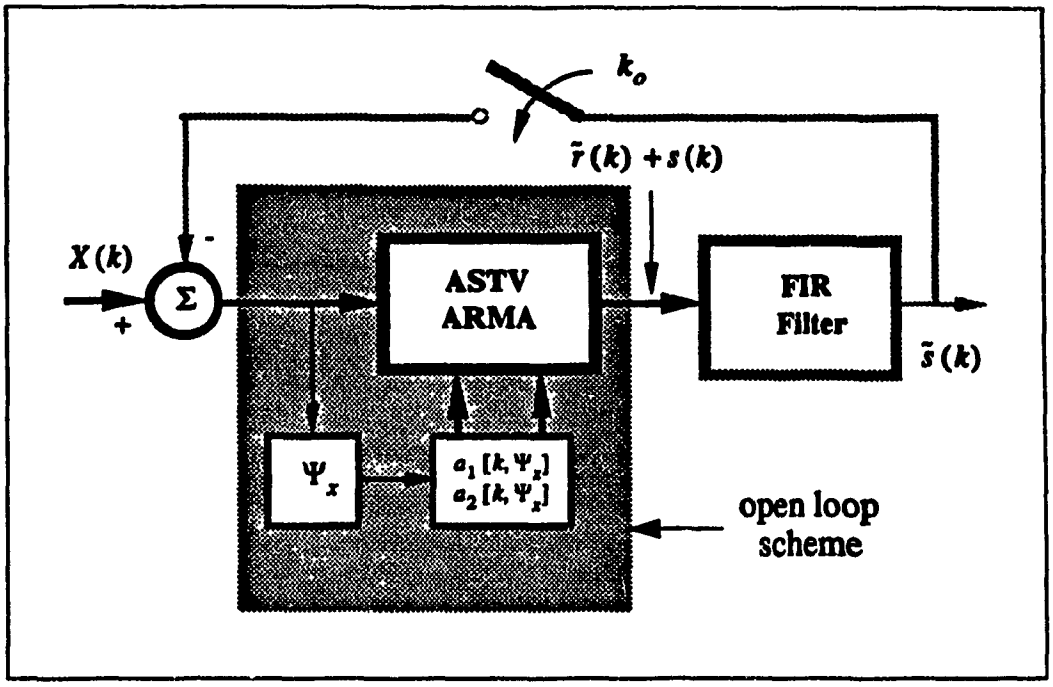

Fig.6.6 A Closed Loop Phase Controlled ASTV-ARMA Model

Lemma 6.2.2 *The new phase perturbation in the closed-loop is given by the following recursive expression*

$$\delta\psi^{\dagger}(k) = \sum_{i=1}^{N} \phi_i(k) \tag{6.2.20}$$

where

$$\phi_i(k) = \frac{\beta_k^{i+1}}{2^i i!} \sin\left(i\Phi(k) - \Psi_r(k) - \sum_{l=1}^{i-1} \phi_l(k) \right)$$

Proof: From (6.2.16) denoting the $l-th$ term of the residual signal as

$$A_l = A_s(k) \frac{\beta_k^l}{2^l l!} e^{j(l+1)\Phi(k)} \tag{6.2.21}$$

we have

$$\frac{A_l(k)}{A_r} = \frac{\beta_k^l}{2^l l!} \ll 1 \qquad l = 1, 2....$$

With the help of the phasor diagram, Fig.6.7, the perturbation in phase can be written as

$$\phi_1(k) = \frac{A_1}{A_r}\sin(\Phi(k) - \Psi_r(k)) \tag{6.2.22}$$

and

$$\phi_2(k) = \frac{A_2}{A_r}\sin(2\Phi(k) - \Psi_r(k) - \phi_1(k)) \tag{6.2.23}$$

By repeated use of (6.2.22) and (6.2.23) the total phase perturbation term of the residual signal $\tilde{r}(k)$ can be expressed as in (6.2.20).

Q.E.D.

Following the same procedure as in the proof of Theorem 6.2.1, the output of the new residual signal is

$$\tilde{r}^{\dagger}(k) = A_s(k)\sum_{m=0}^{\infty}\frac{\beta_k^m}{2^m m!}e^{j\delta\Psi\dagger(k)} \tag{6.2.24}$$

It is straightforward to show

$$\left\|\tilde{r}^{\dagger}(k)\right\|_2^2 = \left\|A_s(k)\right\|_2^2 = \left\|\tilde{r}(k)\right\|_2^2$$

and therefore the energy of such a new residual remains the same.

In this direct feedback situation, the phase perturbation due to the signal $s(k)$ is eliminated, while the perturbation from the residual signal $\tilde{r}(k)$ is introduced.

Since the energies of the residual signal $\tilde{r}(k)$ and the signal $s(k)$ are the same, according to the Theorem 6.2.1, the new phase perturbation introduced through the feedback loop produces another new residual signal at the output, and *the separation performance remains the same.*

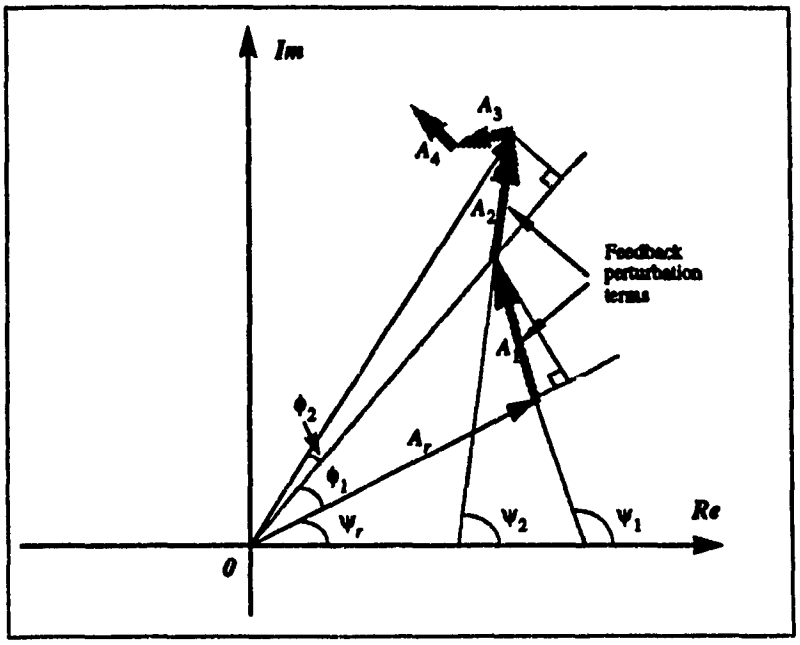

Fig.6.7 The Phasor Diagram for Calculating the Phase Perturbation

In order to improve the separation performance, one has to reduce the phase perturbation term, by cancelling or attenuating the residual signal in the feedback loop; on the other hand the signal $s(k)$ has to be kept unchanged. Note that the residual signal $\tilde{r}(k)$ is still a wideband signal, while the bandwidth of the signal $s(k)$ remains the same.

In the following theorem, we give the condition that leads the closed-loop phase-controlled ASTV-ARMA model to accomplish complete separation.

Theorem 6.2.2 *The condition for complete separation is that the loop gain of the phase perturbation is less than unity.*

Proof: At time k_o, the open loop system reaches the steady state, and we close feedback loop. Assuming a filter in the feedback path, which introduces an attenuation factor ς_l to the residual signal $\vec{r}^{\dagger}(k)$, the phase perturbation term becomes

$$\delta\psi^{\dagger}(k) = \sum_{i=1}^{N}\sum_{l=1}^{N}\frac{\beta_k^{l+1}}{2^l l!}\varsigma_l^{(k-k_o)}\sin\left((l+1)\Phi^{(k)}(k) - \Psi_r(k) - \sum_{i=1}^{l}\phi_i^{(k)}(k)\right)$$

If $0 \leq \varsigma_l < 1$ then we have $\delta\psi^{\dagger}(k) \rightarrow 0$, which means that the ASTV-ARMA

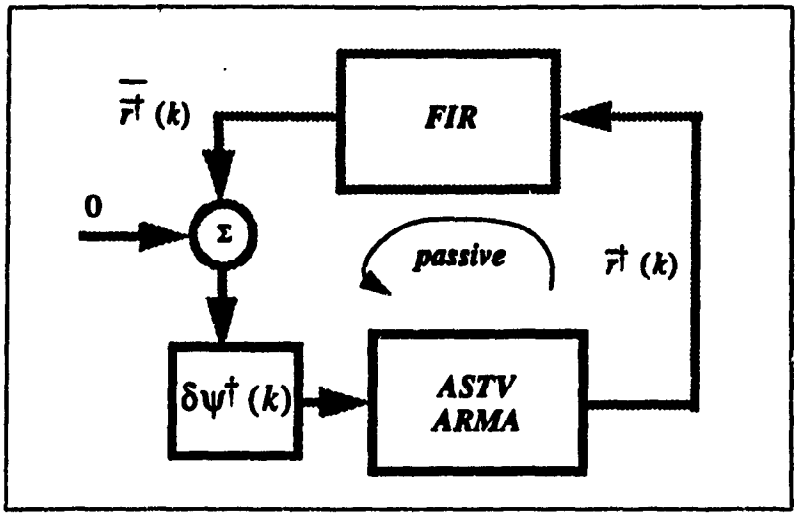

Fig.6.8 The Feedback Loop of the Residual Signal

model is controlled by the true phase of $\Psi_r(k)$. Even though the controlling phase is estimated from the input mixture, a complete separation achieved as the closed-loop system reaches steady state.

Q.E.D.

The perturbation phase loop is shown in Fig.6.8. Note that this loop consists of a phase detector, and a phase-controlled ARMA model. The condition given in Theorem 6.2.2 is an ideal one, since it requires that the filter used in the loop provide an attenuation to the residual signal, without in any way affecting the signal $s(k)$. Hence, we assume that such a filter in the feedback path has the ability to distinguish between the signal $s(k)$ and the residual $\vec{r}^{\dagger}(k)$.

In the course of the following discussion, we investigate an example with two classes of signal $s(k)$: (1) $s(k)$ is a bandlimited signal with *a priori* known bandwidth; (2) $s(k)$ is a multitone signal, with unknown frequencies.

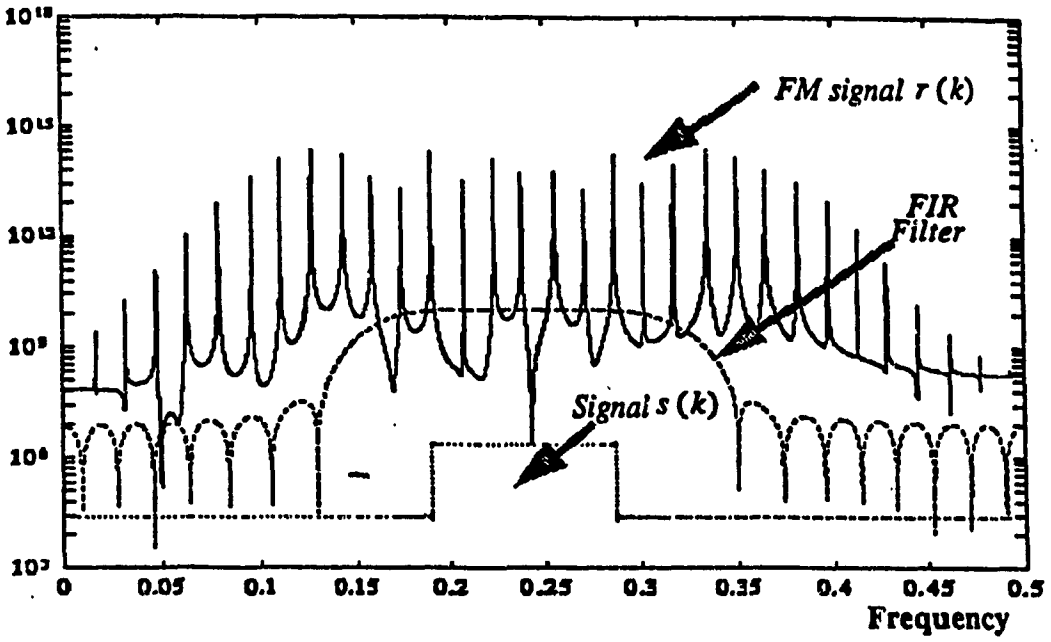

Fig.6.9 The Fourier Power Spectrum of the Input Mixture

Example 6.2.1 Consider an input mixture of a strong FM signal $r(k)$ with unknown parameters and a signal $s(k)$, whose bandwidth of $s(k)$ is *a priori* known to be $0.2rad$ to $0.3rad$. The FM signal $r(k)$ is strong compare to the signal $s(k)$, $\beta = -20dB$. see Fig.6.9. We use a phase controlled AS-ARMA model and a conventional 20th order FIR bandpass filter[1] to retrieve the weak signal $s(k)$. The results of two cases are presented.

(1) (Open Loop Scheme) The Fourier power spectrum of the output is illustrated in Fig.6.10. The power spectrum of the residual signal $\tilde{r}(k)$ is a wideband and the spectrum of the signal $s(k)$ can be identified in the spectrum, its energy being equal to the energy of the signal $s(k)$. The separation performance index is improved by 20dB.

(2) (Closed Loop Scheme) At the output of the open loop ASTV-ARMA model, we use the FIR filter to cancel part of the residual signal $\tilde{r}(k)$. Since a high quality FIR

1. We choose FIR1 package with a Hamming window option in Matlab to perform this simulation.

filter is not chosen, the separation performance index is improved only by $2.3dB$. The Fourier spectrum of the output of the FIR filter is shown in Fig.6.11 (dotted plot). In this case, the passive loop condition is partially satisfied, because the FIR filter provides attenuation outside the bandwidth of the signal $s(k)$. If we close the feedback loop, the residual signal is further cancelled significantly, because the attenuation condition is satisfied outside the bandwidth of the signal $s(k)$, see Fig.6.11. The separation performance index is improved by about $10dB$.

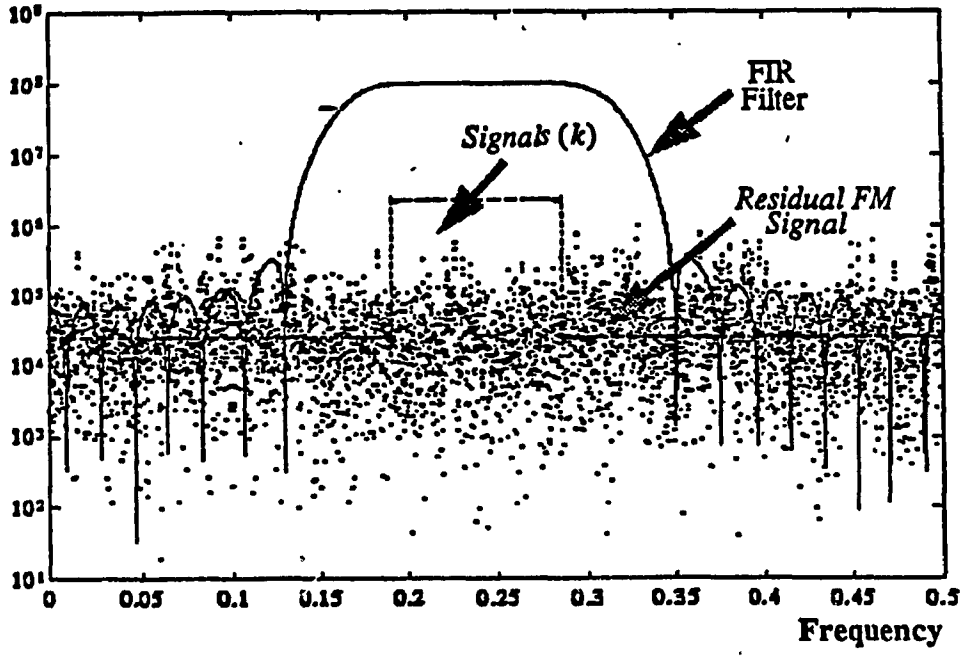

Fig.6.10 Fourier spectrum of the open loop phase controlled ASTV-ARMA model.

The signal separation by using an open loop scheme can be carried out in the sense of blind separation (i.e. the signal $s(k)$ is an arbitrary one), if the results of the performance of the separation are acceptable. However, if the separation performance is to be further improved, then some knowledge about the signal $s(k)$ is essential, for example the signal bandwidth. Even in this situation, closed-loop scheme can not provide complete separation, because the attenuation condition can not be satisfied within the entire spectrum, but as already shown by Example 6.2.1, it significantly improve the separation performance. It is easy to see that the narrower the bandwidth of the signal $s(k)$, better the improvement.

Complete separation can be achieved only if the signal bandwidth is close to zero, i.e. the signal $s(k)$ is a multitone signal. In this case blind separation can be achieved even if the parameters of the multitone signal are *a priori* unknown. [6.11]. An AS-ARMA model based adaptive line enhancer can be used to ideally retrieve the multitone signal.

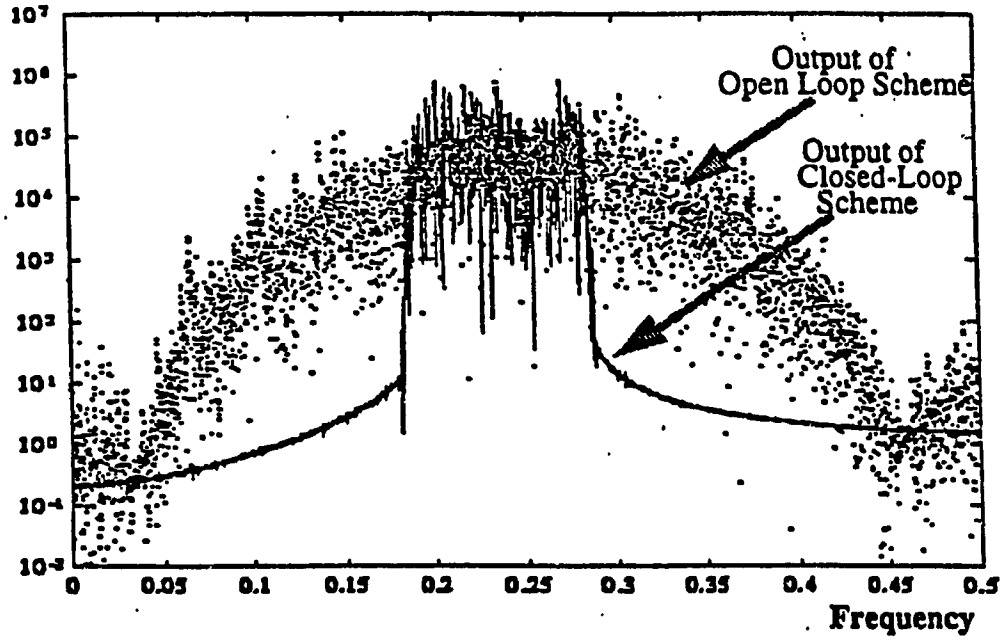

Fig.6.11 Fourier Power Spectrum of Output of Closed-Loop Phase Controlled ASTV-ARMA Model

From this example we see that with a closed-loop scheme, by using a simple low-order FIR filter (filter length=20), we can obtain an excellent separation performance. Such a result may be achieved by using open-loop scheme and a high order FIR filter (filter length=180) through a careful design of the cutoff frequency, which means more information has to be known about the spectrum of the signal $s(k)$.

The separation of signals using phase -controlled ASTV-ARMA model relies upon our ability to obtain the true phase to control the time-varying coefficients. A closed loop ASTV-ARMA model has been designed to achieve a so called *self-synchronization* for this time-varying system. Based on this principle, two novel

schemes were proposed to deal with the time-varying jamming problem in [6.11].

6.3. Tracking Capability of Gauss-Newton Adaptive Algorithm

6.3.1. Introduction

In the blind signal separation context, first of all one has to find a suitable model for the signals, and then find the parameters of the model to perform the signal separation. In this situation, it is very desirable, for the blind signal separation task, to use an adaptive algorithm to update and find the true coefficients of such a model. A lot of attentions have been paid to solve this problem. However, the design and analysis of these algorithms are based on the assumption that the system under modelling are time-invariant or it is slowly time-varying. Very few results available regarding a system which is fast time-varying, and it is well known that this is a more difficult problem. Nevertheless, in many applications a fast-time varying model is required, and in this section, we show that the standard adaptive algorithm fails to work, if the system is fast time-varying.

In what follows, we present an analysis of the Gauss-Newton adaptive algorithm for an AS-ARMA model. The Gauss-Newton algorithm is considered to be with a fast convergence, independent of the input signal once the cost function is quadratic, which is true for an AS-ARMA model. We show that such an adaptive algorithm as applied to a simple second order AS-ARMA model contains a tracking threshold; this constitutes a serious limitation for applying the standard adaptive algorithm to update the coefficients of a fast time-varying AS-ARMA model.

6.3.2. Formulation of Gauss-Newton Algorithm

Given a signal $x(k)$ whose parameters are time-varying, e.g. an AM/FM signal, such a signal can be modelled by a second order time-varying AS-ARMA model with time-varying coefficients $W(k)$. If the coefficients of such a model are the true ones, i.e. calculated from its corresponding Wronskian system, then the signal $x(k)$ satisfies the MA part of the ASTV-ARMA model, and the output becomes zero; otherwise, we denote the output of the AS-ARMA model as an error signal $e(k)$. Let us formulate

the energy equation of such an error signal as:

$$V_e = \sum_{k=1}^{\infty} e^2(k) \tag{6.3.1}$$

The standard Gauss-Newton algorithm is now applied to minimize the cost V_e by Taylor expanding around the coefficients $W(k)$

$$W(k) = W(k-1) - \mu\left[\frac{\partial^2 V_e}{\partial W^2}\right]^{-1}\left[\frac{\partial V_e}{\partial W}\right] \tag{6.3.2}$$

where μ is the step size chosen *a priori*.

The update procedure is listed in Table 6.3.1. Now we consider the stochastic properties of this algorithm.

6.3.3. An ODE Approach to Analysis of Gauss-Newton Algorithm

Denote the difference between the estimation values obtained through the Gauss-Newton algorithm, and the true values by

$$\Gamma^{\mu}(k) = W^{\mu}(k) - W^{\dagger}(k) \tag{6.3.3}$$

Let us define an interpolated process

$$\hat{\gamma}^{\mu}(\tau) = \Gamma^{\mu}(k) \qquad \tau \in [k\mu, (k+1)\mu]$$

Lemma 6.3.1[6.14] *$\hat{\gamma}^{\mu}(k\mu)$ weakly converges to its limiting process $\hat{\gamma}(\tau)$, as the step size $\mu \to 0$ and $k \to \infty$, such that $k\mu \to \tau$. Moreover such a limiting process $\hat{\gamma}(\tau)$ satisfies the following ordinary differential equations (ODEs)*

$$\frac{d}{d\tau}\hat{\gamma}(\tau) = -R(\tau)^{-1}\left[H(\tau)\left[\hat{\gamma}(\tau) + W^{\dagger}(\tau)\right] - P(\tau)\right] - \frac{d}{d\tau}W^{\dagger}(\tau)$$

$$\frac{d}{d\tau}R(\tau) = -R(\tau) + Q(\tau)$$

$$\Gamma(0) = \Gamma_o$$

$$R(0) = R_o$$

$$\hat{\gamma}(\tau) = \left[\gamma_1(\tau), \gamma_2(\tau)\right]^T$$

$$H(\tau) = E\{\tilde{X}(\tau)\tilde{X}^T(\tau) - \Lambda\tilde{E}(\tau)\tilde{E}^T(\tau)\Lambda\} \tag{6.3.4}$$

$$P(\tau) = E\{\tilde{X}(\tau)\tilde{X}(\tau) - \tilde{e}(\tau)\Lambda\tilde{E}(\tau)\} \tag{6.3.5}$$

$$Q(\tau) = E\{[\tilde{X}(\tau) - \Lambda\tilde{E}(\tau)][\tilde{X}(\tau) - \Lambda\tilde{E}(\tau)]^T\} \tag{6.3.6}$$

where, $E\{\ \}$ *denote the ensemble average operator.*

Proof: See [6.14]

Q.E.D.

Lemma 6.3.1 associates the stochastic Gauss-Newton algorithm with ordinary deferential equations, which are analytically tractable. This linkage is established based on the framework of weak convergence theory. Note that the time τ of the limiting process is held constant, by forcing $k \to \infty$ as $\mu \to 0$. This is to ensure that at different times τ, the parameters of the signal under analysis are different, since we are dealing with the tracking problem of a time-varying system. According to weak convergence theory, the *ODEs* given in Lemma 6.3.1. describe the tracking behavior of the mean values of the coefficients of the adaptive Gauss-Newton algorithm.

Our objective is to consider the tracking behavior of such a Gauss-Newton algorithm in the case where the system is fast time-varying. The following analysis is based on the tracking of a frequency varying sinusoid. We approach this objective by directly solving the *ODEs*.

In order to find $H(\tau)$, $P(\tau)$ and $Q(\tau)$, let us *freeze the time* τ and introduce a new discrete time j. The input signal therefore becomes

$$x_j(\omega(\tau)) = A_x(\tau)\sin(\omega(\tau)j + \phi) \tag{6.3.7}$$

where ϕ is uniformly distributed in $[-\pi,\pi]$. The signal $x_j(\omega(\tau))$ as a function of j, represents a harmonic signal with amplitude $A_x(\tau)$ and frequency $\omega(\tau)$ where τ is frozen.

Table6.3.1: Gauss-Newton Algorithm for AS-ARMA Model

2nd-order ASTV-AMAR model:

$$x(k)+w_1(k-1)x(k-1)+w_2(k-1)x(k-2)$$
$$=e(k)+\alpha w_1(k-1)e(k-1)+\alpha^2 w_2(k-1)e(k-2)$$

Parameter Update Algorithm:

$$W(k) = W(k-1)+\mu R^{-1}(k)\Xi(k)e(k)$$
$$R(k) = R(k-1)+\mu[\Xi(k)\Xi^T(k)-R(k-1)]$$

where,

$$\Xi(k) = \tilde{X}(k)-\Lambda\tilde{E}(k)$$
$$\tilde{X}(k) = [\tilde{x}(k-1),\tilde{x}(k-2)]^T$$
$$\tilde{E}(k) = [\tilde{e}(k-1),\tilde{e}(k-2)]^T$$
$$W(k) = [w_1(k),w_2(k)]^T$$
$$\Lambda = \begin{bmatrix}\alpha & 0\\ 0 & \alpha^2\end{bmatrix}$$

Auxiliary filtering:

$$\tilde{x}(k) = x(k)-\alpha w_1(k-1)\tilde{x}(k-1)-\alpha^2 w_2(k-2)\tilde{x}(k-2)$$
$$\tilde{e}(k) = e(k)-\alpha w_1(k-1)\tilde{e}(k-1)-\alpha^2 w_2(k-1)\tilde{e}(k-2)$$
$$e(k) = \tilde{x}(k)+w_1(k-1)\tilde{x}(k-1)+w_2(k-1)\tilde{x}(k-2)$$

Since the input of the model is a sine-wave with a constant frequency $\omega(\tau)$ and amplitude $A_x(\tau)$, the AS-ARMA becomes a time-invariant one, with fixed coefficients $w_1(\tau)$ and $w_2(\tau)$. From Table 6.3.1, we have

$$A_e^2(\tau) = \frac{A_x^2(\tau)}{\left| W\left[\frac{e^{-j\omega(\tau)}}{\alpha}, \gamma(\tau)\right]\right|^2} \tag{6.3.8}$$

where, $A_e(\tau)$ is the amplitude of the harmonic signal $x_j(\omega(\tau), \gamma(\tau))$ and the frozen-time transfer function of the MA part is given by

$$W[e^{-j\omega(\tau)}, \gamma(\tau)] = 1 + w_1(\tau)\, e^{-j\omega(\tau)} + w_2(\tau)\, e^{-j2\omega(\tau)} \tag{6.3.9}$$

and the update coefficients of the adaptive algorithm are

$$w_1(\tau) = w_1^{\dagger}(\tau) + \gamma_1(\tau)$$

$$w_2(\tau) = w_2^{\dagger}(\tau) + \gamma_2(\tau)$$

In the above, $w_1^{\dagger}(\tau)$ and $w_2^{\dagger}(\tau)$ are the true coefficients, while $\gamma_1(\tau)$ $\gamma_2(\tau)$ are the bias of the estimation by Gauss-Newton algorithm. Now we evaluate the correlation function of the input and output of a particular frozen time AS-ARMA model. Since the frozen-time model is a time-invariant one, the correlation can be found by using the Weiner-Khinchin theorem.

The auto-correlation function $R_{e,e}(i-j, \tau)$ of $e_j[\omega(\tau), \gamma(\tau)]$ is therefore

$$R_{e,e}(i-j, \tau) = \frac{A_e^2(\tau)}{2} \cos[\omega(\tau)\,(i-j)] \tag{6.3.10}$$

Similarly, we have for the auxiliary filtering process $\tilde{e}(\tau)$:

$$A_{\tilde{e}}^2(\tau) = A_x^2(\tau) \frac{\left| W[e^{-j\omega(\tau)}, \gamma(\tau)]\right|^2}{\left| W\left[\frac{e^{-j\omega(\tau)}}{\alpha}, \gamma(\tau)\right]\right|^4} \tag{6.3.11}$$

The auto-correlation function of the process $\tilde{e}(\tau)$ is calculated in a similar manner and is:

$$R_{\tilde{e},\tilde{e}}(i-j,\tau) = A_{\tilde{e}}^2(\tau)\cos\left[\omega(\tau)(i-j)\right] \tag{6.3.12}$$

using (6.3.10) and (6.3.12) we have

$$H(\tau) = \begin{bmatrix} R_{\tilde{e},\tilde{e}}(0,\tau) - \alpha^2 R_{e,e}(0,\tau) & R_{\tilde{e},\tilde{e}}(0,\tau) - \alpha^2 R_{e,e}(1,\tau) \\ R_{\tilde{e},\tilde{e}}(0,\tau) - \alpha^2 R_{e,e}(1,\tau) & R_{\tilde{e},\tilde{e}}(0,\tau) - \alpha^2 R_{e,e}(0,\tau) \end{bmatrix} \tag{6.3.13}$$

$$P(\tau) = \begin{bmatrix} R_{\tilde{e},\tilde{e}}(1,\tau) - \alpha R_{e,e}(1,\tau) \\ R_{\tilde{e},\tilde{e}}(2,\tau) - \alpha R_{e,e}(2,\tau) \end{bmatrix} \tag{6.3.14}$$

$$Q(\tau) = H(\tau) - \begin{bmatrix} 2\alpha R_{e,e}(0,\tau) R_{\tilde{e},\tilde{e}}(0,\tau) & \alpha(\alpha+1) R_{e,e}(0,\tau) R_{\tilde{e},\tilde{e}}(1,\tau) \\ \alpha(\alpha+1) R_{e,e}(0,\tau) R_{\tilde{e},\tilde{e}}(1,\tau) & 2\alpha^2 R_{e,e}(0,\tau) R_{\tilde{e},\tilde{e}}(0,\tau) \end{bmatrix}$$

Now, in order to study the tracking ability of the Gauss-Newton algorithm, the ***ODEs*** in Lemma 6.3.1 must be solved. For this, however, it is necessary to find $\omega(\tau)$. The instantaneous frequency of the input signal is

$$\omega_x(\tau) = 2\pi f_r + 2\pi\Delta f\cos\left[\frac{2\pi f_m \tau}{\mu}\right] \tag{6.3.15}$$

while the instantaneous phase becomes

$$\bar{\Psi}_x(\tau) = 2\pi f_r \tau + \frac{\mu f_r}{f_m}\sin\left[\frac{2\pi f_m \tau}{\mu}\right] + \phi_0 \tag{6.3.16}$$

As shown in Chapter 2 the true coefficients $W^{\dagger}(\tau)$ are given by

$$w_1^{\dagger}(\tau) = -\frac{\sin\left[\bar{\Psi}_x(\tau) - \bar{\Psi}(\tau-2\mu)\right]}{\sin\left[\bar{\Psi}_x(\tau-\mu) - \bar{\Psi}(\tau-2\mu)\right]} \tag{6.3.17}$$

$$w_2^{\dagger}(\tau) = \frac{\sin\left[\bar{\Psi}_x(\tau) - \bar{\Psi}(\tau-\mu)\right]}{\sin\left[\bar{\Psi}_x(\tau-\mu) - \bar{\Psi}(\tau-2\mu)\right]}$$

Using the standard ***Runge-Kutta*** routine, we can find the numerical solution of the ***ODEs***. From weak convergence theory, for a small step size μ, $E\{\Gamma^{\mu}(k)\} \approx \hat{\gamma}(\tau)$; therefore the solutions of the ***ODEs*** represent the mean value of the coefficient error, i.e. the bias of the estimation obtained by the Gauss-Newton algorithm. It is found that for $f_m < f_{th}$ such a bias is very small, while $f_m > f_{th}$ the bias increases significantly, see[6.17]. Thus *the threshold effect* is explicitly observed. The tracking capability of the Gauss-Newton algorithm has its limitation in tracking fast varying parameters.

6.3.4. Computer Simulations

Let us define following ratio to measure the performance of the tracking capability of the Gauss-Newton algorithm

$$\eta = 10\log\frac{\|e(k)\|_2^2}{\|x(k)\|_2^2} \tag{6.3.18}$$

Considering the input FM signal with a sine-tone modulating frequency as $x(k) = \cos\left[2\pi f_r k + \frac{\Delta f}{f_m}\sin(f_m k)\right]$, we chose following *normalized frequency* parameters to perform the simulation: $f_r = 0.25$ $\Delta f = 0.2$ and $f_m = [0.001, 0.15]$ The simulation results are plotted in Fig.6.12. It is seen that at $f_m = f_{th} = 0.03$, the tracking performance presents a threshold effect.

In order to understand the tracking behavior of the Gauss-Newton adaptive algorithm, we also plot the trajectory plane of the both the true AS-ARMA model for a single-tone modulated FM signal and the tracking trajectories of the adaptive algorithm in Figs 6.13 a) and b). These plots bring some new light into the understanding of the tracking threshold effect of the Gauss-Newton algorithm. Note that in this example, the labeling a)-e) corresponds to the a)-e) points in the plot of Fig.6.14. We can see as the parameter f_m increases (the frequency varying becomes fast), the true trajectories begin to expand horizontally, and the curvature of the trajectories begins to increase; at a certain point namely $f_m = f_{th}$ the adaptive algorithm can not follow the shape of the true trajectories, and the tracking performance degrades rapidly.

The mechanism behind the threshold behavior is twofold: on the one hand, any recursive adaptive algorithm has a certain memory which leads to a certain limitation in being able to update fast varying parameters, and on the other hand, as shown in our

example, the frequency variation parameter f_m may be considered as a parameter of the trajectory, increase in f_m implies a stretch of the trajectories in the $w_2(k)$ direction, because in the $w_1(k)$ direction the width of the trajectories at the level $w_2(k) = 1$ is fixed (it is determined by the fixed value Δf). So as the curvature increases in the $w_2(k)$ direction, the adaptive algorithm fails to track the true trajectories.

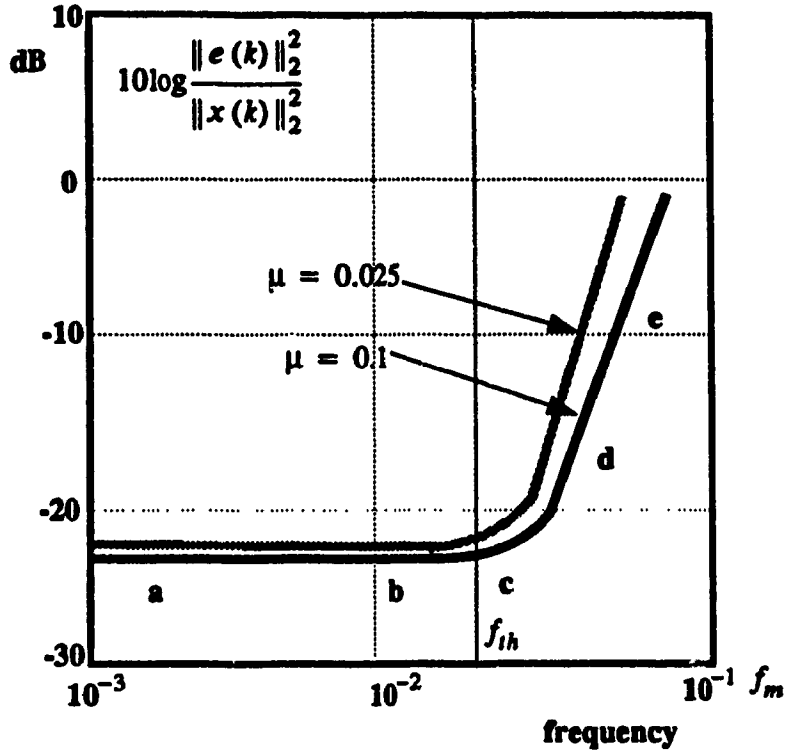

Fig.6.12 Computer Simulation Result for the Gauss-Newton Algorithm to Track a Single Tone Modulated FM Signal, a Tracking Threshold Effect is Displayed for the Larger Frequency Variation Rate

The existence of tracking threshold prohibits the application of a conventional adaptive algorithm to estimate the fast varying parameters, and constitutes a major obstacle in extending the standard algorithms directly to the fast time-varying setting. It also provides a challenge for the development of algorithms to track fast time-varying signals.

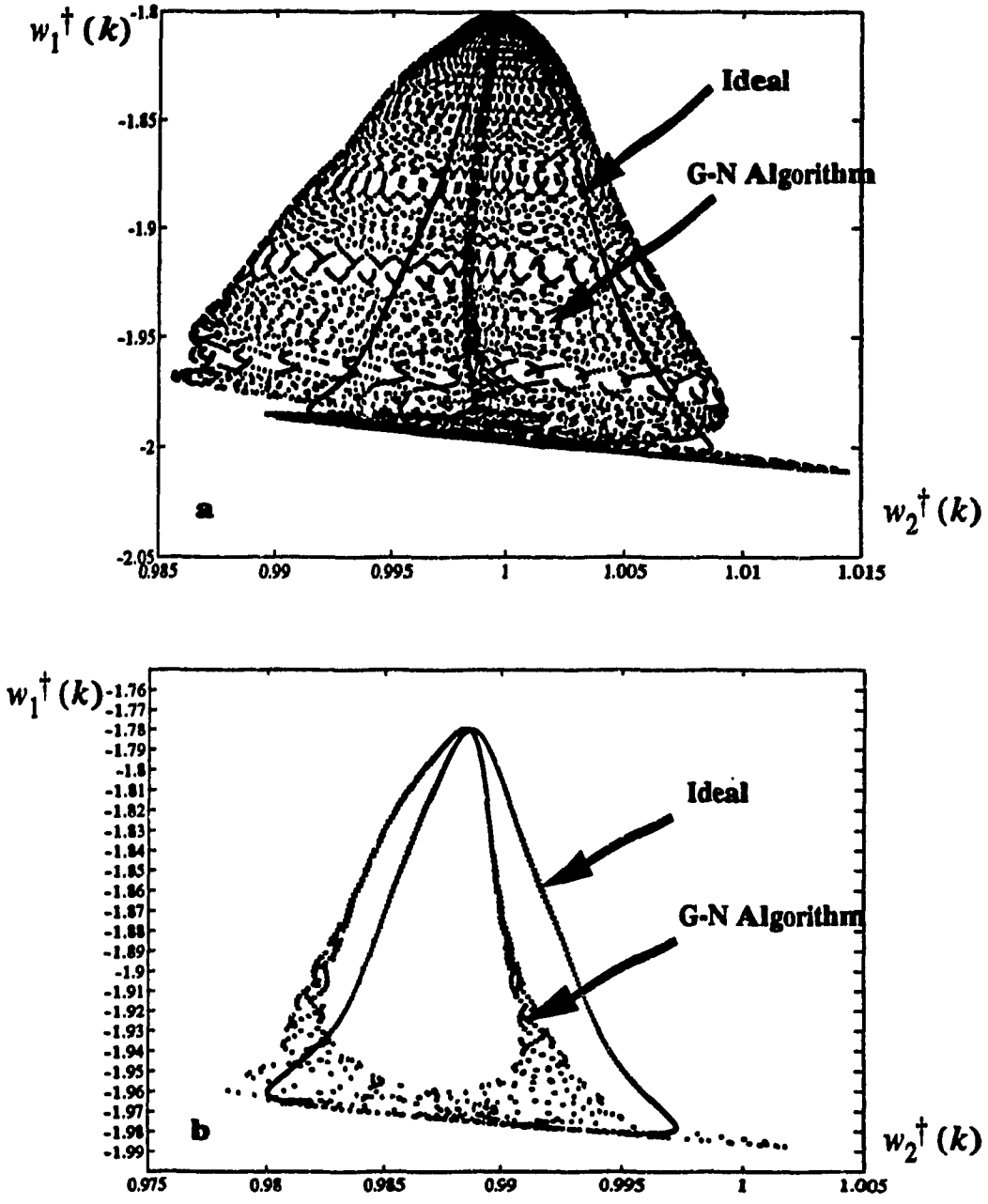

Fig.6.13 A Computer Simulation to Illustrate the Gauss-Newton Algorithm Tracking the Fast Variation of the Trajectory of a Single Tone Modulated FM Signal a)-b) $f_m < f_{th}$

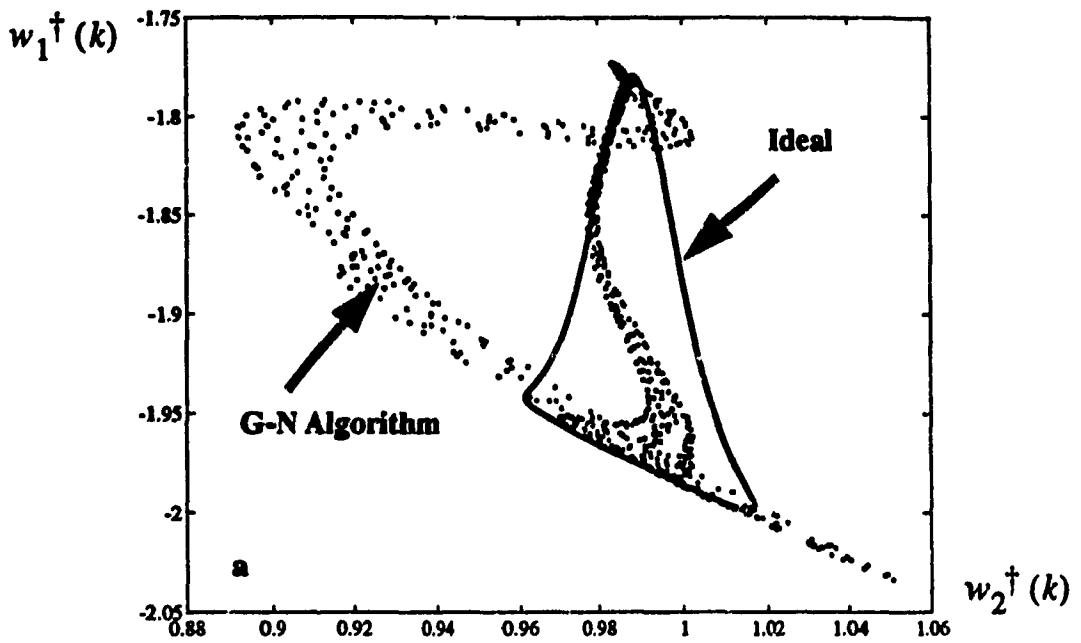

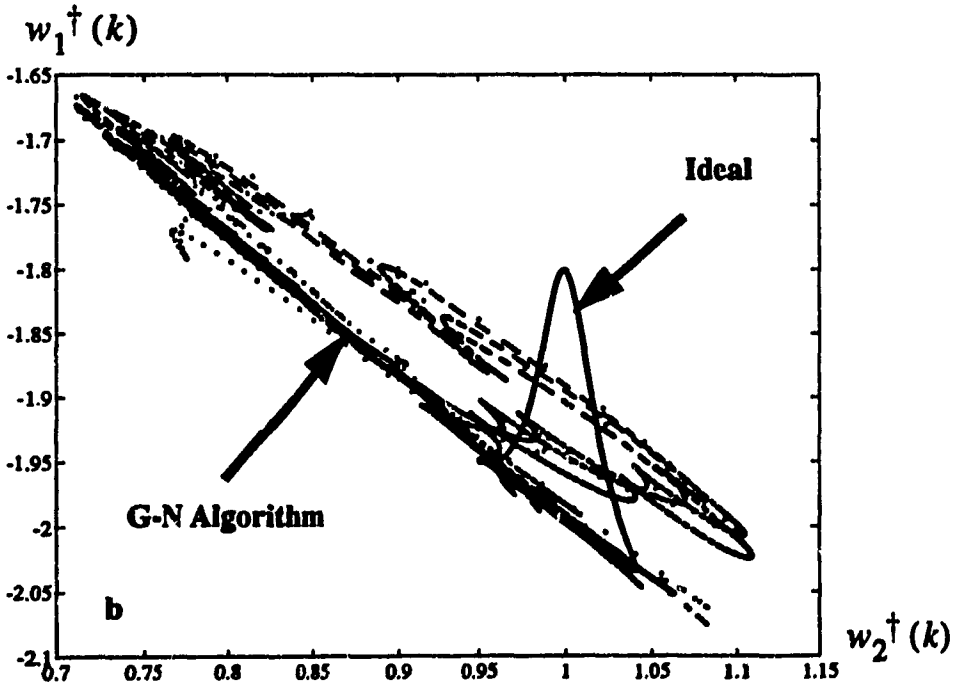

Fig.6.14 A Computer Simulation to Illustrate the Gauss-Newton Algorithm Fails to Track the Fast Variation of the Trajectory of a Single Tone Modulated FM Signal a) $f_m = f_{th}$ and b) $f_m > f_{th}$

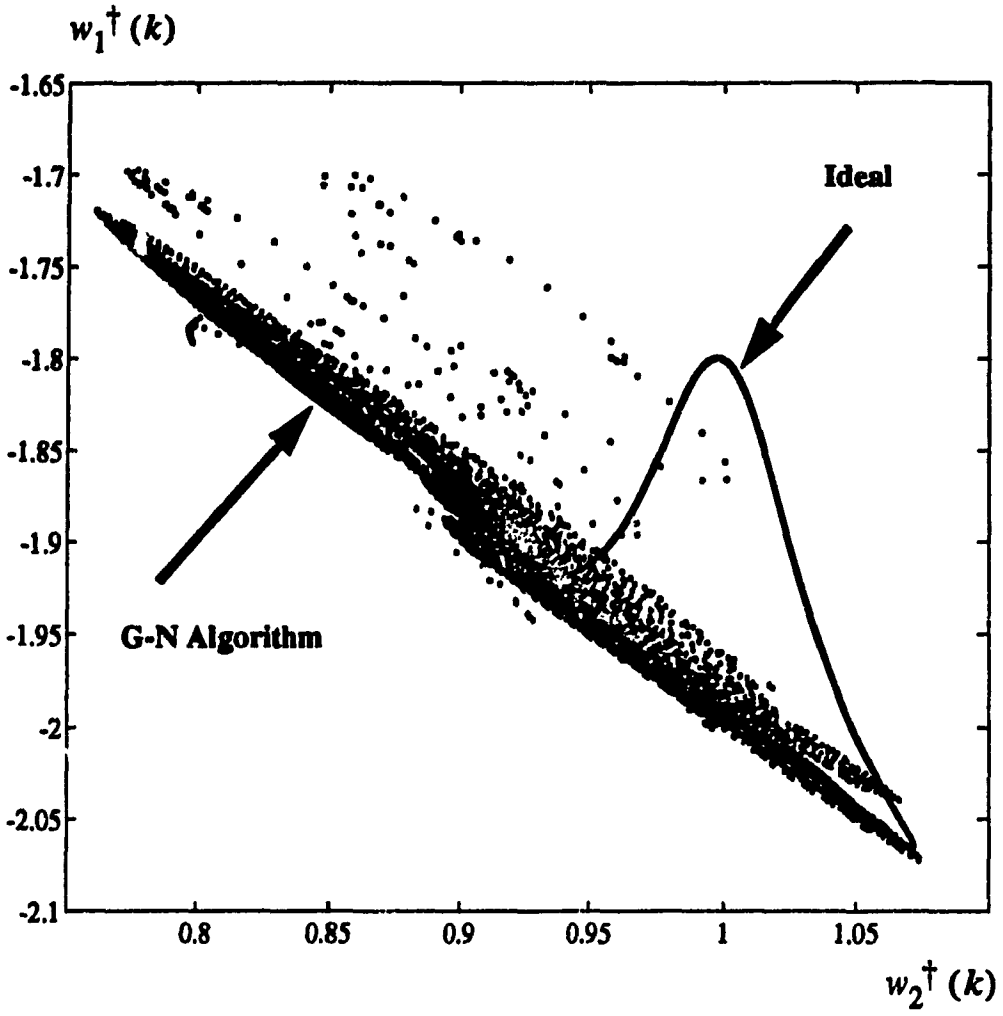

Fig.6.15 Computer Simulation to Illustrate the Gauss-Newton Algorithm Fails to Track the Fast Variation of the Trajectory of a Single Tone Modulated FM Signal $f_m > f_{th}$

References

[6.1] A. V. Oppenheim and R.W. Schafer, "*Digital Signal Processing*", Prentice-Hall, Eglewood Cliffs, N.J. 1975

[6.2] T. M. Apostal, "*Introduction to Analytic Number Theory*", Springer-Verlag, New-York, 1976

[6.3] A. Papoulis, "*Signal Analysis*", McGraw-Hill, New York, 1977

[6.4] H. J. Landau, "Sampling, Data, Transmission, and Nyquest Rate", *Proceeding of IEEE* Vol. 55, No.10, pp. 1701-1706, Oct. 1967

[6.5] R. J. Duffin and A.C. Schaeffer, "A Class of Nonharmonic Fourier Series", *Trans Amer. Math. Soc.*, Vol. 72, pp. 341-266, 1952

[6.6] A. Jerri, "The Shannon Sampling Theorem, Its Various Extension and Applications: A Tutorial Review", *Proceeding of IEEE*, Vol. 65, No. 11, pp. 1565-1596, Nov. 1977

[6.7] D. Slepian, "On Bandwidth", *Proceeding of IEEE*, Vol. 64, pp. 292-300, March, 1976

[6.8] B. Ya Levin, "*Distribution of Zeros of Entire Functions*", Providence, R.I., Amer Math Soc., 1964

[6.9] E. I. Plotkin, L. M. Roytman and M. N. S Swamy, "Non-Uniform Sampling of Bandlimited Modulated Signals", *Signal Processing*, Vol.4, pp. 295-303, 1982

[6.10] E. I. Plotkin and M. N. S. Swamy, "Signal Reconstruction from the Non-Equally Spaced Samples with Application to Jitter Error Reduction and Bandwidth Compression", *ISSPA87*, pp. 337-341., Aug. 1987

[6.11] W. Tong, E. I. Plotkin, D. Wulich and M. N. S. Swamy, "Self-Synchronized Signal Controlled Constrained Notch Filter for Rejection of Non-Stationary Interference", Proceedings *ICASSP91*, pp. 1937-1940, May, 1991

[6.12] D. Wulich, E. I. Plotkin and M. N. S. Swamy, "Constrained Notch Filtering of Non-Uniformly Spaced Sapmles for Enhancement of an Arbitrary Signal Corrupted by a Strong FM Interference", *IEEE Trans. on Signal Processing*, Vol.39, No. 10 pp. 2359-2363, Oct. 1991

[6.13] N. M. McLeanchan, "*Bessel Function for Engineers*", Oxford at the Clarendon Press, 1961

[6.14] B. D. Rao and R. Peng, "Tracking Characteristic of the Constrained IIR Adaptive Notch Filter", *IEEE Trans. on ASSP*, Vol. 36, pp. 1466-1479, Sept. 1988

[6.15] A. Nehorai, "A Minimum Parameter Adaptive Notch Filter with Constrianed Poles and Zeros", *IEEE Trans on ASSP*, Vol. 33, pp. 983-996, Aug. 1985

[6.16] D. Wulich, E. I. Plotkin and M. N. S. Swamy and W. Tong, "PLL Synchronized Time-Varying Constrained Notch Filter for Retrieving a Weak Multiple Sine Signal Jammed

by FM Interference", *IEEE Trans. on Signal Processing*, Vol. 40, No. 11, pp. 2866-2870, Nov. 1992

[6.17] D. Wulich, E. I. Plotkin, M. N. S. Swamy and W. Tong, "Externally Controlled Time-Varying Notch Filter", *Proceedings ISCAS91*, pp. 2061-2064, June, 1991

[6.18] W. Tong, E. I. Plotkin, M. N. S. Swamy and D. Wulich, "Closed-Loop Self-Synchronized Signal Controlled Constrained Notch Filter with Application for Rejection of Arbitrary Frequency Variation Speed Sinusoidal Interference", *Proceedings ISCAS91*, pp. 1440-1443, June, 1991

[6.19] D. Wulich, E.I. Plotkin and M. N. S. Swamy, " Synthesis of Discrete Time-Variant Null Filters for Frequency Varying Signals using Time-Warping Technique", *IEEE Trans. on Circuit and Systems*, Vol. .37, pp. 977-990, Aug. 1990

[6.20] D. Wulich, E. I. Plotkin, M. N. S. Swamy and Wen Tong, "PLLBased Discrete Time-Varying Filter for Estimation of Parameters of a Sine Signal Corrupted by a Closely Spaced FM Interference", *ISCAS90*, pp. 771-774, May, 1990

[6.21] A. Benvensite, "Design of Adaptive Algorithms for Tracking of Time-Varying Systems", *Inter. Journal of Adaptive Control and Signal Processing*, Vol.1, pp. 3-29, 1987

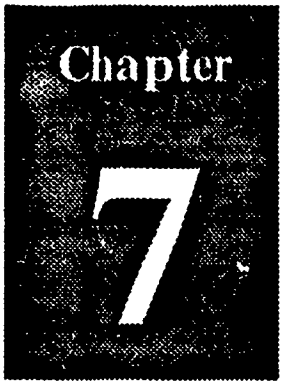

Blind Deconvolution Based on ASTV-ARMA Model

7.1. Introduction

In this chapter, we present a new method to cope with the blind deconvolution problem. Blind deconvolution deals with the propagation of *an unknown source* through a linear multipath channel with *an unknown transfer function*. One has to estimate both the channel and the source from the data observed at the channel output, no other auxiliary access to the source being available. Blind deconvolution finds applications in seismology, radio astronomy, acoustics, and channel equalization in data communication [7.1] [7.2] [7.3].

The key to the proposed method lies in exploiting the ASTV-ARMA to model a class of non-stationary analytical signals. Up till now, there are two major categories of blind equalization algorithms, namely the on-line Godard algorithm [7.7], and higher-order- statistic-based off-line algorithms [7.5] [7.8]. An essential condition of these algorithms is that they require the *higher-order statistics to be ergodic*, i.e. time-invariant.

It is a well known fact that the standard second-order-moment-based methods, such as the linear prediction, are restricted only to systems with minimum phase [7.3]. On the other hand, estimation of higher-order statistics (cumulants, and polyspectra, etc.) often contains a considerable bias, especially for a short length of observation data. Moreover, these algorithms possess a long convergence time, which is unacceptable

especially in the situation of on-line transmissions [7.5].

The main advantages of the proposed method are: (1) it can handle time-varying sources without any *a priori* information about the behavior of its parameters; (2) it guarantees the global convergence and uniqueness of the deconvolution solution; (3) the algorithm is simple to implement and possesses a fast convergence property.

Two different blind deconvolution schemes are presented in this chapter: *the one-sensor-scheme* and *the two-sensors-scheme.*

7.2. Statement of the Problem

7.2.1. Channel Model

Let us denote the *unobservable* source by $\{s_k\}$ and the observed data by $\{x_k\}$. The source $\{s_k\}$ propagates through an unknown multipath channel $\Im \equiv \{h_k\}$ given by

$$\Im(q^{-1}) = \sum_{i=0}^{N} h_i q^{-i} \tag{7.2.1}$$

Thus, the observed data becomes:

$$x_k = \sum_{i=0}^{N} h_j s_{k-j} \tag{7.2.2}$$

where q^{-1} is a delay operator, N is the length of the channel impulse response. The channel may be a FIR or IIR one with a minimum phase or non-minimum phase transfer function[1]. The channel output $\{x_k\}$ is also called a *reverberated source.*

The objective of the deconvolution is to find an inverse channel $\Im^{-1} \equiv \{\theta_k^*\}$, i.e. the equalizer

$$\Im^{-1}(q^{-1}) = \sum_{i=0}^{M} \theta_i^* q^{-i} \tag{7.2.3}$$

1. We will also discuss time-varying channel, in this situation, the concept of transfer function is not applicable.

such that the following condition is satisfied

$$\Im \otimes \Im^{-1} = \sum_{j=0}^{N+M} h_k \theta_{k-j} q^{-j} = \delta_k \tag{7.2.4}$$

where $\otimes$ denotes the convolution of the channel $\Im$ and the equalizer $\Im^{-1}$. Note that both channels $\Im$ and $\Im^{-1}$ are BIBO stable, i.e. $\{h_k\}, \{\theta_k^*\} \in l_1$, where l_1 denotes the set of all absolutely summerable real sequence[1]. Let us denote an *adjustable* sequence by $\Theta \equiv \{\theta_k\} \in l_1$ which is implemented in the form of a tapped delay line of length N. The impulse response of the channel cascade connected with the equalizer $\Im \otimes \Theta$ is given by

$$\sigma_k = \sum_{i=0}^{Q} h_i \theta_{k-i} \qquad \{\sigma_k\} \in l_1 \tag{7.2.5}$$

which is also called the impulse response of *combined channel*, and where $Q = M + N$. The output of the combined channel is

$$y_k = \sum_{i=0}^{Q} \sigma_i s_{k-i} \tag{7.2.6}$$

The deconvolution is accomplished iff the impulse response $\sigma_k = c\delta_{k-K}$. This will be referred to as the equalization condition of the combined channel.

In practice, the non-causality is handled by introducing an appropriate delay for the finite length equalizer. In what follows, we will present two new schemes for the blind deconvolution task. The analysis is carried out for a minimum-phase channel model, but is also valid for a non-minimum-phase channel situation, if the equalizer is implemented in the form of a finite length tapped delay line FIR structure. For the non-minimum phase channel, without loss of generality, we focus our attention to the case where the channel has one zero inside the unit disc and the other outside. The *two side taped equalizer* is given as

$$\sum_{i=-L}^{Q} \Xi_i q^{-i} \qquad \Xi_i = \begin{cases} a^i & i \geq 0 \\ b^i & i < 0 \end{cases} \qquad |b| > 1 > |a| > 0$$

Fig. 7.1 highlights the relationship between the channel, the equalizer, and the

1. In this chapter, we assume that the IIR channel is truncated to a finite length N.

combined channel model.

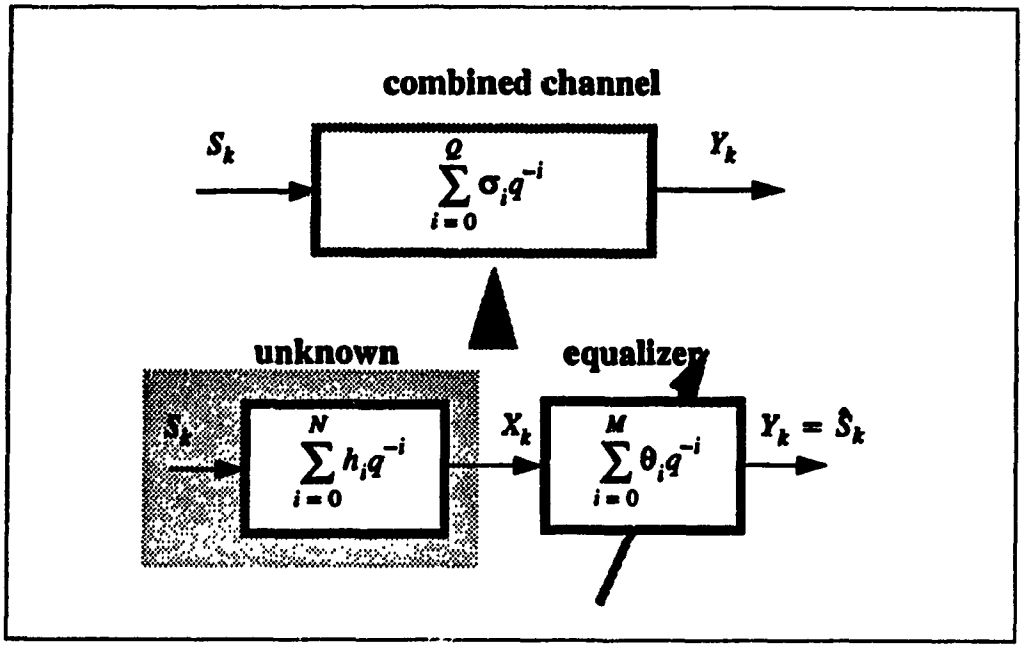

Fig. 7.1 The Relationship between the Channel, Equalizer and Combined Channel

In order to justify the relationship between the channel, the equalizer, the combined channel and the deconvoltuion (equalization) conditions, we state the following lemmas related to channel equalization.

Lemma 7.2.1 *(Channel equalization) The impulse response of the combined channel* $\{\sigma_k\}$ *can be expressed in the form of an infinite Hankel Matrix* H_p *with the following properties: (1) The rank of the matrix is equal to the number of unequalized poles of the combined channel. (2) The coefficients of the channel* $\Im(q^{-1})$ *and the equalizer* $\Theta(q^{-1})$ *are related by*

$$\begin{vmatrix} h_0 & h_1 & h_2 & \cdots & h_{2p-1} \\ \theta_0 & \theta_1 & \theta_2 & \cdots & \theta_{2p-1} \\ 0 & h_0 & h_1 & \cdots & h_{2p-2} \\ 0 & \theta_0 & \theta_1 & \cdots & \theta_{2p-2} \\ \cdots & \cdots & & & \cdots \end{vmatrix} = h_0^{2p} det(H_p) \qquad H_p = \begin{bmatrix} \sigma_0 & \sigma_1 & \cdots & \sigma_{p-1} \\ \sigma_1 & \sigma_2 & \cdots & \sigma_p \\ \cdots & \cdots & & \cdots \\ \sigma_{p-1} & \sigma_p & \cdots & \sigma_{2p-1} \end{bmatrix}$$

Proof:

(1) *Proof of the first property:*

Assuming that the channel $\Im(q^{-1})$ is FIR. The combined channel is given by

$$\Im(q^{-1})\tilde{\Theta}(q^{-1}) = \frac{\Im(q^{-1})}{\tilde{\Theta}(q^{-1})} \qquad \tilde{\Theta}(q^{-1}) = \tilde{\theta}_0 + \tilde{\theta}_1 q^{-1} + \ldots + \tilde{\theta}_m q^{-m}$$

Furthermore, the channel $\Im(q^{-1})$ and the equalizer $\Theta(q^{-1})$ are co-prime, i.e. they do not have a common factor; thus, we have the combined channel response to be

$$\frac{\Im(q^{-1})}{\Theta(q^{-1})} = \sigma_{-1} + \sigma_0 q^{-1} + \sigma_1 q^{-2} + \ldots \tag{7.2.7}$$

From (6.3.5) and (7.2.7) we have the following relationship (null condition)

$$\begin{aligned} \theta_0\sigma_{-1} &= h_0 \\ \theta_0\sigma_0 + \theta_1\sigma_{-1} &= h_1 \\ &\cdots \\ \theta_0\sigma_{M-1} + \theta_1\sigma_{M-2} + \ldots + \theta_M\sigma_{-1} &= h_M \\ \theta_0\sigma_k + \theta_1\sigma_{k-1} + \ldots + \theta_M\sigma_{k-M} &= 0 \qquad k = M, M+1\ldots \end{aligned} \tag{7.2.8}$$

Denote the row vector of a Hankel matrix H_p as

$$\Gamma_0 = \begin{bmatrix} \sigma_0 & \sigma_1 & \ldots & \sigma_{p-1} \end{bmatrix}$$

$$\Gamma_1 = \begin{bmatrix} \sigma_1 & \sigma_2 & \ldots & \ldots & \sigma_p \end{bmatrix}$$

$$\ldots\ldots\ldots\ldots$$

$$\Gamma_{p-1} = \begin{bmatrix} \sigma_{p-1} & \sigma_p & \ldots & \sigma_{2p-1} \end{bmatrix}$$

Based on the last equation of (7.2.8), it is easy to find the following linear combination relationship

$$\Gamma_{l+1} = \sum_{i=1}^{M} \theta_i \Gamma_{p-i+1}$$

Moreover, it is evident that from the structure of the Hankel matrix, the rows of the matrix may be generally expressed as

$$\Gamma_{l+1+k} = \sum_{i=1}^{M} \theta_i \Gamma_{p-i+k+1} \qquad \forall k = M, M+1, \ldots$$

This means that there are only m independent rows in the Hankel matrix; therefore, the rank of the infinite Hankel matrix is equal to the order of the polynomial $\Theta(q^{-1})$, which is equal to the number of unequalized poles of the combined channel, in view of the assumption that $\Im(q^{-1})$ and $\Theta(q^{-1})$ are co-prime.

(2) Proof of the second property:

Using (7.2.5) and (7.2.8) we can find a determinant relationship between the Hurwitz matrix and the Hankel matrix

$$\begin{vmatrix} h_0 & h_1 & h_2 & \cdots & h_{2p-1} \\ \theta_0 & \theta_1 & \theta_2 & \cdots & \theta_{2p-1} \\ 0 & h_0 & h_1 & \cdots & h_{2p-2} \\ 0 & \theta_0 & \theta_1 & \cdots & \theta_{2p-2} \\ \cdots & \cdots & & \cdots & \end{vmatrix} = \begin{vmatrix} 1 & 0 & 0 & \cdots & 0 \\ \sigma_0 & \sigma_1 & \sigma_2 & & \sigma_{2p} \\ 0 & 1 & 0 & & 0 \\ 0 & \sigma_0 & \sigma_1 & \cdots & \sigma_{2p-1} \\ \cdots & \cdots & & & \cdots \end{vmatrix} \begin{vmatrix} \theta_0 & \theta_1 & \theta_2 & \cdots & \theta_{2p-1} \\ & \theta_0 & \theta_1 & \cdots & \theta_{2p-2} \\ & & \theta_0 & & \theta_{2p-3} \\ & \mathbf{0} & & & \cdots \\ & & & & \theta_0 \end{vmatrix}$$

$$= (-1)^{\frac{p(p-1)}{p}} h_0^{2p} \begin{vmatrix} \sigma_p & \sigma_{p-1} & \cdots & \sigma_{2p} \\ \sigma_{p-1} & \sigma_{p-2} & \cdots & \sigma_{2p-1} \\ \cdots & & & \cdots \\ \sigma_1 & \sigma_2 & \cdots & \sigma_{2p} \end{vmatrix} = h_0^{2p} \begin{vmatrix} \sigma_0 & \sigma_1 & \cdots & \sigma_p \\ \sigma_1 & \sigma_2 & \cdots & \sigma_{p+1} \\ \cdots & \cdots & & \cdots \\ \sigma_p & \sigma_{p-1} & \cdots & \sigma_{2p} \end{vmatrix} = h_0^{2p} det(H_p)$$

Q.E.D.

The first statement of Lemma 7.1.1. is valid for both the time-invariant channel and the equalizer, while the second statement is valid only for the time-varying channel response. It is well known that the equalization of time-invariant channel is equivalent to finding the inverse transfer function of the channel, which is based on the relationship between the Z-transforms of the channel input and the channel output. This is not so for the case of equalization for a time-variant channel. The following lemma is true for both the time-invariant and time-varying channels.

Lemma 7.2.2 *The equalization condition for the combined channel is that the channel $\Im(q^{-1})$ and the equalizer $\Theta(q^{-1})$ must possess the same polynomial function up to a constant scale factor and a constant phase shift.*

Proof: Assuming that $\sigma_i = 0 \quad i = 1, 2, ..., Q$ for the Hankel matrix H_1, we have

$$\begin{vmatrix} h_0 & h_1 \\ \theta_0 & \theta_1 \end{vmatrix} = h_0^2 \sigma_0 = 0 \Rightarrow \begin{matrix} \theta_0 = ch_0 \\ \theta_1 = ch_1 \end{matrix} \tag{7.2.9}$$

For H_2

$$\begin{vmatrix} h_0 & h_1 & h_2 & h_3 \\ \theta_0 & \theta_1 & \theta_2 & \theta_3 \\ 0 & h_0 & h_1 & h_2 \\ 0 & \theta_0 & \theta_1 & \theta_2 \end{vmatrix} = h_0^4 \begin{vmatrix} \sigma_0 & \sigma_1 \\ \sigma_1 & \sigma_2 \end{vmatrix} = 0 \tag{7.2.10}$$

By Sylvester expansion of the Hurwitz determinant (7.2.10) we get

$$\begin{vmatrix} h_0 & h_2 \\ \theta_0 & \theta_2 \end{vmatrix}^2 = 0 \Rightarrow \theta_2 = ch_2$$

In general we have,

$$\begin{vmatrix} h_0 & h_p \\ \theta_0 & \theta_p \end{vmatrix}^p = 0 \Rightarrow \theta_p = ch_p$$

Q.E.D.

From the second result of Lemma 7.2.1, we know that given an impulse response of the true channel $\Im(q^{-1})$, and the impulse response of the combined channel $\{\sigma_i\}$, the equalizer $\Theta(q^{-1})$ is not uniquely determined. The equalizer is uniquely determined iff the combined channel satisfies the perfect equalization condition, as stated in the Lemma 7.2.2.

In order to evaluate the equalization performance, we choose the Hankel norm as a criterion. Hankel norm is defined as

$$\|H_p\|_H = \prod_{i=0}^{m} \gamma_i = det(H_p)$$

where γ_i is the non-zero singular value of matrix H_p. The Hankel norm has the property, $\|H_p\|_2 \leq \|H_p\|_H \leq \|H_p\|_\infty$. From Lemma 7.1.2, if a channel is perfectly equalized then $\|H_p\|_H = 0$. So the equalization problem becomes one of finding an

equalizer such that for a given channel $\Im(q^{-1})$, the Hankel norm of the combined channel is minimized.

Remark 7.2.1 The Hankel norm is directly related to the impulse response of the combined channel, therefore, the Hankel norm is a more appropriate criterion to evaluate the performance of equalization. Perfect equalization condition corresponds to the Hankel norm being equal to zero.

7.2.2. The Source Model:

The source signal can be modelled by an analytic function $s_k = A(k)e^{j\Psi(k)}$, where the phase $\Psi(k)$ is a stochastic process with *an arbitrary distribution function*, and $A(k)$ is an envelope with $A(k) \geq 0$. The key assumption made in this chapter is that the instantaneous frequency of the source is time-varying, with a non-constant variation rate $E\{\ddot{\Psi}(k)\} \neq 0$, where $E\{\ \}$ denotes the ensemble mean operation. In what follows, we discuss two categories of sources, the constant-envelope source, and the time-varying envelope source. We propose two blind deconvolution schemes to reconstruct such signals which belong to a very general class of non-stationary analytic signals with randomly varying parameters. It should be mentioned that for such a source, the higher-order statistics are *time-dependent*; therefore, the higher-order-moments-based algorithm is not applicable [7.8].

7.3. A New Criterion for Blind Deconvolution

Choosing a suitable criterion for the blind deconvolution is a crucial issue. Based on such a criterion, the cost function for the blind deconvoltuion may be established. It is necessary for such a cost function to be unimodal, so that the blind deconvolution algorithm, starting from arbitrary initial value, will be guaranteed to converge to the unique true deconvoltuion solution. However finding such a criterion turns out to be a notoriously difficult task [7.6]. The widely accepted Gordard blind equalization algorithm has recently been shown to have the local convergence problem in some practical applications [7.7]. Moreover, it has been shown that the standard criterion based on a memoryless non-linearity will always lead to convergence problems, and no successful blind equalization scheme has been found using memoryless non-linearity as a deconvolution criterion.

The core element of the proposed blind deconvolution method is based on the establishment of a new criterion. The basic idea is to determine the structural model for the source s_k. We construct an ASTV-ARMA model which possesses the following unique features:

(1) It contains a **functional null singularity** to the true source with arbitrary parameters.

(2) It provides a **transparency** output for the reverberated source.

In what follows we will use a simple second order linear time-varying AS-ARMA model which satisfies the above mentioned features. A time-varying linear model, combined with second-order moment statistic is used to constitute the cost function. Our effort is to explore the idea that the reverberated source will satisfy such an ASTV-ARMA model if and only if the channel is equalized. It will be shown that under such a criterion, the uniqueness of the solution for blind equalization is guaranteed.

Now, let us find the time-varying moving average model for the source $s_k = A(k)\, e^{j\Psi(k)}$, that is, construct the null singularity for the source s_k:

$$s_k + a_1(k)\, s_{k-1} + a_2(k)\, s_{k-2} = 0 \tag{7.3.1}$$

Theorem 7.3.1 (*Coefficient splitting*) *The time-varying coefficients can be expressed as a product of two parts*

$$a_l(k) = \gamma_l^A(k)\,\gamma_l^\Psi(k) \qquad l = 1, 2 \tag{7.3.2}$$

where

$$\gamma_1^A(k) = \frac{A(k)}{A(k-1)} \qquad \gamma_2^A(k) = \gamma_1^A(k)\,\gamma_1^A(k-1) \tag{7.3.3}$$

and

$$\gamma_2^\Psi(k) = \frac{\sin[\dot{\Psi}(k)]}{\sin[\dot{\Psi}(k-1)]} \tag{7.3.4}$$

$$\gamma_1^\Psi(k) = -\gamma_2^\Psi(k)\cos[\dot{\Psi}(k-1)] - \cos[\dot{\Psi}(k)] \tag{7.3.5}$$

Proof: The Hilbert transform of s_k gives

$$\mathfrak{s}_k = H\{A(k)e^{j\Psi(k)}\} = jA(k)e^{-j\Psi(k)}$$

Both s_k and $\mathfrak{s}_k$ constitute complete and independent solutions of the linear homogeneous equation with time-varying coefficients given by (7.3.1). Therefore, the *augmented Wronskian* of the two independent solutions of (7.3.1) is given by

$$\begin{vmatrix} A(k-0)e^{j\Psi(k-0)} & H\{A(k-0)e^{j\Psi(k-0)}\} & s_{k-0} \\ A(k-1)e^{j\Psi(k-1)} & H\{A(k-1)e^{j\Psi(k-1)}\} & s_{k-1} \\ A(k-2)e^{j\Psi(k-2)} & H\{A(k-2)e^{j\Psi(k-2)}\} & s_{k-2} \end{vmatrix} = 0$$

Using Laplace expansion and comparing with (7.3.1), we obtain (7.3.2)-(7.3.5).

Q.E.D.

It should be noted that the time-varying coefficients of the ASTV-ARMA model can be split into a product of two independent parts, one being a function of the source envelope and the other of the instantaneous frequency. This results in a decoupling of the signal phase and the envelope. Therefore, we can perform signal processing by treating the phase and envelope separately. The splitting of the coefficients of the ASTV-ARMA model leads us to a study of the blind deconvolution problem with respect to two categories of sources; a constant-envelope source and a time-varying-envelope source.

7.4. Blind Deconvolution of a Constant-Envelope Source

7.4.1. System Descriptions

A source s_k with $A(k) = Const\ \forall k \in Z^+$ passes through the channel and the equalizer, then the output of the equalizer is fed into a second order time-varying ARMA model and the energy of the output of such a ARMA model is used as a cost function for the LMS adaptive algorithm to update the coefficients of the equalizer. The

two time-varying coefficients are controlled by the instantaneous phase $\Phi(k)$ of the channel output signal by using equations (7.3.4) and (7.3.5). The adjustment of the equalizer terminates when the value of the cost function reaches its minimum.

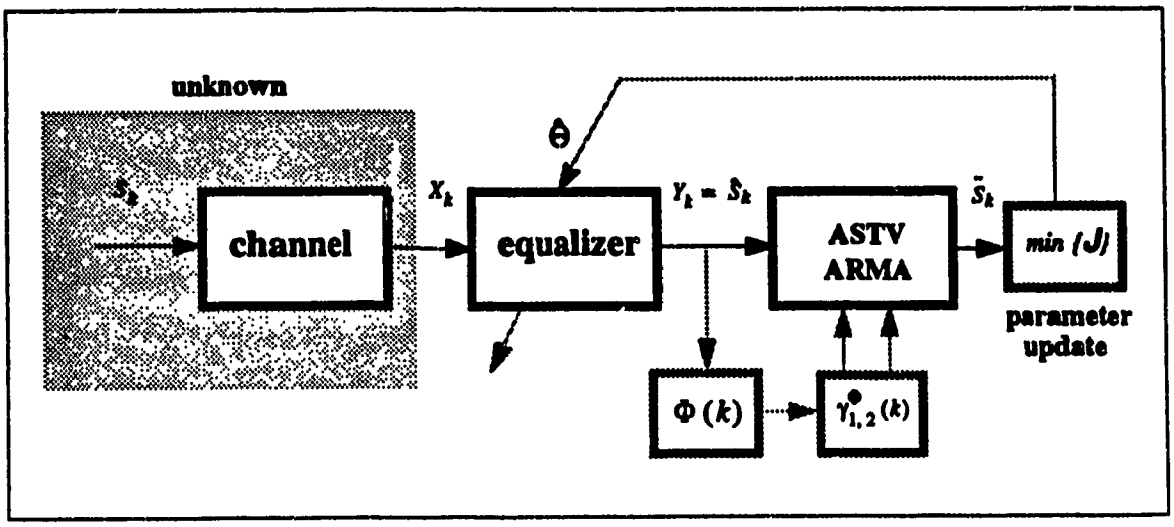

Fig. 7.2 One-Sensor Scheme for the Deconvolution of a Constant-Envelope Source

We prove that the equalizer can converge to the true inverse channel, once the deconvolution is achieved and the source is recovered. The block diagram of the one-sensor deconvolution scheme is shown in Fig.7.2

7.4.2. Global Minimum of the Cost Function

Let us consider a source with a constant envelope,

$$s_k = e^{j\Psi(k)}$$

The output of the combined channel becomes

$$\hat{s}_k = \tilde{A}(k)\, e^{j\Phi(k)} \tag{7.4.1}$$

where the envelope is written as

$$\tilde{A}(k) = \left[\left(\sum_{i=0}^{Q} \sigma_i \sin\Psi(k-i) \right)^2 + \left(\sum_{i=0}^{Q} \sigma_i \cos\left(\Psi(k-i)\right) \right)^2 \right]^{1/2} \tag{7.4.2}$$

and the phase

$$\Phi(k) = arc\tan\left[\frac{\sum_{i=0}^{Q}\sigma_i\sin\Psi(k-i)}{\sum_{i=0}^{Q}\sigma_i\cos\Psi(k-i)}\right] \tag{7.4.3}$$

From (7.4.2), we see that the envelope of the output signal from the combined channel is no longer a constant one. In what follows, we are going to elaborate on expression (7.4.2)

$$\tilde{A}(k) = \left(\sum_{i=0}^{Q}\sigma_i^2 + 2\sum_{i\neq j}^{Q}\sigma_i\sigma_j\cos\dot{\Psi}_{ij}\right)^{1/2} \tag{7.4.4}$$

where we denote $\sum_{i\neq j}^{Q} \equiv \sum_{i=1}^{Q}\sum_{j=1,j\neq i}^{Q}$ and $\dot{\Psi}_{ij} = \Psi(k-i) - \Psi(k-j)$, The Taylor expansion of the envelope $\tilde{A}(k)$ is obtained as

$$\tilde{A}(k) = \sqrt{\sum_{i=0}^{Q}\sigma_i^2}\left\{1 + \frac{1}{2}\frac{2\sum_{i\neq j}^{Q}\sigma_i\sigma_j\cos\dot{\Psi}_{ij}}{\sum_{i=0}^{Q}\sigma^2{}_i} + \frac{1}{2\cdot 4}\left(\frac{2\sum_{i\neq j}^{Q}\sigma_i\sigma_j\cos\dot{\Psi}_{ij}}{\sum_{i=0}^{Q}\sigma^2{}_i}\right)^2 + O(\sigma_i^2)\right\}$$

Using the inequality

$$\left|\frac{2\sum_{i\neq j}^{Q}\sigma_i\sigma_j\cos\Psi_{ij}}{\sum_{i=0}^{Q}\sigma_i^2}\right| \leq \frac{2\sum_{i\neq j}^{Q}|\sigma_i||\sigma_j|}{\sum_{i=0}^{Q}\sigma_i^2} \leq 1$$

and neglecting the higher order terms, $\tilde{A}(k)$ can be written as

$$\tilde{A}(k) \cong \left(\sum_{i=0}^{Q}\sigma_i^2\right)^{1/2} + \frac{\sum_{i\neq j}^{Q}\sigma_i\sigma_j\cos\dot{\Psi}_{ij}}{\left(\sum_{i=0}^{Q}\sigma_i^2\right)^{1/2}} \tag{7.4.5}$$

By (7.4.1) and (7.4.5) the channel output is expressed as

$$\tilde{s}_k = \left(\sum_{i=0}^{Q}\sigma_i^2\right)^{1/2} e^{j\Phi(k)} + \frac{\sum_{i\neq j}^{Q}\sigma_i\sigma_j\cos\Psi_{ij}}{\left(\sum_{i=0}^{Q}\sigma_i^2\right)^{1/2}} e^{j\Phi(k)} \tag{7.4.6}$$

The first term of (7.4.6) is a constant envelope component, and will be cancelled at the output of the ASTV-ARMA model, while the second term is a time-varying component of the envelope which will pass through the ASTV-ARMA *transparently*, i.e. the residual output of ASTV-ARMA model becomes:

$$\tilde{s}_k = \hat{A}(k)\, e^{j\Phi(k)} = \frac{\sum_{i\neq j}^{Q}\sigma_i\sigma_j\cos\Psi_{ij}}{\left(\sum_{i=1}^{Q}\sigma_i^2\right)^{1/2}} e^{j\Phi(k)} \tag{7.4.7}$$

The mean square error of the residual output as a cost function used to update the coefficients of the equalizer is defined as

$$J = E\{\tilde{s}_k^2\} = E_\Psi\{\hat{A}(k)^2\}$$

The uniqueness of the minimum of such a cost function is equivalent to the uniqueness of the solution deconvolution problem.

The stationary or the points of minima of the cost function are obtained by letting

$$\frac{\partial}{\partial\theta}J(\sigma) = E_\Psi\{\hat{A}(k)\}\frac{\partial}{\partial\theta}E_\Psi\{\hat{A}(k)\} = 0 \tag{7.4.8}$$

which yields

$$\boxed{E_\Psi\{\hat{A}(k)\} = 0} \tag{7.4.9}$$

$$\boxed{\frac{\partial}{\partial\theta}E_\Psi\{\hat{A}(k)\} = 0} \tag{7.4.10}$$

Note that these two system of equations are *not equivalent*, (7.4.10) $\Rightarrow$ (7.4.9), but it is not true that (7.4.10) $\Leftarrow$ (7.4.9). The uniqueness of the solution for both the equations is the key point to the uniqueness of the solution of the deconvolution problem.

7.4.3. Uniqueness of the Blind Deconvoltuion Solution

Let us denote the ensemble mean of the instantaneous frequency as $E_{\Psi}\{\Psi_{ij}(k)\} = \dot{\psi}_{ij}(k)$, where $E_{\Psi}\{\ \}$ is the mathematical expectation with respect to variable Ψ. The instantaneous frequency of the source $\dot{\psi}_{ij}(k)$ is time-varying, and is also called the *parameter* of the constant -envelope source. From condition (7.4.8), we have

$$\frac{\sum_{i\neq j}^{Q}\sigma_i\sigma_j\cos\dot{\psi}_{ij}}{\left(\sum_{i=0}^{Q}\sigma_i^2\right)^{1/2}} = 0 \tag{7.4.11}$$

It is easy to see that the solution of (7.4.11) is given by

$$\boxed{\sigma_j = c \quad \sigma_i = 0 \qquad i = 0, \ldots, Q \quad j \neq i} \tag{7.4.12}$$

This is a *desired deconvolution solution*. In order to show the uniqueness of the solution, it is necessary to study equation (7.4.10) to find the other possible equilibrium points of the cost function $J\{\ \}$ in (7.4.10)

From Appendix 7.1, (7.4.10) can be expressed as following linear homogenous equation

$$\boxed{\sum_{j>i}^{Q} g_{ij}(h,\sigma)\cos\dot{\psi}_{ij}(k) = 0} \tag{7.4.13}$$

where $g_{ij}(h,\sigma)$ is a function of the channel response $\{h_i\}$ and the response of the combined channel $\{\sigma_i\}$, (see A.7.1.8). Since the channel is time-invariant, the coefficients of $g_{ij}(h,\sigma)$ are fixed values and independent of time k. Now (7.4.13) implies that $\cos\dot{\psi}_{ij}(k)$ is a fundamental solution of the homogenous equation. Considering the source parameter $\dot{\psi}_{ij}(k)$ as an instantaneous *"phase"* of the cosine function, denote its *"frequency"* as $\dot{\psi}(k) = \dot{\psi}_{1,0}(k) - \dot{\psi}_{0,0}(k)$, which is called the

variation rate of the source parameter. Let us invoke the following property of the relationship between the coefficients of a homogenous equation and its fundamental solutions.

Lemma 7.4.1 *For a homogeneous equation with fixed value coefficients, the Wronskian associated with such an equation is a constant, and the frequency* $\ddot{\psi}(k)$ *of the fundamental solution* $\cos\dot{\psi}_{ij}(k)$ *is time-invariant. If the coefficients of the homogenous equation are time-varying, then the corresponding Wronskian is also time-varying and the frequency* $\ddot{\psi}(k)$ *of the fundamental solution* $\cos\dot{\psi}_{ij}(k)$ *is not a constant.*

Proof: This is an extension of Proposition 2.3.3 and 2.3.4 in Chapter 2.

Q.E.D.

According to Lemma 7.2.1, if (7.4.13) is satisfied, we have two cases for the relationship between the coefficients $g_{ij}(h,\sigma)$ and parameter variation rate $\ddot{\psi}(k)$;

$$\text{(i) } \ddot{\psi}(k) \neq Const \quad \text{and } g_{ij}(h,\sigma) = 0,$$

$$\text{(ii) } \ddot{\psi}(k) = Const \text{ and } g_{ij}(h,\sigma) \neq 0.$$

For the first case, by (A.7.8) in Appendix 7.1, $g_{ij}(h,\sigma) = 0$ implies that the solution of (7.4.13) is the desired deconvolution solution given by (7.4.12). However, in the second case, $g_{ij}(h,\sigma) \neq 0$ indicates there exists at least one solution for the combined channel response σ_i, which is different form the desired deconvolution solution; therefore the cost function $J\{\ \}$ has a local minima. On the other hand, the variation rate of the source parameter being not a constant, i.e. $\ddot{\psi}(k) \neq Const$, implies $E_{\Psi}\{\ddot{\Psi}_{ij}(k)\} \neq 0$. These two cases lead to following result.

Lemma 7.4.2 (*Channel Identifiability*) *The channel is uniquely identifiable, iff the variation rate of of the source parameter is not constant, i.e.* $E_{\Psi}\{\ddot{\Psi}(k)\} \neq 0$.

Proof: If $E_{\Psi}\{\ddot{\Psi}(k)\} = 0$ then $\ddot{\psi}(k) = Const$, thus we have

$$\psi_{i,i+1}(k) = \vartheta \quad \psi_{i,i+2}(k) = 2\vartheta \quad \text{and} \quad \psi_{i,i+l}(k) = l\vartheta$$

Hence (7.1.35) can be written as

$$\sum_{n=1}^{Q} g'_n(h,\sigma)\cos(n\vartheta) = 0 \tag{7.4.14}$$

It is seen immediately, by using the augmented Wronskian approach, that we can find analytically the expression for the coefficients $g'_n(h,\sigma)$, and then find the corresponding impulse response σ_i for the combined channel. Such a solution is not unique and does not satisfy the desired deconvolution condition (7.4.12). On the other hand, if the source parameter is shift varying $\exists l$ such that $\dot{\psi}_{l,l-1}(k) \neq \dot{\psi}_{i,i-1}(k)$ $\forall i,j = max|i-j| = Q$, then $\dot{\psi}(k+i) \neq Const$ $\forall i \in 1,2,...Q$.

According to Lemma 7.4.1, if (7.4.13) is valid, we must have

$$g_{ij}(h,\sigma) = 0$$

The use of (A.7.1.8) in Appendix 7.1 leads to (7.4.12).

Q.E.D.

Lemma 7.4.2 simply states a paradox that the transfer function of a channel can not be identified by using a single sine signal with a fixed frequency, besides the condition $E_{\psi}\{\ddot{\psi}(k)\} \neq 0$ also indicates that the linear chirp FM signal can not be used to identify the channel.

Lemma 7.4.2 also indicates that the local minima of the cost function $J\{\ \}$ is generated due to the slow variation of the source parameter (instantaneous frequency). If within the length of impulse response of the combined channel, the instantaneous frequency variation is sufficiently slow, the cost function will generate undesirable local minima. Nevertheless, the cost function $J\{\ \}$ is a function of time, thus the ASTV-ARMA output energy surface becomes time-varying, and the location of the minima points of such a surface are also time-varying. In addition to these time-varying minima, the cost function contains a *unique time-invariant* global minimum.

Theorem 7.4.1 *(Uniqueness) There exists an unique time-invariant stable global minima of the cost function $J\{\ \}$, and such a global minima corresponds to the equalization of the combined channel.*

Proof: According to the Lemma 7.4.1 and Lemma 7.4.3, Equation (7.4.12) is the only stationary equilibrium point of the cost function $J\{\ \}$.

Q.E.D.

Corollary 7.4.1 *The blind deconvolution is unique iff the parameter variation rate is not a constant.*

Proof: According to Lemma 7.4.2 and Lemma 7.4.3.

Q.E.D.

Example1: In order to give a clear explanation about the unique global minima of the cost function $J\{\ \}$, let us consider a channel with two paths and a two-tap equalizer.

In this case, using (A.7.8) in Appendix 7.1, (7.4.13) becomes

$$\begin{aligned}&[h_1(\sigma_2^2-\sigma_0^2)\sigma_1+h_2(\sigma_2^2-\sigma_1^2)\sigma_0]\cos\dot{\psi}_{01}(k)\\&+[h_1(\sigma_1^2-\sigma_0^2)\sigma_2-2h_2\sigma_0\sigma_1\sigma_2]\cos\dot{\psi}_{02}(k)\\&+[-2h_1\sigma_0\sigma_1\sigma_2+h_2(\sigma_0^2-\sigma_1^2)\sigma_2]\cos\dot{\psi}_{12}(k)\ =\ 0\end{aligned}\tag{7.4.15}$$

and

$$\begin{aligned}&[h_1(\sigma_1^2-\sigma_2^2)\sigma_0-2h_2\sigma_0\sigma_1\sigma_2]\cos\dot{\psi}_{01}(k)\\&+[-2h_1\sigma_0\sigma_1\sigma_2+h_2(\sigma_1^2-\sigma_2^2)\sigma_0]\cos\dot{\psi}_{02}(k)\\&+[h_1(\sigma_0^2-\sigma_1^2)\sigma_2+h_2(\sigma_0^2-\sigma_2^2)\sigma_1]\cos\dot{\psi}_{12}(k)\ =\ 0\end{aligned}\tag{7.4.16}$$

with the constraint: $\sum_{i=0}^{2}\sigma_i^2\neq 0$.

Since the parameters of the source are time-varying $\dot{\psi}_{i,i+1}(k)\neq C_1\ \ i=0,1,2,$

$$\begin{aligned}\dot{\psi}_{01}(k)-\dot{\psi}_{02}(k)\ &=\ \dot{\psi}_{12}(k)\neq Const\\ \dot{\psi}_{02}(k)-\dot{\psi}_{12}(k)\ &=\ \dot{\psi}_{01}(k)\neq Const\end{aligned}\qquad \forall k\in Z^{+}$$

On the other hand, once the equalizer converges to a steady state, the coefficients of the homogeneous equation (7.4.15) and (7.4.16) are constants. Hence, the only possible solution is $\sigma_i = Cons \quad \sigma_j = 0,\ i\neq j$.

If the parameter of the source is time-invariant, then

$$\dot{\psi}_{01}(k)\ =\ \dot{\psi}_{12}(k)\ =\ \vartheta \qquad \dot{\psi}_{02}(k)\ =\ 2\vartheta$$

Thus we have,

$$\frac{2h_1\sigma_0\sigma_1\sigma_2 - h_2(\sigma_0^2-\sigma_1^2)\sigma_2 - h_1(\sigma_2^2-\sigma_0^2)\sigma_1 - h_2(\sigma_2^2-\sigma_1^2)\sigma_0}{h_1(\sigma_1^2-\sigma_0^2)\sigma_2 - 2h_2\sigma_0\sigma_1\sigma_2} = \frac{\cos 2\vartheta}{\cos\vartheta}$$

$$\frac{-h_1(\sigma_0^2-\sigma_1^2)\sigma_2 - h_2(\sigma_0^2-\sigma_2^2)\sigma_1 - h_1(\sigma_1^2-\sigma_2^2)\sigma_0 + (2h_2\sigma_0\sigma_1\sigma_2)}{-2h_1\sigma_0\sigma_1\sigma_2 + h_2(\sigma_1^2-\sigma_2^2)\sigma_0} = \frac{\cos 2\vartheta}{\cos\vartheta}$$

(7.4.17)

Using the relationship between the Hurwitz and the Hankel determinants as given in Lemma 7.2.1, and considering at the same time the above two equations as constraints, it is straight forward to show that the above two equations allow at least one solution for $\sigma_i \neq 0$ $i = 0, 1, 2$; such a solution is a local minima of the cost function $J\{\ \}$, which leads to a false deconvolution solution. We state following result as a counterpart of Theorem 7.4.1 for the time-varying channel. We assume that time-varying channel is BIBO stable, the channel variation is independent to the source.

Corollary 7.4.1 *(Condition of Equalization of Time-varying Channel) If the channel is time-varying, the condition for the cost function $J\{\ \}$ to be unimodal is that the parameter of source has a non-constant variation rate.*

Proof: See Appendix 7.2.

Q.E.D.

As shown in (7.4.2), a constant-envelope source passing through an unequalized combined channel becomes a time-varying envelope. In what follows, we present a relationship between the impulse response of the combined channel and the envelope variation of the channel output. Let us denote the envelope variation rate as $\partial\gamma^A(k) = \left|\gamma_1^A(k) - \gamma_1^A(k-1)\right|$,

Lemma 7.4.4 *(Bound on Envelope Variation Rate) For a constant-envelope source, the variation rate of the envelope observed at the output of combined channel has an upperbound given by*

$$\partial\gamma^A(k) \leq 2\left\{\left(1 - \frac{\sum_{i\neq j}^{Q}|\sigma_i\sigma_j|}{\sum_{i=0}^{Q}\sigma_i^2}\right)^{-1} - 1\right\}$$

Proof: By definition the envelope variation rate is

$$\partial\gamma^{\tilde{A}}(k) = \left| \frac{\tilde{A}(k)}{\tilde{A}(k-1)} - \frac{\tilde{A}(k-1)}{\tilde{A}(k-2)} \right|$$

with

$$\frac{\tilde{A}(k)}{\tilde{A}(k-1)} = \frac{\sum_{i=0}^{Q} \sigma_i^2 + \sum_{i \neq j}^{Q} \sigma_i \sigma_j \cos\psi_{ij}(k)}{\sum_{i=0}^{Q} \sigma_i^2 + \sum_{i \neq j}^{Q} \sigma_i \sigma_j \cos\psi_{ij}(k-1)}$$

Then

$$\partial\gamma^{\tilde{A}}(k) \leq \frac{4\sum_{i=1}^{Q} \sigma_i^2 \sum_{i \neq j}^{Q} |\sigma_i \sigma_j| + 2\left(\sum_{i \neq j}^{Q} |\sigma_i \sigma_j|\right)^2}{\left(\sum_{i=1}^{Q} \sigma_i^2 - \sum_{i \neq j}^{Q} |\sigma_i \sigma_j|\right)^2}$$

$$= 2\left\{\left(1 - \frac{\sum_{i \neq j}^{Q} |\sigma_i \sigma_j|}{\sum_{i=0}^{Q} \sigma_i^2}\right)^{-1} - 1\right\} \qquad (7.4.18)$$

Q.E.D.

Denoting $\tilde{\sigma} = \left(\sum_{i \neq j}^{Q} |\sigma_i \sigma_j|\right)\left(\sum_{i=0}^{Q} \sigma_i^2\right)^{-1}$, we notice that $0 \leq \tilde{\sigma} \leq 1$.

Remark 7.3.1 From (7.4.18) we see that an unequalized pole close to the unit circle, $\tilde{\sigma} \rightarrow 1$, may result in a fast variation of the envelope at the output of the combined channel. Conversely, if the channel is equalized, i.e. $\tilde{\sigma} = 0$, the observed envelope becomes a constant one.

Theorem 7.4.2 *For a constant-envelope source with a non-constant parameter variation rate, the observed envelope of the combined time-invariant channel output is constant, iff the channel is equalized.*

Proof: "*if*" part is seen from the fact that (7.4.13) will become a constant, when the combined channel response is given by $\sigma_i = \delta_{i0}$ $i = 0, \ldots, Q$. The channel is

equalized, and the output of the equalizer possesses a constant envelope.

"only if" is seen by setting $\sigma_i = 0 \quad i = 1, 2..., Q$ which is equivalent to the channel equalization condition. Thus we have from (7.4.18)

$$\gamma^{\tilde{A}}(k) = 0$$

The envelope of the equalizer output is constant, which implies the equalization of the channel.

Q.E.D.

The key to the deconvolution of a constant-envelope source is based on Theorem 7.4.2; the envelope variation of the channel output signal is an important information to achieve channel equalization. In what follows, we investigate a more general case, where the envelope of the true source is time-varying.

7.5. Blind Deconvolution of a Time-Varying Envelope Source

7.5.1. Reverberated Envelope of a Time-Varying Envelope Source

Now we consider the case where the true source contains a time-varying envelope.

$$s_k = A(k)\, e^{-j\Psi(k)}$$

The output of the combined channel becomes

$$\tilde{s}_k = \tilde{A}(k)\, e^{-j\tilde{\Phi}(k)}$$

where the reverberated envelope is expressed as

$$\tilde{A}(k) = \left[\sum_{i=0}^{Q} A^2(k-i)\,\sigma_i^2 + \sum_{i=1}^{Q}\sum_{j=1}^{Q} A(k-i)A(k-j)\,\sigma_i\sigma_j \cos\psi_{ij}(k) \right]^{1/2} \qquad (7.5.1)$$

We expand the reverberated envelope (7.5.1) by Taylor series and neglect the higher-order terms. Let us denote

$$\tilde{A}(k-l) = A(k-l) f_l \sigma_0 \;\; ; \;\; l = 0, 1, 2, \qquad (7.5.2)$$

where

$$f_l = f_l(A(k), \sigma) = \left(1 + \frac{\sum_{i=1}^{Q} A^2(k-i-l)\sigma_i^2}{A^2(k-l)\sigma_0^2} \right)^{1/2} \times \left(1 + \frac{\sum_{i=1}^{Q}\sum_{j=1}^{Q} A(k-i-l)A(k-j-l)\sigma_i\sigma_j \cos\psi_{ij}(k)}{\sum_{i=0}^{Q} A^2(k-i-l)\sigma_i^2} \right)$$

Then the variation rate of the envelope of the channel output is given by

$$\partial\gamma^{\tilde{A}}(k) = \left| \frac{\tilde{A}(k)\tilde{A}(k-2) - \tilde{A}^2(k-1)}{\tilde{A}(k-1)\tilde{A}(k-2)} \right| \tag{7.5.3}$$

Substitution of (7.5.1) and (7.5.2) into (7.5.3) gives

$$\gamma^{\tilde{A}}(k) = \gamma^{A}(k)\left[\frac{f_0}{f_1} + \frac{f_1}{f_2}\right] - \left[\frac{\tilde{A}(k)f_1}{\tilde{A}(k-1)f_2} - \frac{\tilde{A}(k-1)f_0}{\tilde{A}(k-2)f_1}\right] \tag{7.5.4}$$

The envelope variation rate of the combined channel output $\gamma^{\tilde{A}}(k)$ is different from the variation rate of the true source $\gamma^{A}(k)$, because it is dependent on the impulse response of the combined channel σ_i. If the channel is equalized, i.e. the combined channel satisfies condition (7.4.12), then we have by (7.5.2) and (7.5.4)

$$\partial\gamma^{\tilde{A}}(k) = \partial\gamma^{A}(k) \tag{7.5.5}$$

This is the key for the blind deconvolution of a time-varying-envelope source.

Lemma 7.5.1 *If the envelope of the true source is a priori known, then the channel can be identified iff the instantaneous frequency has a non-constant variation rate.*

Proof: If $A(k)$ is known *a priori*, then following the same procedure as in Appendix 7.1, we have

$$\sum_{j>i}^{Q} \tilde{g}_{ij}(h, \sigma, A(k)) \cos\psi_{ij}(k) = 0$$

By Lemma 7.4.1, if the frequency variation rate $\ddot{\psi}(k) \neq Const$, then the above equation has only the solution given by(7.4.12). If $\ddot{\psi}(k) = Const$, the solution of the above equation will result in local minima of the cost function.

Q.E.D.

In general, equation (7.5.4) indicates that the envelope of the reverberated source will be different from the time-varying envelope of the true source which is *a priori* unknown.

Lemma 7.5.2 *The deconvolution of a source with a priori unknown time-varying envelope can not be achieved from the output of one channel*

Proof: From (7.5.4), the uncertainty of the envelope variation of the channel output indicates that one senor to collect the observation data is not sufficient to identify the channel.

Q.E.D.

7.5.2. A Two-Sensor Blind Deconvolution Scheme

In order to cope with deconvolution of the source with a time-varying envelope, we propose a two-sensor scheme, see Fig.7. 3. In addition to the unknown *channel-1*, we simultaneously collect another set of observation data by using an independent sensor through another unknown *channel-2*. With these two sets of observation data, we carry out the deconvolution of the source with a time-varying envelope. Here we assume that the propagation delay of the source propagating through the channels to the sensors are known, and have been compensated. The impulse response of combined channel-1 is denoted by $\sigma_{i1}, i = 0, 1, 2, \ldots, Q$, and the impulse response of combined channel-2 by σ_{i2}.

The envelopes observed at the two sensors are given by

$$\tilde{A}_1(k) = \left(\sum_{i=1}^{Q} A^2(k-i)\sigma_{i1}^2 + 2\sum_{i=1}^{Q}\sum_{j=1, j\neq i}^{Q} A(k-i)A(k-j)\sigma_{i1}\sigma_{j1}\cos\psi_{ij}(k) \right)^{1/2}$$

$$\tilde{A}_2(k) = \left(\sum_{i=1}^{Q} A^2(k-i)\sigma_{i2}^2 + 2\sum_{i=1}^{Q}\sum_{j=1, j\neq i}^{Q} A(k-i)A(k-j)\sigma_{i2}\sigma_{j2}\cos\psi_{ij}(k) \right)^{1/2}$$

The source reconstructed from the both channels should be the same, if the deconvolution is achieved. Let us impose the constraint on the partial coefficients

$$\gamma_i^{A_1}(k) = \gamma_i^{A_2}(k) \tag{7.5.6}$$

This constraint implies

$$\tilde{A}_1(k)\tilde{A}_2(k-1) = \tilde{A}_2(k)\tilde{A}_1(k-1)$$
$$\tilde{A}_1(k)\tilde{A}_2(k-2) = \tilde{A}_2(k)\tilde{A}_1(k-2)$$

resulting in

$$\sigma_{i1}^2 - l\sigma_{i2}^2 = 0$$
$$\sigma_{i1}\sigma_{j1} - l^2\sigma_{i2}\sigma_{j2} = 0$$

where l is a scale value. The above equations require that the two combined channels have the relationship

$$\sigma_{i1} = l\sigma_{i2} \tag{7.5.7}$$

This is the equilibrium point of the 2-senor system. It is therefore important to investigate the uniqueness of this equilibrium point.

Theorem 7.5.2 *The reverberated time-varying envelope source can be uniquely reconstructed from the data collected by two sensors under the condition that the two unknown channels have no common poles/zeros.*

Proof: From (7.5.7) we know that the Hankel determinants for the two channels given by

$$H_{p1} = \begin{bmatrix} \sigma_{11} & \sigma_{21} & \sigma_{31} & \cdots \\ \sigma_{21} & \sigma_{31} & \cdots & \cdots \\ \sigma_{31} & \cdots & \cdots & \cdots \\ \cdots & \cdots & \cdots & \cdots \end{bmatrix} \qquad H_{p2} = \begin{bmatrix} \sigma_{12} & \sigma_{22} & \sigma_{32} & \cdots \\ \sigma_{22} & \sigma_{32} & \cdots & \cdots \\ \sigma_{32} & \cdots & \cdots & \cdots \\ \cdots & \cdots & \cdots & \cdots \end{bmatrix}$$

are related by

$$det(H_{p1}) = l^p det(H_{p2})$$

According to Lemma 7.2.1, condition (7.5.7) implies that the ranks of the Hankel matrices constructed by $\{\sigma_{i1}\}$ and $\{\sigma_{i2}\}$ are the same; therefore, the responses of the combined channels 1 and 2 must satisfy one of the two conditions: *(1) both are perfectly equalized; or, (2) both the combined channels have the same unequalized poles / zeros.*

Q.E.D.

Let us study the situation when the two combined channels have common poles or common zeros. We first study the second condition. Considering all the possible combinations of the channel and the equalizer, we have the following three possible combinations of the channel and the equalizer

$$(1)\ \frac{\Im_1(q^{-1})}{\Theta_1(q^{-1})} = \frac{\Im_2(q^{-1})}{\Theta_2(q^{-1})} \quad (2)\ \frac{\Theta_1(q^{-1})}{\Im_1(q^{-1})} = \frac{\Theta_2(q^{-1})}{\Im_2(q^{-1})} \quad (3)\ \frac{\Theta_1(q^{-1})}{\Im_1(q^{-1})} = \frac{\Im_2(q^{-1})}{\Theta_2(q^{-1})}$$

which are equivalent to two different cases given by

$$\begin{aligned} &\textbf{CASE-1} \quad \Theta_1(q^{-1})\Theta_2(q^{-1}) = \Im_1(q^{-1})\Im_2(q^{-1}) \\ &\textbf{CASE-2} \quad \Im_1(q^{-1})\Theta_2(q^{-1}) = \Im_2(q^{-1})\Theta_1(q^{-1}) \end{aligned} \tag{7.5.8}$$

In case-1 of (7.5.8), if $\Im_1(q^{-1})$ and $\Im_2(q^{-1})$ do not have common factors, then neither can $\Theta_1(q^{-1})$ and $\Theta_2(q^{-1})$ have, since the order of the polynomial of the left hand side of (7.5.8) must be the same as that of the right hand side.

However, in case-2 of (7.5.8), it can be shown that the two equalizers may have common factors, even if the channels $\Im_1(q^{-1})$ and $\Im_2(q^{-1})$ do not have common factors; such possible common factors of the equalizers $\Theta_1(q^{-1})$ and $\Theta_2(q^{-1})$ become the unequalized poles/zeros. Because the unequalized poles/zeros will lead to a false deconvolution solution, (i.e. the equilibrium is a local minima), it is important to check if our reconstructed source is a true one.

In order to check for such unequalized poles/zeros, we first look at the relationship between the equalizer $\Theta_1(q^{-1})$ and its tapped delay-line counterpart $\tilde{\Theta}_1(q^{-1})$. If the equalizer $\Theta_1(q^{-1})$ is an IIR one,

$$\frac{1}{\Theta_1(q^{-1})} = \frac{1}{(1-p_1q^{-1})(1-p_2q^{-1})\ldots(1-p_{Mp}q^{-1})} = \prod_{l=1}^{M_p}\left[\sum_{i=0}^{\infty}(q^{-1}p_l)^i\right] \tag{7.5.9}$$

If L_p is a sufficiently large number (7.5.9)becomes

$$\frac{1}{\Theta_1(q^{-1})} = \left(\sum_{i=0}^{L_1}(q^{-1}p_1)^i\right)\left(\sum_{i=0}^{L_1}(q^{-1}p_2)^i\right)\cdots\left(\sum_{i=0}^{L_1}(q^{-1}p_{M_p})^i\right) \tag{7.5.10}$$

$$= \tilde{\Theta}_1(q^{-1}) = \sum_{i=0}^{M}\theta_i^{(1)}q^{-i}$$

Hence, checking for the existence of common factors between $\Theta_1(q^{-1})$ and $\Theta_2(q^{-1})$ is equivalent to checking for the common factors of $\tilde{\Theta}_1(q^{-1})$ and $\tilde{\Theta}_2(q^{-1})$.

After the equalization update converges to a steady state, we must check for possible *unequalized hidden common poles/zeros* for the channels. Let us assume that for *channel-1* equalizer the estimated coefficients are $\{\theta_i^{(1)}\}$ $i = 1, \ldots, M1$, while those for *channel-2* are $\{\theta_i^{(2)}\}$ $i = 1, \ldots, M2$. Let us now construct the resolvent matrix::

$$R_{M1\times M2} = \begin{bmatrix} \theta_0^{(1)} & \theta_1^{(1)} & \cdots & \theta_{M1}^{(1)} & & & 0 \\ & \theta_0^{(1)} & \theta_1^{(1)} & \cdots & \theta_{M1}^{(1)} & & \\ & & \cdots & \cdots & \cdots & \cdots & \\ & & & \theta_0^{(1)} & \theta_1^{(1)} & \cdots & \theta_{M1}^{(1)} \\ 0 & & & \theta_0^{(2)} & \theta_1^{(2)} & \cdots & \theta_{M2}^{(2)} \\ & & & \cdots & \cdots & \cdots & \\ \theta_0^{(2)} & \theta_1^{(2)} & \cdots & \cdots & \theta_{M2}^{(2)} & & 0 \end{bmatrix}$$

It is well known that, equalizer-1 $\tilde{\Theta}_1(q^{-1})$ and equalizer-2 $\tilde{\Theta}_2(q^{-1})$ are coprime, iff $det(R_{M1\times M2}) \neq 0$.

If $det(R_{M1\times M2}) = 0$, then, both equalizer-1 $\tilde{\Theta}_1(q^{-1})$ and equalizer-2 $\tilde{\Theta}_2(q^{-1})$ contain the same extra unequalized poles/zeros, and this will lead to a local minima solution for the deconvolution. In such a situation, we can use the Euclidean algorithm to find the largest common factor, and find the order l_c of such a common factor. Then we reduce the order of both the equalizers by l_c and perform the estimation again, until the determinant of the resolvent $det(R_{M1\times M2}) \neq 0$.

In practice, the physical location of the sensors is different, therefore the propagation path of the true source through the two different channels are different, and hence the transfer functions of the two channels usually do not contain the same poles/ zeros.

7.5.3. Partial Adaptive Gauss-Newton Algorithm

In order to model a signal with unknown time-varying envelope, one needs to develop an adaptive algorithm to track the partial coefficients for the time-varying envelope. According to Theorem 7.3.1, the time-varying coefficients of the ARTV-ARMA model can be explicitly split into a product of two independent parts: one $\gamma_l^{\Psi}(k)\ l = 1, 2$ which is controlled by the instantaneous phase $\Psi(k)$, and the other $\gamma_l^{A}(k)\ l = 1, 2$ which depends only on the envelope $A(k)$. The partial coefficients $\gamma_l^{\Psi}(k)$ are calculated from the instantaneous phase retrieved from the input mixture by using a phase detector, while the partial coefficients $\gamma_l^{A}(k)$ are estimated adaptively. The product of these two partial coefficients $\gamma_l^{\Psi}(k)\gamma_l^{A}(k)$ is injected into the ASTV-ARMA model. Usually, the source signal has a fast time-varying instantaneous frequency but the envelope is slowly time-varying. Thus by splitting the time-varying coefficients of the ASTV-ARMA model into two independent partial coefficients, we can model the non-stationary signal with a fast time-varying instantaneous frequency.

The partial adaptive algorithm for the estimation of $\gamma_l^{A}(k)$, the partial coefficients of the envelope, is listed in Table 7.1; it is basically a modification of the Gauss-Newton algorithm and possesses a fast convergence property. However we have to point out that this algorithm also contains a threshold effect when the variation of the coefficients of the envelope becomes fast.

7.6. Deconvolution Performance in the Presence of Additive Noise

Based on the result of the sensitivity analysis of the signal-controlled time-varying filter, if the variance of the input noise is given by σ_n^2, then at the output of the ASTV-ARMA model the variance of the noise remains σ_n^2, after the channel is equalized. Due to noise perturbation in the time-varying coefficients, there is a residual output signal at the output of the ASTV-ARMA model, and by Theorem 6.3.1, the variance of such a residual output is $\sigma_s^2 = \sigma_n^2$. In the steady state, after the deconvolution is accomplished, the minimum energy at the output of ASTV-ARMA model is

$$J_{min}\{\ \} = 2\sigma_n^2 \tag{7.5.11}$$

Since the update of the equalizer coefficients is based on a LMS criterion, the variance may be written as

$$cov(\Theta) = \mu J_{min} I_{MxM} = 2\mu\sigma_n^2 I_{MxM} \tag{7.5.12}$$

where Θ is the estimated equalizer coefficient, μ is the step size, I_{MxM} is a unity matrix.

$$\gamma^A(k+1) = \gamma^A(k) - \mu\Gamma_{II}^{-1}(k)\Gamma_I(k)$$

$$\Gamma_{II}(k) = (1-\mu)\Gamma_{II}(k-1) + \mu\Phi(k)\Phi^T(k) + \Pi(k)Re\{y(k)\}$$

$$\Gamma_I(k) = \Gamma_I(k-1) - \Phi(k)Re\{y(k)\}$$

$$\Phi(k) = \begin{bmatrix} \gamma_1^{\Psi}(k) & 0 \\ 0 & \gamma_2^{\Psi}(k) \end{bmatrix} \left\{ \begin{bmatrix} 1 & 0 \\ 0 & 1 \end{bmatrix} Re\left\{ \begin{bmatrix} \phi_1(k) \\ \phi_2(k) \end{bmatrix} \right\} + Re\left\{ \left[\Phi(k-1) \;\; \Phi(k-1) \right] \right\} \begin{bmatrix} \alpha & 0 \\ 0 & \alpha^2 \end{bmatrix} \gamma^A(k-1) \right\}$$

$$\gamma^A(k) = \left[\gamma_1^A(k) \;\; \gamma_2^A(k) \right]^T \qquad \Phi(k) = \left[\phi_1(k) \;\; \phi_2(k) \right]^T$$

$$\Pi(k) = \begin{bmatrix} \pi_{11}(k) & \pi_{12}(k) \\ \pi_{21}(k) & \pi_{22}(k) \end{bmatrix}$$

$$\phi_1(k) = -y(k-1) - \alpha x(k-1)$$
$$\phi_2(k) = -y(k-2) - \alpha^2 x(k-2)$$

$$\pi_{11}(k) = -2\alpha\phi_1(k-1) - \alpha\gamma_1^A(k)\pi_{11}(k-1) - \alpha^2\gamma_2^A(k)\pi_{11}(k-2)$$
$$\pi_{22}(k) = -2\alpha^2\phi_2(k-1) - \alpha\gamma_1^A(k)\pi_{22}(k-1) - \alpha^2\gamma_2^A(k)\pi_{22}(k-2)$$
$$\pi_{12}(k) = \pi_{21}(k)$$
$$= -2\alpha^2\phi_2(k-1) - \alpha\gamma_1^A(k)\pi_{22}(k-1) - \alpha^2\gamma_2^A(k)\pi_{22}(k-2)$$

Table 7.1: Partial Adaptive Gauss-Newton Algorithm

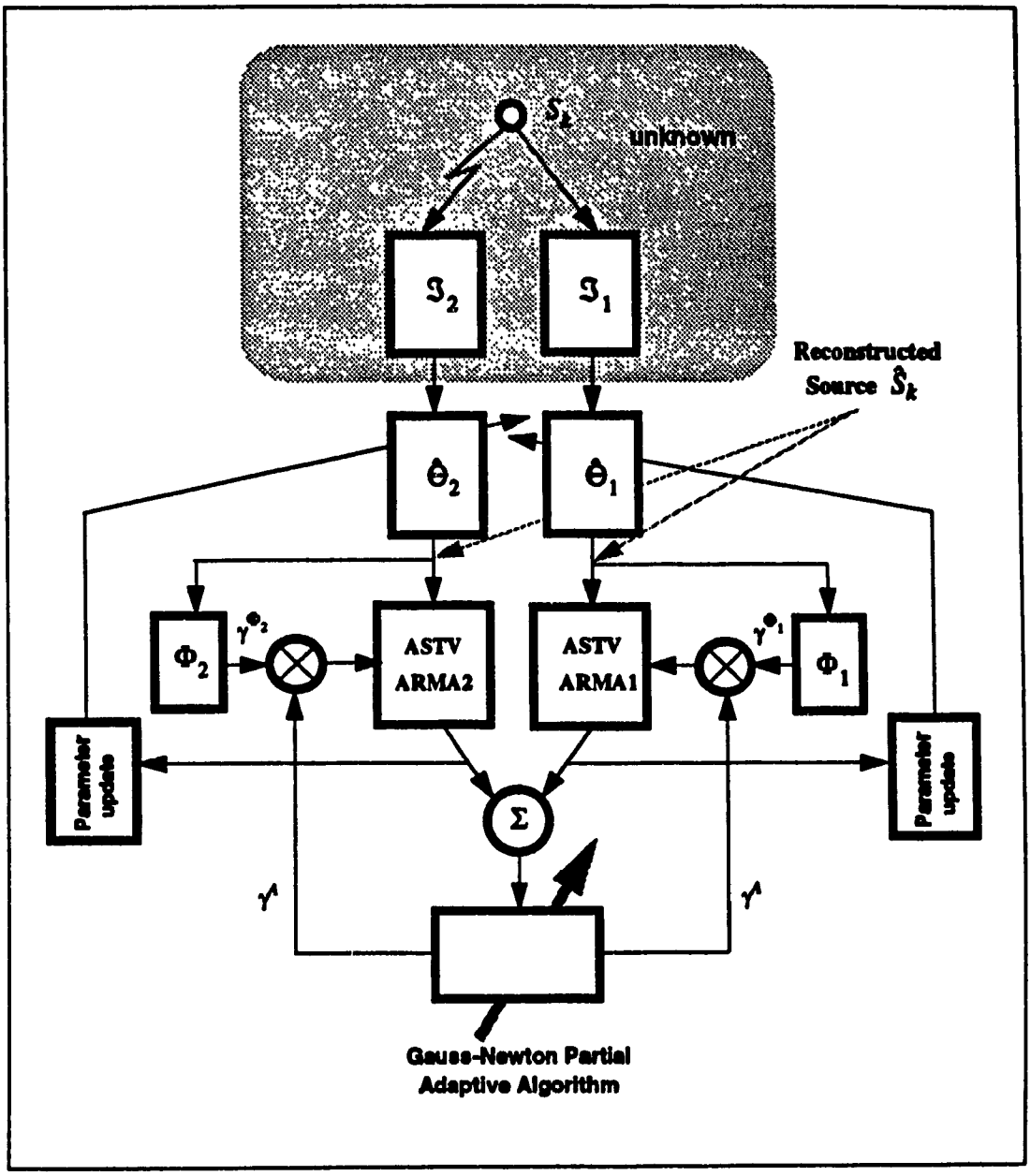

Fig. 7.3 Two-Sensor Scheme for the Blind Deconvolution of a Time-Varying Envelope Source

7.7. Summary of Blind Deconvolution Based on ASTV-ARMA Model

In this section, we summarize and extend the scope of the applications of the proposed blind deconvolution schemes (one-sensor scheme and two-sensor scheme). The results associated with different type of sources and channels are presented; the applicability of the proposed schemes in different situations are illustrated in Table 7.2 and Table 7.3.

Source Envelope	Channel Type
Constant-Envelope	*Time-Invariant (TIC)*
Time-Varying Envelope	*Time-Varying (TVC)*

Table 7.2: Source and Channel Types

$\partial A(k) = 0$	TIC	TVC
$\ddot{\psi}(k) \neq 0$	*YES*	*ill convergence*
$\ddot{\psi}(k) = 0$	*NO*	*YES*

Table 7.3: Blind Deconvolution of Constant Envelope Source with One-Sensor Scheme

$\partial A(k) \neq 0$	TIC	TVC	$\partial A(k) = 0$	TIC	TVC
$\ddot{\psi}(k) \neq 0$	*YES*	*YES*	$\ddot{\psi}(k) \neq 0$	*YES*	*YES*†
$\ddot{\psi}(k) = 0$	*YES*	*YES*	$\ddot{\psi}(k) = 0$	*NO*	*YES* +

Table 7.4: Blind Deconvolution of Time-Varying Envelope Source with Two-Sensor Scheme

† - using phase constraint for both channel $\gamma_{l1}^{\Psi}(k) = \gamma_{l2}^{\Psi}(k) \quad l = 1,2$

+ - using the envelope constraint $\gamma_{l1}^{A}(k) = \gamma_{l2}^{A}(k) = 1 \quad l = 1,2$

As we can see from the above tables, it is always impossible to use a sine signal with a fixed frequency to identify an unknown channel. The two-sensor scheme can

deal with a wider range of blind deconvolution problems. However we have to point out that such a scheme is based on a partial adaptive algorithm used to track the envelope variation. Such an algorithm (see Chapter 6) possesses an inherent tracking capability threshold. Therefore the two-sensor scheme is restricted only to a *slow time-varying envelop source.*

Example 2: ***Blind deconvolution of a constant envelop source based on one-sensor scheme.***

The source is represented by a frequency modulated signal. The modulating signal is a Gaussian stochastic process. The channels are

(***Channel-1***) A FIR channel with a *nonminimum phase* transfer function.

$$\mathfrak{I}_1(q^{-1}) = -1.5 + 3.5q^{-1} - 1.0q^{-2}$$

(***Channel-2***) An IIR channel with a *minimum phase* transfer function.

$$\mathfrak{I}_2(q^{-1}) = \frac{1}{3.3 - 5.0q^{-1} + 2.6q^{-2}}$$

Channel-1 contains two zeros, one is inside the unit disc, the other outside the unit disc. Channel-2 has two complex conjugate poles inside the unit disc. The constant-envelope random frequency-modulated signal passes through the channels, and only one-sensor scheme is used to reconstruct the source.

The Lissajous diagrams shown in Fig.7.4 illustrate the channel output before the deconvolution. In this example, we use a second order FIR equalizer to find the inverse channel of Channel-1. The statistical results are listed in Table 7.5, where $MSE^{\dagger}$ indicates the theoretical results obtained by applying equation (6.3.52).

We observe that the reconstructed source is very close to the true one. For the blind equalization of the nonminimum phase Channel-2, we use a two-sided non-causal equalizer. The simulation results are listed in Table 7.5.

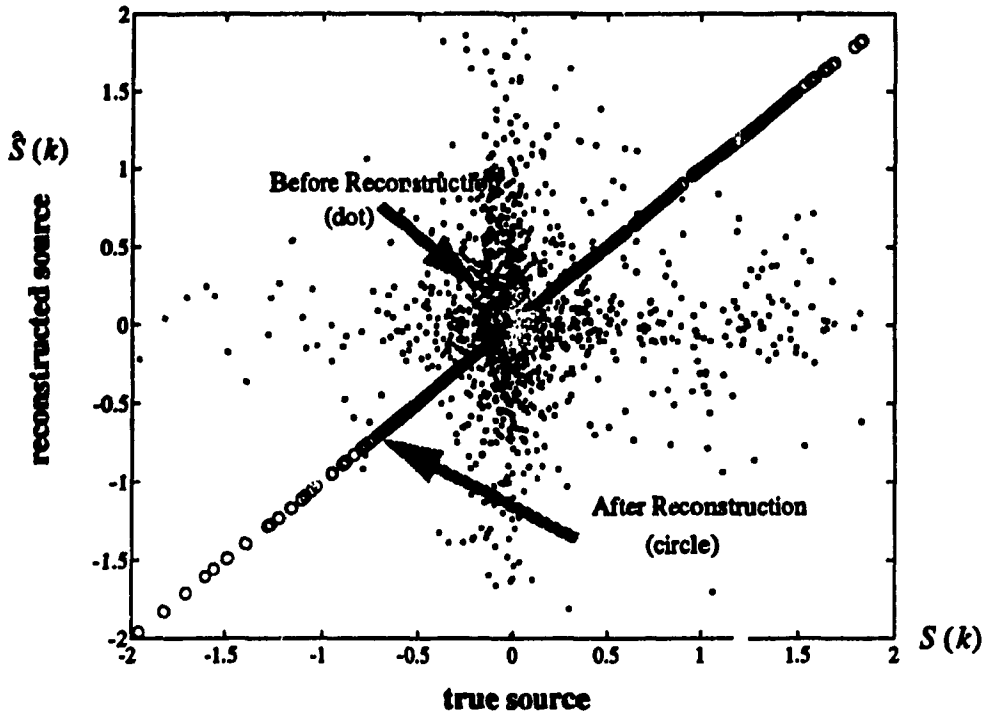

Fig. 7.4 The Lissajous Diagram for Convoluted and Recovered Source.

SNR	$\theta_1 = -1.5$		$\theta_2 = 0.8$		MSE†
	BIAS	MSE	BIAS	MSE	
50dB	-5.0×10^{-4}	5.1×10^{-6}	-1.3×10^{-4}	5.1×10^{-6}	3.2×10^{-6}
40dB	5.5×10^{-4}	3.9×10^{-5}	-1.4×10^{-3}	8.9×10^{-5}	3.9×10^{-5}
30dB	3.4×10^{-3}	8.8×10^{-4}	6.6×10^{-3}	1.2×10^{-4}	3.2×10^{-4}
20dB	2.1×10^{-3}	9.3×10^{-3}	4.0×10^{-3}	2.1×10^{-3}	4.2×10^{-3}
10dB	-5.0×10^{-2}	3.4×10^{-2}	4.5×10^{-2}	2.6×10^{-2}	3.2×10^{-2}

Table 7.5: Performance of Equalization Channel-2 Using One-Sensor Scheme

SNR	$a = 0.33$		$b = 2.0$		MSE†
	BIAS	MSE	BIAS	MSE	
50dB	2.1×10^{-3}	9.7×10^{-6}	7.9×10^{-4}	8.2×10^{-6}	3.2×10^{-6}
40dB	-3.4×10^{-3}	8.6×10^{-5}	-4.5×10^{-3}	9.4×10^{-5}	3.9×10^{-5}
30dB	1.7×10^{-2}	5.8×10^{-4}	8.7×10^{-3}	5.8×10^{-4}	3.2×10^{-4}
20dB	2.1×10^{-2}	7.8×10^{-3}	7.0×10^{-3}	7.0×10^{-3}	4.2×10^{-3}
10dB	7.4×10^{-2}	9.4×10^{-2}	8.5×10^{-2}	6.7×10^{-2}	3.2×10^{-2}

Table 7.6: Performance of Equalization Channel-1 Using One-Sensor Scheme

Example 3 ***Blind deconvolution of a time-varying-envelope source using a two-sensor scheme.***

The source is an AM/FM signal where both the instantaneous frequency and the amplitude are independently modulated by two sinusoids with different frequencies.

The observation data are collected from two different channels, Channel-1 and Channel-2. The convoluted source and reconstructed source are illustrated in Fig.7.5. Blind Deconvolution of a time-varying-envelope source is a more general and difficult task. To our knowledge, the proposed two-sensor scheme is the first such on-line algorithm. Since the design of the two-sensor scheme involves the partial adaptive Gauss-Newton algorithm, and such an adaptive algorithm possesses a threshold effects the proposed algorithm is applicable only if the envelope of the true source is a slowly time-varying one.

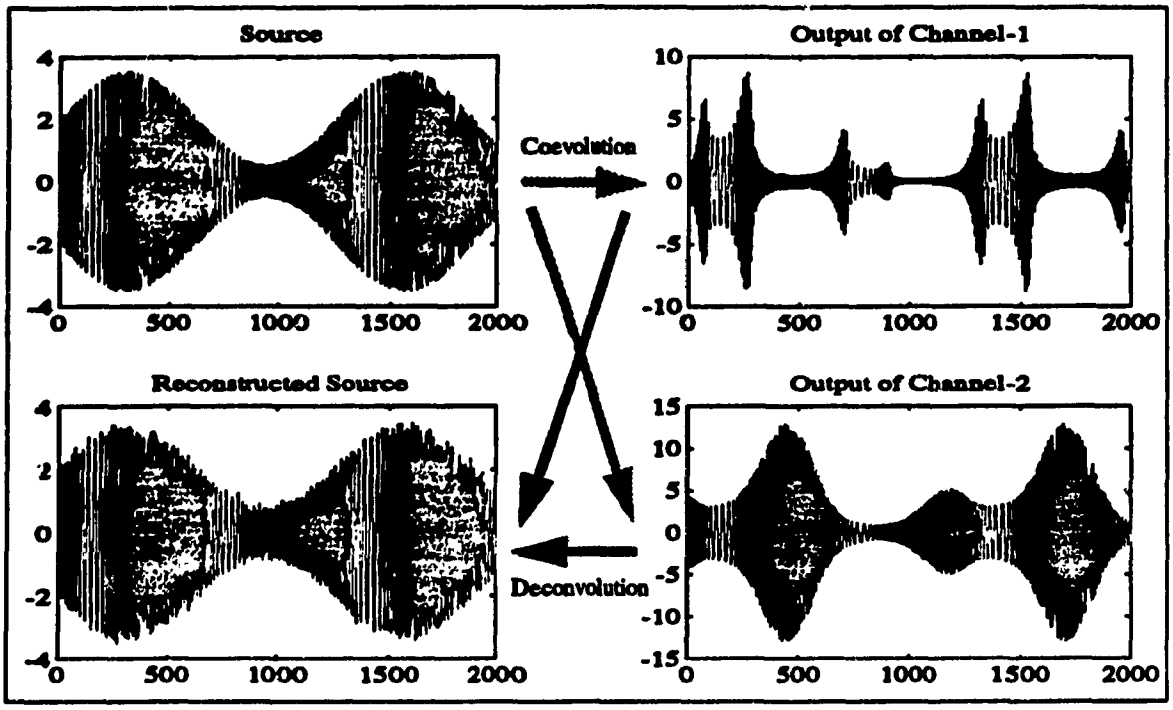

Fig. 7.5 Blind Deconvolution of Time-Varying Envelope Source Using Two Sensors Scheme

Example 4: ***Blind Equalization of digital Communication Channels***

For the equalization of the data communication channel the transmitter sends a known pattern of sequence called the training sequence, prior to the transmission session of the information data. Based on the receiving signal and a known training sequence, we adjust the equalizer of the receiver. Since the training sequence is *a priori* known, it does not bear any information. So during the equalization period there is no information transmission. Such a standard strategy has a serious drawback when applied to a continuously varying channel. In such a case one has to send the training sequence and to adjust the equalizer continuously, thus making the transmission efficiency dramatically degraded.

Blind equalization aims not to use an *a priori* known training sequence to equalize the channel; equalization is carried out as the transmission of the information data starts transmit. So it is obvious that the convergence time required for the blind equalizer is very crucial.

Blind equalization algorithm was proposed in digital communication nearly a decade ago [7.3] [7.4], and the constant-module algorithm or the so called Godard algorithm is a typical practically implemented algorithm [7.5]. However up till now, none of these algorithms can be effectively used for data transmission, the main weakness being the requirement of long observation time for convergence. Usually it takes *more than* 10^4 *symbol* (!) to reach the convergence state, apart form the recently discovered problem of local minima associated with the cost function of such an algorithm [7.7] [7.6]. On the other hand, algorithms such as the Godard algorithm or the higher-order-statistic-based algorithms resort to the use of higher-order statistical information, which means that the probability distribution function should be a non-Gaussian one. Nevertheless, in communication systems scramble coding is usally used, so that the actual transmitted data has a Gaussian shape distribution function. Therefore, the existing higher-order-statistic-based algorithma are not practically applicable.

In this example, we apply our ASTV-ARMA model to implement a blind equalization for digital communication. The significant advantage is that it exhibits *a fast convergence.* Simulation results demonstrates that the convergence time is dramatically reduced to *20 symbols.* Our proposed algorithm is simple to implement and may become very attractive to such applications as mobile communication and HF data communication.

In what follows, we discuss blind equalization with respect to two standard communication signals: the QAM signal and the raised cosine pulse shaped QAM signal.

(1) QAM signal;

A QAM signal can be written as $d_k = e^{j\psi(k)} en(k)$, where $\psi(k) = \omega_c k$, ω_c is the carrier frequency, $en(k)$ is the multilevel signal $en(lT) \in \{-L_m, -L_m+1, \ldots, 1, 0, -1, \ldots, L_m-1, L_m+1\}$; $lT, l \in Z^+$ is the synchronization instant, and T is the width of a symbol. For each individual channel, the QAM signal can be expressed as a synchronized sum of BPSK signals, i.e. the phase is keying for 0 to $\pm\pi$. For a standard QAM signal design, the carrier satisfies $\sin\psi(lT) = 0$, and the phase is discontinuously shifted $+\pi$ or $-\pi$ at any symbol synchronization instant.

We use our ASTV-ARMA model to null the unmodulated carrier, that is the null singularity of the AS-ARMA model is set to null the carrier signal $e^{j\psi(k)}$. Then at the symbol synchronization points, due the discontinuous phase keying, the null property of the AS-ARMA model will not be satisfied, and the MA part of this model will generate an impulse at these synchronous points. Let us keep the coefficients of the AS-ARMA model as constants: $\gamma_1 = -2\cos\omega_c$ and $\gamma_2 = 1$

Suppose we have the BPSK signal

$$s_{k-1} = \sin[\psi(lT-1)] \quad s_k = \sin[\psi(lT)+\pi] \quad s_{k+1} = \sin[\psi(lT+1)+\pi]$$

The output of MA part of AS-ARMA model becomes

$$r_{k-1} = s_{k-2} + a_1 s_{k-1} + a_2 s_k = 0$$

$$r_k = s_{k-1} + a_1 s_k + a_2 s_{k+1} = 2\sin\psi(lT-1)$$

$$r_{k+1} = s_k + a_1 s_{k+1} + a_2 s_{k+2} = 0$$

It is seen that an impulse exists at the phase keying point. This is an important key to our blind equalization scheme. Since the symbol transmission rate is *a priori* known, in the received sequence, we can blank the impulse at synchronous points in the output of the MA part, and the output of the MA part is always equal to zero if the channel is equalized. In this case the output of AS-ARMA model will also be zero, i.e. the ASTV-ARMA model will match the QAM signal.

If the channel is not equalized, then the MA part will generate impulses at non-synchronous points; the impulses of the MA part will excite the symmetrical AR part, resulting in a non-zero output. It is easy to see that the energy of the AS-ARMA output is minimized iff the channel is equalized, and such an energy function contains a unique minimum.

(2) Raised cosine pulse shaped QAM signal.

The raised cosine pulse shaped QAM signal is given by:

$$A(k-lT) = \left[\frac{\sin\omega_c(k-lT)}{\omega_c(k-lT)}\right]\left\{\frac{\cos\zeta\omega_c(k-lT)}{1-\left[\frac{2\zeta\omega_c(k-lT)}{\pi}\right]^2}\right\}$$

If the raised cosine factor ζ is known, (which is fixed once the system is designed) then the partial coefficient for the envelope can be pre-calculated as

$$\gamma_1^A(k-lT) = \frac{\sin(\omega_c k)\cos[\zeta\omega_c(k-lT)]}{\sin[\omega_c(k-lT-1)]\cos[\zeta\omega_c(k-lT-1)]}\left[1-\frac{1}{k-lT}\right]$$

$$\times\left\{\frac{1-\left[\frac{2\zeta\omega_c(k-lT-1)}{\pi}\right]^2}{1-\left[\frac{2\zeta\omega_c(k-lT)}{\pi}\right]^2}\right\} \qquad (7.5.13)$$

which in the case $k = lT$ becomes

$$\gamma_1^A(lT) = \frac{\omega_c\{-\left[\frac{2\zeta\omega_c}{\pi}\right]^2\}}{\sin\omega_c\cos\zeta\omega_c} \qquad (7.5.14)$$

In the case where the QAM signal is raised cosine shaped, the coefficients of the model can be written as

$$\gamma_1(k) = -2\cos\omega_c\gamma_1^A(k) \qquad \gamma_2(k) = \gamma_2^A(k)$$

The block diagram for the raised cosine equalizer is shown in Fig.7.6. The algorithm for the blind equalization of the QAM signal is listed in Table 7.6

By a direct extension of Theorem 7.4.1, we may conclude that *the blind deconvolution of the QAM signal can be achieved, if the symbol transmission rate is a priori known. The blind equalization of raised cosine QAM signals can be achieved if the symbol rate and raised cosine factor are a priori known.*

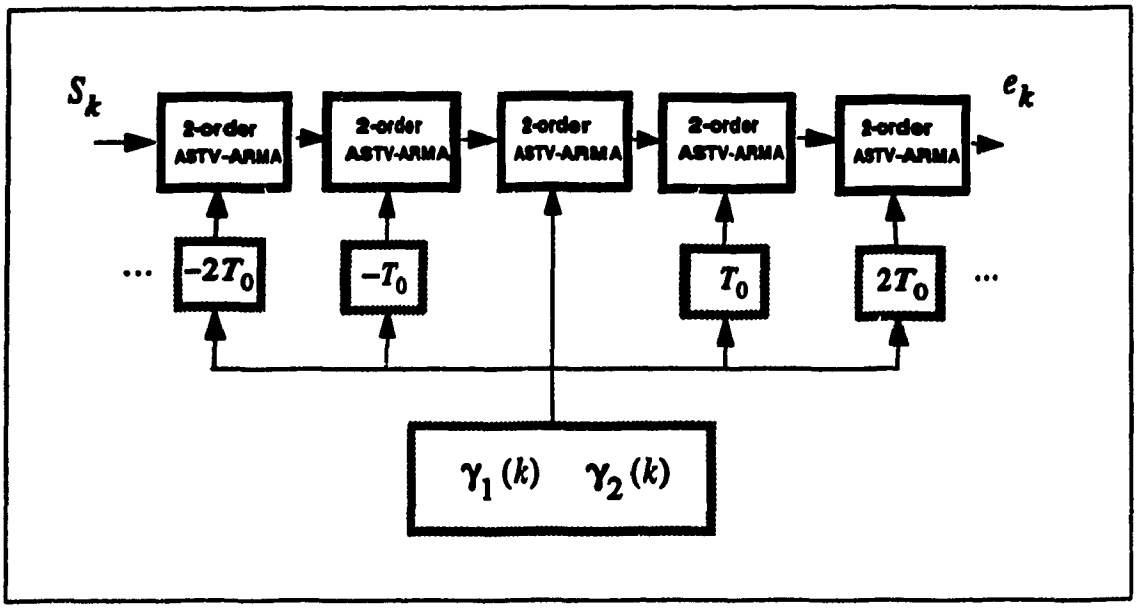

Fig. 7.6 Nonminimum Phase Equalizer for the Raised Cosine Shaped QAM signal

Table 7.7: Blind Equalization Algorithm for QAM Signal

Channel Output: $$s_k = \sum_{l=0}^{N} h_l e^{j\Psi(k-l)}$$

Step 0 *Parameter Setup:*

$$\alpha = 0.99 \qquad \gamma_1(k) = \gamma_1^{\Psi}(k) = -2\cos\omega_c$$

$$\gamma_2(k) = \gamma_2^{\Psi}(k) = 1$$

Step 1 *Equalizer Output:*

$$y_k = \sum_{l=1}^{L1}\sum_{m=0}^{M1} (r_{l,1}^{(k)})^m \cos(\omega_{l,1}^{(k)} m)\, s_{k+m} + \sum_{l=1}^{L2}\sum_{m=0}^{M2} \left(\frac{1}{r_{l,2}^{(k)}}\right)^m \cos(\omega_{l,2}^{(k)} m)\, s_{k-m}$$

$$+ \sum_{l=1}^{L3}\sum_{m=0}^{M3} (r_{l,3}^{(k)})^m s_{k+m} + \sum_{l=1}^{L4}\sum_{m=0}^{M4} \left(\frac{1}{r_{l,2}^{(k)}}\right)^m s_{k-m}$$

Step 2 *ASTV-ARMA Output:*

$$r_k = y_k + \gamma_1(k)\, y_{k-1} + \gamma_2(k)\, y_{k-2}$$

if $k = lT \rightarrow r_k = 0$ *(remove discontinuity singularity)*

$$e_k = r_k - \alpha\gamma_1(k)\, e_{k-1} - \alpha^2\gamma_2(k)\, e_{k-2}$$

Step 3 *Coefficients Update:*

$$\Theta_k = \left[r_{1,1}^{(k)}, \omega_{1,1}^{(k)} \ldots r_{1,2}^{(k)}, \omega_{1,2}^{(k)} \ldots r_{1,3}^{(k)} \ldots r_{1,4}^{(k)} \ldots\right]^T$$

$$Y_k = \left[y_k\, y_{k-1} \ldots y_{k-ML}\right]^T \qquad ML = L1 + L2 + L3 + L4$$

$$\Theta_{k+1} = \Theta_k - \mu Y_k e_k$$

Step 4 *Go to Step 1*

$M1$ is the number of pairs of complex conjugate poles inside unit disc;
$M2$ is the number of pairs of complex conjugate poles outside unit disc;
$M3$ is the number of pairs of real poles inside unit disc;
$M4$ is the number of pairs of real poles outside unit disc;
$M = max\{L1 + L2, L3 + L4\}$ is the length of the central tapped equalizer;
μ is the step size of the LMS algorithm.

The simulation results are listed in Tables 7.7-7.8 for equalization of Channel-1 and Channel-2

SNR	$a = 0.33$		$b = 2.0$		$MSE^{\dagger}$	H-Norm
	BIAS	*MSE*	*BIAS*	*MSE*		
50dB	3.7×10^{-5}	4.2×10^{-5}	9.0×10^{-3}	5.4×10^{-5}	3.2×10^{-5}	8.3×10^{-4}
40dB	3.5×10^{-4}	3.9×10^{-4}	2.2×10^{-3}	4.1×10^{-4}	3.9×10^{-4}	9.1×10^{-4}
30dB	6.5×10^{-3}	4.0×10^{-3}	7.1×10^{-2}	4.8×10^{-3}	3.2×10^{-3}	1.5×10^{-2}
20dB	9.4×10^{-3}	2.4×10^{-2}	4.2×10^{-1}	1.1×10^{-1}	4.2×10^{-2}	8.6×10^{-1}

Table 7.8: Performance of Blind Equalization of Channel-1 Using 64-QAM Signal

SNR	$\theta_1 = -1.5$		$\theta_2 = 0.8$		$MSE^{\dagger}$	H-Norm
	BIAS	*MSE*	*BIAS*	*MSE*		
50dB	1.2×10^{-5}	1.3×10^{-5}	1.0×10^{-5}	9.4×10^{-6}	3.2×10^{-5}	5.6×10^{-5}
40dB	8.3×10^{-5}	2.1×10^{-4}	2.1×10^{-5}	7.8×10^{-5}	3.9×10^{-4}	7.4×10^{-4}
30dB	9.1×10^{-4}	8.9×10^{-4}	4.3×10^{-4}	2.1×10^{-4}	3.2×10^{-3}	3.7×10^{-3}
20dB	1.2×10^{-3}	7.8×10^{-3}	2.2×10^{-4}	1.6×10^{-3}	4.2×10^{-2}	1.3×10^{-2}

Table 7.9: Performance of Blind Equalization of Channel-2 Using 64-QAM Signal

The above table also shows the Hankel norm for impulse response of the combined channel, which is evaluated by using the estimated coefficients of the inverse channel.

To illustrate the performance of blind equalization of QAM signals, convergence

characteristics of the equalizer is plotted in Fig.7.7. It is seen that the equalizer converges in about 20 symbols. Note that we use oversampled data, so our scheme belongs to the fractional blind equalization.

Fig.7.8 and Fig.7.10 show the unequalized QAM constellation diagram for Channels-1and 2, respectively. Fig.7.9 and Fig.7.11 show the blind equalization results.

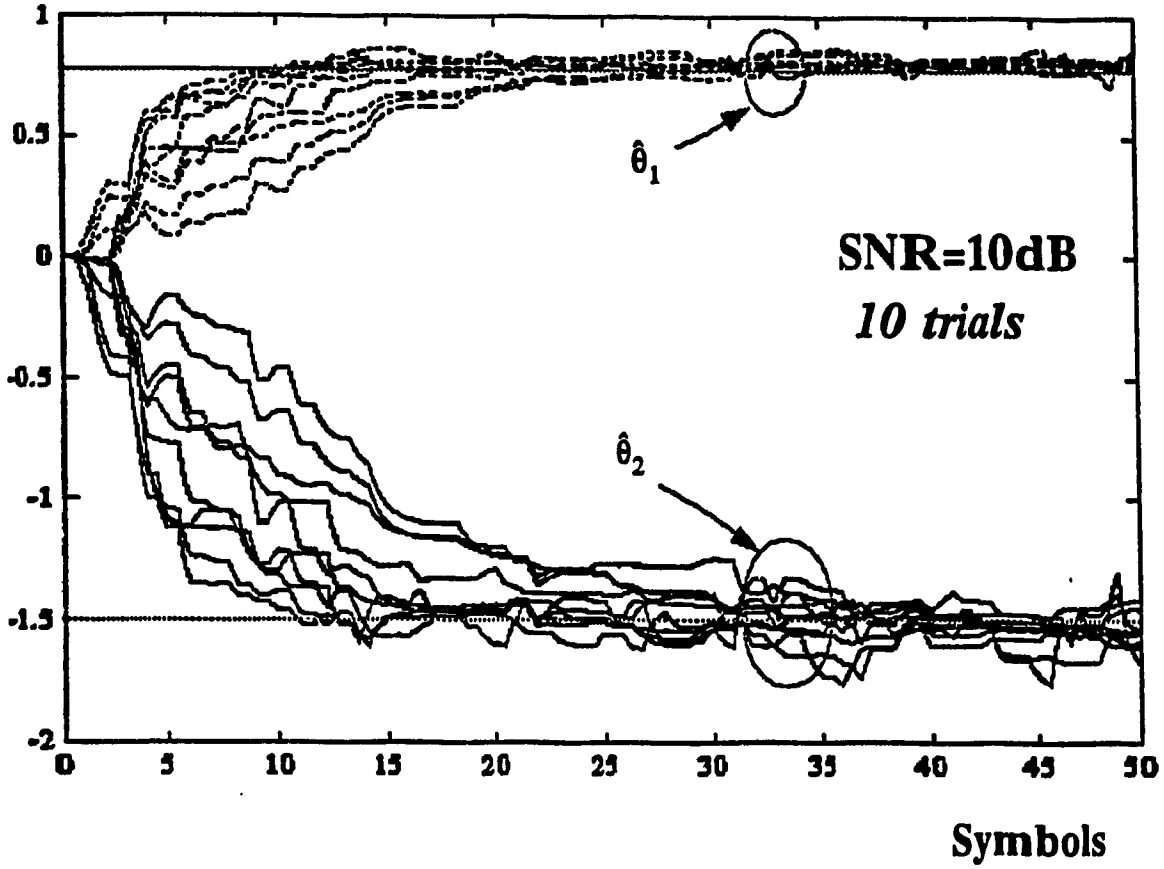

Fig. 7.7 Convergence Characteristic of Bind Equalizer

Example 5 ***Blind Equalization for BPSK Transmission of Images.***

AS a final example, we consider the use of blind equalization algorithm to combat the multipath problem of image transmission. Suppose the image is digitized and BPSK is used to transmit the signal in a multipath environment (channel-2). Fig.7.12 shows the received image, where the details of the text can not been recognized. Fig.7.13 presents the recovered image after the channel is equalized.

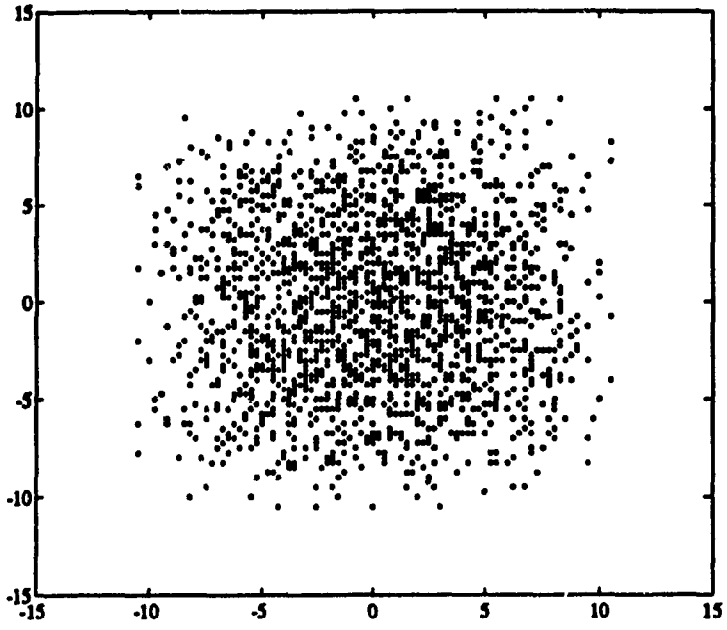

Fig. 7.8 The Output of Multipath Channel-1 of 64-QAM Signal

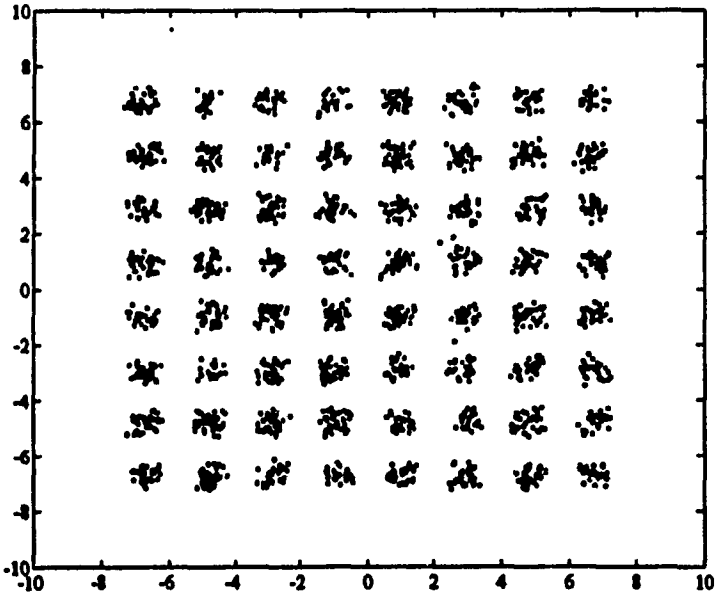

Fig. 7.9 The Equalized 64-QAM Signal for Multipath Channel-1

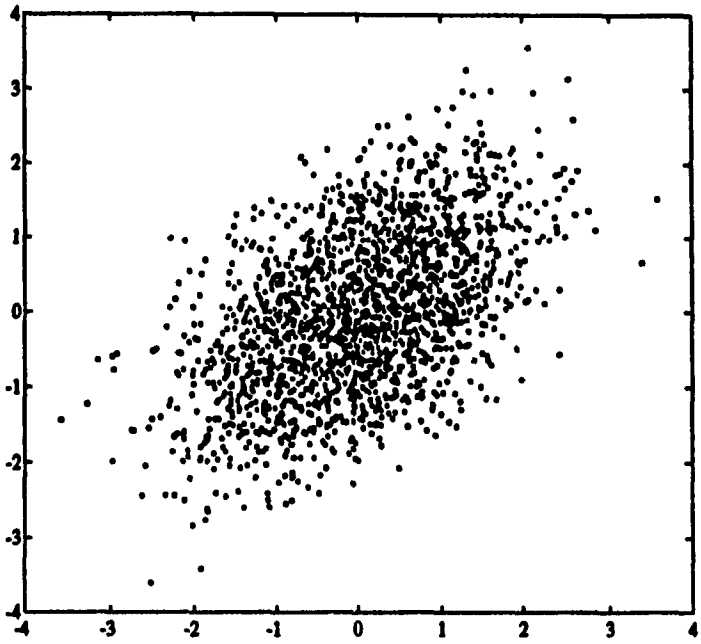

Fig. 7.10 The Output of Multipath Channel-2 of 64-QAM Signal

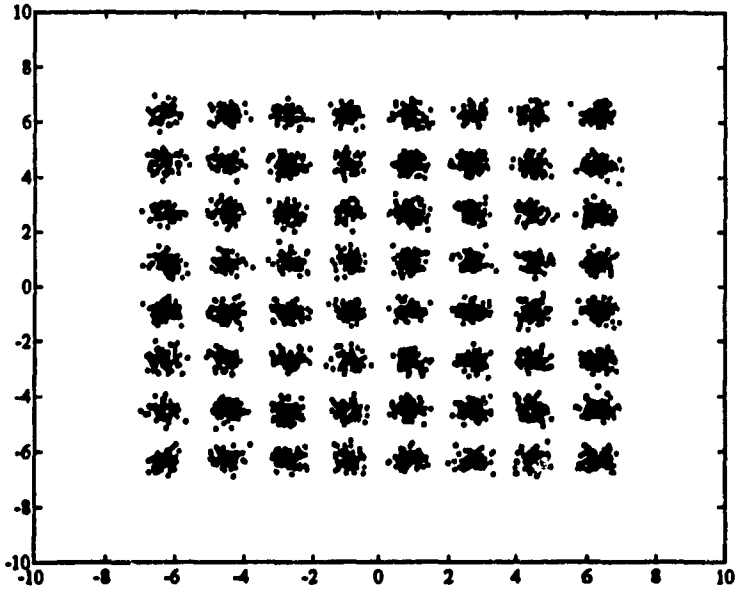

Fig. 7.11 The Equalized 64-QAM Signal for Multipath Channel-2

Fig. 7.12 Image Transmission via a Multipath Channel-1

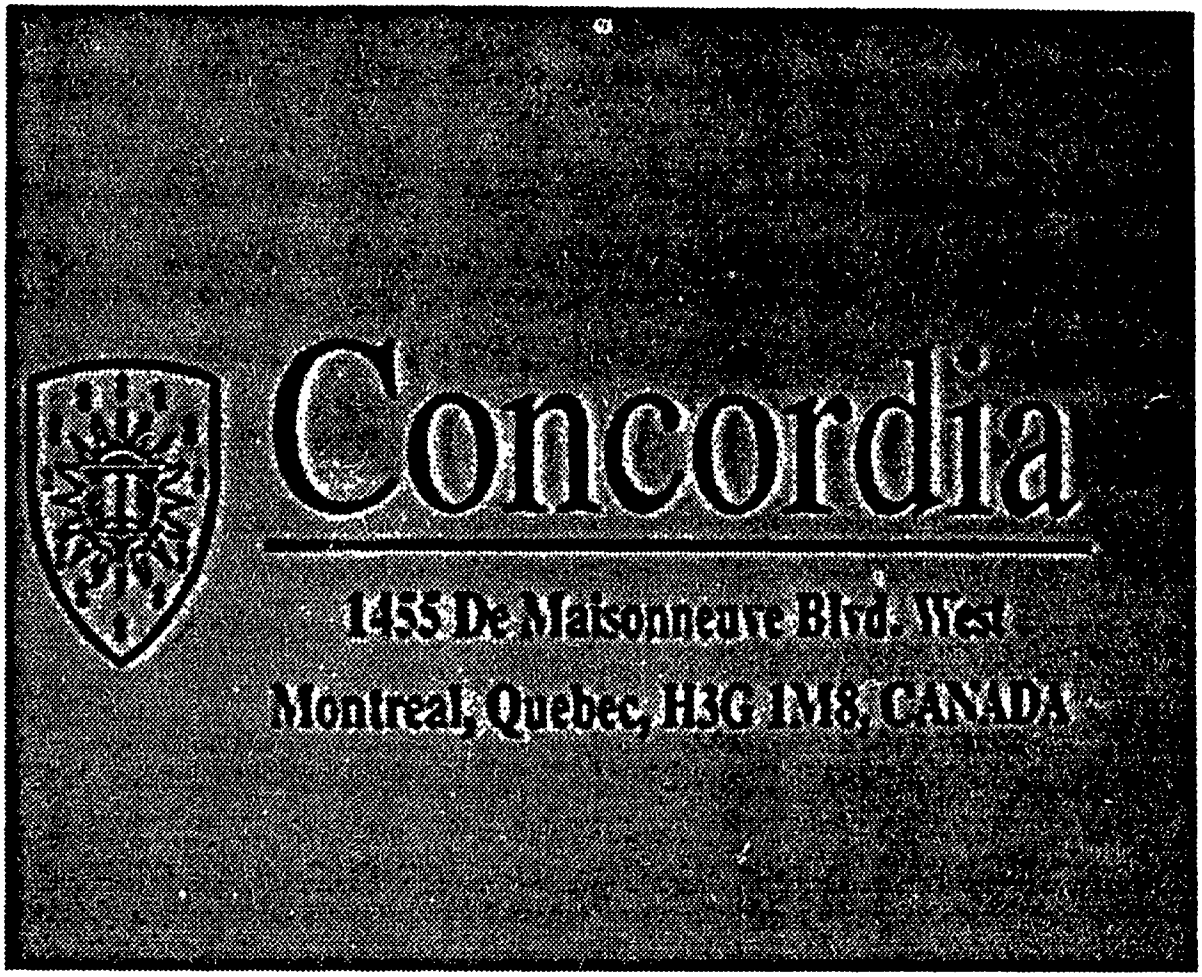

Fig. 7.13 Reconstructed Image

References

[7.1] A. V. Oppenheim and R. W. Schafer, "*Digital Signal Processing*", Prentice-Hall, Edlewood, N.J., 1975

[7.2] T. G. Stockham, T. M. Cannon and R. B. Ingeberstein, "Blind Deconvolution Through Digital Signal Processing", *Proceedings of IEEE*, Vol. 64, No.4, pp. 678-692, April, 1975

[7.3] A. Benvensite, M. Goursat and G. Ruget, "Robust Identification of a Non-minimum Phase System: Blind Adjustment of a Linear Equalizer in Data Communications", *IEEE Trans. on Automatic Control*, Vol. 25, pp. 385-399, June 1980

[7.4] J. R. Treichler and M. G. Agee, "A New Approach to Multipath Correction of Constant Modulus Signals", *IEEE Trans. ASSP*, Vol. 28, No. 8 pp. 349-472, 1982

[7.5] D. Hatzinakos and C. L. Nikias, "Blind Equalization Using a Tricepstrum Based Algorithm", IEEE Trans on Communications, Vol. 39, No. 5, pp. 669-681,May 1991

[7.6] C. R. Johnson Jr., "Admissibility in Blind Adaptive Channel Equalization", *IEEE Control Systems Magazine*, pp. 3-15, Jan. 1991

[7.7] Z. Ding, C. R. Johnson Jr. and R. A. Kennedy, "On the (Non) Existence of Undesirable Equilibria of the Godard Blind Equalizers", *IEEE Trans on Signal Processing* Vol.40, No.10, Oct. 1992

[7.8] A. P. Petropulu and C. L. Nikias, "Blind Deconvolution Using Signal Reconstruction from Partial Higher-Order Cepstrial Information", *Proceedings ICASSP91*, pp.1757-1760, May, 1991

Chapter 8

Cross-Coupled ASTV-ARMA Model and Separation of Superimposed Frequency Modulated Sinusoids

8.1. Introduction

In this chapter, the problem of separation of superimposed random frequency-modulated sinusoids (FMSs) is addressed. Such a superimposed signal may be considered as a set of broadband sources propagating through a memoryless additive channel. We propose a Cross-Coupled Almost-Symmetrical Time-Varying ARMA (CC-ASTV-ARMA or CC-AA) model to separate each individual source from the sum of the FMS signals whose power spectra may *completely overlap*. In practice, it is highly desirable to separate such kind of superimposed sources in a blind fashion. By blind separation, we mean the separation which is carried out using a signal received from only *one sensor*, without any other auxiliary inputs. Recently an attempt has been made for the separation of two FMSs by using a cross-coupled phase locked-loop technique (see [8.1] *loc. cit*). However, such a technique utilizes the assumption that the amplitudes of each spectrum-overlapping FMSs are *a priori* known, which makes it unrealistic in the context of blind signal separation. The other major category of methods based on an analysis of the time-frequency representation using the Wigner-Ville distribution [8.5]. Nevertheless, these methods can neither separate the superimposed FMSs in an *on-line* manner nor can they provide a high resolution of closely-spaced FMSs, due to the interfernce effects of the cross terms.

The advantage of the proposed CC-AA model is that one does not has to impose any assumption on the superimposed FMSs (SFMSs). The main idea is based on the fact

that any FMS, *regardless of its parameters*, satisfies a second order ASTV-ARMA model with time-varying coefficients, which depend only on the instantaneous phase of the FMS. An adaptive algorithm is used to estimate the instantaneous values of these *time-varying coefficients*; these coefficients are injected then into the second order ASTV-ARMA models in a cross-coupled manner. In this chapter, it is shown that the proposed special cross-coupled structure of the second-order ASTV-ARMA models possesses only one equilibrium state, which is globally stable and leads to a complete separation of the SFMSs. We also show that such an equilibrium state corresponds to the slowest variation of the ASTV-ARMA trajectory with minimum *Lipschitzian* constant. Finally, we show that the CC-AA model tends to converge to this particular equilibrium state and results in an unique separation of the SFMSs.

The condition for separability of the SFMS is described in terms of the crossing of the time-varying coefficients of the second-order ASTV-ARMA model. A trajectory monitoring is used to overcome any random switching between the separated FMSs at the output when a crossing of the trajecories occur.

8.2. Preliminaries

Let us consider a sum of M SFMSs with time-dependent frequencies

$$S(k) = \sum_{i=1}^{M} r_i(k) = \sum_{i=1}^{M} A_i \cos(\psi_i(k) + \phi_i) \qquad (8.2.1)$$

$$k \subset Z^+ \qquad \phi_i \in [0, \pi]$$

where A_i, ϕ_i are fixed value parameters, Z^+ denotes the positive integer set, while the phase $\psi_i(k)$ is associated with an instantaneous frequency $\dot{\psi}_i(k)$, such that

$$\psi_i(k) = \int_0^k \dot{\psi}_i(\tau)\, d\tau$$

An instantaneous frequency $\dot{\psi}_i(k)$ represents an information carried by the FMS from each source. In this chapter, we assume that $\dot{\psi}_i(k)$ are independent random processes for $\forall i \in \{1, 2, ..., M\}$, with *unknown distribution functions*. The

instantaneous frequency is always positive and satisfies the Nyquest sampling criterion, hence

$$0 < \psi_i(k) < \pi \tag{8.2.2}$$

We also assume that the *number M* of the FMSs is *a priori* known[1]. In what follows, we are interested in the case where the Fourier spectrum of each FMSs component $r_i(k)$ possesses the *same bandwidth* and hence the separation of the superimposed FMs can not be carried out by means of conventional time-invariant filters using the knowledge of their Fourier spectra.

It is known that an FMS $r_i(k) \in \Re$ satisfies the following second order time-varying MA model

$$r_i(k) + a_{i,1}(k)\, r_i(k-1) + a_{i,2}(k)\, r_i(k-2) = 0 \tag{8.2.3}$$

Explicit expressions for the coefficients $\{a_{i,1}(k), a_{i,2}(k)\}$ have been first found in [8.2]. By constructing an AR part which is symmetrically constrained to the MA part (8.2.3) with a symmetrical factor $\alpha \to 1^-$, we obtain a second-order ASTV-ARMA model for the FMS

$$\begin{aligned} & y(k) + \alpha a_{i,1}(k)\, y(k-1) + \alpha^2 a_{i,2}(k)\, y(k-2) \\ & \quad = x(k) + a_{i,1}(k)\, x(k-1) + a_{i,2}(k)\, x(k-2) \end{aligned} \tag{8.2.4}$$

As seen from (8.2.3), the signal $r_i(k) \in \Re$ is represented by the time-varying coefficients $\{a_{i,1}(k), a_{i,2}(k)\}$. Let us define $a_{i,1}[a_{i,2}(k)] \in \Re \times \Re$ as the *trajectory* of the second-order ASTV-ARMA model or the *trajectory* of the signal $r_i(k)$.

The solution of (8.2.3) may be represented in the form

$$y(k) = Q_i^{(a_1, a_2)}[x(k)]$$

where the operator $Q_i^{(a_1, a_2)}$ is as defined in Chapter 4.

Let us define the signal subspace which is spanned by the W-system associated with

1. The analysis in Section 8.5 indicates that this assumption can be eliminated.

(8.2.3) by

$$\Omega_i = \{r_i(k) = A_i\cos(\psi_i(k) + \phi_i) \,|\, A_i \in (0,\infty), \phi_i \in (0,\pi)\}$$

Therefore, the operator $Q_i^{(a_1, a_2)}$ has a null singularity within the subspace Ω_i and provides a transparent output to the signals which belong to the subspace $\bar{\Omega}_i$ (complementary to Ω_i) i.e.

$$\textbf{Prop-I } \textit{(Null Singularity)} \qquad \underset{x(k) \in \Omega_i}{Q_i^{(a_1, a_2)}}[x(k)] = 0 \tag{8.2.5}$$

$$\textbf{Prop-II } \textit{(Transparency)} \qquad \underset{x(k) \in \bar{\Omega}_i}{Q_i^{(a_1, a_2)}}[x(k)] = x(k) \tag{8.2.6}$$

where $\Omega_i \cap \bar{\Omega}_i = \varnothing$ and $\Omega_i \oplus \bar{\Omega}_i = I$. Hence we can see that $Q_i^{(a_1, a_2)}[\ \cdot\ ] \in I - \Omega_i$. Thus we have: (1)the ASTV-ARMA model is defined by the trajectory $a_{i,1}[a_{i,2}(k)]$, and (2) such an ASTV-ARMA model can be employed to separate the signal $r_i(k)$ having this particular trajectory. We will use these properties to design the CC-AA model to separate SFMSs.

8.3. System Description

A block diagram of the proposed CC-AA model is shown in Fig. 8.1. The CC-AA model consists of M parallel branches and a set of M adaptive second-order ASTV-ARMA models. Each branch contains *(M-1)* second-order ASTV-ARMA models in *cascade* connection. Suppose that in a certain branch all these *(M-1)* ASTV-ARMA models are properly tuned to cancel *(M-1)* FMSs, then only one FMS passes through transparently at the output of this branch. In this way, at the output of the different M branches, one can have M separated FMSs components. At the output of each branch, an adaptive ASTV-ARMA model is used to track the branch output in such a manner that the energy of the residual output of the adaptive second-order ASTV-ARMA model is minimized. The purpose of using an adaptive ASTV-ARMA model at each branch is to estimate the time-varying coefficients which are needed to control and accurately tune the ASTV-ARMAs. By injecting these estimated time-varying

coefficients to the ASTV-ARMA models in the various branches of the cross-coupled structure, the system becomes a closed one.

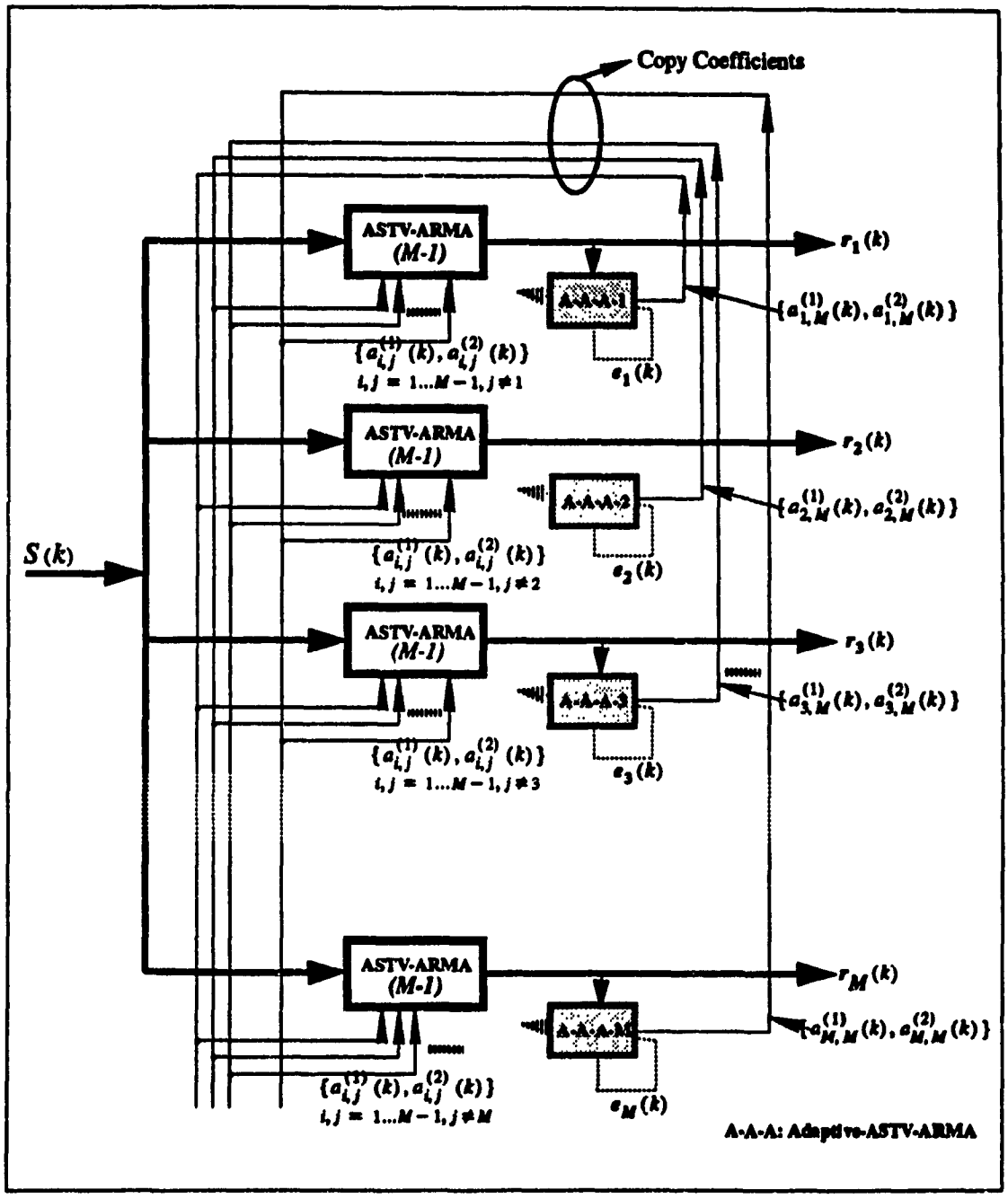

Fig. 8.1 Cross-Coupled ASTV-ARMA Model

Without lost of generality, the cross-coupled nature of the proposed system may be

easily demonstrated by considering the case of the separation of two SFMSs as shown in Fig.8.2, where

$$S(k) = r_1(k) + r_2(k) \tag{8.3.1}$$

The outputs of the cross-coupled ASTV-ARMA models can be described by

$$\begin{aligned} y_i(k) = {} & S(k) + a_{i,1}(k) S(k-1) + a_{i,2}(k) S(k-2) \\ & -\alpha a_{i,1}(k) y_i(k-1) - \alpha^2 a_{i,2}(k) y_i(k-2) \end{aligned} \tag{8.3.2}$$

while those of the Adaptive ASTV-ARMA models by:

$$\begin{aligned} e_i(k) = {} & y_i(k) + a_{i,1}^{\dagger}(k) y_i(k-1) + a_{i,2}^{\dagger}(k) y_i(k-2) \\ & -\alpha a_{i,1}^{\dagger}(k) e_i(k-1) - \alpha^2 a_{i,2}^{\dagger}(k) e_i(k-2) \end{aligned} \tag{8.3.3}$$

where $i = 1, 2$.

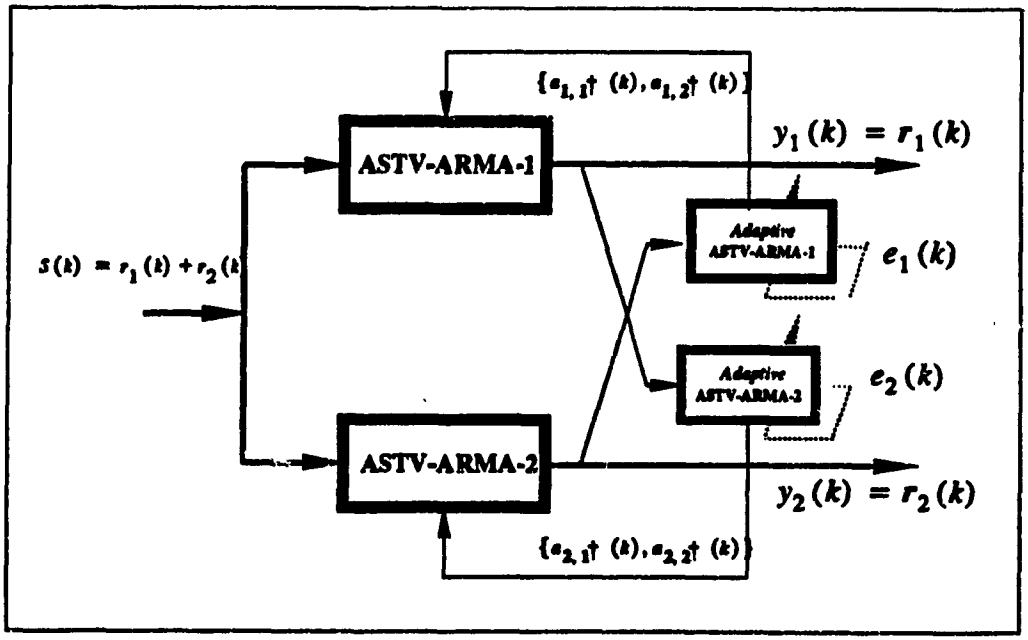

Fig. 8.2 A Basic CC-ASTV-ARMA Model

The time-varying coefficients $a_{i,1}^{\dagger}\,[a_{i,2}^{\dagger}(k)]$ are adjusted using the Gauss-Newton algorithm (see Table 6.2) and copied to the cross-coupled ASTV-ARMA model:

$$a_{i,1}(k) = a_{i,1}^{\dagger}(k) \quad ; \quad a_{i,2}(k) = a_{i,2}^{\dagger}(k)$$

Suppose that the system reaches its steady state, then the residual outputs of the adaptive ASTV-ARMA-1,2 will be zero[1], *iff* the following null singularity conditions are satisfied

$$r_1(k) + a_{2,1}^{\dagger}(k) r_1(k-1) + a_{2,2}^{\dagger}(k) r_1(k-2) = 0$$

$$r_2(k) + a_{1,1}^{\dagger}(k) r_2(k-1) + a_{1,2}^{\dagger}(k) r_2(k-2) = 0$$

Then the output for ASTV-ARMA-1 is

$$y_1(k) = r_1(k)$$

and for ASTV-ARMA-2

$$y_2(k) = r_2(k)$$

This results in a desired separation of the two superimposed FMSs mixture $S(k)$. In what follows we will prove the CC-AA model converges to a desired separation of the superimposed FMSs and show that such a separation result is a unique one.

8.4. SFMS Separability and Equilibria of CC-AA Model

Since the proposed CC-AA model is a *linear* time-varying one which obeys null singularity and transparency propositions (8.2.4),(8.2.5), the output of the second order ASTV-ARMA model in each branch should be a linear combination of the components of the FMSs:

$$y_{i,M-1}(k) = \sum_{j=1}^{M} \xi_{i,j} A_j \cos(\psi_j(k) + \phi_j) \tag{8.4.1}$$

where $\xi_{i,j} \in (0,1)$, and $y_{i,j}(k)$ denotes the output of *jth ASTV*-ARMA cascaded

1. Throughout this chapter, we assume that the Gauss-Newton algorithm can sustain a sufficient tracking capability to minimize the residual output energy.

connecting the ASTV-ARMA model in the *ith* branch. Then we have the following lemma.

Lemma 8.4.1 *The output of the CC-AA model satisfies the following condition.*

$$\sum_{i=1}^{M} \xi_{i,j} = 1 \tag{8.4.2}$$

Proof: Let us first prove the result for the simplest model for CC-AA shown in Fig.8.2. Consider branch 1 where ASTV-ARMA-1 is controlled by the Adaptive ASTV-ARMA-1 of branch 2. Let the output of ASTV-ARMA-1 be wirrten as

$$y_1(k) = \xi_{1,1} A_1 \cos(\psi_1(k) + \phi_1) + \xi_{1,2} A_2 \cos(\psi_2(k) + \phi_2) \tag{8.4.3}$$

Suppose Adaptive ASTV-ARMA-2 can track this output perfectly, and the trajectory of Adaptive ASTV-ARMA-2 $a_{2,1}[a_{2,2}(k)]$ is injected into ASTV-ARMA-2, and ASTV-ARMA-2 is controlled by the Adaptive ASTV-ARMA-2. Then the output of ASTV-ARMA-2 can be expressed as

$$y_2(k) = S(k) - \xi_{1,1} A_1 \cos(\psi_1(k) + \phi_1) - \xi_{1,2} A_2 \cos(\psi_2(k) + \phi_2) \tag{8.4.4}$$

On the other hand, by definition (8.4.1), the output of ASTV-ARMA-2 can be written as

$$y_2(k) = \xi_{2,1} A_1 \cos(\psi_1(k) + \phi_1) + \xi_{2,2} A_2 \cos(\psi_2(k) + \phi_2) \tag{8.4.5}$$

By comparing (8.4.4) and (8.4.5), it is easy to see

$$\xi_{1,1} + \xi_{2,1} = 1 \quad \text{and} \quad \xi_{1,2} + \xi_{2,2} = 1 \tag{8.4.6}$$

Similarly, using the general models given in Fig.8.1, and using induction, (8.4.2) can be established.

Q.E.D.

Lemma 8.4.1. indicates that if an Adaptive-ASTV-ARMA model can completely cancel the output of each branch of CC-AA, i.e. the Gauss-Newton algorithm has sufficient track capability, the FMS component $A_k \cos(\psi_k(k) + \phi_k)$ appeares at the

output of *pth* branch as $\xi_{p,k}A_k\cos(\psi_k(k)+\phi_k)$, but the total energy of such an FMS component at the outputs of all branches remains the same as the input.

Definition 8.4.1 Let us introduce the notion of a *separation ratio* w.r.t. the FMS component $r_p(k)$ for the output of *the CC-AA* model at branch p *as*

$$\rho_{p,l} = \frac{\xi_{p,l}A_l}{\xi_{p,p}A_p} \geq 0, \qquad p, l = 1, 2, \ldots, M$$

If the SFMSs are ideally separated, i.e. $y_{p,M-1}(k) = r_p(k)$, we have $\xi_{i,j} = \delta_{i,j}$ where $\delta_{i,j}$ is the Kronecker delta and thus

$$\rho_{p,j} = \delta_{p,j} \tag{8.4.7}$$

From Lemma 8.4.1, it follows that (8.4.7) is a particular case of condition (8.4.2). Condition (8.4.7) for complete separation also indicates that the separation is unique up to the permutation of the branch index p.

Denote

$$\Delta_{i,j}(k,l,m) = \sin(\psi_i(k-l) - \psi_j(k-m))$$

$$\Delta_p^{\Sigma}(k,l,m) = \sum_{i=1,j=1}^{M} \rho_{i,p}\rho_{j,p}\Delta_{i,j}(k,l,m)$$

where $\Delta_{p,p}(k,1,2)$ is the *normalized Wronskian* of the FMS $r_p(k)$, and $\Delta_p^{\Sigma}(k,1,2)$ is the *normalized composite Wronskian* of the output in branch p with respect to the FMS component $r_p(k)$. With the above notations, we may state the following theorem for the equilibria of the CC-AA model.

Theorem 8.4.1 *(Equilibria) For the output of branch p, the trajectory* $a_{p,1}[a_{p,2}(k)]$ *has the following equilibrium states*

$$a_{p,1}(k) = -\frac{\Delta_p^{\Sigma}(k,0,2)}{\Delta_p^{\Sigma}(k,1,2)} \qquad a_{p,2}(k) = \frac{\Delta_p^{\Sigma}(k,0,1)}{\Delta_p^{\Sigma}(k,1,2)} \tag{8.4.8}$$

Proof: Let us find the time-varying coefficients for the MA model (8.2.3) with input

$$x(k) = \sum_{i=1}^{M} \xi_{p,i} A_i \cos(\psi_i(k) + \phi_i)$$

The augmented Wronskian may be written as

$$\begin{vmatrix} \sum_{i=1}^{M} \xi_{p,i} A_i \cos(\psi_i(k) + \phi_i) & \sum_{i=1}^{M} \xi_{p,i} A_i \sin(\psi_i(k) + \phi_i) & x(k) \\ \sum_{i=1}^{M} \xi_{p,i} A_i \cos(\psi_i(k-1) + \phi_i) & \sum_{i=1}^{M} \xi_{p,i} A_i \sin(\psi_i(k-1) + \phi_i) & x(k-1) \\ \sum_{i=1}^{M} \xi_{p,i} A_i \cos(\psi_i(k-2) + \phi_i) & \sum_{i=1}^{M} \xi_{p,i} A_i \sin(\psi_i(k-2) + \phi_i) & x(k-2) \end{vmatrix} = 0$$

By Laplace expansion, after some manipulations, we have

$$a_{p,1}(k) = -\frac{\sum_{i,j=1}^{M} \rho_{i,p}\rho_{j,p}\Delta_{i,j}(k,0,2)}{\sum_{i,j=1}^{M} \rho_{i,p}\rho_{j,p}\Delta_{i,j}(k,1,2)} \qquad a_{p,2}(k) = \frac{\sum_{i,j=1}^{M} \rho_{i,p}\rho_{j,p}\Delta_{i,j}(k,0,1)}{\sum_{i,j=1}^{M} \rho_{i,p}\rho_{j,p}\Delta_{i,j}(k,1,2)}$$

This completes the proof.

Q.E.D.

The trajectory $a_{p,1}[a_{p,2}(k)]$ given in (8.4.8) is in fact the trajectory of all possible outputs given by (8.4.1); such trajectories preserve the property (8.4.2) of Lemma 8.4.1.

Corollary 8.4.1 *The condition for the complete separation of superimposed FMSs is that the trajectory* $a_{p,1}^{*}[a_{p,2}^{*}(k)]$ *is given by*

$$a_{p,1}^{*}(k) = -\frac{\Delta_{p,p}(k,0,2)}{\Delta_{p,p}(k,1,2)} \qquad a_{p,2}^{*}(k) = \frac{\Delta_{p,p}(k,0,1)}{\Delta_{p,p}(k,1,2)} \tag{8.4.9}$$

We will call such a trajectory as the complete separation trajectory (CST)

Proof: It is a direct consequence of the substitution of the complete separation

condition (8.4.7) into (8.4.8).

Q.E.D.

It can be seen from (8.4.7) along with the definition of $\Delta_p^{\Sigma}(k, 1, 2)$ that the equilibria of the CC-AA model are dependent on the separation ratio ρ. The different equilibrium states will provide different separation results. However, there exists only one equilibrium state $a_{p,1}^{*}[a_{p,2}^{*}(k)]$ which results in a *unique* and *complete* separation.

In Theorem 8.4.1, the trajectories of the equilibria of the CC-AA model are expressed in terms of the various combinations of the second order Wronskians. It allows us to study these equilibria states based on the basic properties of a Wronskian. Corollary 8.4.1. explicitly shows that the CST should be constructed by the Wronskian of only one FMS component.

Theorem 8.4.2. *(Stability) The equilibrium state* $a_{p,1}^{*}[a_{p,2}^{*}(k)]$ *given in (8.4.8), (8.4.9) is globally BIBO stable.*

Proof: Since the trajectory $a_{p,1}^{*}[a_{p,2}^{*}(k)]$ is constructed solely using the Wronskian of one FMS component $r_p(k)$, therefore by a direct extension of Lemma 6.4.2, we may conclude that the equilibrium state given in (8.4.9) is globally BIBO stable.

Q.E.D.

In what follows, we investigate the variation properties of the trajectory to show that the CC-AA model will always converge to the complete separation equilibrium state.

8.5. Variation Properties of SFMS Trajectory

In this section, we study the variation properties of the trajectory $a_{p,1}[a_{p,2}(k)]$ from the point of view of continuity of functions, especially the *uniform boundness*. Such an uniform boundness may be described in terms of the Lipschitzian constant. It is interesting to show that the complete separation trajectory possesses a minimum

Lipschitzian constant. This property is used to prove the convergence of the CC-AA to separate the SFMSs.

It should be noted that the Wronskain of the CST (8.4.9) is always positive, i.e. $0<\Delta_{p,p}(k,1,2)<1$; such a condition is satisfied independent of the frequency variations of $r_p(k)$. Therefore the trajectory $a_{p,1}^{*}[a_{p,2}^{*}(k)]$ is bounded, within a certain admissible region as show in Chapter 5. In what follows, we are going to show that the trajectory of the other equilibrium states, namely, $a_{p,1}[a_{p,2}(k)]$ may not necessarily be bounded. Since $\Delta_p^{\Sigma}(k,1,2)$ may not be positive $\forall k \in Z^{+}$, it is possible that at a certain time instant $k \in G$, $G \subset Z^{+}$, the Wronskian $\Delta_p^{\Sigma}(k,1,2)$ could changes its sign, and the zero-crossing of $\Delta_p^{\Sigma}(k,1,2)$ result in an unbounded trajectory.

Lemma 8.5.1 *The composite Wronskian* $\Delta_p^{\Sigma}(k,1,2)$ *is not strictly positive*

Proof: By the definition of $\Delta_p^{\Sigma}(k,1,2)$, it is a linear combination of M 2nd-order Wronskians; therefore, the determinat $\Delta_p^{\Sigma}(k,1,2)$ is not necessarily a Wronskian of the W-system associated with a 2nd-order homogeneus equation. Thus the positiveness of such a determinant is not guarrenteed.

Q.E.D.

Remark 8.5.1 Since we assume that the frequency modulation is a random function with an *arbitrary* distribution, the Wronskain is time-varying too. In addition, the composite Wronskian $\Delta_p^{\Sigma}(k,1,2)$ may vanish for a certain time instant $k \in G$. Thus the unboundedness of the trajectory $a_{p,1}[a_{p,2}(k)]$ is only local. Although the trajectory $a_{p,1}[a_{p,2}(k)]$ has local discontinuity singularity $\forall k \in G$, we may still argue that $\forall k \in \tilde{G}$ such that $G \cap \tilde{G} = \emptyset$; such a trajectory may be locally bounded.

Let us define a norm for the *variation rate* of the trajectory of ASTV-ARMA model by

$$\|\partial A_p(k)\|_{\infty} = max\{|a_{p,1}(k)-a_{p,1}(k-1)|, |a_{p,2}(k)-a_{p,2}(k-1)|\}$$

Following [8.7], we say a trajectory is totally stable, i.e. $\forall k, l \in Z^{+}$

$$\| a_{p,1}[a_{p,2}(k)] - a_{p,1}[a_{p,2}(k-l)] \|_\infty$$
$$= \| a_{p,1}[a_{p,2}(k)] - a_{p,1}[a_{p,2}(k-1)] \|_\infty \le L \tag{8.5.1}$$

where L also called the *Lipschitzian* constant. If (8.5.1) is true only for $\exists k, l \in \tilde{G}$, $\tilde{G} \subset Z^+$, then $a_{p,1}[a_{p,2}(k)]$ is only practical stable.

Theorem 8.5.1 *(Trajectory Bound) The complete separation trajectory $a_{p,1}^*[a_{p,2}^*(k)]$ given by (8.4.9) is strictly Lipschitzian and totally stable, while all the other non-complete separation trajectories $a_{p,1}[a_{p,2}(k)]$ given by (8.4.8) are locally Lipschitzian and only practical stable.*

Proof: For the CST,

$$|\partial a_{p,1}^*(k)| = |a_{p,1}(k) - a_{p,1}(k-1)|$$
$$= \left| \frac{\Delta_{p,1}(k,0,2)}{\Delta_{p,1}(k,1,2)} - \frac{\Delta_{p,1}(k-1,0,2)}{\Delta_{p,1}(k-1,1,2)} \right|$$
$$\le \left| \frac{\Delta_{p,1}(k,0,2)}{\Delta_{p,1}(k,1,2)} \right| + \left| \frac{\Delta_{p,1}(k-1,0,2)}{\Delta_{p,1}(k-1,1,2)} \right| \le 2\frac{\varepsilon_{max}}{\varepsilon_{min}}$$

Similarly, we have

$$|\partial a_{p,2}^*(k)| \le 2\frac{\varepsilon_{max}}{\varepsilon_{min}}$$

Hence,

$$\| \partial A_p^*(k) \|_\infty = 2\frac{\varepsilon_{max}}{\varepsilon_{min}} \qquad \forall k \in Z^+ \tag{8.5.2}$$

This proves the first statement; also (8.5.2) implies that the CST is *Lipschitzian* continuous.

Now let us evaluate the *Lipschitzian* constant of trajectory $a_{p,1}[a_{p,2}(k)]$ corresponding to the other equilibrium states. From (8.4.8)

$$|a_{p,1}(k)| = \left| \frac{\Delta_p^{\Sigma}(k,0,2)}{\Delta_p^{\Sigma}(k,1,2)} \right| \tag{8.5.3}$$

$\forall k \in \tilde{G}$. We consider the best case for the boundness of trajectory $a_{p,1}[a_{p,2}(k)]$, assuming $\Delta_{i,j}(k,1,2) \geq 0$ in the denominator of (8.5.3); thus

$$|a_{p,1}(k)| = \left| \frac{\sum_{i=1,j=1}^{M} \rho_{i,p}\rho_{j,p}\Delta_{i,j}(k,0,2)}{\sum_{i=1,j=1}^{M} \rho_{i,p}\rho_{j,p}\Delta_{i,j}(k,1,2)} \right| \leq \frac{\sum_{i=1,j=1}^{M} \rho_{i,p}\rho_{j,p}|\Delta_{i,j}(k,0,2)|}{\sum_{i=1,j=1}^{M} \rho_{i,p}\rho_{j,p}\Delta_{i,j}(k,1,2)}$$

Using Holder inequality, for $r>0, s>0$, and $\frac{1}{r}+\frac{1}{s}=1$

$$|a_{p,1}(k)| \leq \frac{sup\left\{ \left(\sum_{i=1,j=1}^{M} \rho_{i,p}^2\rho_{j,p}^2 \right)^{1/r} \left(\sum_{i=1,j=1}^{M} \Delta_{i,j}^2(k,0,2) \right)^{1/s} \right\}}{inf\left\{ \left(\sum_{i=1,j=1}^{M} \rho_{i,p}^2\rho_{j,p}^2 \right)^{1/r} \left(\sum_{i=1,j=1}^{M} \Delta_{i,j}^2(k,1,2) \right)^{1/s} \right\}}$$

$$\leq \frac{\varepsilon_{max}}{\varepsilon_{min}} \left(1 + \frac{M-1}{2\varepsilon_{max}^2} \right)^{1/s}$$

Therefore

$$\| \partial A_p(k) \|_{\infty} = \frac{\varepsilon_{max}}{\varepsilon_{min}} \left(1 + \frac{M-1}{2\varepsilon_{max}^2} \right)^{1/s} \tag{8.5.4}$$

Q.E.D.

Based on (8.5.2), we see that the complete separation trajectory possesses a nice *global Lipschitzian* property.This is a key property in establishing the existence of a blind separability of SFMSs using CC-AA, since all the other non-complete separation trajectories are only locally *Lipschitzian*, and may contain unbounded singularities.

Corollary 8.5.1 *The complete separation trajectory (CST) possesses the*

minimum variation rate.

Proof: From (8.5.10) and (8.5.12)

$$inf\frac{\|\partial A_p(k)\|_\infty}{\|\partial A_p^*(k)\|_\infty} = inf\left(1+\frac{M-1}{2\varepsilon^2_{max}}\right)^{1/s} = \left(\frac{3}{2}\right)^{1/s} > 1 \ , \quad s>1$$

Q.E.D.

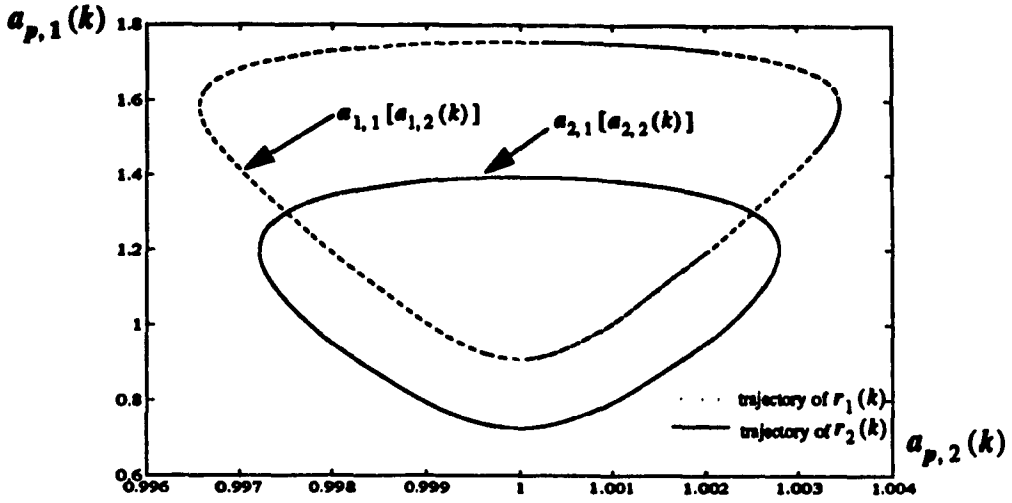

Fig. 8.3 Complete Separation Trajectories for two SFMSs

Corollary 8.5.1 presents a very interesting property for the trajectory $a_{p,1}[a_{p,2}(k)]$. It shows that the CST has a minimum *Lipschtzian* constant, and thus a minimum variation rate bound. This means that such a trajectory is the smoothest one among all possible trajectories, and any other trajectory which results in a non-complete separation of the SFMs, will have a larger variation rate.[1]

Corollary 8.5.1 also establishes a relationship between the equilibria of the CC-AA and the variation rates of the corresponding trajectories. Let us recall that CC-AA is driven by a set of adaptive ASTV-ARMA models. Thus the kind of trajectory the adaptive algorithm tracks, determines the equilibrium state that the system will converge to. In what follows, we will show that the Gauss-Newton algorithm tends to

1. In the light of this results, the assumption on the number of source M is *a priori* known may be relaced by the number of the source is unknown but the CC-AA branch number must be larger than M.

"choose" the trajectory with minimum *Lipschitzian* constant (the most smooth trajectory).

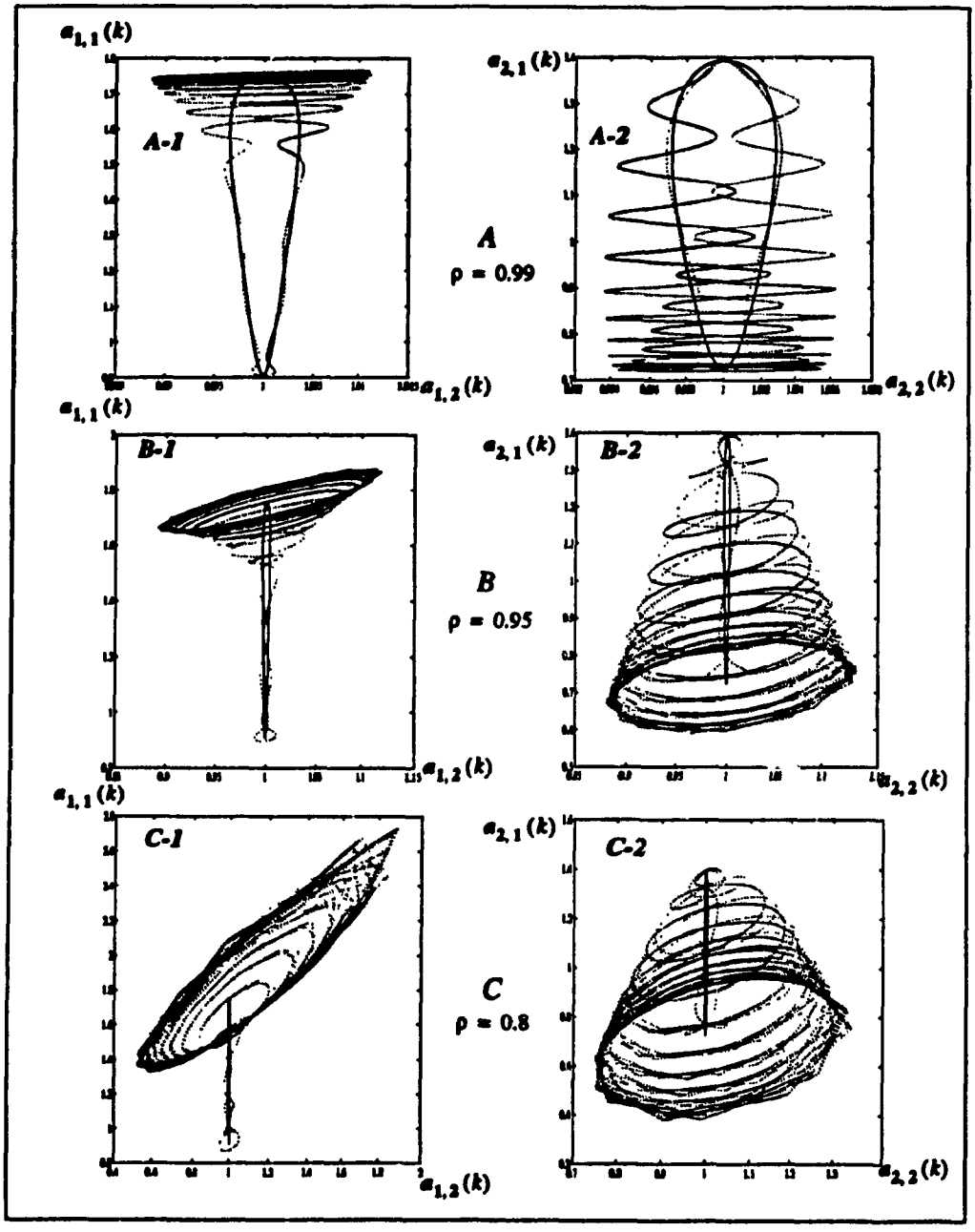

Fig. 8.4 Trajectory Variation vs. Separation Ratio ρ (bold lines represent the CST)

In Fig.8.3 and Fig.8.4, we present an illustrative example to show the trajectory

variations in accordance with Corollary 8.5.1.

In this example, two SFMSs $r_1(k)$ and $r_2(k)$ are considered; the trajectories of these two FMSs are shown in Fig.8.3, which also represent the CST of these two FMSs. If the separation is not complete, i.e. the separation ratio ρ is not equal to unity, the corresponding trajectories of these non-complete separation outputs are shown in Fig.8.4. It can be seen that as ρ decreases the trajectory become more rapidly varying and the path of the trajectories become less smooth and more complicated.

We have thus shown that among the equilibria of the CC-AA, the complete separation equilibrium is globally stable and possesses a trajectory with minimum variation rate. Now we are going to show that the CC-AA model will converge to and track such a trajectory.

8.6. Convergence and Tracking Properties of CC-AA

The Gauss-Newton algorithm used for Adaptive ASTV-ARMA model to track the output of each branch of the CC-AA is listed in Table 6.1. For convenience of analysis, we re-write the adaptive algorithm in the following recursive form [8.7] [8.8].

$$\tilde{a}(k+1) = \tilde{a}(k) + K(k)\,[y_M(k) - \Psi^T(k)\tilde{a}(k)]$$

$$K(k) = \frac{P(k)\Psi(k)\Psi^T(k)}{\gamma + \Psi^T(k)P(k)\Psi(k)}$$

$$P(k+1) = \frac{1}{\gamma}\left[P(k) - \frac{P(k)\Psi(k)\Psi^T(k)P(k)}{\gamma + \Psi^T(k)P(k)\Psi^T(k)}\right] \qquad (8.6.1)$$

where the gradient is given by

$$\Psi(k) = \left[y_M(k) - \alpha e(k),\ \ y_M(k-1) - \alpha^2 e(k-1)\right]^T ,$$

the estimate trajectory $\tilde{a}_{p,1}[\tilde{a}_{p,2}(k)]$ is denoted as a vector; $\tilde{a}(k) = \left[\tilde{a}_1(k)\ \tilde{a}_2(k)\right]^T$ the tracking error is denoted as a vector $\bar{a}(k) = \left[a_1(k) - \tilde{a}_1(k) \quad a_2(k) - \tilde{a}_2(k)\right]^T$; $\gamma = 1 - \mu$ is the forgetting factor,

and μ is the step size or the so called speed of adaptation. From (8.6.1), we can derive the expression for the tracking error as follows:

$$\begin{aligned} \bar{a}(k+1) &= G(k)\bar{a}(k) + z(k+1) \\ G(k) &= I - K(k)\Psi^T(k) \\ z(k+1) &= -K(k)w(k) + \partial A(k+1) \end{aligned} \tag{8.6.2}$$

where $w(k)$ is an additive input noise, and the trajectory variation rate is denoted as

$$\partial A(k) = \left[a_1(k) - a_1(k-1) \quad a_2(k) - a_2(k-1)\right]^T$$

Now we establish a relationship between the tracking error $\bar{a}(k)$ and the *Lipschitzian* constant of the trajectory which the adaptive algorithm is tracking to. We state the results in the following theorem. In the following derivations the matrix norms are defined as $\|A\|_2 = (\sigma_{max}(AA^T))^{1/2}$ and $\|A\|_\infty = max(a_{ij})$

Theorem 8.6.1 *(Tracking Error Bound) The tracking error of the Gauss-Newton algorithm is bounded by the Lipschitzian constant of the true trajectory.*

$$\lim_{k\to\infty} \|\bar{a}(k)\|_2^2 \le E[\|w(k)\|_2^2 + \|\partial A(k)\|_\infty^2]^{1/2} \tag{8.6.3}$$

Proof: The proof is lengthy, the details are provided in Appendix 8.1-4. A sketch of the proof is presented as follows

First, let us denote a Lyapunov function for the tracking error as

$$V(k) = \bar{a}^T(k)P^{-1}(k)\bar{a}(k) \tag{8.6.4}$$

Hence the mathematical expectation of the Euclidean norm of tracking error can be written as

$$\begin{aligned} E\{\|\bar{a}(k)\|_2^2\} &\le E\{\|P^{-1/2}(k)\|_2^2 \|P^{-1/2}(k)\bar{a}(k)\|_2^2\} \\ &\le E\{\|P(k)\|_2^8\}^{1/8} E\{V^{8/7}(k)\}^{7/8} \end{aligned} \tag{8.6.5}$$

It is shown in Appendix 8.1

$$sup E\{\|P(k)\|_2^8\} = C_o < \infty \tag{8.6.6}$$

By definition (8.6.1), and (8.6.2) (8.6.5), we have the expansion

$$\begin{aligned} V(k+1) &= \bar{a}^T(k)\, G^T(k)\, P^{-1}(k+1)\, G(k)\, \bar{a}(k) \\ &\quad + 2z^T(k+1)\, P^{-1}(k+1)\, G(k)\, \bar{a}^T(k) \\ &\quad + z^T(k+1)\, P^{-1}(k+1)\, z(k+1) \end{aligned} \tag{8.6.7}$$

For the first term in (8.6.8), we have (see Appendix 8.2)

$$G^T(k)\, P^{-1}(k+1)\, G(k) \le \left[1 - \frac{1}{1+\gamma \| P(k) \|_2^2}\right] P^{-1}(k) \tag{8.6.8}$$

Using (8.6.5), we can show $V(k) > \bar{a}^T(k)\, G^T(k)\, P^{-1}(k+1)\, G(k)\, \bar{a}(k)$. Hence the Lyapunov function may be written as

$$\begin{aligned} V(k+1) \le & \left(1 - \frac{1}{2(1+\gamma \| P(k+1) \|_2^2)}\right) V(k) \\ & + z^T(k+1)\, P^{-1}(k+1)\, z(k+1)\ (3 + 2\gamma \| P(k+1) \|_2^2) \end{aligned} \tag{8.6.9}$$

From Appendix 8.3,

$$2 \left| z^T(k+1)\, P^{-1}(k+1)\, z(k+1) \right| \le C_1 (\| w(k) \|_2^2 + \| \partial A(k+1) \|_2^2) \tag{8.6.10}$$

where $C_1 < \infty$.

By invoking the constant variation method of the theory of difference equation [8.7], we may denote a transition function as

$$\Phi(k+1, n) = \left(1 - \frac{1}{2(1+\gamma \| P(n+1) \|_2^2)}\right) \Phi(k, n) \tag{8.6.11}$$

and rewrite the Lyapunov function as

$$V(k+1) \le \Phi(k, 0)\, V(0) + C_2 \sum_{n=1}^{k-1} \Phi(k, n)\ (\| w(k) \|_2^2 + \| \partial A(k+1) \|_2^2) \tag{8.6.12}$$

where $C_2 < \infty$. Using Minkovski inequality it is found that

$$[E\{V^{8/7}(k)\}]^{7/8} \le [(E\{\Phi(k,0)\,V(0)\})^{8/7}]^{7/8} \tag{8.6.13}$$
$$+C_2\sum_{n=1}^{k-1}\left[(E\{\Phi(k,n)\,(\|w(k)\|_2^2+\|\partial A(k+1)\|_2^2)\})^{8/7}\right]^{7/8}$$

By using Appendix 8.4, we have

$$E\{\Phi(k+1,n)\} \le C_3\varsigma^{k-n+1} \quad \text{where} \quad \varsigma\in(0,1) \quad k-n>0 \quad C_3<\infty \tag{8.6.14}$$

We see that $\Phi(k,n)<1$. The first term of (8.6.12) decreases as $n\to\infty$. For the second term

$$\begin{aligned} &E\{[\Phi(k,n)\,(\|w(k)\|_2^2+\|\partial A(k+1)\|_2^2)]^{8/7}\} \\ &\le E\{[\Phi(k,n)]^{8/7}(\|w(k)\|_2^{16/7}+\|\partial A(k+1)\|_2^{16/7})\} \\ &\le (E\{[\Phi(k,n)]^{16/7}\})^{3/14}E\{(\|w(k)\|_2^4+\|\partial A(k+1)\|_2^4)^{4/7}\} \\ &\le E\{[\Phi(k,n)]^{3/14}\}\,E\{(\|w(k)\|_2^2+\|\partial A(k+1)\|_2^2)^{4/7}\} \end{aligned} \tag{8.6.15}$$

By (8.6.27), it is not difficult to see

$$\lim_{n\to\infty} sup\,E\{V^{8/7}(k)\} \le C_4E\{(\|w(k)\|_2^2+\|\partial A(k+1)\|_2^2)^{4/7}\} \tag{8.6.16}$$

where $C_4<\infty$. Considering (8.6.5) and (8.6.6), (8.6.16) is expressed as

$$\lim_{k\to\infty}\|\bar{a}(k)\|_2^2 \le E[\|w(k)\|_2^2+\|\partial A(k)\|_2^2]^{1/2} \tag{8.6.17}$$

By applying the norm inequality $\|\partial A(k)\|_2 \le \|\partial A(k)\|_\infty$, we prove this theorem.

Q.E.D.

Corollary 8.6.1 *The minimum tracking error is achieved when the Gauss-Newton algorithm tracking a trajectory possesses a minimum Lipschitzian constant.*

Proof: From (8.6.3), we have

$$\lim_{k\to\infty} sup\frac{1}{k}\sum_{n=1}^{k}\|\bar{a}(k)\|_2^2 \le \lim_{k\to\infty} sup\frac{1}{k}\sum_{n=1}^{k} E[\|w(k)\|_2^2+\|\partial A(k)\|_\infty^2]^{1/2} \quad (8.6.18)$$

Suppose the additive noise of input is negligible, $\|w(k)\|_2^2 \to 0$; then for a slow variation trajectory $\|\partial A(k)\|_\infty^2 \to 0$,

$$\lim_{k\to\infty} sup\frac{1}{k}\sum_{n=1}^{k}\|\bar{a}(k)\|_2^2 \to 0$$

Q.E.D.

Corollary 8.6.1 gives an expression for the mathematical expectation of the tracking error. The Gauss-Newton algorithm is designed to minimize the cost function of the output of the ASTV-ARMA model. Ideally, if the cost function is minimized then the tracking error should approach error. In the following theorem, we demonstrate that the cost function of the CC-AA is minimized as the tracking error is minimized.

Theorem 8.6.2 *(Global Convergence) The CC-AA globally converges to the minimum value of the cost function, and results in a complete separation SFMSs.*

Proof: If the Adaptive-ASTV-ARMA model at *pth* branch of the CC-AA tracks the complete separation trajectory $a_{p,1}^*[a_{p,2}^*(k)]$

$$\begin{aligned} y_{p,M}(k)+a_{p,1}^*(k)y_{p,M}(k-1)+a_{p,2}^*(k)y_{p,M}(k-2) &= 0 \\ e_{p,M}(k)+\alpha a_{p,1}^*(k)e_{p,M}(k-1)+\alpha^2 a_{p,2}^*(k)e_{p,M}(k-2) &= 0 \end{aligned} \quad (8.6.19)$$

However, for the estimated trajectory $\tilde{a}_{p,1}[\tilde{a}_{p,2}(k)]$, the output of MA and AR part of the Adaptive CC-AA model at branch p are given as

$$\begin{aligned} \tilde{y}(k) &= y_{p,M}(k)+\tilde{a}_{p,1}(k)y_{p,M}(k-1)+\tilde{a}_{p,2}(k)y_{p,M}(k-2) \neq 0 \\ e_{p,M}(k) &= -\alpha a_{p,1}^*(k)e_{p,M}(k-1)-\alpha^2 a_{p,2}^*(k)e_{p,M}(k-2)+\tilde{y}(k) \end{aligned} \quad (8.6.20)$$

If we denote the tracking error of the Adaptive-ASTV-ARMA model as

$\bar{a}_{p,i}(k) = \tilde{a}_{p,i}(k) - a_{p,i}^{*}(k)$, $i = 1, 2$ then (8.6.20) can be written as

$$\begin{aligned} e_{p,M}(k) = & -\alpha a_{p,1}^{*}(k)\, e_{p,M}(k-1) - \alpha^2 a_{p,2}^{*}(k)\, e_{p,M}(k-2) \\ & + \bar{a}_{p,1}(k)\, y_{p,M}(k-1) + \bar{a}_{p,2}(k)\, y_{p,M}(k-2) \end{aligned} \tag{8.6.21}$$

Taking the norm of (8.6.21), and using the norm inequality $\| \ \|_2 \le \| \ \|_\infty$

$$\begin{aligned} & (1 - \alpha^2 \| a_{p,1}^{*}(k) \|_2 - \alpha^4 \| a_{p,2}^{*}(k) \|_2) \| e_{p,M}(k) \|_2 \\ & \le (\| \bar{a}_{p,1}(k) \|_\infty + \| \bar{a}_{p,2}(k) \|_\infty) \| y_{p,M}(k) \|_2 \end{aligned} \tag{8.6.22}$$

Assuming $C_{min} = inf(1 - \alpha^2 \| a_{p,1}^{*}(k) \|_2 - \alpha^4 \| a_{p,2}^{*}(k) \|_2) \neq 0$, we have

$$\| e_{p,M}(k) \|_2 \le \frac{1}{C_{min}} \| \bar{a}_p(k) \|_\infty \| y_{p,M}(k) \|_2 \tag{8.6.23}$$

Hence the cost function of the CC-AA can be expressed as the total output energy of the Adaptive-ASTV-ARMA model at all branches

$$\| e_{total}(k) \|_2 = \sum_{p=1}^{M} \| e_{p,M}(k) \|_2 \le \frac{\| S(k) \|_2}{C_{min}} \sum_{p=1}^{M} \| \bar{a}_p(k) \|_\infty \tag{8.6.24}$$

$$\lim_{k \to \infty} \frac{1}{k} sup \| e_{total}(k) \|_2 \le \frac{\| S(k) \|_2}{C_{min}} \lim_{k \to \infty} sup \frac{1}{k} \sum_{n \to \infty}^{k} E[\| w(k) \|_2^2 + \| \partial A(k) \|_\infty^2]^{1/2} \tag{8.6.25}$$

The LHS of (8.6.25) is minimized as $\| \partial A(k) \|_\infty^2 \to 0$.

Q.E.D.

Theorem 8.6.2 concludes our proof of convergence and tracking of the CC-AA to an equilibrium which leads to the desired complete separation of the SFMSs. Also, it establishes an inherent relationship between the tracking behavior of the CC-AA and the variation properties of the trajectory of the signal. Based on this relationship we may conclude that there exists a global convergence of the CC-AA and that it will always converge to the complete separation of SFMSs.

8.7. Intersection of CC-AA Trajectories

In this section, we investigate the trajectory-crossing of two ASTV-ARMA models. By trajectory-crossing, we mean that at a certain time-instant these trajectories have the same coordinates [8.9]. If the trajectories of two or more ASTV-ARMA models intersect, two problems are arise: (1) at the crossing instant, the SFMSs are non-separable, and (2) after crossing, the tracking of the trajectories may result in a random switch between the ASTV-ARMA outputs. The following lemma shows the mechanism of the trajectory-crossing.

Lemma 8.7.1 *(Trajectoryi-Crossing) The trajectories of two ASTV-ARMA models intersect each other at an instant* $\exists k \in Z^+$ *, iff the instantaneous frequencies of the signals associated with these models have the same sample value at this instant k.*

Proof: Consider an FMS $r_p(k) = \sin[\psi(k)]$ with instantaneous frequency $\dot{\psi}(k)$; then the trajectory of the ASTV-ARMA model representing such an FMS can be written as

$$a_{p,2}(k) = \frac{\sin[\dot{\psi}(k)]}{\sin[\dot{\psi}(k-1)]} \tag{8.7.1}$$

$$a_{p,1}(k) = -\frac{\sin[\dot{\psi}(k)+\dot{\psi}(k-1)]}{\sin[\dot{\psi}(k-1)]}$$

Thus the instantaneous frequency function in the plane $\{\dot{\psi}(k), \dot{\psi}(k-1)\}$ and the trajectory of the ASTV-ARMA model in the plane $\{a_{p,1}(k), a_{p,2}(k)\}$ constitute a certain mapping relationship, which is characterized by the Jacobian J:

$$J = \begin{vmatrix} \dfrac{\partial a_{p,1}(k)}{\partial \dot{\psi}(k)} & \dfrac{\partial a_{p,2}(k)}{\partial \dot{\psi}(k)} \\ \dfrac{\partial a_{p,1}(k)}{\partial \dot{\psi}(k-1)} & \dfrac{\partial a_{p,2}(k)}{\partial \dot{\psi}(k-1)} \end{vmatrix} = a_{p,1}(k)\, a_{p,2}(k) \tag{8.7.2}$$

Since the Wronskian $\Delta_p(k, 0, 1) = \sin[\dot{\psi}(k)] > 0$, $\forall k \in Z^+$ we have, $|J| < \infty$ and $a_{p,2}(k) > 0$. Because the instantaneous frequency is a positive function, the only situation where the Jacobian vanishes is

$$\dot{\psi}(k) + \dot{\psi}(k-1) = \pi \quad , \tag{8.7.3}$$

Hence,the mapping between the instantaneous frequency and trajectory is an one-to-one mapping, except for the pathological case when (8.7.3) is satisfied.

Q.E.D.

If the input mixture of the SFMSs contains two or more FMs whose trajectories intersect one another, the FMSs components of the input mixture degenerate to sinusoids having the same instantaneous frequency. It is obvious that one can not separate sinusoids having the same frequency. More importantly, in the CC-AA model such a trajectory-crossing is random in nature and may result in a random switching between the trajectories; thus, this crossing will cause an uncertainty in the identification of the outputs of the CC-AA.

Computer simulation results are presented in Fig.8.5. The FMSs are single-tone modulated, and the instantaneous frequencies of the two FMSs crosss each other at a certain time instant, which results in trajectory-crossing . The random crossing between the trajectories is clearly seen.

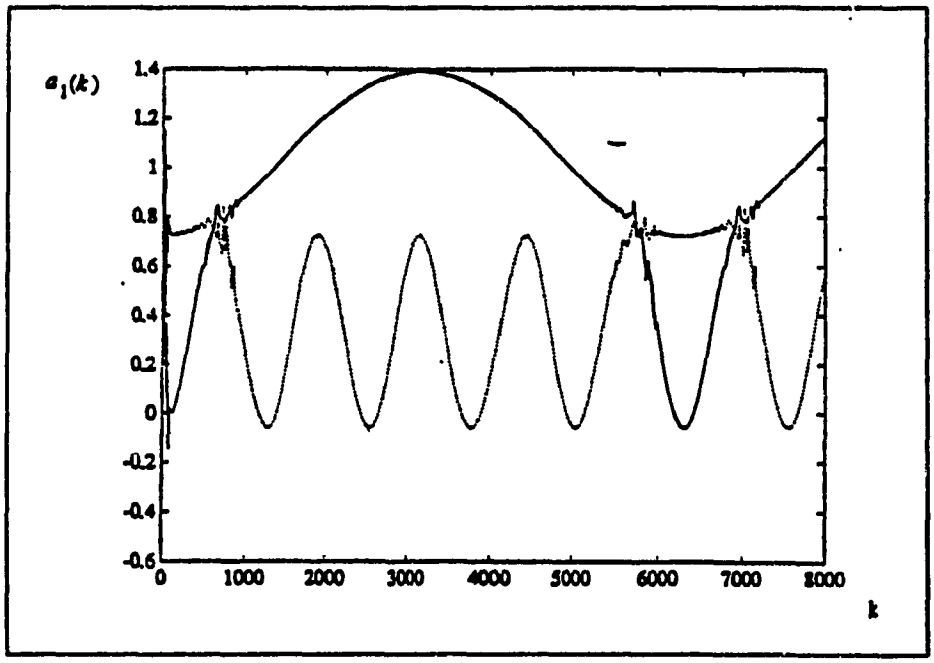

Fig. 8.5 Random Switching of CC-AA Trajectories

In order to avoid a random switch between the trajectories of the different ASTV-

ARMA models, we suggest use of the instantaneous Euclidean distance between the two trajectories given by

$$d_{ij}(k) = \left[|a_{i,1}(k) - a_{i,1}(k-1)|^2 + |a_{i,2}(k) - a_{i,2}(k-1)|^2\right]^{1/2}$$

$$\forall i, j \in \{1, 2, \ldots M\}$$

If the distance $d_{ij}(k) < c$, where c is a certain threshold, then a simple trajectory extrapolation is used for the next few iterations $k+1, k+2, \ldots$ to control the gradient of the trajectory tracking until the distance $d_{ij}(k)$ becomes larger than the chosen threshold value.

Another way of overcoming the random switching problem is based on the assumption that the probability of the event that the instantaneous frequencies as well as the derivatives of the two FMSs are the same at a given instant of time is practically close to zero. So if the adaptation speeds of the two Gauss-Newton algorithms could be adjusted so that at the crossing instant each adaptive algorithm possesses a different adaptation speed, namely the step size, then the possibility of the random switching can be drastically reduced. In what follows, we present a modification of Gauss-Newton algorithm which has the ability to adjust the step size in a local sense.

The local cost function at time instant k is written as $F\{\tilde{a}(k), \mu_{(k)}\}$. Let us minimize this cost function w.r.t. the step size μ_k

$$\min_{\mu(k)} F\{\tilde{a}(k), \mu(k)\} \tag{8.7.4}$$

By substituting (8.6.1) into (8.7.4) and taking into account that

$$\frac{\partial F}{\partial \mu(k)} = -\Psi^T(k) P(k) \Psi(k) [y_M(k) - \Psi^T(k) \tilde{a}(k)] = 0 \tag{8.7.5}$$

the step size can be adjusted as

$$\mu(k+1) = \mu(k) - \iota \Psi^T(k) P(k) \Psi(k) [y_M(k) - \Psi^T(k) \tilde{a}(k)] \tag{8.7.6}$$

where ι is the gain for updating the step size.

If the trajectory-crossing occurs, which implies the corresponding FMSs degenerate into one FMS component at this particular instant, the number of SFMSs is reduced and although the random crossing could be avoided (by using extrapolation or updating step size suggested above), the separation performance is degraded.

Example 1: *Separation of Gaussian random function modulated SFMSs having the same Fourier spectra*

In this example, we consider a practical application of the separation of signals whose Fourier spectra are completely overlapped. In this case, we assume that the number of SFMSs is *M*, all FMSs have the *same central frequency*, the instantaneous frequency of each FMS is modulated by a zero-mean Gaussian process with the same variance σ^2. Further we assume condition (8.2.2) is satisfied. We use a CC-AA to separate the SFMSs. Since the random FMS component is a stochastic process, it obeys a certain distribution, but according to the Central Limit Theorem [8.9], the sum of a large number of such stochastic processes may be approximated by a Gaussian process.

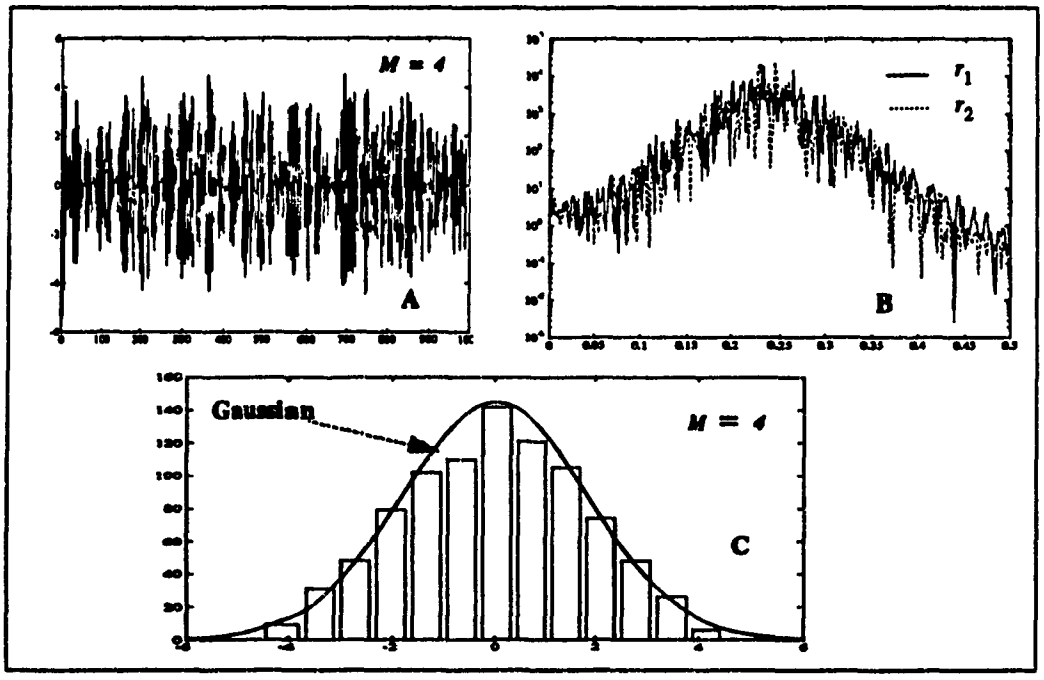

Fig. 8.6 A) Waveform B) Fourier Spectra C) Histogram of Input Mixture

To illustrate the characteristic of such an input mixture, its waveform, its Fourier

spectrum, and histogram are presented in Fig. 8.6.

A computer simulation result is given to show the use of a CC-AA for separation of two SFMSs. The two random modulating functions are differnet realizations of the same Gaussian noise. The Lissajous diagram representing the two random modulating sources is illustrated in Fig. 8.7.

After the two SFMSs are separated, these FMSs are demodulated, and the modulating functions are compared with the true modulating functions using Lissajous diagram as shown in Fig.8.8. It is seen that for both the separated sources $\hat{S}_1(k)$ and $\hat{S}_2(k)$, a good separation performance is achieved.

Now one may consider such a separation of SFMSs as a transmission of random sources through the same channel with a given bandwidth [8.8] [8.9]. Our transmission model is described in Fig.8.10. By exploiting the CC-AA model, it is possible to transmit several superimposed FMSs within the same bandwidth.

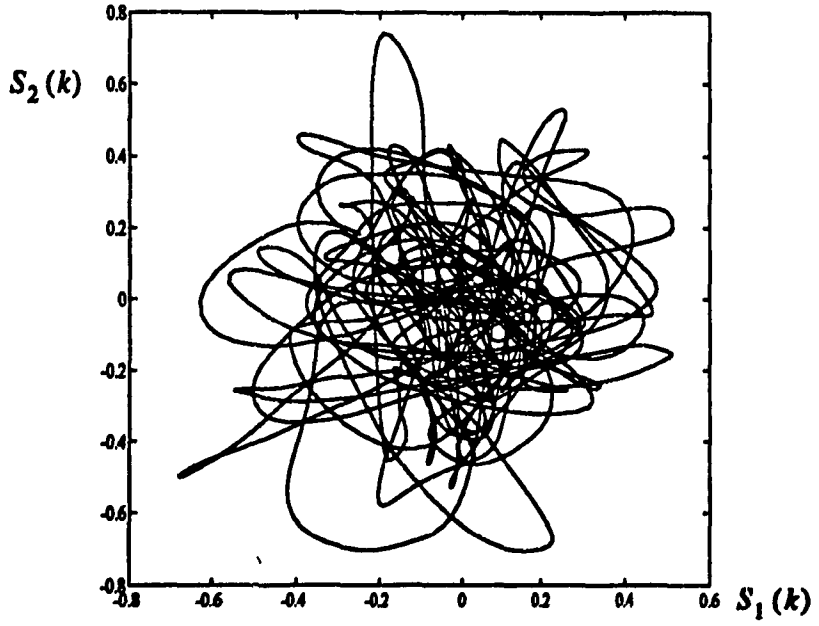

Fig. 8.7 Lissajous Diagram of Relationship of Two Independent Source

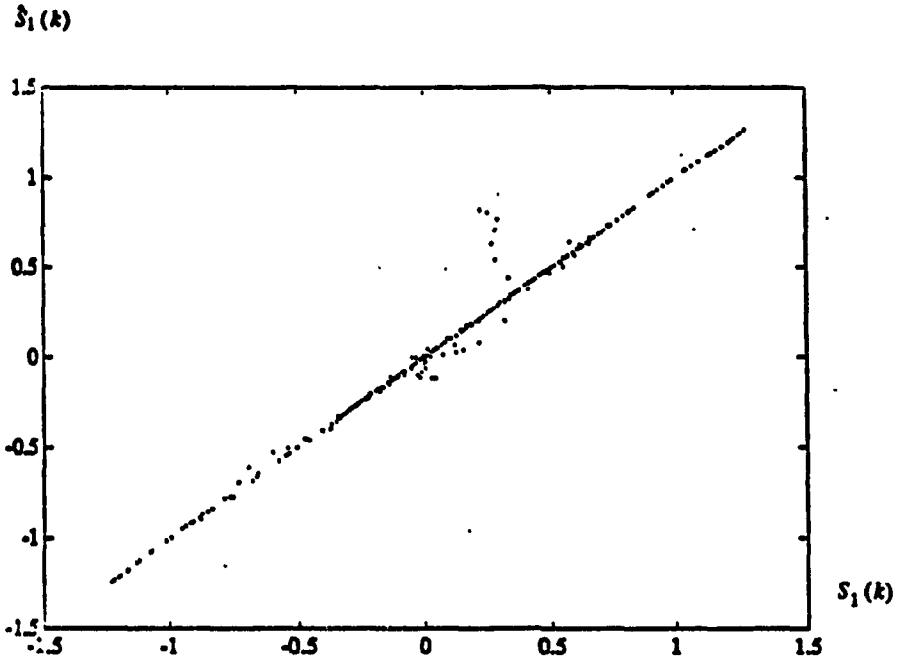

Fig. 8.8 Lissajous Diagram of Separation Results

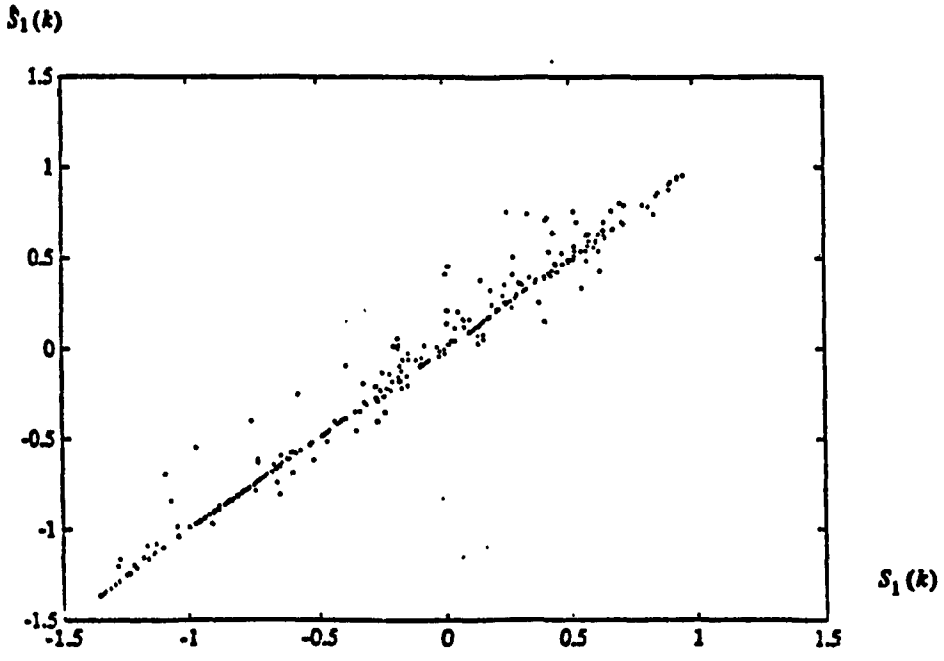

Fig. 8.9 Lissajous Diagram of Separation Results.

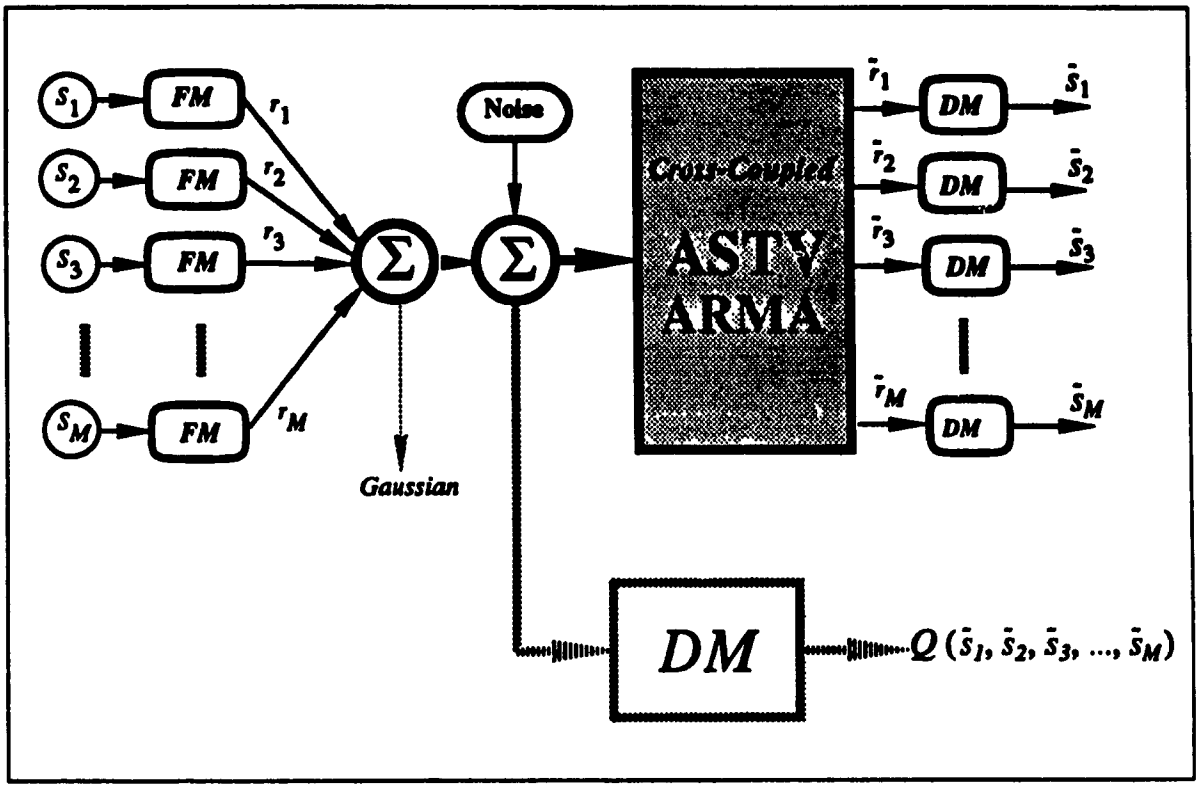

Fig. 8.10 Transmission Model Using CC-AA

Example 2: *Decomposition of Exponentially damped SFMS.*

In this example, we are interested in studying decomposition of a transient signal into a sum of exponentially damped FMSs with overlapping Fourier spectra.

Suppose that a transient is composed of two exponentially damped FMSs as shown in Fig.8.11. Using the CC-AA model, the transient is decomposed into two exponentially damped FMSs as shown in Fig. 8.12. The Fourier spectrum of each

exponentially damped FMS is plotted in Fig.8.13.

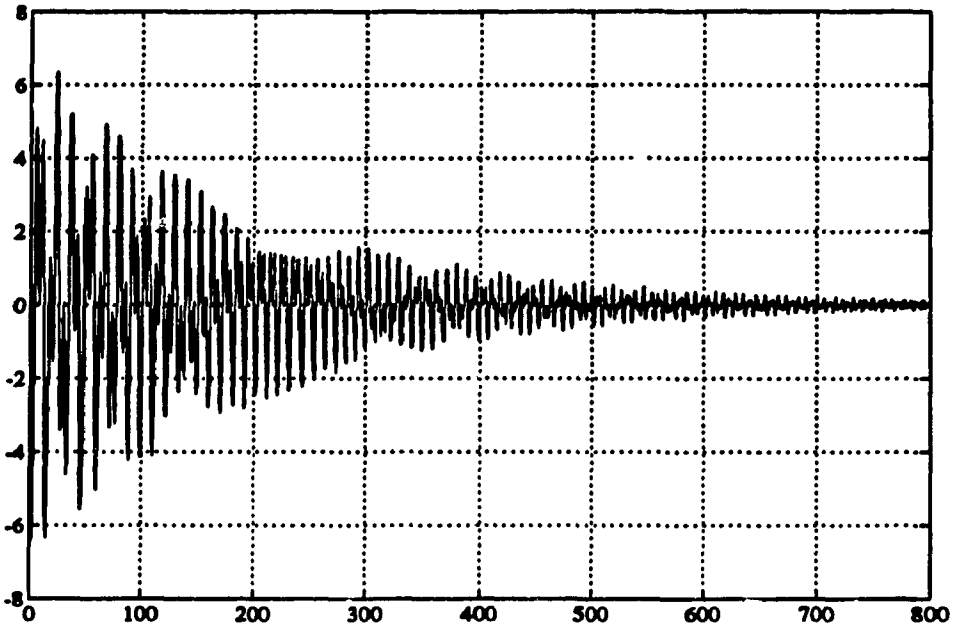

Fig. 8.11 A Transient Signal

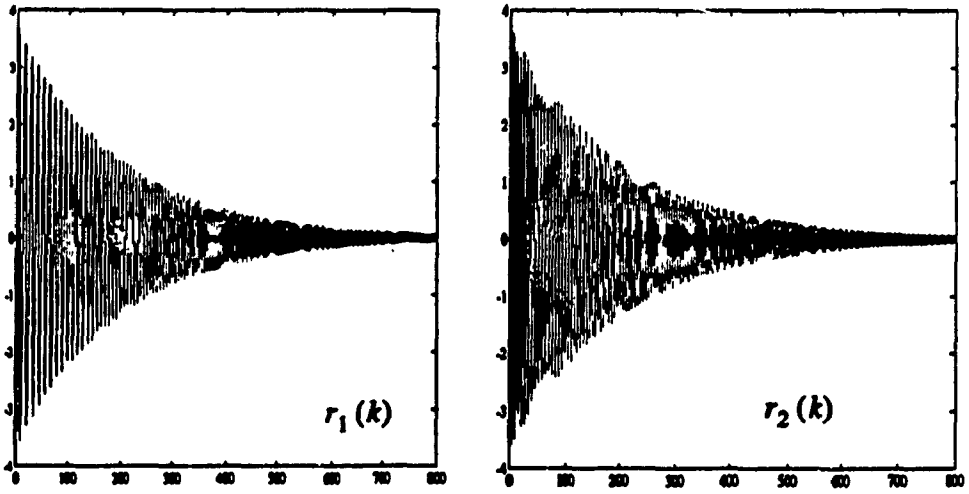

Fig. 8.12 Decomposed Two Exponential Damped FMSs

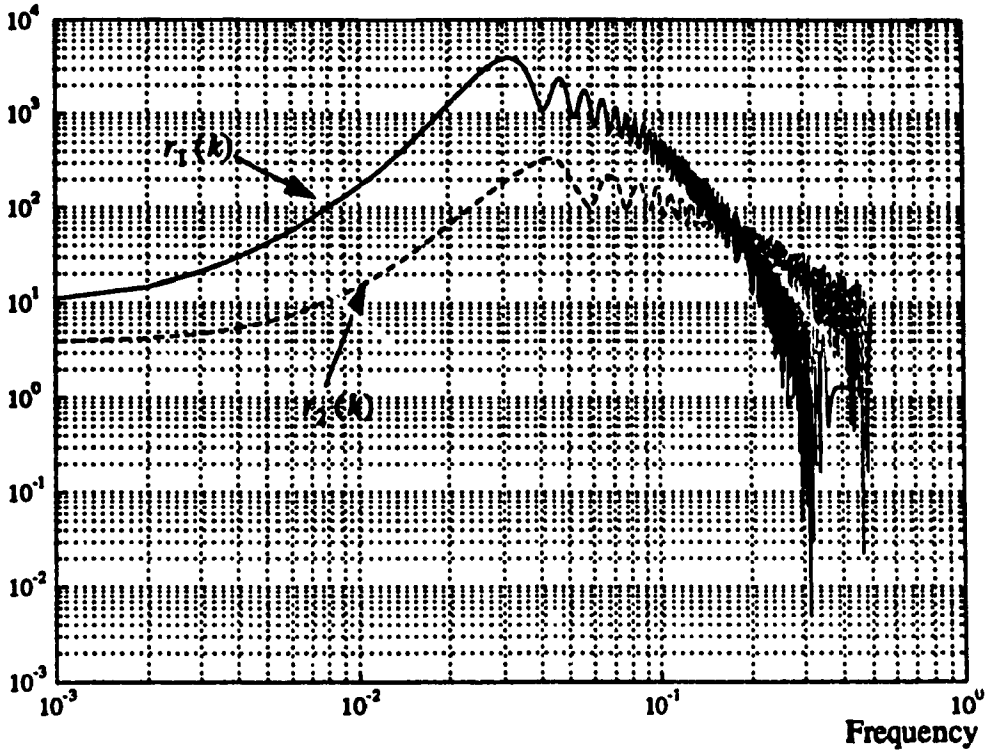

Fig. 8.13 Fourier Spectrum of Two Exponentially Damped FMS Components

References

[8.1] D. Wulich, E. I. Plotkin, M.N.S. Swamy and E. Kashi, "A Modified CCPLL for Demodulation of Two FM Signals with Overlapping Sepctra", *Electronic Letters*, Vol. 24, pp. 1588-1570, Dec.1988

[8.2] W. Tong, E. I. Plotkin and M. N. S. Swamy, "Cross-Coupled Constrained Null Filter and Separation of Superimposed Frequency Modulated Sinusoids", *Proceedings ISCAS92*, pp. 1479-1482, May, U.S.A.

[8.3] T. A. C. M. Classen and W. F. G. Mecklenbranker, "The Vigner Distribution - A Tool for Time-Frequency Analysis, Pats I-II", *Pilips,J. Res.* Vol. 35, pp. 217-250, 276-300, 372-389, 1980

[8.4] G.H. Goulb and C.F. Van Loan, "*Matrix Computations*", John Hopkins University Press, 1983

[8.5] Lakshimikantham and D. Trigiante, "*Theory of Difference Equation*", Academic Press Inc. 1988

[8.6] L. Ljung and T. Soderstrom, "*Theory and Practice of Recursive Identification*", The MIT Press, Cambridge, Mass. 1986

[8.7] A. Benvensite, "Design of Adaptive Algorithms for Tracking of Time-varying Systems", *Inter. Journal of Adaptive Control and Signal Processing*, Vol.1, pp. 3-29, 1987

[8.8] C. E. Shannon and Weaver, "*The Mathematical Theory of Communications*", The University of Illinois, Urbana, 1949

[8.9] H. Cramer and M. R. Leadbetter, "*Stationary and Related Stochastic Processes*", John Wiley & Sons, Inc., New York, 1967

Chapter 9

Conclusions

9.1. Summary of the Results

In this thesis, we have investigated, in detail, an ASTV-ARMA model, and studied two aspects of such a model; (1) its synthesis and various properties; and (2) its applications to the problem of separation of superimposed signals with overlapping Fourier spectra.

We have presented the concept of a linear time-varying null-operator, and showed that the existence of a time-varying null operator is associated with the positiveness of the Wronskian which defines the geometrical properties of the signal space; it has been shown that if a signal can be represented by an N-dimensional W-system, then one can find a time-varying null operator to represent such a signal. It is also shown that for a certain class of signals time-varying modelling is more efficient than time-invariant one, i.e. such a model has an order significantly lower than the corresponding time-invariant model.

It has been shown that the construction of a higher-order time-varying null operator determined by a higher-order Wronskian can be synthesized by using lower-order Wronskians combined with certain pivots. Two algorithms for the construction of higher-order Wronskian were discussed: the Choi-McMillan and the Sylvester algorithms. We further explored the fundamental properties of a higher-order time-varying operator and showed that a time-varying operator can neither be decomposed by using root-factorization nor can it be commuted with other time-varying and/or

time-invariant null operators.

We introduced a time-varying anti-null operator which is perfectly symmetrical to the null operator. A system which is built using these two operators is found to be perfectly transparent to any signal that is not rejected by a null operator. By exploring the properties of the impulse response of an anti-null time-varying operator, we have clearly brought out the role of the anti-null operator in the design of a transparent system. On the other hand, it is also established that a perfect transparent operator is not physically realizable, due to the uncertainty in the initial states and the stability problem of the transparent system. By investigating the trade-off between the transparency and the observation time of an almost symmetrical time-varying operator, it has also been shown that the one-sided almost symmetrical time-varying transparent operator can asymptotically approximate the ideal transparent one.

A general study of a linear time-varying anti-null operator has been carried out. Two kinds of local instabilities, namely the local instability of the first kind and local instability of the second kind, have been discussed. It is shown that for a linear time-varying system having a local instability of the first kind, the module of the eigenvalues can be temporarily outside the unit disc, and the system is still globally BIBO stable. It is also shown that even if the module of the eigenvalues of the system is located strictly inside the unit disc, the system may be globally unstable. A general test for the necessary and sufficient conditions of the stability of a linear time-varying system has been presented. It is proved that the construction of a second order anti-null operator based on the W-system is BIBO globally stable.

Applications of the proposed model for signal separation was presented in Chapters 6,7,and 8. First, we investigated a specific phase unwarping procedure to convert a constant-envelope signal of arbitrary phase to another constant-envelope signal of a given phase. The non-equally spaced sampling technique plays a fundamental role in this transform. Once a signal has been converted to a sinewave with fixed frequency, an almost symmetrical time-invariant model can be used for the implementation of the null and anti-null operators. Based on this approach some practical schemes have been suggested for separation of constant-envelope signals with overlapping Fourier spectra. A phase perturbation analysis has been carried out, and a closed-loop scheme suggested to improve the separation performance. In addition, we have also performed a theoretical analysis of the tracking capability of the Gauss-Newton adaptive

algorithm. It is has been shown that such an algorithm has an inherent threshold effect when applied to track signals with fast time-varying parameters.

This concept was then applied for solving the problem of blind channel deconvolution. Based on the main properties of the ASTV-ARMA model (null singularity and transparency), a new criterion for channel equalization has been proposed. It has been shown that the time-varying coefficients of an ASTV-ARMA model may be split into two distinct parts, one depending on the variations of the phase and the other on the variation of the envelope of the signal. By combining the adaptation of the envelope dependent part and the signal controlling of the phase dependent part, we have established a new approach for the implementation of blind deconvolution. The proposed scheme for blind deconvolution was investigated with respect to a nonstationary source signal propagating through a rational channel. Two different blind deconvolution schemes, namely the one-sensor scheme and the two-sensor scheme, have been repectively proposed for the constant-envelope source and the time-varying envelope source. We have further shown that the proposed blind deconvolution schemes guarantee the unique convergence to the desired deconvolution solution. Several examples have been presented to show the advantages of using the proposed blind deconvolution algorithm.

Finally a Cross-Coupled ASTV-ARMA(CC-AA) model, which can be used to separate superimposed frequency modulated sinusoids with complete overlapping Fourier spectra, has been presented. The stability of the equilibria states of the CC-AA model and their trajectory variation properties have been also discussed. We shave further shown that the CC-AA always converges to the solution resulting in a complete separation of the superimposed FM signals whose Fourier spectra overlap.

9.2. Further Research Directions

Since research in the area of time-varying null operators is rather new, many issues related to this filed are still open. In what follows, we discuss possible future research directions:

1) Synthesis of time-varying null operators, on an arbitrary building basis, which may lead to new methods of designing signal transparent

systems with given null singularities.

2) Development of a more general approach for the decomposition of a time-varying null operator; for example, using Krylov subspace decomposition method to find the lower order time-varying null operators.

3) Synthesis of a practical approach to overcome the perfect symmetry reqiurement for the realization of an ideal transparent operator, and at the same time achieve better transparency. A study of the optimal trade-off between transparency quality and the duration of the observation time, a very important aspect for the processing of transparent signals.

4) Extention of the results on BIBO stability of a linear time-varying system to verify the two conjectures proposed in Chapter 5.

5) A study of the non-equally spaced sampling (NESS) technique with emphasis on spectrum synthesis. Given a Fourier spectrum, to find the condition for the NESS to obtain the desired spectrum in a new time-domain.

6) Design of a more powerful adaptive algorithm for tracking a fast time-varying system.

7) A study of the blind deconvolution problem for a time-varying channel, especially, a statistical-channel model. Application of the ASTV-ARMA model for the blind equalization of communication channels.

8) Generalization of the concept of a cross-coupled ASTV-ARMA model for the separation of arbitrary superimposed signals, and a study of the separability of superimposed signals based on their trajectory properties.

Appendix 3.1 *Proof of Lemma 3.6.1*

Consider the roots $q_1, q_2, \ldots q_N$ of the following equation

$$1 + a_1 q^{-1} + \ldots + a_N q^{-N} = 0 \tag{A-3.1.1}$$

Let us study the following expression

$$\frac{1}{\phi(q^{-1})} = \frac{1}{(1-q_1 q^{-1})(1-q_2 q^{-1})\ldots(1-q_N q^{-1})} = \tag{A-3.1.2}$$

$$(1+q_1 q^{-1}+q_1^2 q^{-2}+\ldots)(1+q_2 q^{-1}+q_2^2 q^{-2}+\ldots)\ldots(1+q_N q^{-1}+q_N^2 q^{-2}+\ldots)$$

Then we have expansion

$$\frac{1}{\phi(q^{-1})} = 1+\gamma_1 q^{-1}+\gamma_2 q^{-2}+\ldots \tag{A-3.1.3}$$

Taking derivative of $\phi(q^{-1})$ with respect to q^{-1}, we have

$$-\frac{\phi'(q^{-1})}{\phi(q^{-1})} = \frac{\gamma_1+2\gamma_2 q^{-1}+3\gamma_3 q^{-2}+\ldots}{1+\gamma_1 q^{-1}+\gamma_2 q^{-2}+\ldots} \tag{A-3.1.4}$$

By a well known equality

$$-\frac{\phi'(q^{-1})}{\phi(q^{-1})} = \frac{q_1}{1-q_1 q^{-1}}+\frac{q_2}{1-q_2 q^{-1}}+\ldots+\frac{q_N}{1-q_N q^{-1}} \tag{A-3.1.5}$$

$$= q_1+q_1^2 q^{-1}+q_1^3 q^{-2}+\ldots+q_2+q_2^2 q^{-1}+q_2^3 q^{-2}+\ldots+q_N+q_N^2 q^{-1}+q_N^3 q^{-2}$$

$$= s_1+s_2 q^{-1}+s_3 q^{-2}+\ldots$$

By (A-3.1.4) and (A-3.1.5)

$$s_1+s_2 q^{-1}+s_3 q^{-2}+\ldots = \frac{\gamma_1+2\gamma_2 q^{-1}+3\gamma_3 q^{-2}+\ldots}{1+\gamma_1 q^{-1}+\gamma_2 q^{-2}+\ldots} \tag{A-3.1.6}$$

Equating the corresponding coefficients of q^{-i} in (A-3.1.6) yields

$$\begin{aligned} \gamma_1 &= s_1 \\ 2\gamma_2 &= s_2+\gamma_1 s_1 \\ 3\gamma_3 &= s_3+\gamma_1 s_2+\gamma_2 s_1 \\ &\ldots\ldots\ldots\ldots \\ r\gamma_r &= s_r+\gamma_1 s_{r-1}+\ldots+\gamma_{r-1} s_1 \end{aligned} \tag{A-3.1.7}$$

Using Newton's formula

$$s_r + a_1 s_{r-1} + \ldots + a_{r-1} s_1 = -r a_r \tag{A-3.1.8}$$

and multiplying both sides of (A-3.1.7) respectively by $a_{r-1} a_{r-2} \ldots, 1$ and adding both sides, we have

$$\begin{aligned} &a_{r-1}\gamma_1 + 2a_{r-2}\gamma_2 + \ldots + r\gamma_r \\ &\quad = -\{r a_r + (r-1)\, a_{r-1}\gamma_1 + \ldots + a_1 \gamma_{r-1}\} \end{aligned} \tag{A-3.1.9}$$

Hence

$$\gamma_r + a_1\gamma_{r-1} + a_2\gamma_{r-2} + \ldots + a_r = 0 \quad r = 1, 2, \ldots N \tag{A-3.1.10}$$

Thus we have a set of linear equations for $i = 1, 2, \ldots, N$, and the solution of such a Gauss system of equations can be written by following compact expression

$$\gamma_l = (-1)^l \begin{vmatrix} a_1 & 1 & & \\ a_2 & a_1 & 1 & \\ \ldots & \ldots & \ldots & \ldots \\ a_{l-1} & a_{l-2} & \ldots & \ldots & 1 \\ a_l & a_{l-1} & \ldots & & a_1 \end{vmatrix}_{l \times l} \quad l = 1, 2, \ldots, N \tag{A-3.1.11}$$

Appendix 3.2 *Proof of Lemma 3.7.1*

Assume that $\lambda = \lambda_1$ is the largest eigen value of B and $\phi(\lambda)$ is its probability density. Let R be the region of the $(N-1)$-dimensional space $\lambda_i \geq 0$ $(i = 1, 2, \ldots, N)$ and for each $\lambda > 0$, let R_λ be the sub-region of R consisting of all $(\lambda_2, \lambda_3, \ldots, \lambda_N)$ such that $\lambda \geq \lambda_2 \geq \ldots \geq \lambda_N \geq 0$ .We then see that

$$\phi(\lambda) = K_N \lambda^{-1/2} exp\left(-\frac{\lambda}{2\sigma^2}\right) \int_{R_\lambda} exp\left[-\frac{\sum_{i=2}^{N} \lambda_i}{2\sigma^2}\right] \prod_{2 \leq i < j}^{N} (\lambda_i - \lambda_j) \prod_{j=2}^{N} (\lambda - \lambda_j) \lambda_j^{-1/2} d\lambda_j \tag{A-3.2.1}$$

$$\leq K_N \lambda^{N-\frac{3}{2}} exp\left(-\frac{\lambda}{2\sigma^2}\right) \int_{R} exp\left[-\frac{\sum_{i=2}^{N} \lambda_i}{2\sigma^2}\right] \prod_{2 \leq i < j}^{N} (\lambda_i - \lambda_j) \prod_{j=2}^{N} \lambda_j^{-1/2} d\lambda_j$$

$$= \lambda^{N-\frac{3}{2}} exp\left[-\frac{\lambda}{2\sigma^2}\right] K_N K_{N-1}^{-1}$$

Because of the fact that $\lambda - \lambda_j \leq \lambda$ $(j = 2, 3, \ldots, N)$, it is easy to see that

$$\frac{K_N}{K_{N-1}} = \frac{\pi^{1/2}}{(2\sigma^2)^{(N-1)/2} (\Gamma(N/2))^2} \tag{A-3.2.2}$$

Thus, (A-3.2.1) may be expressed as

$$\phi(\lambda) \leq \frac{\pi^{1/2}}{(2\sigma^2)^{(N-1)/2} (\Gamma(N/2))^2} \lambda^{N-\frac{3}{2}} exp\left[-\frac{\lambda}{2\sigma^2}\right] \tag{A-3.2.3}$$

Now let us calculate

$$Prob(\lambda > 2\sigma^2 rN) = \int_{2\sigma^2 rN}^{\infty} \phi(\lambda) d\lambda \tag{A-3.2.4}$$

$$\leq \frac{\pi^{1/2}}{(2\sigma^2)^{(N-1)/2} (\Gamma(N/2))^2} \int_{2\sigma^2 rN}^{\infty} \lambda^{N-\frac{3}{2}} exp\left[-\frac{\lambda}{2\sigma^2}\right] d\lambda$$

$$< \frac{(rN)^{(N-1)/2} exp[-rN] \pi^{1/2}}{(\Gamma(N/2))^2 (r-1)N}$$

Using Stirling's formula

$$\left(\Gamma\left(\frac{N}{2}\right)\right)^2 > \frac{\pi N^{N-1}}{exp\,(N)\,2^{N-2}} \qquad \text{(A-3.2.5)}$$

we get

$$Prob\,(\lambda > 2\sigma^2 rN) < \frac{(rN)^{(N-1)/2} exp\,[-rN]\,\pi^{1/2} exp\,(N)\,2^{N-2}}{(\pi N^{N-1})\,(r-1)\,N} \qquad \text{(A-3.2.6)}$$

$$= \left(\frac{2r}{e^{r-1}}\right)^N \frac{1}{4\,(r-1)\,(r\pi N)^{1/2}}$$

Appendix.4.1 *Expressions for coefficients* $p_l(k)$

First let us rewrite Newton's rule (A-3.1.8)

$$\begin{aligned} s_1 + a_1 &= 0 \\ s_2 + a_1 s_1 + 2a_2 &= 0 \\ &\cdots\cdots\cdots\cdots \end{aligned} \qquad \text{(A-4.1.1)}$$

Following the same procedure as in (A-3.1.10) and (A-3.1.11), we get

$$s_r = (-1)^r \begin{vmatrix} a_1 & 1 & & \\ 2a_2 & a_1 & 1 & \\ \cdots & \cdots & \cdots & \cdots \\ (l-1)a_{l-1} & a_{l-2} & \cdots & \cdots & 1 \\ la_l & a_{l-1} & \cdots & & a_1 \end{vmatrix}_{r \times r} \qquad \text{(A-4.1.2)}$$

Considering the two polynomials

$$g(q^{-1}) = 1 + a_1 q^{-1} + \ldots + a_N q^{-N} \qquad \text{(A-4.1.3)}$$

$$f(q^{-1}) = 1 + b_1 q^{-1} + \ldots + b_M q^{-M} \qquad \text{(A-4.1.4)}$$

our goal is to find the expression for the coefficients of the following expansion

$$\frac{g(q^{-1})}{f(q^{-1})} = 1 + p_1 q^{-1} + p_2 q^{-2} + \ldots \qquad \text{(A-4.1.5)}$$

Let us recall (A-3.1.5). If $g(q^{-1}) = f'(q^{-1})$ then $p_j = s_{j+1}$; thus by comparison, if we substitute the coefficients of $g(q^{-1})$ in (A-4.1.4) in the first column of determinant (A-4.1.2), we have

$$p_l = (-1)^l \begin{vmatrix} 1 & 1 & & \\ a_1 & b_1 & 1 & \\ \cdots & \cdots & \cdots & \cdots \\ a_{l-1} & b_{l-1} & \cdots & \cdots & 1 \\ a_l & b_l & \cdots & & b_1 \end{vmatrix}_{(l+1)\times(l+1)} = (-1)^l \begin{vmatrix} a_1 - b_1 & 1 & & \\ a_2 - b_2 & b_1 & 1 & \\ \cdots & \cdots & \cdots & \cdots \\ a_{l-1} - b_{l-1} & b_{l-1} & \cdots & \cdots & 1 \\ a_l - b_l & b_l & \cdots & & b_1 \end{vmatrix}_{l \times l} \qquad \text{(A-4.1.6)}$$

Appendix.4.2 *Expression for a 2-D ASTV-ARMA Model*

Let us consider the 2-D sinusoid signal as

$$x(i,j) = \sin[\psi^{(1)}(i) + \psi^{(2)}(j)] \qquad \text{(A-4.2.1)}$$

Then such a class of sinusoidal singals can be repreosented by a Wronskian system of functions given by

$$\{s_1 s_1, s_1 s_2, s_1 c_1, s_1 c_2, s_2 c_1, c_1 c_2, c_2 c_2\} \qquad \text{(A-4.2.2)}$$

where,

$$s_1(i) = \sin\psi^{(1)}(i) \qquad s_2(j) = \sin\psi^{(2)}(j)$$
$$c_1(i) = \cos\psi^{(1)}(i) \qquad c_2(j) = \cos\psi^{(2)}(j)$$

In fact the W-system of funtions in (A-4.1.2) is an orthogonal system. Denoting $\psi_{i,j}^{(l)} = \psi^{(l)}(i-j)$, we can formulate the augmented Wronskain for the W-system of funtions (A-4.1.2) as shown in Table A.4.1. By using the minor expansion along the last column we may compute the coefficients $a_{i,j}(k)$, $i,j = \{0,1,2\}$, we have the following 2-D ASTV-ARMA model:

$$\sum_{i=0}^{2}\sum_{j=0}^{2} \alpha^{i+j} a_{i,j}(k)\, q_1^{-i} q_2^{-j} y(i,j) = \sum_{i=0}^{2}\sum_{j=0}^{2} a_{i,j}(k)\, q_1^{-i} q_2^{-j} x(i,j) \qquad \text{(A-4.2.3)}$$

and the filtering operation is based on the following 3×3 window.

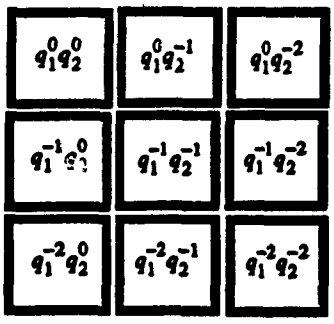

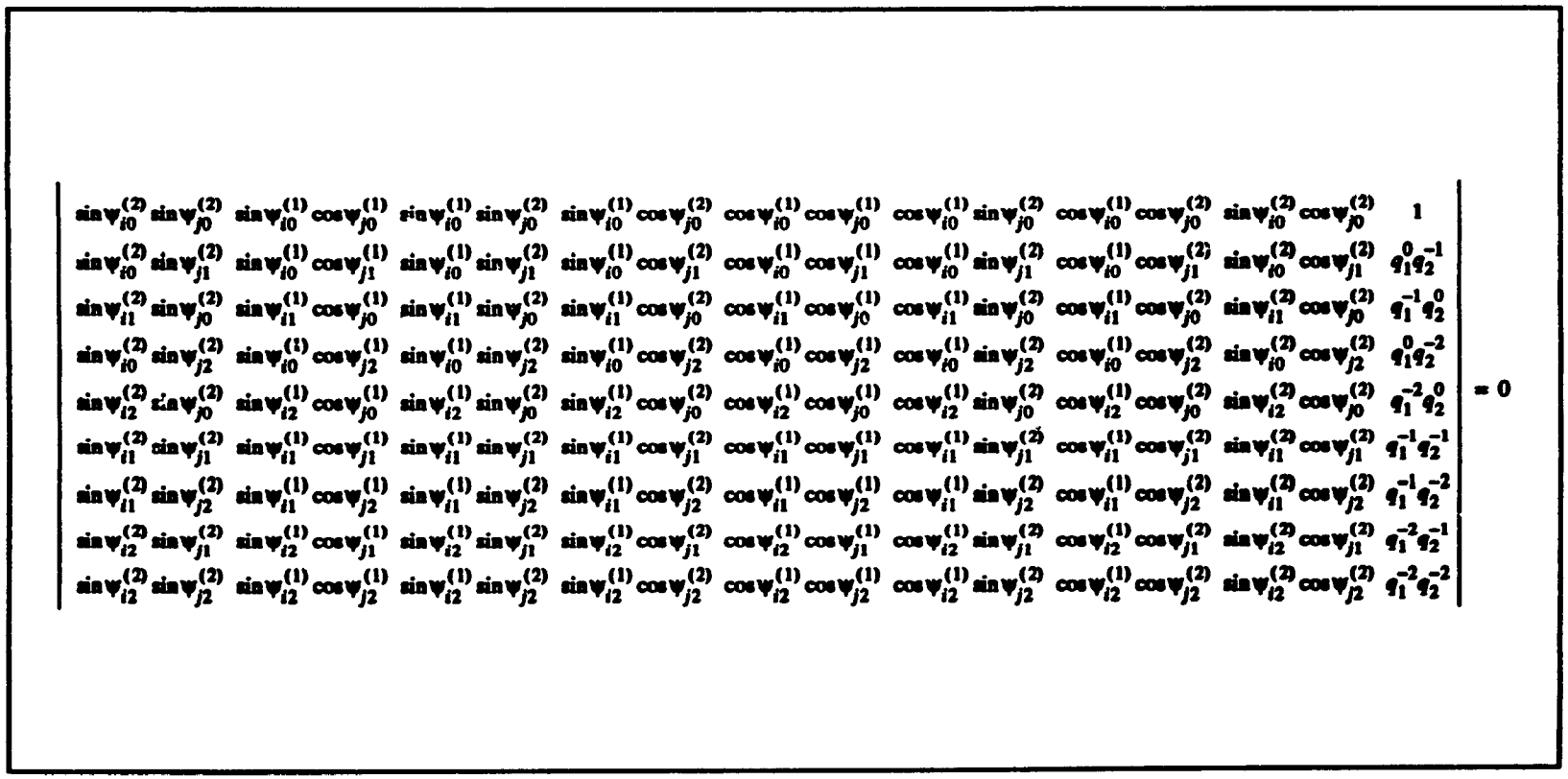

$$
\begin{vmatrix}
\sin\psi_{i0}^{(2)}\sin\psi_{j0}^{(2)} & \sin\psi_{i0}^{(1)}\cos\psi_{j0}^{(1)} & \sin\psi_{i0}^{(1)}\sin\psi_{j0}^{(2)} & \sin\psi_{i0}^{(1)}\cos\psi_{j0}^{(2)} & \cos\psi_{i0}^{(1)}\cos\psi_{j0}^{(1)} & \cos\psi_{i0}^{(1)}\sin\psi_{j0}^{(2)} & \cos\psi_{i0}^{(1)}\cos\psi_{j0}^{(2)} & \sin\psi_{i0}^{(2)}\cos\psi_{j0}^{(2)} & 1 \\
\sin\psi_{i0}^{(2)}\sin\psi_{j1}^{(2)} & \sin\psi_{i0}^{(1)}\cos\psi_{j1}^{(1)} & \sin\psi_{i0}^{(1)}\sin\psi_{j1}^{(2)} & \sin\psi_{i0}^{(1)}\cos\psi_{j1}^{(2)} & \cos\psi_{i0}^{(1)}\cos\psi_{j1}^{(1)} & \cos\psi_{i0}^{(1)}\sin\psi_{j1}^{(2)} & \cos\psi_{i0}^{(1)}\cos\psi_{j1}^{(2)} & \sin\psi_{i0}^{(2)}\cos\psi_{j1}^{(2)} & q_1^{0}q_2^{-1} \\
\sin\psi_{i1}^{(2)}\sin\psi_{j0}^{(2)} & \sin\psi_{i1}^{(1)}\cos\psi_{j0}^{(1)} & \sin\psi_{i1}^{(1)}\sin\psi_{j0}^{(2)} & \sin\psi_{i1}^{(1)}\cos\psi_{j0}^{(2)} & \cos\psi_{i1}^{(1)}\cos\psi_{j0}^{(1)} & \cos\psi_{i1}^{(1)}\sin\psi_{j0}^{(2)} & \cos\psi_{i1}^{(1)}\cos\psi_{j0}^{(2)} & \sin\psi_{i1}^{(2)}\cos\psi_{j0}^{(2)} & q_1^{-1}q_2^{0} \\
\sin\psi_{i0}^{(2)}\sin\psi_{j2}^{(2)} & \sin\psi_{i0}^{(1)}\cos\psi_{j2}^{(1)} & \sin\psi_{i0}^{(1)}\sin\psi_{j2}^{(2)} & \sin\psi_{i0}^{(1)}\cos\psi_{j2}^{(2)} & \cos\psi_{i0}^{(1)}\cos\psi_{j2}^{(1)} & \cos\psi_{i0}^{(1)}\sin\psi_{j2}^{(2)} & \cos\psi_{i0}^{(1)}\cos\psi_{j2}^{(2)} & \sin\psi_{i0}^{(2)}\cos\psi_{j2}^{(2)} & q_1^{0}q_2^{-2} \\
\sin\psi_{i2}^{(2)}\sin\psi_{j0}^{(2)} & \sin\psi_{i2}^{(1)}\cos\psi_{j0}^{(1)} & \sin\psi_{i2}^{(1)}\sin\psi_{j0}^{(2)} & \sin\psi_{i2}^{(1)}\cos\psi_{j0}^{(2)} & \cos\psi_{i2}^{(1)}\cos\psi_{j0}^{(1)} & \cos\psi_{i2}^{(1)}\sin\psi_{j0}^{(2)} & \cos\psi_{i2}^{(1)}\cos\psi_{j0}^{(2)} & \sin\psi_{i2}^{(2)}\cos\psi_{j0}^{(2)} & q_1^{-2}q_2^{0} \\
\sin\psi_{i1}^{(2)}\sin\psi_{j1}^{(2)} & \sin\psi_{i1}^{(1)}\cos\psi_{j1}^{(1)} & \sin\psi_{i1}^{(1)}\sin\psi_{j1}^{(2)} & \sin\psi_{i1}^{(1)}\cos\psi_{j1}^{(2)} & \cos\psi_{i1}^{(1)}\cos\psi_{j1}^{(1)} & \cos\psi_{i1}^{(1)}\sin\psi_{j1}^{(2)} & \cos\psi_{i1}^{(1)}\cos\psi_{j1}^{(2)} & \sin\psi_{i1}^{(2)}\cos\psi_{j1}^{(2)} & q_1^{-1}q_2^{-1} \\
\sin\psi_{i1}^{(2)}\sin\psi_{j2}^{(2)} & \sin\psi_{i1}^{(1)}\cos\psi_{j2}^{(1)} & \sin\psi_{i1}^{(1)}\sin\psi_{j2}^{(2)} & \sin\psi_{i1}^{(1)}\cos\psi_{j2}^{(2)} & \cos\psi_{i1}^{(1)}\cos\psi_{j2}^{(1)} & \cos\psi_{i1}^{(1)}\sin\psi_{j2}^{(2)} & \cos\psi_{i1}^{(1)}\cos\psi_{j2}^{(2)} & \sin\psi_{i1}^{(2)}\cos\psi_{j2}^{(2)} & q_1^{-1}q_2^{-2} \\
\sin\psi_{i2}^{(2)}\sin\psi_{j1}^{(2)} & \sin\psi_{i2}^{(1)}\cos\psi_{j1}^{(1)} & \sin\psi_{i2}^{(1)}\sin\psi_{j1}^{(2)} & \sin\psi_{i2}^{(1)}\cos\psi_{j1}^{(2)} & \cos\psi_{i2}^{(1)}\cos\psi_{j1}^{(1)} & \cos\psi_{i2}^{(1)}\sin\psi_{j1}^{(2)} & \cos\psi_{i2}^{(1)}\cos\psi_{j1}^{(2)} & \sin\psi_{i2}^{(2)}\cos\psi_{j1}^{(2)} & q_1^{-2}q_2^{-1} \\
\sin\psi_{i2}^{(2)}\sin\psi_{j2}^{(2)} & \sin\psi_{i2}^{(1)}\cos\psi_{j2}^{(1)} & \sin\psi_{i2}^{(1)}\sin\psi_{j2}^{(2)} & \sin\psi_{i2}^{(1)}\cos\psi_{j2}^{(2)} & \cos\psi_{i2}^{(1)}\cos\psi_{j2}^{(1)} & \cos\psi_{i2}^{(1)}\sin\psi_{j2}^{(2)} & \cos\psi_{i2}^{(1)}\cos\psi_{j2}^{(2)} & \sin\psi_{i2}^{(2)}\cos\psi_{j2}^{(2)} & q_1^{-2}q_2^{-2}
\end{vmatrix} = 0
$$

Table A-1, Augmented Wronakisn for Computing the Coefficients of 2-D ASTV-ARMA Model

Appendix 5.1 *Derivation of (5.3.13)*

Now using (5.3.9) yields the following matrix equations:

$$\Pi(j+1) = I + A^T(j)\Pi(j+1)A(j)$$

$$\Pi(j) = I + A^T(j-1)\Pi(j)A(j-1)$$

Let us compute

$$A^T(j)\,(\Pi(j+1) - \Pi(j))A(j) - (\Pi(j+1) - \Pi(j))$$

$$= A^T(j)\Pi(j+1)A(k) - A^T(j)\Pi(j)A(j) - \Pi(j+1) + \Pi(j)$$

$$= -(A^T(j) - A^T(j-1))\Pi(j)A(j) - A^T(j)\Pi(j)A(j) - A(j-1))$$

$$= W(j) \qquad \text{(A.5.1.1)}$$

Taking the matrix norm on (A.5.1.1) yields

$$\|W(j)\| \le 2\|A(j) - A(j-1)\|\|\Pi(j)\|\|A(j)\|$$

$$\le 2\|\partial A(j)\|\Gamma_\rho(j)\rho_A(j) \qquad \text{(A.5.1.2)}$$

where $\|\partial A(j)\| = \|A(j) - A(j-1)\|$ denotes the *variation rate* of the LTV system $A(j)$. From (5.3.14), we can evaluate

$$\Pi(j+1) - \Pi(j) = W(j) + A^T(j)\,(\Pi(j+1) - \Pi(j))A(j) \qquad \text{(A.5.1.3)}$$

Applying the chain substitution procedure as in(5.3.10), we get

$$\Pi(j+1) - \Pi(j) = W(j) + \sum_{l=1}^{\infty} (A^T(j))^l W(j)\,(A(j))^l, \qquad \text{(A.5.1.4)}$$

$$\|\Pi(j+1) - \Pi(j)\| = \|W(j)\| + \|W(j)\| \frac{\rho_A^2(j)}{1-\rho_A^2(j)} = \Gamma_\rho(j)\|W(j)\|$$

By substituting (A.5.1.2) we get:

$$\|\Pi(j+1) - \Pi(j)\| \leq 2\|\partial A(j)\|\Gamma_\rho^2(j)\rho_A(j) \qquad \textbf{(A.5.1.5)}$$

Appendix 7.1 *Proof of uniqueness of the deconvolution solution*

Equation (7.4.10) can be further expressed as

$$\frac{\partial}{\partial\theta}E_{\Psi}\{\tilde{A}(k)\} = \sum_{j=1}^{Q}\frac{\partial\sigma_j}{\partial\theta_i}\frac{\partial}{\partial\sigma_j}E_{\Psi}\{\tilde{A}(k)\} = 0 \qquad \text{(A.7.1.1)}$$

where

$$E_{\Psi}\{\frac{\partial}{\partial\sigma_m}\tilde{A}(k)\} = \frac{\sum_{j=1}^{Q}\sum_{i\neq m}^{Q}\sigma_j^2\sigma_i\cos\dot{\psi}_{mi}(k) - \sum_{i\neq j}^{Q}\sigma_i\sigma_j\sigma_m\cos\dot{\psi}_{ij}(k)}{\left(\sum_{i=1}^{Q}\sigma_i^2\right)^{3/2}} \qquad \text{(A.7.1.2)}$$

Let us express (A.7.1.1) into the following matrix form[1]

$$\Pi V = 0 \qquad \text{(A.7.1.3)}$$

where

$$V = \left[\frac{\partial\tilde{A}(k)}{\partial\sigma_1}\ \frac{\partial\tilde{A}(k)}{\partial\sigma_2}\ \cdots\ \frac{\partial\tilde{A}(k)}{\partial\sigma_Q}\right]^T$$

and the channel matrix is written as

$$\Pi = \frac{\partial\Sigma}{\partial\Theta} = \begin{bmatrix} \frac{\partial\sigma_1}{\partial\theta_0} & \frac{\partial\sigma_2}{\partial\theta_0} & \cdots & \frac{\partial\sigma_Q}{\partial\theta_0} \\ \frac{\partial\sigma_1}{\partial\theta_1} & \frac{\partial\sigma_2}{\partial\theta_1} & \cdots & \frac{\partial\sigma_Q}{\partial\theta_1} \\ \cdots & \cdots & \cdots & \cdots \\ \frac{\partial\sigma_1}{\partial\theta_M} & \frac{\partial\sigma_2}{\partial\theta_M} & \cdots & \frac{\partial\sigma_Q}{\partial\theta_M} \end{bmatrix} = \begin{bmatrix} h_0\ h_1\ \cdots\ h_N & & \mathbf{0} \\ & h_0\ h_1\ \cdots\ h_N & \\ & & \cdots\ \cdots \\ \mathbf{0} & & h_0\ \cdots\ h_{N-1}\ h_N \end{bmatrix}$$

Obviously, $V = 0$ is one solution of (A.7.1.3), which leads to the same solution

1. The formulation of the problem for the non-minimum phase situation is similarly done by using the two-sided non-causal equalizer and introducing a certain amount of delay. The results of the analysis for the non-minimum phase case is the same as the minimum phase one, since both cases will have the same sturcture for the matrix Π.

as in (7.4.12); such a solution is the desired one, However, the matrix is not a full-rank matrix, and hence may have a solution other than $V = 0$; the existence of such a solution indicates that the vector V may fall into the null space of the matrix Π which satisfies (A.7.1.3), due to the fact that the number equations is less than the number of unknown varaibles. Such a class of solutions can cause undesired local minima.

An interesting observation is that $\frac{\partial}{\partial \sigma_i}\hat{A}(k)$ represents a solution of the follwoing system of homogeneous equations.

$$h_0\frac{\partial \tilde{A}(k)}{\partial \sigma_{0+l}} + h_1\frac{\partial \tilde{A}(k)}{\partial \sigma_{1+l}} + \ldots + h_N\frac{\partial \tilde{A}(k)}{\partial \sigma_{Q+l}} = 0 \qquad \text{(A.7.1.4)}$$

$$l = 1, 2, \ldots, M-1$$

After some manipulations of the matrix equation (A.7.1.3) we can find the set of following homogeneous equation

$$\sum_{p=1}^{N} h_p\left[\left(\sum_{i\neq p+l}^{Q}\sigma_i\cos\dot{\psi}_{p+l,i}(k)\right)\left(\sum_{i=1}^{Q}\sigma_i^2\right) - \sigma_{p+l}\left(\sum_{i\neq j}^{Q}\sigma_i\sigma_j\cos\dot{\psi}_{ij}(k)\right)\right] = 0 \qquad \text{(A.7.1.5)}$$

$$l = 1, 2, \ldots, M$$

With the constraint $\sum_{i=1}^{Q}\sigma_i^2 \neq 0$, (A.7.1.5) can also be written as

$$\sum_{p=1}^{N}\sum_{i\neq m}^{Q}\sigma_i\left(\sum_{i=1}^{Q}\sigma_i^2\right)h_p\cos\dot{\psi}_{p+l,i}(k) - \sum_{p=1}^{N}\sum_{i\neq j}^{Q}h_p\sigma_{p+l}\sigma_i\sigma_j\cos\dot{\psi}_{ij}(k) = 0 \qquad \text{(A.7.1.6)}$$

Combining all the coefficients of the term $\cos\psi_{ij}(k)$, (A.7.1.6) can be rewriten as a set of homogeneous equations with coefficients of fixed values

$$\sum_{j>i}^{Q} g_{ij}(h,\sigma)\cos\dot{\psi}_{ij}(k) = 0 \qquad \text{(A.7.1.7)}$$

where

$$g_{ij}(h,\sigma) = h_i\sigma_j\left(\sum_{\substack{n\neq i\\ n\neq j}}^{Q}\sigma_n^2 - \sigma_i^2\right) + h_j\sigma_i\left(\sum_{\substack{n\neq i\\ n\neq j}}^{Q}\sigma_n^2 - \sigma_j^2\right) - 2\sum_{\substack{p\neq i\\ p\neq j}}^{N}h_p\sigma_{p+l}\sigma_i\sigma_j \qquad \text{(A.7.1.8)}$$

and $$\sum_{\substack{n=1 \\ n\neq i \\ n\neq j}}^{Q} = \sum_{n=1}^{Q} \sum_{i=1, i\neq n}^{Q} \sum_{j=1, j\neq n}^{Q}$$

The following relationships between the instantaneous frequency is also useful:

$$\dot{\psi}_{ij}(k) = E_{\Psi}\{\Psi_i(k) - \Psi_j(k)\}$$

$$= E_{\Psi}\{\Psi_i(k) - \Psi_{i-1}(k) + \Psi_{i-1}(k) - \Psi_{i-2}(k) + \ldots + \Psi_j(k) - \Psi_{j-1}(k-1)\}$$

$$= \dot{\psi}_{i-1,i}(k) + \dot{\psi}_{i-2,i-1}(k) + \ldots + \dot{\psi}_{j-1,j}(k)$$

Then according to the assumption that the source parameter is time-varying, we have

$$\begin{aligned} \dot{\psi}_{i,j}(k) - \dot{\psi}_{i,j-1}(k) &= \ddot{\psi}(k-j) \neq Const \\ \dot{\psi}_{i,j}(k) - \dot{\psi}_{i-1,j}(k) &= \ddot{\psi}(k-i) \neq Const \end{aligned} \quad \forall k \in Z^{+} \qquad \text{(A.7.1.9)}$$

Appendix 7.2 *Proof of Corollary 7.4.2*

In the case where the channel is time-varying, the combined channel response is denoted as σ_{k-j}, and the envelope of the received signal is given by

$$\tilde{A}(k) = \left(\sum_{i=0}^{Q}\sigma_{k-j}^2 + 2\sum_{i\neq j}^{Q}\sigma_{k-i}\sigma_{k-j}\cos\dot{\psi}_{ij}\right)^{1/2}$$

Let

$$\frac{\partial}{\partial\sigma_j}\tilde{A}(k) = \frac{1}{\tilde{A}(k)}\left(\sigma_{k-j} + \sum_{i\neq j}^{Q}\sigma_{k-j}\cos\dot{\psi}_{ij}\right) = 0$$

Assuming that the source is a chirped sine tone, then $\dot{\psi}_{ij} = |i-j|\varphi$; this yields

$$\Pi\begin{bmatrix} 1 & \cos\varphi & \cos 2\varphi & \dots & \cos Q\varphi \\ \cos\varphi & 1 & \cos\varphi & \dots & \cos(Q-1)\varphi \\ \dots & \dots & & \dots & \dots \\ \cos(Q-1)\varphi & \dots & \dots & 1 & \cos\varphi \\ \cos Q\varphi & \dots & \dots & \cos\varphi & 1 \end{bmatrix}\begin{bmatrix} \sigma_k \\ \sigma_{k-1} \\ \dots \\ \sigma_{k-Q-1} \\ \sigma_{k-Q} \end{bmatrix} = 0$$

or

$$\sum_{i=1}^{Q}h_{k-i}\sigma_{k-i} + \sum_{n=1}^{N}\sum_{i=1}^{Q}h_{k-i}(\sigma_{k-i+n}+\sigma_{k-i-n})\cos n\varphi = 0 \qquad \text{(A.7.2.1)}$$

The coefficients are time-varying, i.e.

$$\sum_{i=1}^{Q}h_{k-i}\sigma_{k-i} \neq Const$$

$$\sum_{i=1}^{Q}h_{k-i}(\sigma_{k-i+n}+\sigma_{k-i-n}) \neq Const$$

According to Lemma 7.4.1, if (A.7.2.1) is satisfied, then the parameters of the source should be time-varying. This indicates that if the parameter of the source is time-varying then the cost function contains local minima. Therefore, if the parameter of the source posesses a non-constant varaition rate, then the only solution for (A.7.2.1) is $\{\sigma_k = 1, \sigma_{k-j} = 0\}$ $j = 1, 2, \dots Q$, and thus the time-varying channel is uniquely identifiable.

Appendix 8.1 *Proof for Theorem 8.6.1 (derivation of (8.6.6))*

First we present a result about the persistence exciting condition [8.6] for Adaptive-ASTV-ARMA model.

The gradient $\Psi(k)$ is a mixing process, $\exists \delta > 0$ and $h > 2$ such that

$$E\left[\sum_{k=lh}^{(l+1)h-1} \frac{\Psi(k)\Psi^T(k)}{1+\|\Psi(k)\|^2}\right] \geq \delta I$$

To show this, let us denote $Y(k) = \left[y_M(k)\ \ y_M(k-1)\right]^T$ and $E(k) = \left[e_M(k)\ \ e_M(k-1)\right]^T$, we have

$$\Psi(k)\Psi^T(k) = Y(k)Y^T(k) - \begin{bmatrix}\alpha & 0\\ 0 & \alpha^2\end{bmatrix} E(k)E^T(k)$$

Since $\alpha \neq 1$ thus $Y(k) \neq E(k)$, therefore $\Psi(k)\Psi^T(k)$ is matrix of rank unity, in this case, $h > 2$

$$\sum_{k=lh}^{(l+1)h-1} \Psi(k)\Psi^T(k) \quad \text{is positive definite.}$$

Next, Let us derive the following expression for the trace of the matrix $P(k)$

$$tr\{\gamma P(k+1)\}^n = tr\left\{\left[P^{-1}(k) + \frac{1}{\gamma}\Psi(k)\Psi^T(k)\right]\right\}^n$$

$$< tr\left\{\left[P^{-1}(k+lh) + \frac{1}{\gamma}\Psi(k)\Psi^T(k)\right]^{-1}\right\}^n \qquad \text{(A.8.1.1)}$$

$$< tr\left\{\left[P^{-1}(k+lh) + \frac{1}{\gamma}\Psi(k)\Psi^T(k)\right]^{-1} P^{n-1}(k+lh)\right\}^n$$

$$= tr\left\{P^{n-1}(k+lh)\left[P(k+lh) - \frac{P(k+lh)\Psi(k)\Psi^T(k)P(k+lh)}{\gamma+\Psi^T(k)P(k+lh)\Psi(k)}\right]\right\}$$

$$= tr\{P^n(k+lh)\} - \frac{tr\{P^{n+1}(k+lh)\}\Psi(k)\Psi^T(k)}{\gamma+\Psi^T(k)P(k+lh)\Psi(k)}$$

Now cosidering a positive definite function defined as

$$V_l = \sum_{k=(l-1)h}^{lh-1} tr\{\gamma P(k+1)\}^8 \qquad \text{(A-8.1.2)}$$

and using (A-8.1.1) with $n = 8$, we have

$$\begin{aligned} V_l &\le h tr\{P^8(k+lh)\} - \frac{\delta tr\{P^8(k+lh)\}\, tr\{P(k+lh)\}}{p^8(\gamma+\|P(k+lh)\|_2)} \\ &\le \left[1 - \frac{\delta tr\{P(k+lh)\}}{p^8 h(\gamma+\|P(k+lh)\|_2)}\right] h tr\{P^8(k+lh)\} \end{aligned} \qquad \text{(A-8.1.3)}$$

From (A-8.1.1) and (A-8.1.2) we see

$$V_l \ge h tr\{P^8(k+lh)\} \qquad \text{(A-8.1.4)}$$

Therefore, we have

$$E[V_{l+1}] \le \left(1 - \frac{\delta\|P(k+lh)\|_2}{p^8 h(\gamma+\|P(k+lh)\|_2)}\right) E[V_l] \qquad \text{(A-8.1.5)}$$

From elementary calculus, we know, that for

$$w = \frac{u}{\gamma+u} \quad \text{we have} \quad \frac{dw}{du} = \frac{\gamma}{(\gamma+u)^2} > 0 \qquad \text{(A-8.1.6)}$$

Using (A-8.1.5), we can show that

$$sup\, E[V_l] \le \infty \quad \text{and} \quad sup\, E[\|P(k)\|_2^8] \le C_o \le \infty \qquad \text{(A-8.1.7)}$$

Similarly, we can show that

$$sup\, E[\|P(k)\|_2^4] \le \infty \qquad sup\, E[\|P(k)\|_2^2] \le \infty \qquad \text{(A-8.1.8)}$$

Appendix 8.2 *Proof for Theorem 8.6.1 (derivation of (8.6.8))*

Using (8.6.2) and the matrix inversion lemma in [8.6], we have

$$G^T(k)P^{-1}(k+1)G^T(k) = G^T(k)\left(\frac{1}{\gamma}G(k)P(k)G^T(k) + K(k)K^T(k)\right)G^T(k)$$

$$= \gamma G^T(k)G^{-1}(k)\left[P(k) + \frac{1}{\gamma}G^{-1}(k)K(k)K^T(k)\left(G^T(k)\right)^{-1}\right]^{-1}G^{-1}(k)G^T(k)$$

$$= \gamma\left[P(k) + \frac{1}{\gamma}G^{-1}(k)K(k)K^T(k)\left(G^T(k)\right)^{-1}\right]^{-1}$$

$$= \gamma[P^{-1/2}(k)P^{-1/2}(k)$$

$$-\left(\gamma P^{-1/2}(k)P^{-1/2}(k)G^T(k)\left[K(k)K^T(k)\right]^{-1}G(k)P^{-1/2}(k)P^{-1/2}(k)\right)^{-1}\Big]$$

Using Cauchy-Schwartz inequality, we get

$$G^T(k)P^{-1}(k+1)G^T(k)$$

$$\leq \gamma\left[1-\left(1+\left\|\left[K(k)K^T(k)\right]^{-1}\right\|_2\left\|G(k)P(k)G^T(k)\right\|_2\right)^{-1}\right]P^{-1}(k)$$

$$\leq \left(\left[1-\left(1+\gamma\|P(k)\|_2^2\right)^{-1}\right]P^{-1}(k) = \left[1-\frac{1}{1+\gamma\|P(k)\|_2^2}\right]P^{-1}(k)\right)$$

Appendix 8.3 *Proof for Theorem 8.6.1 (derivation of (8.6.11))*

By using the basic norm inequality, we have

$$z^T(k+1)P^{-1}(k+1)z(k+1) < \left\| P^{-1/2}(k+1)\left(K(k)w(k) - \partial A(k+1)\right)\right\|_2^2$$

$$\leq \left\| K^T(k)P^{-1}(k+1)K(k)\right\|_2 \|w(k)\|_2^2 + \left\|P^{-1}(k+1)\right\|_2 \|\partial A(k+1)\|_2^2$$

$$\leq \left(\|P(k+1)\|_2^4 + \|P(k+1)\|_2^2\right)\left(\|w(k)\|_2^2 + \|\partial A(k+1)\|_2^2\right)$$

from (A-8.1.8) we known that

$$\|P(k+1)\|_2^4 < \infty \text{ and } \|P(k+1)\|_2^2 < \infty$$

thus for a bounded value C_1, we reach

$$z^T(k+1)P^{-1}(k+1)z(k+1) < C_1\left(\|w(k)\|_2^2 + \|\partial A(k+1)\|_2^2\right)$$

Appendix 8.4 *Proof for Theorem 8.6.1 (derivation of (8.6.14))*

Consider the following recursion, for $0<\nu<1$ and $\varepsilon<\infty$

$$\boldsymbol{E}\{\phi(k+1)\} \le \nu\phi(k)+\varepsilon \tag{A-8.4.1}$$

If we chose $\varepsilon \ge 1$ and $c = \varepsilon/\nu$, so that

$$p(k) = \frac{\phi(k)+c}{c(1-\nu)+\varepsilon} > \frac{c}{c(1-\nu)+\varepsilon} > 1 \tag{A-8.4.2}$$

Then also we have

$$\boldsymbol{E}\{p(k+1)\} \le \nu p(k)+1 \tag{A-8.4.3}$$

Now, for any $n>m$, define a sequence $\{x(k), m \le k \le n\}$ as

$$x(k) = (1-\frac{1}{p(k)})x(k-1) \qquad x(m-1) = 1 \tag{A-8.4.4}$$

Thus

$$p(k)x(k) = p(k)x(k-1) - x(k-1) \tag{A-8.4.5}$$

Consequently, by (A-8.4.3)

$$\begin{aligned} \boldsymbol{E}\{p(k)x(k)\} &= \boldsymbol{E}\{p(k)\}x(k-1) - x(k-1) \\ &\le (\nu p(k-1)+1)x(k-1) - x(k-1) \\ &= \nu p(k-1)x(k-1) \end{aligned} \tag{A-8.4.6}$$

Note that by (A-8.4.3)

$$\boldsymbol{E}\{p(m)\} \le \boldsymbol{E}\{p(0)\} + \frac{1}{1-\nu}$$

Thus

$$\begin{aligned} \boldsymbol{E}\{p(n)x(n)\} &\le \nu(\boldsymbol{E}\{p(n-1)x(n-1)\}) \le \ldots \le \nu^{n-m+1}\boldsymbol{E}\{p(m-1)x(m-1)\} \\ &= \nu^{n-m+1}\boldsymbol{E}\{p(m-1)\} \le \nu^{n-m+1}\left[\boldsymbol{E}\{p(0)\} + \frac{1}{1-\nu}\right] \end{aligned} \tag{A.8.4.7}$$

Hence by (A-8.4.4)

$$E\prod_{k=m}^{n}(1-\frac{1}{p(k)}) = E\{x(n)\} \le E\{p(n)x(n)\}$$
$$\le \nu^{n-m+1}\left[E\{p(0)\} + \frac{1}{1-\nu}\right]$$

From elementary calculus, it is easy to show that

$$1-y \le (1-gy)^{\frac{(1-r)}{g}} \quad , 0 \le gy \le r \le 1 \; g > 1$$

Using the above, the Holder inequality, and (A-8.4.7), we have

(A-8.4.7)

$$E\{\prod_{k=m}^{n}(1-\frac{1}{\phi(k+1)})\} \le E\{\prod_{k=m}^{n}(1-\frac{1}{\phi(k+1)+c})\}$$

$$\le E\left\{\prod_{k=m}^{n}(1-\frac{c(1-\nu)+\varepsilon}{\phi(k+1)+c})^{\frac{(1-r)}{g}}\right\} \le E\left\{\prod_{k=m}^{n}(1-\frac{1}{p(k)})^{\frac{(1-r)}{g}}\right\}$$

$$\le \left\{E\prod_{k=m}^{n}(1-\frac{1}{p(k)})^{\frac{(1-r)}{g}}\right\} \le \left(\nu^{\frac{(1-r)}{g}}\right)^{n-m+1}\left[E\{p(0)\} + \frac{1}{1-\nu}\right]^{\frac{(1-r)}{g}}$$

Therefore, we have

$$E\{\prod_{k=m}^{n}(1-\frac{1}{\phi(k+1)})\} \le M\eta^{n-m+1}$$

where $\eta = \nu^{\frac{(1-r)}{g}} < 1$ and $g = c(1-\nu)+\varepsilon$, $r = 1-\nu+(\varepsilon/c)$.

Finally, with the help of the result in (A-8.4.7), together with(8.6.12), we obtain

$$E\{\Phi(k+1,n)\} \le C_3\zeta^{k-n+1}$$

Appendix *Audio Demonstrations*

The purpose of these audio demonstrations is to show that the proposed algorithm can be applied to deal with some practical applications. The results of these demonstrations are stored in the floppy disk attached at back of this thesis.[1]

AUDIO DEMO-1 *Separation of a speech signal from a frequency modulated sinusoidal interference*

Consider a weak speech signal superimposed with a strong frequency modulated sinusoid, where the modulating signal is a stochastic process with an arbitrary distribution function. The objective of this simulation is to demonstrate the use of a second-order ASTV-ARMA model to cancel such a strong FM signal, and to recover the speech signal.

We consider two cases: (1) an FM sinusoid with a *a priori* known instantaneous phase; and (2) an FM sinusoid with unknown instantaneous phase (blind separation).

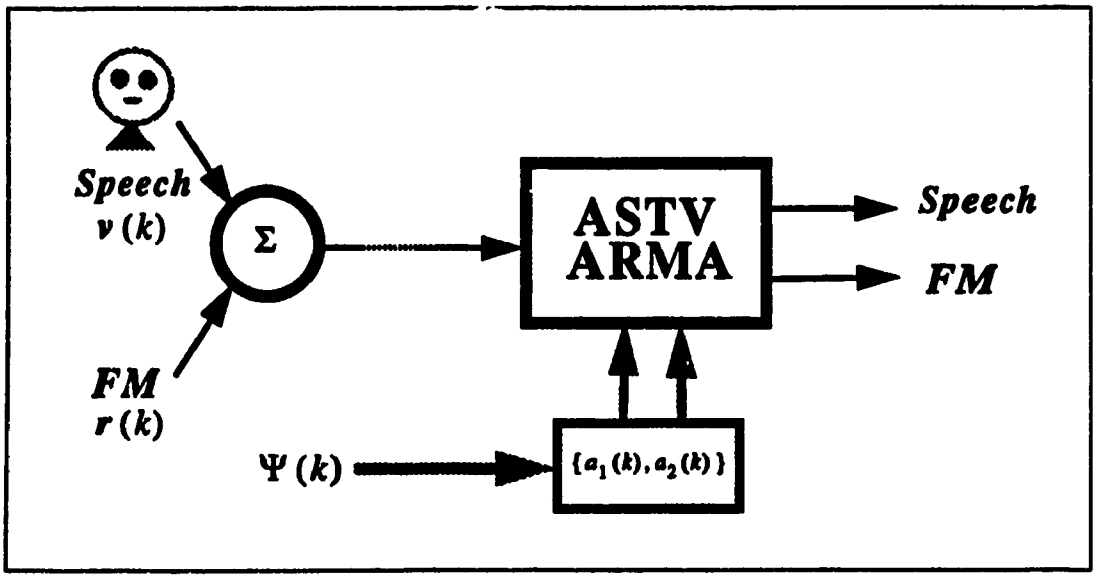

Fig.A-A.1 Block Siagram of Separation of Speech from a Strong FM Sinusoid

In the first case, the phase is used to calculate the time-varying coefficients needed to control the second-order ASTV-ARMA model. This audio demonstration shows that a complete separation of speech from the FM signal may be achieved, while in the

1. the file names of the are listed in Table A-A.4

second case the phase is estimated directly from the input mixture, and then the time-varying coefficients are calculated to control the ASTV-ARMA model.

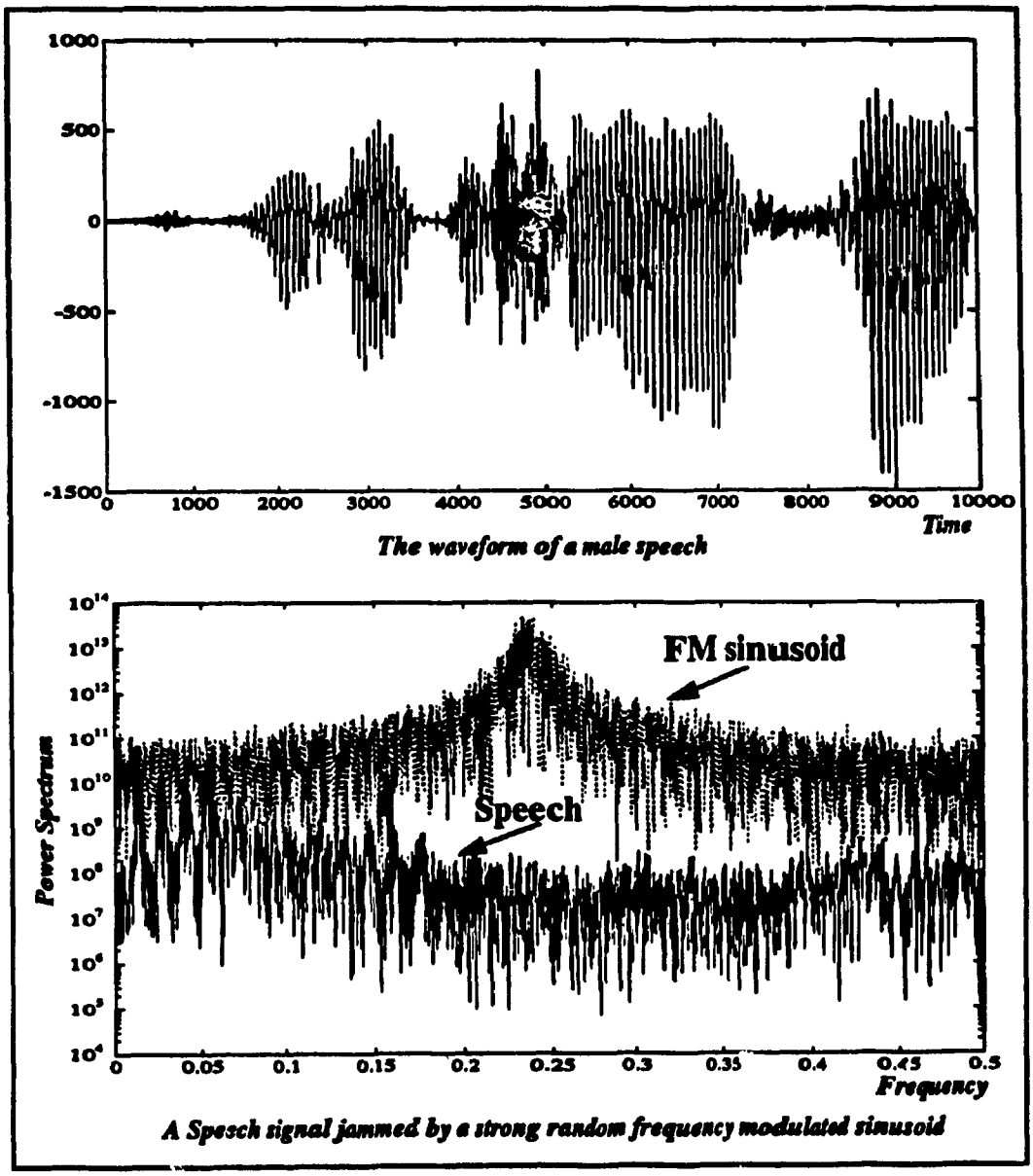

Fig.A-A.2 A Male Speech and Spectra of Input Mixture

The block diagram of the phase-controlled ASTV-ARMA model is shown in Fig.A-A.1, and the algorithm is presented in Table A-A.1. A male speech waveform is shown in Fig.A-A.2. The Fourier spectra of the speech and the FM signal are also shown in Fig.A-A.2. It is clear that the Fourier spectra of these signals are completely

overlapping .A blind phase-controlled ASTV-ARMA model is also shown in Fig. A-A.3.

Input: $x(k) = s(k) + r(k)$

Output: $y(k)$

$s(k)$ ---------- **speech**

$$r(k) = \sin\left(\omega_0 k + \int_0^k n(l)\,dl\right)$$

$$10\log\frac{\|r(k)\|}{\|s(k)\|} \geq 8dB$$

% Step-0 **If** $\psi(k)$ **is known, goto** *Step-2*

% Step-1 (Hilbert Transform)

$$\hat{x}(k) = H[x(k)]$$

$$\psi(k) = \text{atan}\{\frac{\hat{x}(k)}{x(k)}\}$$

% Step-2 (Calculation of Coefficients)

$$a_1(k) = -\frac{\sin(\psi(k) - \psi(k-2))}{\sin(\psi(k-1) - \psi(k-2))}$$

$$a_2(k) = \frac{\sin(\psi(k) - \psi(k-1))}{\sin(\psi(k-1) - \psi(k-2))}$$

% Step-3 (ASTV-ARMA model)

$$y(k) = x(k) + a_1(k)x(k-1) + a_2(k)x(k-2)$$
$$-\alpha a_1(k)y(k-1) - \alpha^2 a_2(k)y(k-2)$$

% Stop

Table A-A.1 ***An Algorithm for Separation of a Strong FM Signal and a Weak Speech Signal***

The phase-controlled ASTV-ARMA model completely eliminates the FM signal if the phase is known *a priori.*

On the other hand, if the phase is estimated from the input mixture (blind separation), the FM signal can not be completely cancelled. However, the quality of the recovered speech can be considerably improved.

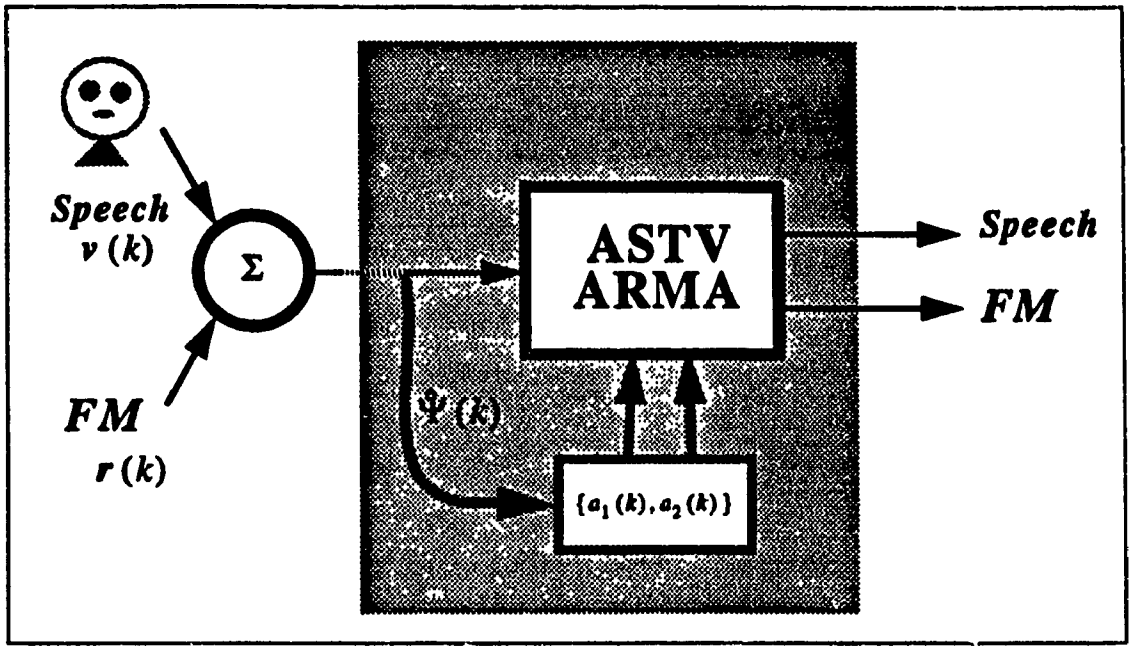

Fig.A-A.3 Blind Separation of Speech from a FM Sinusoids

AUDIO DEMO-2 *Blind enhancement of speech using phase information only*

Our goal is to enhance(retrive) a weak speech signal in the presence of a very strong interfering speech signal (Speaker-2) as is shown in Fig. A-A.3

Based on the assumption that a speech signal can be represented as an AM/FM one, we retrieve the instantaneous phase of the stronger speech, and use such phase information only to calculate the time-varying coefficients to control the ASTV-ARMA model. Although the strong speech can not be completely cancelled by using partial information, it is shown that such a phase-controlled ASTV-ARMA model can

provide satisfactory results for enhancing a weak speech signal.

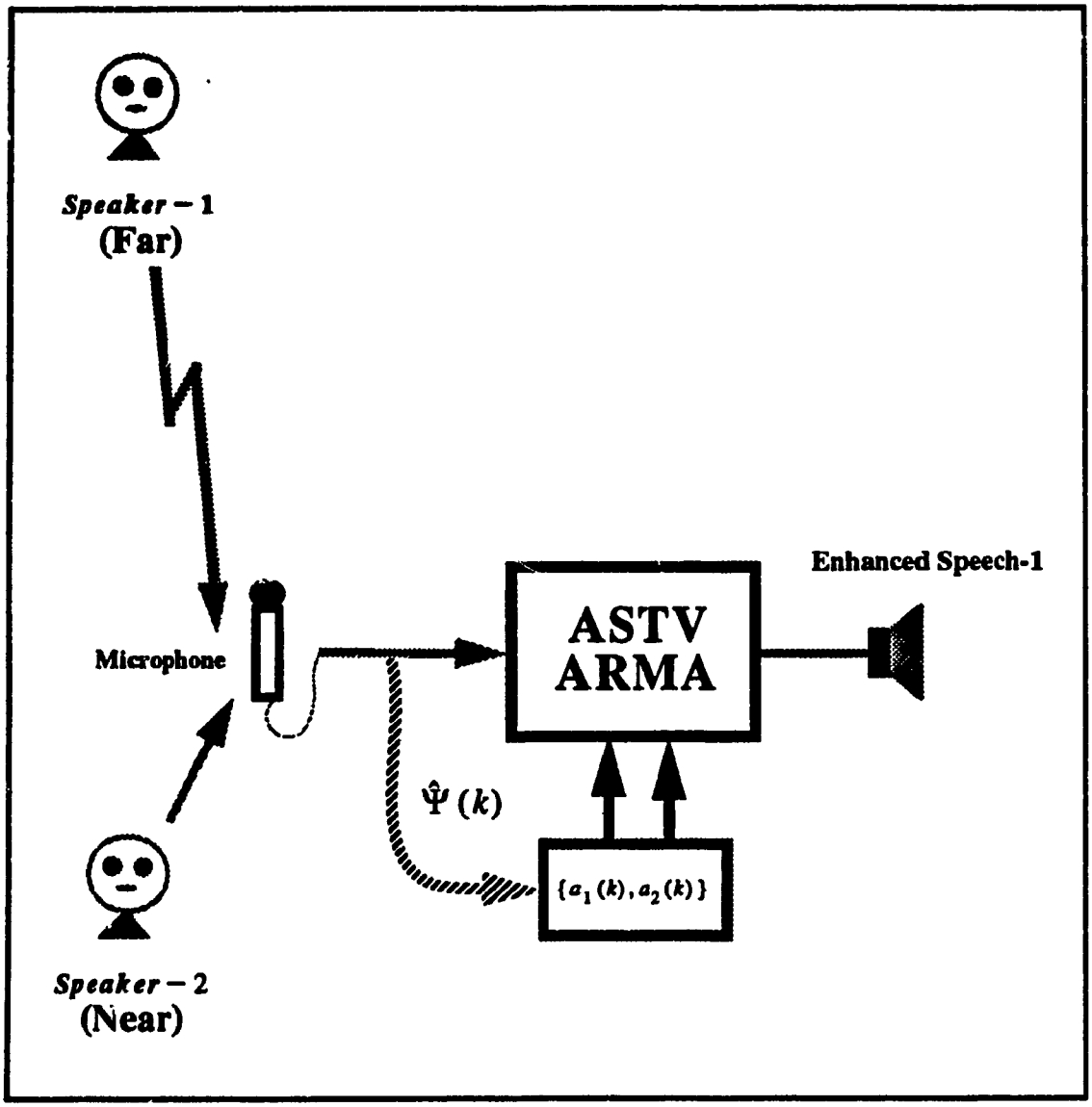

Fig.A-A.3 Blind Enhancement of a Weak Speech

The block diagram of the proposed phase-controlled ASTV-ARMA enhancer is show in Fig. A-A.3, and the corresponding blind enhancement algorithm is given in Table A-A.2

Input: $x(k) = s_1(k) + s_2(k)$

Output: $y(k)$

$s_1(k)$ ---------- **speech -1** *(Far)*

$s_2(k)$ ---------- **speech -2** *(Near)*

$$10\log\frac{\|s_2(k)\|}{\|s_1(k)\|} \geq 8dB$$

% Step-1 (Hilbert Transform)

$$\hat{x}(k) = H[x(k)]$$

$$e(k) = (x^2(k) + \hat{x}^2(k))^{1/2}$$

$$z(k) = x(k)/e(k)$$

$$\hat{z}(k) = H[z(k)]$$

$$\psi(k) = \text{atan}\{\frac{\hat{z}(k)}{z(k)}\}$$

% Goto Step-2 in Algorithm A-A-1

Table A-A.2 A blind Enhancement Algorithm

AUDIO DEMO-3 *Separation of superimposed frequency modulated sinusoids*

In this demo, a Cross-Coupled ASTV-ARMA model is used to separate the superimposed FM signals with *the same carrier;* the modulating signal for each FM sinusoid is a speech signal from a different speaker. The FM sinusoids are superimposed and transmitted through the same channel bandwidth. Fig.A-A.4 shows the completely overlapping Fourier spectra of the superimposed FM sinusoids. We show that using CC-ASTV-ARMA model, such a superimposed FM signal can be

separated at the receiving end. After the separation of the superimposed FM signals is achieved, the corresponding speech signals are recovered by applying conventional demodulation procedures.

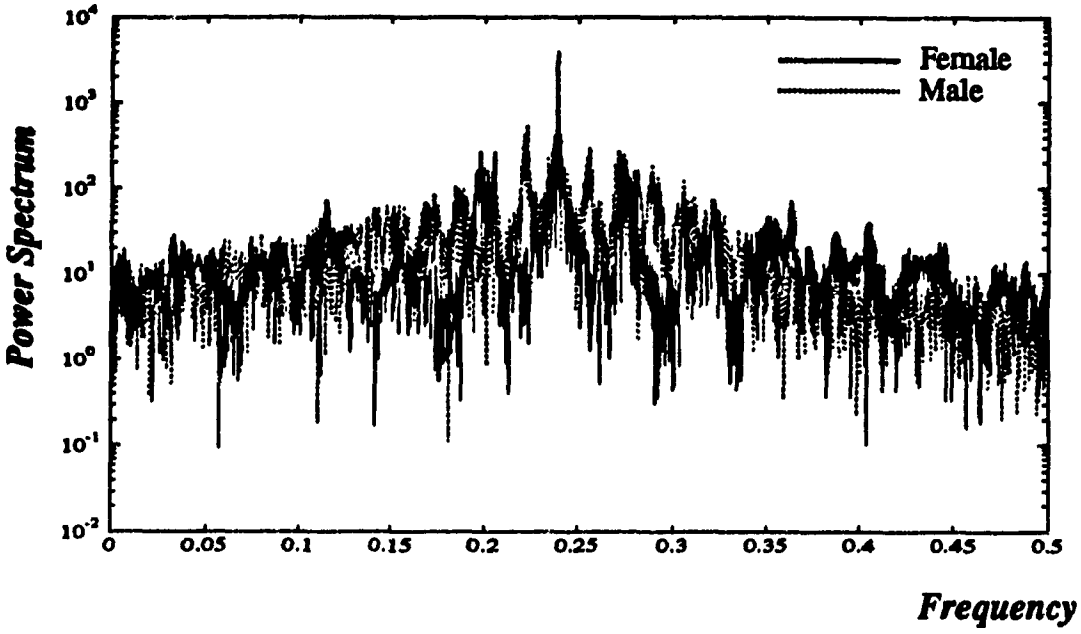

Fig.A-A.4 The Complete Overlapping Fourier Spectra of Superimposed FM Sinusoids

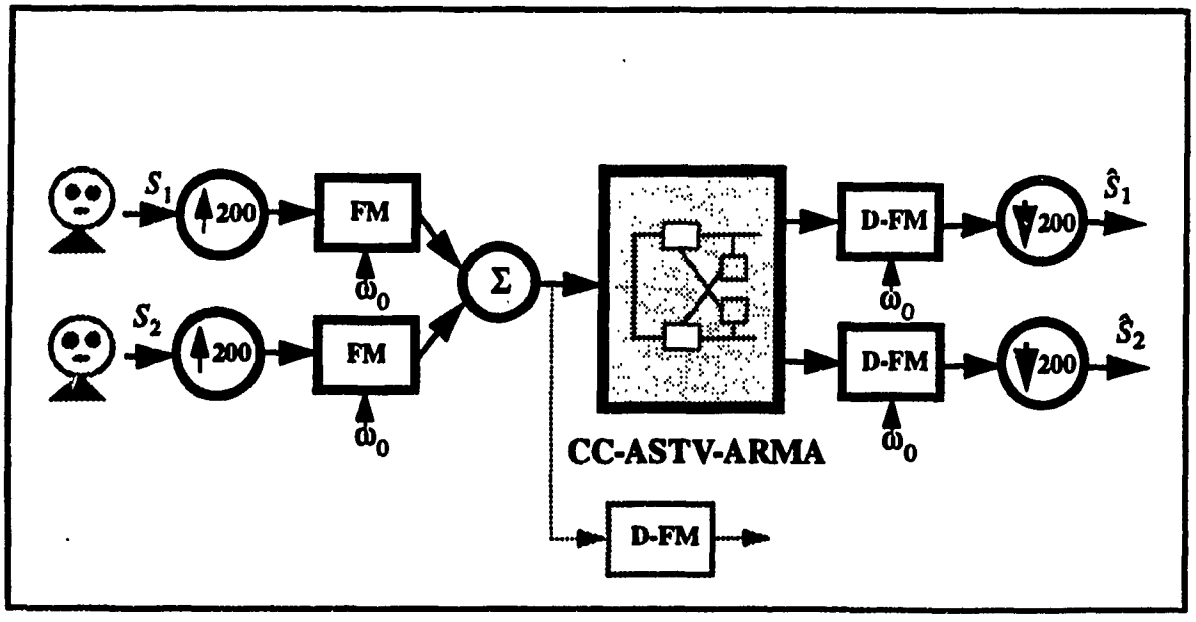

Fig.A-A.5 Cross-Coupled ASTV-ARMA Model for Separation of FM Sinusoids

On the other hand, if a conventional FM receiver is applied to the channel output without using the proposed scheme, the output of the receiver will result in a mixed, un-understandable speech.

Input: $x(k) = s_1(k) + s_2(k) + \ldots + s_N(k)$

Output: $y_1(k)$ $y_2(k)$ ——— $y_N(k)$

$s_1(k)$ ——— **speech -1**

$S_2(k)$ ——— **speech -2**

———

$S_N(k)$ ——— **speech -N**

% Step-1 (Generating Speech Modulating FM Sinusoids)

For i=1 to N

$$s_i(k) = \sin\left(\omega_0 k + \int_0^k S_i(l)\, dl\right)$$

% Step-2 Applying Cross-coupled ASTV-ARMA Model Given in Chapter 8

% Step-3 (Demodulation of FM Sinusoids)

For i=1 to N

$$\Psi_i(k) = \text{atan}\left\{\frac{H[y_i(k)]}{y_i(k)}\right\}$$

% Step-4 (Reconstructing Separated Speech)

For i=1 to N

$$\tilde{S}_i(k) = d\Psi_i(k)$$

% Stop

Table A-A.3 An Algorithm Based on CC-ASTV-ARMA Model

Table A-A.3 presents the algorithm using CC-ASTV-ARMA model for separating superimposed FM signals.

Two simulations are considered: (1) separation of FM sinusoids modulated by a male speech and a female speech[1], and (2) separation of FM sinusoids modulated by two male speeches and a music signal.

The usage of audio-demo files

The audio-demo file can be demonstrated on a SUN Station using either X-Window with the help of Matlab-version4, or by using Open-Window version-3 /audio tools.(files listed in Table A-A.4)

Table A.A.4 ***A List of Demo Files***[a]

	File name (X-Window)	*File name (Open-Window)*	*Description*
Audio Demo-1	audio10.dat	audio10	A weak speech signal jammed by a strong FM interference
	audio11.dat	audio11	Recover speech signal using a priori known instantaneous phase
	audio12.dat	audio12	Recover speech using blind ASTV-ARMA model
Audio Demo-2	audio20.dat	audio20	A weak speech in the presence of another strong one
	audio21.dat	audio21	Enhanced weak speech
Audio Demo-3	audio30.dat	audio30	Direct demodulated speech signal (cross-talk mixture)
	audio31.dat	audio31	Separated (demodulated) speech form channel-1
	audio32.dat	audio32	Separated (demodulated) speech from channel-2
Audio Demo-4	audio40.dat	audio40	Direct demodulated speech signal (cross-talk mixture)
	audio41.dat	audio41	Separated (demodulated) speech from channel-1 (Swamy)
	audio42.dat	audio42	Separated (demodulated) speech from channel-2 (Plotkin)
	audio43.dat	audio43	Separated (demodulated) music signal from channel-3

a. All the files are in compressed versions.

1. The male speech is "*I would like to know all the flights from Pittsburgh to Atlanta*"; the female speech is " *Show me all non-stop flights from Dallas to Atlanta*"